HYDROGEOLOGY OF THE MIDDLE SIGATOKA VALLEY SOUTHWEST VITI LEVU, FIJI

A thesis submitted in partial fulfilment of the requirements of the

Degree of

Master of Science in Engineering Geology

at the

University of Canterbury

By

Ratu Aminisitai Loco

2011

Abstract

Bedrock geology of the middle Sigatoka valley, located ~ 20 km inland of the township of Sigatoka, southwest of Viti Levu, Fiji, includes the steeply inclined Tari Fomation and uplifted Qalimare Limestone of the Wainimala Group of Oligocene to Middle Miocene age. These units are juxtaposed against the steeply inclined and moderately-highly fractured Cici Sandstone and Takaro Conglomerate/Rudite of the Tuva Sedimentary Group of Late Miocene age, northwest of the study area. Surface geology is largely expressed by the sinistral Nasovatava Fault, and its associated faults splays, and unconsolidated Quaternary to Recent Alluvium that fills the incised valley. The valley includes a ~40 km^2 rural area, from Bilalevu to Dubalevu, characterized by semi-commercial agricultural land-use practices. This area is subject to high water resource demand and utilisation, particularly from groundwater sources. Geophysical surveys, through electromagnetic and electrical resistivity methods, at Dubalevu, Tubakeli and Bila Rd, permitted the estimation of depth to bedrock, thickness and extent of alluvial materials and the presence of fractured systems within the mapped units. Groundwater drilling, through mud-rotary circulation, permitted the characterization of the major hydrogeological units, namely surficial confining unit, alluvial aquifer system, and intermediate confining unit and fractured aquifer systems. The hydrogeological framework is capped by low permeability surficial confining unit comprising sandy silt and silty loam with 7.8×10^{-8} m/s at Dubalevu, 2.2×10^{-7} m/s at Tubakeli and 4.3×10^{-8} m/s at Bila Rd. The alluvial aquifer system, comprising unconsolidated coarse-medium gravels with some fine-medium sand in Dubalevu and Bilalevu have an estimated transmissivity and conductivity of 600 m^2/d^{-1} and 30 m/d^{-1} and 1644 m^2/d^{-1} and 274.8 m/d^{-1}, respectively. The intermediate confining unit is composed of the fresh and unweathered sedimentary rock mass. Groundwater bore pump tests showed the fractured sedimentary system has an average transmissivity, storativity and conductivity of 10.9 m^2/d^{-1}, 3.7×10^{-4}, 1.16 m/d^{-1} for the fractured Cici Sandstone at Dubalevu, 26.2 m^2/d^{-1}, 6.1×10^{-4}, 6.1 m/d^{-1} for the fractured Takaro Conglomerate/Rudite at Tubakeli and 48.7 m^2/d^{-1}, 1.7×10^{-3}, 9.1 m/d^{-1} for the fractured Tari Formation at Bila Rd. Hydrogeochemical classification of groundwaters, springs and surface sources, showed the dominance of $Ca(HCO_3)_2$ type water suggesting the dissolution of calcite in the sedimentary units with variable sources of Na^+ and Mg^{2+}. Stable hydrogen and oxygen isotope analyses of groundwater, surface water and precipitation show a local meteoric water line

slope of 4.3, suggesting that water resources in the middle Sigatoka Valley are meteoric in origin with variable modifications via evaporation and mixing with older residual evaporated and connate groundwater. Chloride concentrations confirm the dominance of meteoric recharge-induced dilution. Groundwater recharge estimation, through physical and chemical mass balance models, yielded different results of 0.08 m/month (physical) and 0.2-0.6 m/month (chemical) in the wet season and -0.01 m/month (physical) and 0.1-0.2 m/month (chemical) during the dry season. Groundwater recharge mechanisms in the Sigatoka Valley, include moderate-rapidly dispersing meteoric-derived waters along fractured flow paths and seasonally variable leakage, from surface sources, dispersing along alluvial macro-poses. Groundwater protection and sustainable management in the study area is likely to be threatened by unregulated groundwater drilling, excess groundwater abstraction, absence of groundwater legislation and growing concerns of climatic variability. This thesis concludes by presenting several recommendations for groundwater protection and sustainable management, including sound groundwater exploration and evaluation of geological units, establishing an effective and sustainable legal frameworks, and increasing awareness of inherent groundwater issues such as climatic seasonality, climate change, vulnerability to contamination and unsustainable abstraction.

Table of Content

List of Figures

Chapter 1

Chapter 2

Chapter 3

List of Tables

Chapter 1

Chapter 2

Chapter 3

ACRONYMS

AAS – Alluvial Aquifer System

ADB – Asian Development Bank

API – aerial photo interpretation

CS – Cici Sandstone

Cl^- - chloride (mg/L)

CMB – Chloride mass balance

e - electron

EC – electrical conductivity (mS/m for EM survey and µS/cm for chemical concentration)

EM – Electromagnetic (geophysical method)

ER – Electrical resistivity (geophysical method)

FBS – Fractured Basement System

FG – Fiji Government

FP – Fiji Platform

FMS – Fiji Metereological Services

HD – Horizontal dipole or vertical coplanar coil orientation

ICS – Intermediate Confining System

K – coefficient of permeability or hydraulic conductivity (m/d^{-1})

LWRM – Land and Water Resources Management

MMEA – Ministry of Multi-Ethnic Affairs

MRD – Mineral Resources Department

n – neutron

NF – Nasovatava Fault (ENE-WSW trending and sinistral displacement)

NFB – North Fiji Basin

p – proton

PDW – privately drilled wells

PDC – private drilling companies

PfWG – Programme for Water Governance

PWD – Public Works Department

PWB – Physical water balance

QRA – Quaternary-Recent Alluvium

SCS – Surficial Confining System

SVRDP – Sigatoka Valley Rural Development Project

SV – Sigatoka Valley

SR – Sigatoka Rivers

S – storativity (dimensionless)

T – tranmissivity (m^2/d^{-1})

TDS – total dissolved solutes

TCM – tropical cyclone Mick

TCR – Takaro Conglomerate/Rudite unit

TSG – Tuva Sedimentary Group (Middle Miocene-early Late Miocene)

VD – vertical dipole or horizontal coplanar coil orientation

WG – Wainimala Group (Late Oligocene-Middle Miocene)

YG – Yavuna Group (Late Eocene-Early Oligocene)

Acknowledgements

I am indebted to many people and parties for their overwhelming support during this research project. I would like to thank:

(1) The Fiji Government, through the Ministry of the I-Taukei Affairs, for the opportunity granted to undertake this post-graduate program in this renown institution.

(2) The Mineral Resources Department, particularly the (then) Director (Mr Ian Fong) and Manager Geological Services (Mr Malakai Finau), for financing this project.

(3) My supervisors, Mr. David Bell for the advice and support throughout the research period and Dr. Travis Horton, for always having an open door to help with insights and advice on hydrochemistry, for analyzing my isotope samples and for editing this thesis. Also, thanks to Associate Professor Dr. David Nobes for his advice in the interpretation of geophysical data and for editing the geophysics component of this research.

(4) The HYCOS program of the South Pacific GeoScience Commission (SOPAC), particularly Mr Peter Sinclair (Hydrogeologist), for permitting the use of SOPAC's geophysical equipment and for guidance on geophysical and hydrogeological investigations.

(5) Members of the Dubalevu, Tubakeli and Bila Rd settlements for their hospitality.

(6) The Hydrogeology staff of the Mineral Resources Department for their tireless assistance throughout the data acquisition stages

(7) The drill crewmen who were involved during the drilling and pump test stages.

(8) Staffs of the MRD's Geochemical Laboratory for the analysis of chemical samples.

(9) Mr Joshua Blackstock for his assistance, particularly in the interpretration of hydrochemistry.

(10) Mr Peter Rodda (Geologist) for confirmation of several geological questions.

(11) Mr Jeremaia Taganesia and his family for their friendship, assistances and support during the past two years..VINAKA SIR!!!

(12) My parents ("RATU & NAU"), brothers and sister, for all your prayers and the words of encouragement.

(13) Mr and Mrs Sulio Vuniamatana for providing accommodation, scrumptious meals and transport for last six (6) months.

(14) All my friends and families in Christchurch, Fiji and overseas for the encouragements.

(15) Last but not least, my wife, Mrs Salome Loco, for her continual support in the last three years.

"VINAKA VAKALEVU"

Chapter 1: Introduction

1.1 Project background

The nation of Fiji (Figure 1.1) is comprised of more than 300 islands in the southwest Pacific (176-182°E and 16-20°S), 109 of which are permanently populated (Gale & Booth, 1993). Rapid population growth and economic development in major urban centres has increased demand, usage and exploitation of natural resources, including surface and groundwater systems.

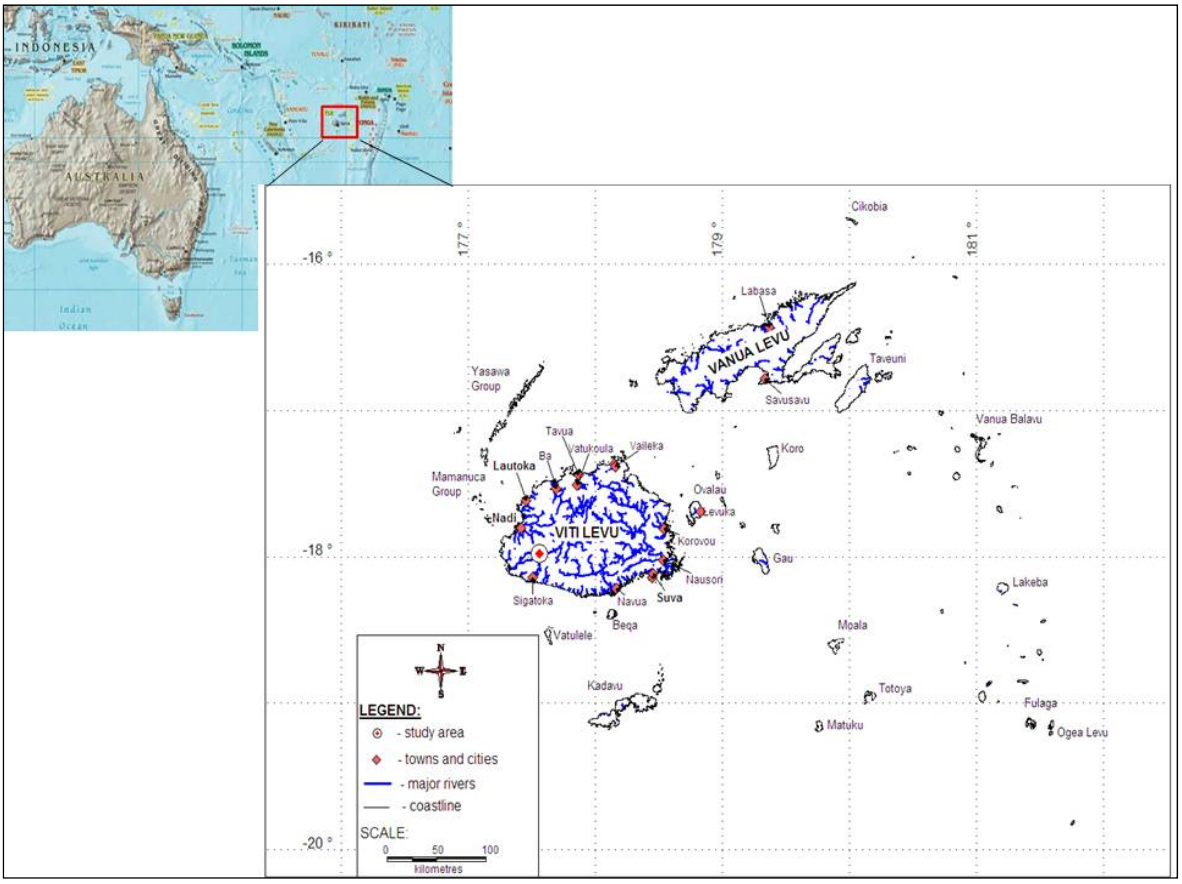

Figure 1.1: location of Fiji Islands (marked by red square) in relation to other countries in the Pacific (Henessey and iventure, 2003) and an inset of the Fiji Islands group with the study area on southwest Viti Levu in relation to the towns and cities (MapInfo Professional 10.0).

Economic activities in Fiji, primarily driven by increases in namely sugar cane farming, infrastructural development, agriculture (e.g. forestry and fishery sectors), as well as the mineral sector, has led to the expansion of urban areas, including Suva, Lautoka and Nadi (Figure 1.1). As a flow-on effect, semi-urban centres, including Ba, Tavua, and rural farming settlements in the Sigatoka Valley (SV), recorded rapid landuse changes, from traditional

subsistence farming to semi-commercial agricultural activities (e.g. root crop, vegetable, sugar cane farming). Increases in tourism had further fueled the changes, increasing stress on natural resources. If not properly monitored and managed, these changes may lead to numerous adverse environmental impacts, such as land degradation through accelerated erosion, contamination of waterways, excess demand and improper use of surface water, excess groundwater abstraction and groundwater quality deterioration via aquifer contamination.

This research was centred on two semi-commercial farming communities in the southwest Viti Levu (southern of the two largest islands in Fiji (Figure 1.1)). The farming areas, namely Dubalevu and Bilalevu, are located in the middle Sigatoka Valley. The valley, known as "Fiji's salad bowl" due to its historical and current agricultural productivity, includes numerous aggradation landforms, namely alluvial fans, terraces and extensive flats in the central Sigatoka River (SR) valley (Figure 1.2). In an attempt to enhance the growth and supply of high-quality fruits and vegetables, throughout the year (Gale and Booth, 1993), the Fiji Government (FG) and Asian Development Bank (ADB) established of the Sigatoka Valley Rural Development Project (SVRDP) in 1986. The SVRDP intends to provide reliable and sustainable irrigation water sources to farmers in the area. In response to SVRDP, the Mineral Resources Department (MRD) conducted an investigation of hydrogeological potential of alluvial materials deposited along the meandering river during which around 21 groundwater wells were drilled across the valley (results of SVRDP will be presented and summarized in the next chapter). This thesis, however, reports on the current hydrogeological conditions present in the middle Sigatoka catchment and investigates potential deeper water-bearing units, namely fracture sedimentary basements, relative to the previously investigated alluvium deposits as per SVRDP that may provide usable groundwater quality and quantity. For ease of referencing, the middle Sigatoka valley (MSV), including the Dubalevu and Bilalevu will, hereafter, be collectively referred to as the "study area".

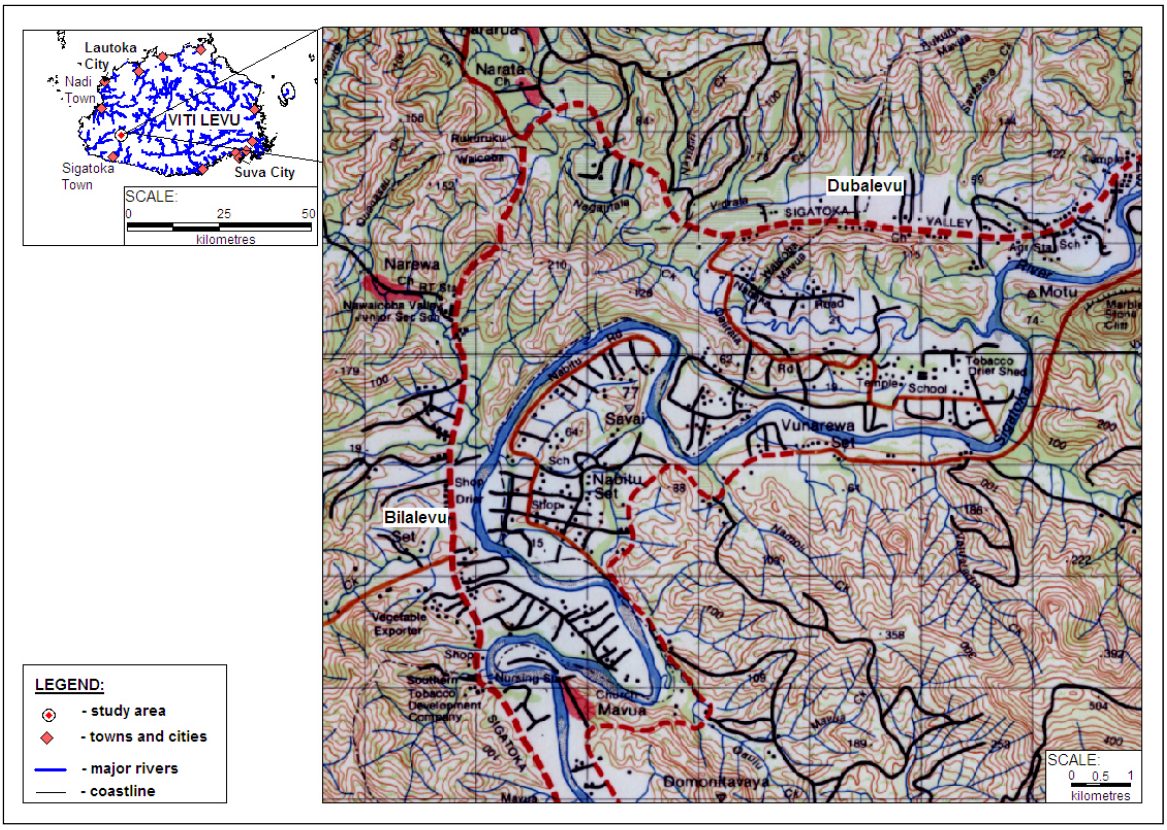

Figure 1.2: location of study area Viti Levu and an inset of the topographical map of the study area, Bilalevu and Dubalevu, with surrounding settlements and villages which were also investigated during this research through groundwater chemical and isotope sampling.

1.2 Thesis Objectives

Several key questions formed my thesis research:

- What is the general geological, geomorphic and tectonic history of the area?
- What are the relationship between this geological history and the hydrogeological conditions present in the study area?
- What are the primary recharge mechanism(s) in the study area?
- What does the aqueous geochemistry indicate about groundwater flow and local hydrological conditions?
- What are the impacts of increase human development and landuse intensification on groundwater resource quantity and quality?

In view of the preceding questions, this thesis is designed to address the following objectives:

- to classify all underlying geological materials relative to groundwater flow and storage potential;
- to examine the influences (if any) of structural controls, namely fault-induced fractures and/or shear zones in controlling groundwater occurrence;
- to determine the dimensions (extent, depth and thickness) of the underlying alluvial aquifer(s) and to locate deeper and fractured water-bearing units when present;
- to identify the major hydrochemical facies of local groundwaters;
- to determine groundwater recharge and flow regime;
- to determine the stable isotopic composition of surface water, groundwater, and rainfall relevant to local hydrological cycling; and
- to determine the sustainability of current groundwater resources utilization practices and recommend mechanisms to equitably allocate groundwater and surface water resources, particularly during the dry season

1.3 Study Area

1.3.1 Location and selection

The 40 km^2 study area is located ~ 15-22 km NNE and inland of Sigatoka Town (Figure 1.2). The study area had been subject to landuse intensification via rural and semi-commercial farming in the past three decades and has since, recorded an escalating demand and use water resources, particularly groundwater, for human security and safety, as well as to optimize plant growth. The selection of study areas has been made due to:

- the presence of geomorphic, geological and structural features, such as the abandoned Qalitala meander valley at Dubalevu, two abandoned (oxbow) lakes at Nabaka and Bilalevu, terraced alluvial deposits at Bilalevu, and the ENE-WSE trending sinistral Nasovatava Fault with its associated splays, suggest areas of potential groundwater storage and flow through possible buried river channels and fractured or sheared sedimentary units;

- the availability of baseline data from the SVRDP at the Mineral Resources Department (MRD) that provides essential hydrogeological constraints upon which this research can be expanded;
- continuous landuse intensification for semi-commercial and commercial agriculture purposes, which could escalate groundwater demand and use for drinking and irrigation, and potentially creates adverse impacts on groundwater resource quality and quantity;
- its close proximity to rainfall stations at Mavua and Nacocolevu, warranting a reliable long-term rainfall data necessary for physical water balance model for groundwater recharge estimation

1.3.2 Geology

The study area is underlain by Tari Formation and Qalimare Limestone of the Wainimala Group (dated Oligocene to Middle Miocene in age) and juxtaposed against the Cici Sandstone and Takaro Conglomerate/Rudite of the Tuva Sedimentary Group of Midddle to Late Miocene in age (Hathway, 1989). These sedimentary units are deformed, and displaced in areas, relative to the rupture of the sinistral Nasovatava Fault (Figure 1.3.). Eustatic fluctuation in the Quaternary to Recent period caused episodic incision of these sedimentary basement upon which Alluvium materials were deposited (Davies, 1992). History and detailed classification of these geological units in relation to their groundwater potential will be examined in the proceeding chapters.

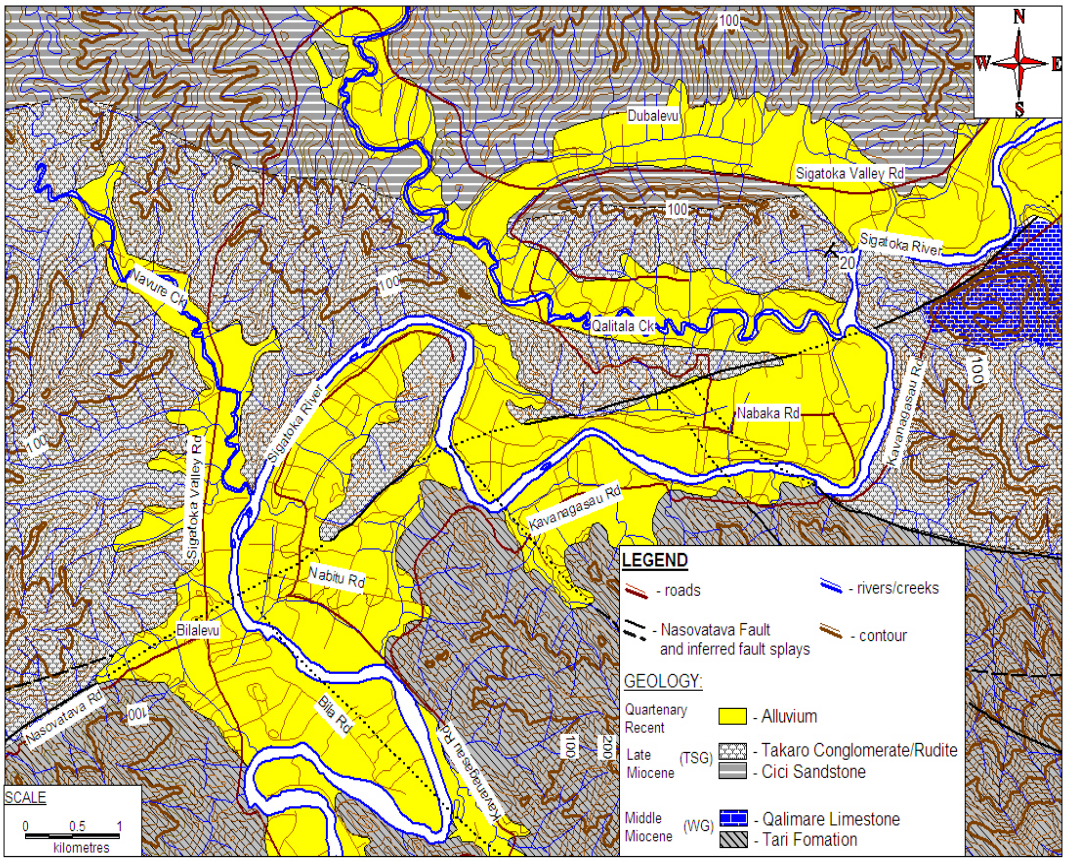

Figure 1.3: Geology of the study area comprising the Tari Formation, Qalimare Limestone of the Wainimala Group, Cici Sandstone and Takaro Conglomerate/Rudite of the Tuva Group and Alluvium materials occupying the reaches of the Sigatoka River (Hathway, 1989). Summary of the geological history and detailled classification of these geological units will be covered in later chapters. Refer to Figure 3.13 for the enlarged version.

1.3.3 Physiography

The physical landscape is characterized by steeply and highly dissected, as well as rolling, submountainous tracts (Figures 1.4 – 1.5), bounded by low-lying alluvial plains that occupy meandering reaches of the SR (Davies, 1992). The topographic high, are mantled by the uplifted and deformed Wainimala and Tuva geological groups, whilst incised valley in the study area is filled with Alluvial materials, comprising unconsolidated gravels, sands and silt.

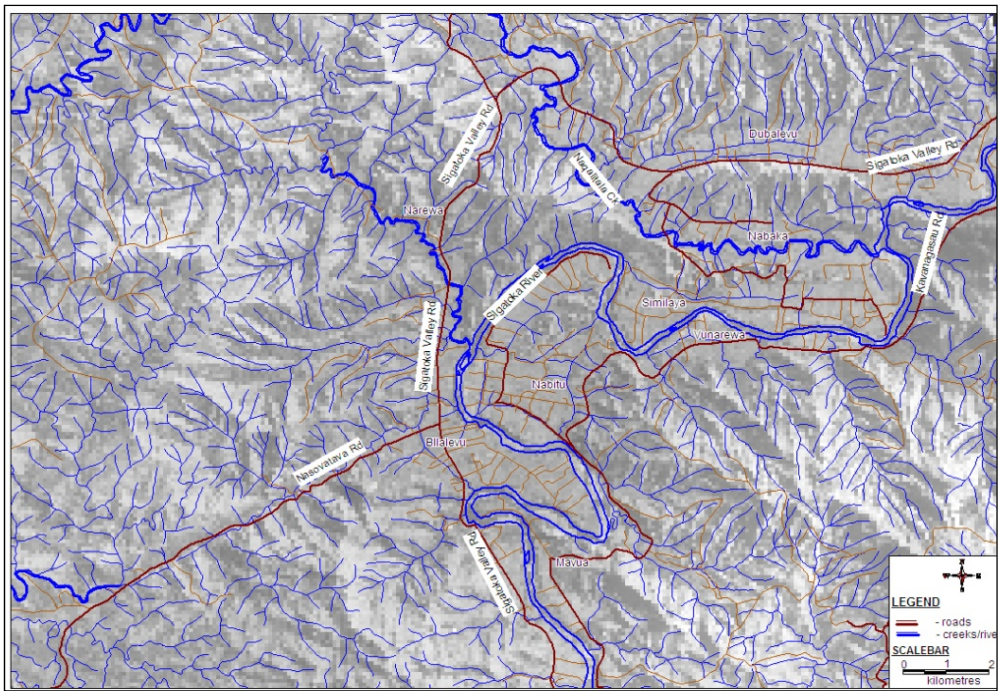

Figure 1.4: Low resolution 1994 aerial photo showing highly dissected hills occupying the topographical highs whilst the contiguous alluvial flats, harnessed for human occupation and commercial agricultural practices, occupy the reaches of the Sigatoka River.

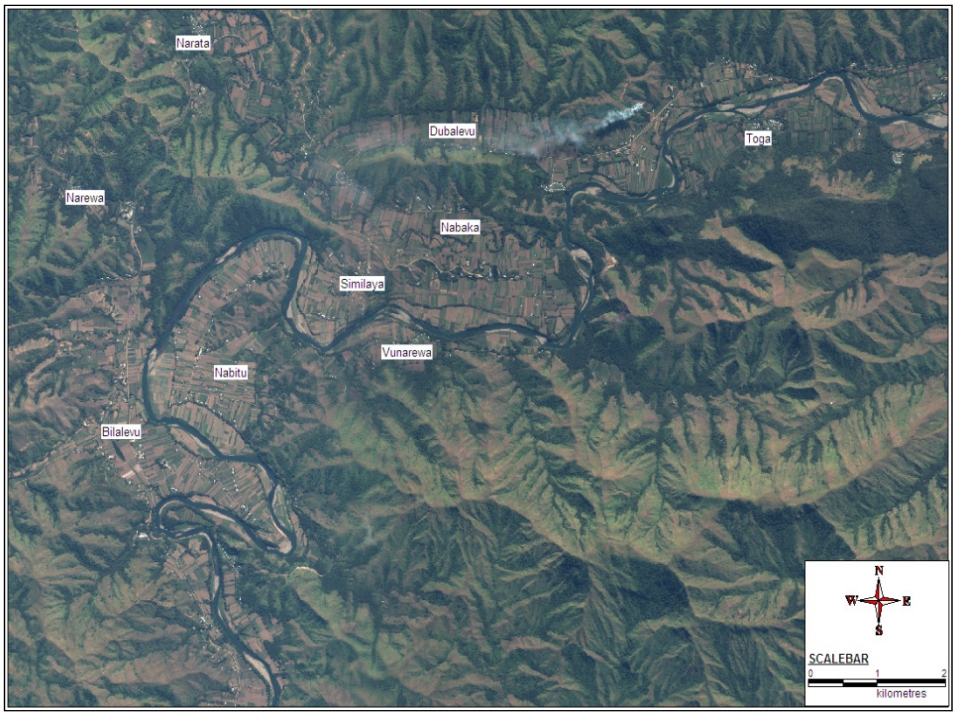

Figure 1.5: 1:10,000 IKONOS satellite image captured in 2005 showing highly dissected landscape with confined alluvial flats occupying the reaches of the Sigatoka River.

Overall, fluvial surface processes are the primary control on the shape of the Middle Sigatoka Valley. These processes, according to Selby (1985), include:

- incision and/or channelizing of landscape by the Sigatoka River;

- base-level responses of river systems and long-term interactions with relatively high relief causing hillslope processes and sediment generation;
- entrainment of sediments and debris to the ocean; and
- production of a suite of erosional and depositional landforms.

These roles are evident in the presence of temporary sediment storages and/or aggradation landforms around the reaches of the SR (Figures 1.2 & 1.5), including flood plains, abandoned river channels and terraces, and alluvial fans, which serve as geomorphic markers representing periods of abrupt climatic and/or environmental changes. Surface slumping, minor landslides and debris flows are ubiquitous in steep and dissected slopes, as manifested by vegetation-covered talus and scree.

1.3.3 Climate

Fiji's climate is classified as seasonal maritime tropical and is controlled by the Southeast (SE) trade winds (Figure 1.6) and seasonal movement of the Inter-tropical convergence zone and associated Hadley cells. This climate is characterized by a pronounced wet and dry seasons from November to April and from May to October, respectively (Gale & Booth, 1993). Up to 80% of the total annual rainfall falls during the wet season, also known as the cyclone season, with maximum rainfall always recorded from January to April (Cox & Hulston, 1980). The dry season is characterized by long (~25 sunshine days/month) dry spells with negligible precipitation. In addition to atmospheric circulation patterns, climate in Viti Levu is strongly influenced by the presence of several north-south mountain ranges (900-1400 m a.s.l) dividing the island into a humid windward (rainfall > 3000 mm y^{-1}) climate zone on the eastern side, and a dry climate zone on the west (rainfall < 2000 mm y^{-1}) (Waterloo, et. al., 1997) (Figure 1.6). The study area is located on the dry side, immediately adjacent to the transitional climatic zone (Figure 1.7), SW Viti Levu.

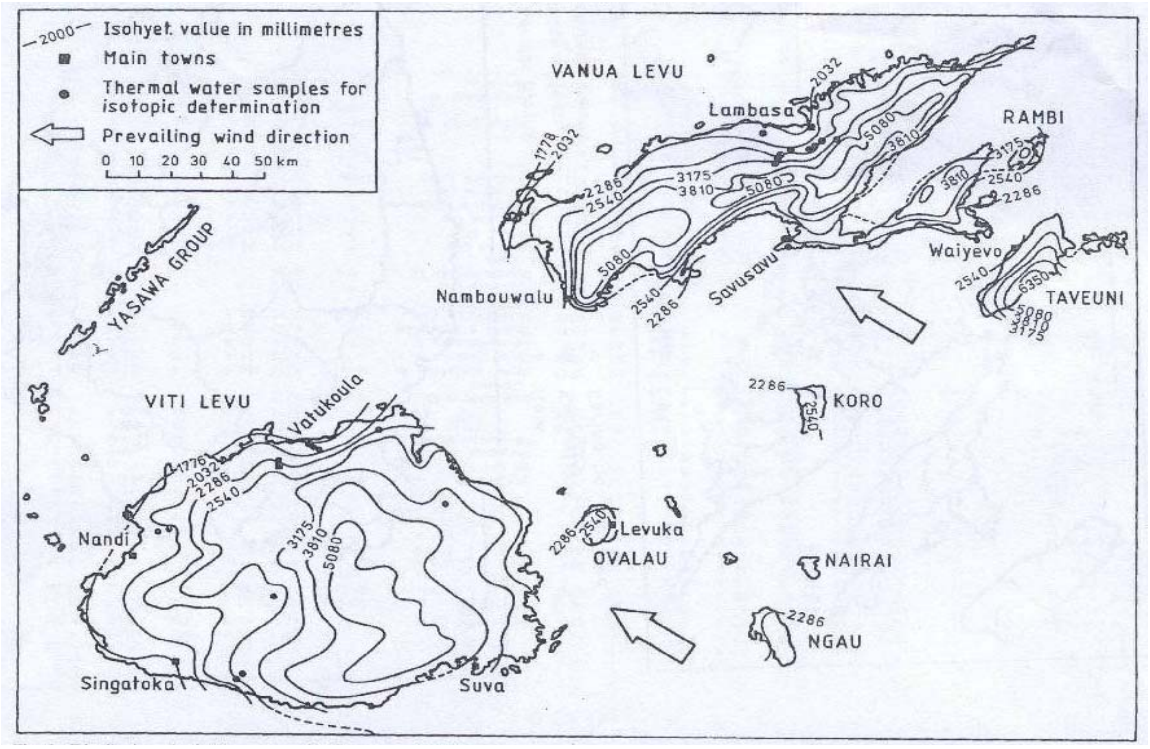

Figure 1.6: distribution of rainfall on the main islands of Fiji as controlled by the SE trade wind. Areas of with area of higher rainfall indicating regions of higher elevation (Cox & Hulston, 1980).

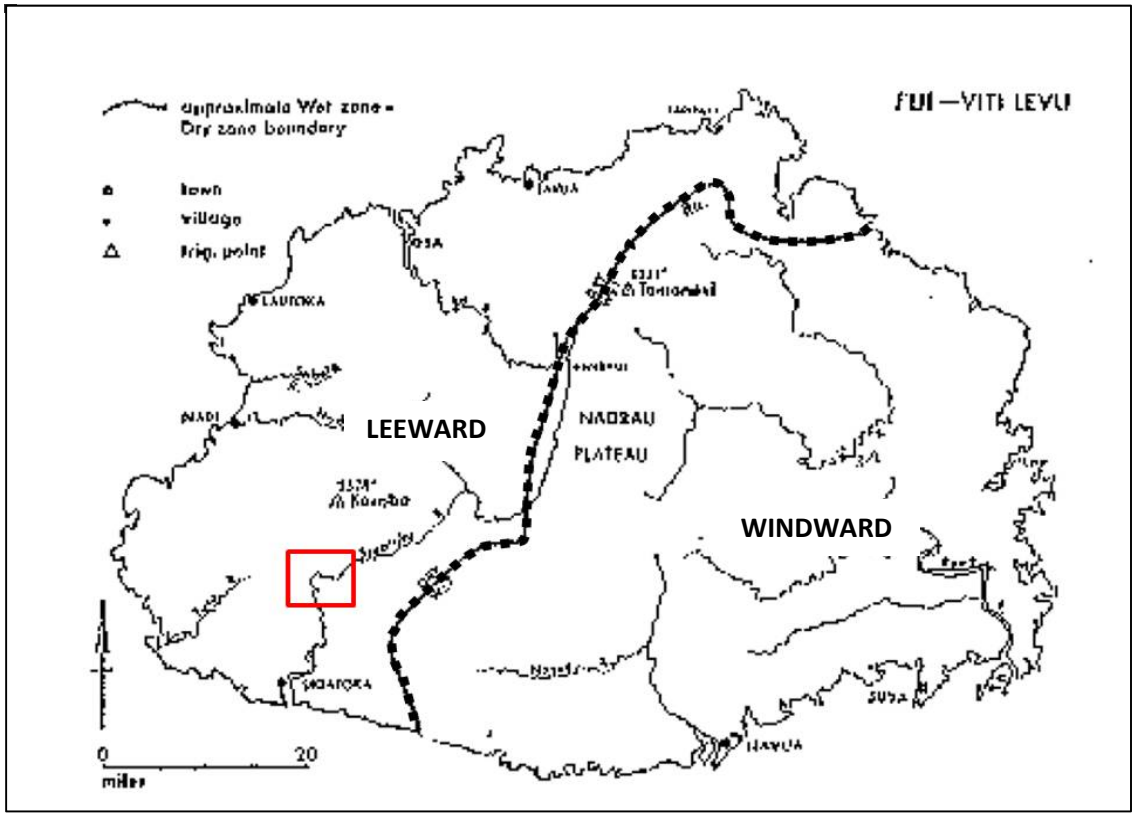

Figure 1.7: approximated windward and leeward boundary in Viti Levu, Fij, as controlled by the SE trade wind and the N-S mountain ranges: the study area shown by the red box located west of transitional boundary (de Brian, 2001).

Months	Jan	Feb	Mar	Apr	May	Jun	Jul	Aug	Sep	Oct	Nov	Dec
Maximum temperature (°C)	31	31	31	30	29	28	27	27	28	29	30	31
Minimum temperature (°C)	22	22	22	21	20	19	18	18	19	20	21	21
Average rainfall (mm)	277	253	295	182	106	74	77	73	99	102	142	189
Number of days with rain	16	16	17	13	10	7	8	7	8	8	10	13
Daily sunshine (hours)	5.5	5.1	4.8	4.7	5.2	4.7	5.2	5.9	5.4	6.1	6	6.2
Monthly evapotranspiration (mm)	156	136	127	105	89	73	76	97	112	139	148	158

Table 1.1: monthly climate data from Nacocolevu Agriculture Research Centre (Average for (1938-1982). Source: Hawaiian Agronomics International (1984).

The warmest period (Table 1.1), December to March, has a mean maximum temperature of 31 °C, with excess precipitation usually recorded and during which tropical cyclone season often occurs (Davies, 1992). The coolest period, July and August, experiences a mean maximum temperature of 27 °C (Gale & Booth, 1993). Davies (1992) added stated the SV experiences dry season between May and October, with little to no rainfall received during June and September and Table 1.1 shows this with an average monthly rainfall of 90 mm from May-October and around 220 mm during the wet or cyclone season. Potential evapotranspiration (PET) during the dry and wet seasons were recorded to be around 100 mm and 140 mm, respectively.

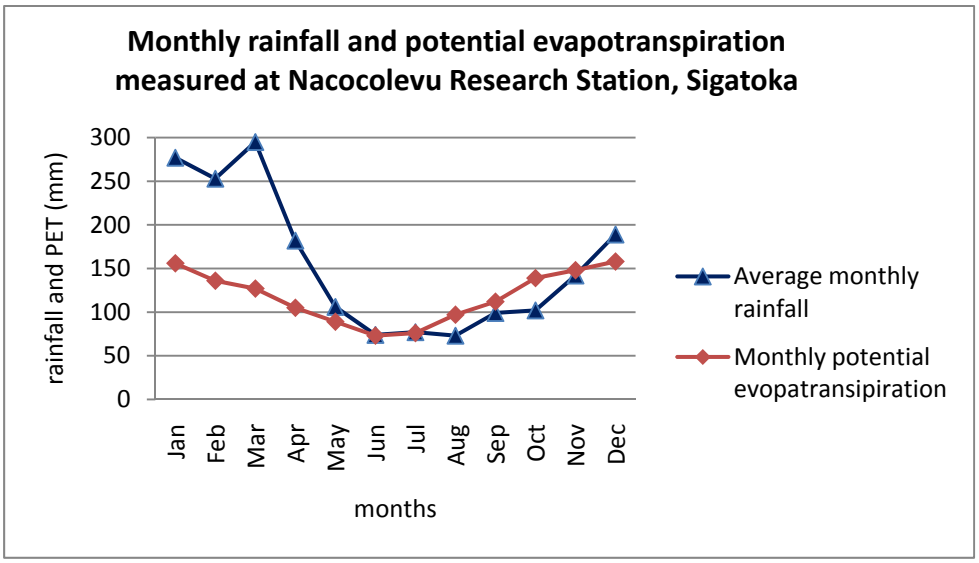

Figure 1.8: monthly average rainafall and PET obtained from Table 1.1 (average for 1938-1982) showind the distinct wet and dry seasons.

Clearly, net recharge is deficit during most of dry season due to high PET period, whilst excess water (i.e. surface and groundwater) is continued to be used and exploited for portable and irrigation purposes. This could threaten the long-term sustainability of water resources and hence, necessitates systematic and conventional investigation, procedures and mechanisms to ensure equitable allocation and sustainable groundwater management: some of which will be addressed in this research.

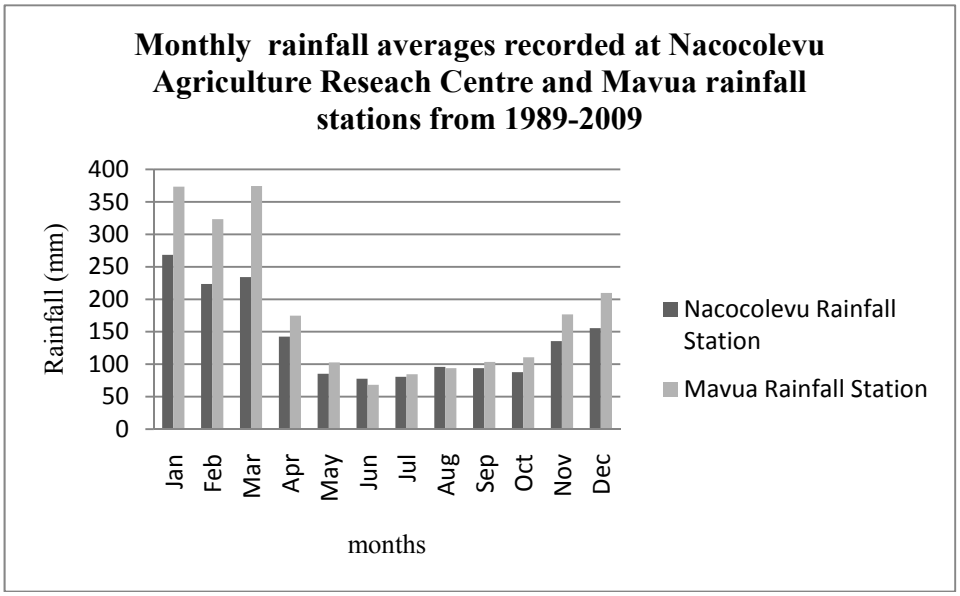

Figure 1.9: monthly rainfall averages recorded at Nacocolevu and Mavua rainfall stations for 1989-2009. Raw rainfall data and location map of the two climate stations in relation to the study area will be provided in Appendix A (Source: Fiji Metereological Service).

1.3.4 Soil, Vegetation and Land Use

Soil capping the study area has been classified by Rijkse (1990) as Sigatoka and Dubalevu series. The Sigatoka soil, occupying the Bilalevu area, are defined as very dark greyish brown to dark brown sticky, plastic, and friable silt derived from the recent alluvium comprising rocks of mixed mineralogy. The Dubalevu soil is characterized by very dark brown and yellowish brown, friable, slightly plastic and slightly sticky, silt loam derived from colluviums comprising sandstone of intermediate and basic composition (Rijkse, 1990). Vegetation cover varies spatially: the topographic highs are covered by grassland and scrub vegetation, together with thick patches of exotic pine trees and native species, whilst the topographic lows and alluvial flats are either covered with grassland or cultivated and thence occupied by human dwellings, such as villages or farm houses. From aerial photograph interpretation (API), thick and heavy vegetation tend to be concentrated around major water ways and river-valley bottoms. Landuse around the valley is controlled by semi-commercial farming whilst villagers are mostly engaged in subsistence farming. In semi-commercial farms, vegetable and root crops, including tomatoes, beans, beet, carrots, lettuce, cauliflower, cabbage, pumpkins, melons, pawpaw, and peanuts, pumpkin, cassava and corn farmers, are grown and harvested.

1.3.5 Population & Water Resources Use

The study area, together with neighboring villages and settlements, has experienced significant changes in population. An increase in the population of most villages had been recorded whilst population in Bilalevu and other farming settlements have decreased in the past two decades (Table 1.2): this may be ascribed to either rural-urban migration or non-renewal of land leases.

LOCALITIES	POPULATION		
	1986	1996	2007
BILALEVU SETTLEMENT	490	505	255
DREKE VILLAGE	104	124	159
KORONISAGANA VILLAGE	194	225	250
MAVUA VILLAGE	101	114	181
NABITU SETTLEMENT	388	427	380
NARATA VILLAGE	No data	129	156
NAREWA VILLAGE	205	205	237
RARARUA VILLAGE	142	200	170
TOGA VILLAGE	242	169	205
VUNAREWA VILLAGE	No data	123	143
TUBAIRATA VILLAGE	No data	65	144
DUBALEVU SETTLEMENT	No data	No data	31
SIMILAYA SETT	183	138	80
NABAKA SETT	417	267	157
Total	2466	2691	2548

Table 1.2 Population of villages and farming settlements within the study area (Source: Fiji Island Bureau of Statistics).

In response to such intensive landuse pattern and fluctuating population (Table 1.2), demand for water resources use is relatively high. A significant amount of surface and groundwater is utilized drinking and irrigation uses for human security and to ensure adequate water availability for optimum plant growth during the dry period. In Bilalevu, due to its close proximity to the SR, many farmers, through the assistance of the Ministry of Primary Industry's Agriculture Department, use low-lift engine-driven pumps for sprinkler irrigation scheme. Groundwater resources had been utilized for drinking purpose and marked by a growing number of 4" diameter privately drilled wells (PDW) around the study area in the last decade. The drilling of these wells were conducted by private drilling companies (PDC) and largely unknown to the MRD until the inception of this project. PDW are pumped at an average rate of 1 L/s for 4-8 hours daily: the details of these wells will be discussed in the next chapter. Dubalevu, having located relatively far from the Sigatoka River, utilizes groundwater for irrigation purpose with a few farmers opting to use these sources for

domestic use during severe dry periods. The SVRDP wells in Dubalevu have the maximum capacity of around 10-20 L/s (Gale & Booth, 1993) but are pumped at an average abstraction rate of 3 L/s. Settlements and villages located within and adjacent to the Dubalevu-Bilalevu corridor, namely Nabitu, Jubairata, Rararua and Laqere, also use groundwater for drinking and sanitation purpose whilst Mavua, Nasovatava, Vunarewa, Narewa and Toga are sustained by perennial streams catchments and spring sources (details of groundwater use in the study area will be discussed in later chapters relevant to the sustainable management of groundwater resources).

1.4 Outline of field investigation and methods

The investigation and characterization of the hydrogeological system around the MSV was conducted through the following methods:

(1) satellite imagery and aerial photos (Appendix B shows a list if aerial photos used) were used during the reconnaissance stage to identify geomorphic, geological and structural features pertinent to the overall geological/tectonic setting, as well as the identification of subjective areas for geophysical surveys.

(2) Global positioning system (GPS) surveys were used, through the use of Garmin76 device to capture location data of rock outcrops, geophysical survey lines, existing and newly installed boreholes, and chemistry and isotope sampling sites. These data were downloaded into MapSource software, and subsequently corrected and converted in formats compatible for GIS platforms, such as MapInfo 10.0.

(3) Literature review was conducted on all existing and relevant geological, hydrogeological, landuse, climatic and isotope datasets available for the Fiji group, particularly the Sigatoka valley.

(4) Engineering geological and geomorphic mapping and classification of surface outcrops, conducted by both vehicle and foot traverses, is conducted to establish of overall geological framework upon which groundwater exploration is guided.

(5) Geophysical survey, using electrical resistivity and electromagnetic methods, is conducted on several sites to produce high resolution subsurface profiles showing variable geophysical properties upon which the selection of potential drill sites and determination of target depths are guided.

(6) Soil permeability tests, through the "falling head method" and using the WF26010permeameter cell, is conducted to determine the permeability of overlying fine material, namely silty loam, in relation to infiltrating meteoric and irrigation was into the groundwater systems;

(7) Water resources inventory was designed, through interviewing owners and attendants of most privately drilled wells to determine the well depth, abstraction rate and duration of use on daily basis and number of families sustained by each of the groundwater sources, to establish the current status of groundwater use and to use as a tool for projecting groundwater or water resources sustainability in the long-term.

(8) Groundwater drilling using mud-rotary method was conducted on 9 sites to permit the collection and assessment of drilled cuttings for lithological logs and proper construction materials were used to ensure strength and stability of groundwater wells and allow optimum water flow to be assessed for aquifer parameters calculations through pumping and recovery tests, respectively.

(9) Pumping and recovery tests were conducted on several wells to permit the analysis and assessment of aquifer properties, namely tranmissivity, storativity and hydraulic conductivity, as well as to allow the collection of groundwater samples for chemical and isotope analysis.

(10) Groundwater levels of existing wells were also measured using a SOLINIST dipper on two occasions to determine the direction of groundwater flow around the Dubalevu and Bilalevu area

(11) Groundwater chemical sampling on existing groundwater wells and on surface water sources, namely creeks, river and springs, in Dubalevu, Nabitu, Nabaka, Similaya and Bilalevu and the analysis of major ionic compositions, total dissolve solutes (TDS) to determine the dominant hydro-chemical facies and any spatial variability.

(12) Isotope sampling and analysis on numerous water sources, namely groundwater wells, creeks, and rivers, was conducted through the mass fractionation of H^1/O^{16} and H^2/O^{18} to establish the abundant isotopic composition and determine if groundwater is derived from either rapidly through flowing rain-derived recharge or dispersed slowly through fractured bedrock areal sources.

(13) Chloride concentration test was also conducted on the isotope samples using the Orbecco-Hellige 975 analyst.

The selection of above methods was primarily controlled by:

- funding availability from government for logistical support, preliminary groundwater chemical analysis, groundwater investigation, groundwater drilling and development, procurement of borehole construction materials and arrangement for suitable pump sizes. Please note that several other pre-planned investigation methods, such as river gauging, pesticide residues analysis in groundwater, and groundwater dating, were not conducted due to financial constraint;
- availability of suitable equipment such as geophysical instrument, permeater, drilling rig, drilling mud and groundwater pumps;
- availability of facilities for chemical analyses at MRD's Geo-chemical Laboratory and isotope analysis at the University of Canterbury; and
- time constraint – A period of 16 months was initially allocated for the completion of this research project and during which all data acquisition through the above-mentioned methods, interpretation and documentation were to be completed. Extensions were granted by the College of Science due to exceptional circumstances, such as several tropical cyclones in Fiji between November, 2009-January, 2010, project breakdowns, funding disbursement delays, delayed student visa renewal procedures in Fiji and, finally, the devastating February 22nd Christchurch earthquake.

1.5 Thesis Organization

The thesis is organized such that:

- chapter 1 provides the project background and primary objectives of this thesis before describing the study area in terms of location, geology, physiography, climate, vegetation and landuse with an introduction to the investigation methods employed for this hydrogeological study,
- chapter 2 presents the literature review of geological and tectonic setting of Fiji with their relevance to the hydrogeological and geomorphic systems in the study area before providing an overview of the hydrogeological system based on the SVRDP.

This reviews the groundwater utilization in Fiji, the status of groundwater policies and legislations before isotope hydrology will be reviewed including previous isotopic survey conducted in Fiji,

- chapter 3 provides field investigation methods and results of geophysical surveys, geological and engineering geological mapping, pumping tests and, groundwater exploration drilling, chemistry and isotope sampling, chloride concentration tests and groundwater recharge calculations,
- chapter 4 provides discussions for geophysics, physical hydrogeology, hydrochemistry and groundwater recharge,
- chapter 5 examines issues and challenges encountered during this research before providing a series of recommendations for groundwater sustainable management, and
- chapter 6 provides the major conclusions of this thesis and outlines areas of further study.

Chapter 2: Literature Review

2.0` Introduction

This chapter presents existing geological, hydrogeological surveys around the SW Viti Levu, as well as relevant water resources studies around Fiji to aid the characterization of the hydrogeological system in question. The chapter is organized to first cover both regional geological and tectonic evolution of southwest Viti Levu, Fiji. This is followed by a review of eustatic/sea level fluctuation records in the Pacific and in Fiji in relation to the deposition of Quarternary and Recent Alluvium before an overview of geological setting of the study area is provided. These are followed by the snapshot of groundwater utilization around Fiji, including progresses and history of groundwater development in Fiji, the hydrogeological setting of the study area as per the Sigatoka Valley Rural Development Project (SVRDP), as well as an overview of the current groundwater utilization in the study are. These are followed by an overview of groundwater policies and legislation before concluding with an introduction to isotope hydrology and results from previous isotopic studies in Fiji.

2.1 Regional geology and tectonic evolution

The Fiji Islands, in the southwest Pacific region, are located between the Pacific and Indo-Australian tectonic plates boundary and sits on a broad, shallow submarine platform close to the ocean deeps delineating the western edge of the Pacific Plates (Hamburger, 1986) (Fig. 2.1.1). Hence, the geological framework, documented in Hamburger (1986), Rodda (1994) and Hathway & Colley (1994), Webb (1999), Rahiman (2006), is dominated by remnants of arc-related volcanic, plutonic rocks with repeated sequences of volcaniclastics sediments as attributed various stages of island arc development. Further, recent phases of magmatism are related to arc fragmentation and rifting in neighboring back-arc basins whilst periods of tectonic quiescence and instances of sea-level fluctuation, are recorded in development of numerous sedimentary basins and deposition of fluvial materials, respectively.

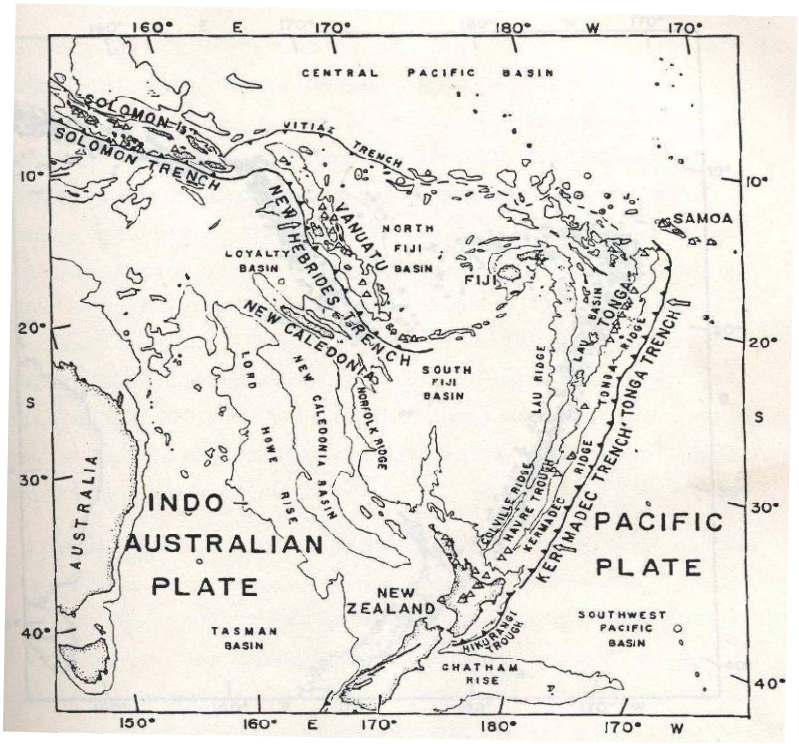

Figure 2.1: regional tectonic setting (Hamburger, 1986).

2.2 Geological and tectonic setting – Fiji

The islands of Fiji comprise of Late Eocene to Recent predominantly plutonic, volcanic, volcaniclastic facies, with sedimentary rocks forming in numerous depositional basin (including a few raised Holocene Limestone islands), together with recent alluvial materials (Gale & Booth, 1993). The oldest dated rock being the Yavuna stock is dated around 40-36 Ma, is found to be outcropping SE of Nadi in Viti Levu, whilst the most recent volcanic eruption occurred approximately 2000 years BP on Taveuni. This timescale included numerous proto-volcanism and sedimentation events, synchronous deformation episodes and neo-volcanism. This next sections will focus on Late Eocene to Late Miocene tectonics event and geological groups concentrated on SW Viti Levu, namely the Yavuna Group, Wainimala Group, Colo Plutonic Group, and Tuva Sedimentary Group: details of Fiji's geology are provided in Rodda (1994), Rahiman (2006) and Hathway and Colley (1994).

2.2.1 Yavuna Group (YG)

The YG is viewed as a proto-volcanic-arc formed following the inception of convergence between the Pacific and Indo-Australian plates in the Eocene (Hathway & Colley, 1994) and

was spanning between Late Eocene and Oligocene (Figure 2.1.2). The group, Fiji's oldest rocks and among the oldest observed in the Southwest Pacific Islands (Hamburger, 1986), has major occurrence outcrop southwest Viti Levu (Figures. 2.2 & 2.3) and is composed of primitive and dominant arc-like dacitic rocks, shallow-water limestone, a tonalite/trondhjemite stock with basaltic pillow lavas (Rodda, 1994). The Yavuna Stock, accepted to be located in the West of the convergence regime, marked last magmatic orogeny in the remnant-arc before the opening of the South Fiji Basin in the Late Oligocene (Figure. 2.5) and prior to its northeastward rift and migration (i.e. 36-25 Ma (Rodda, 1994)).

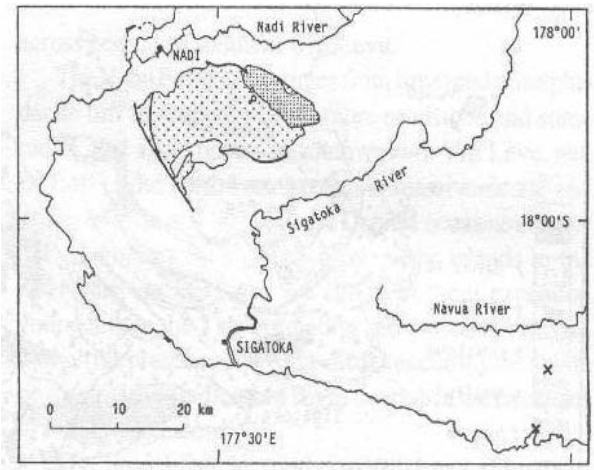

Figure 2.2: southwestern Viti Levu location and distribution of the Yavuna Group ((Rodda, 1994).

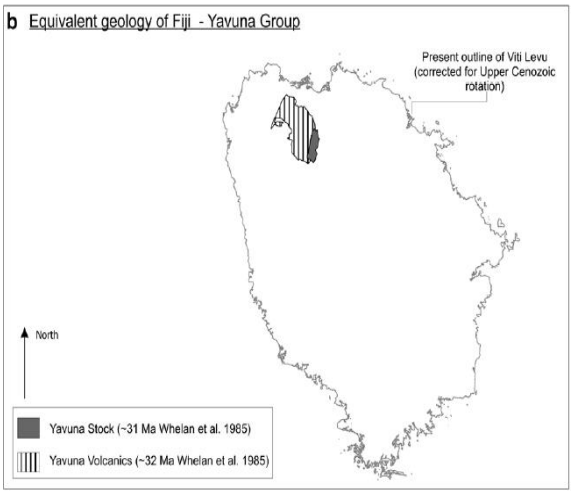

Figure 2.3: possible location and orientation of the Yavuna Group and Viti Levu on the proto-arc (Rahiman,2006).

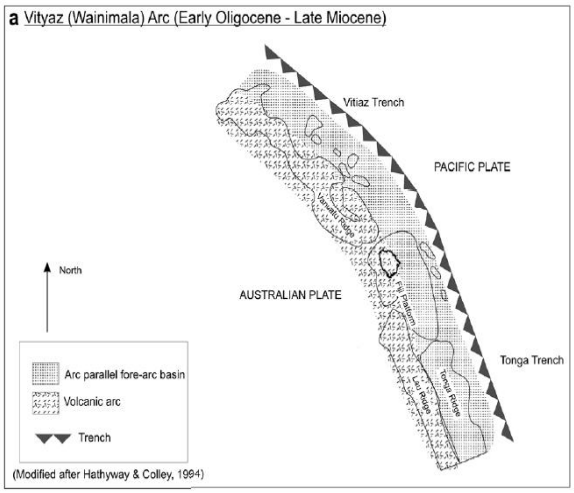

Figure 2.4: Proto-arc and the continuous Vitiyas arc, the Melanesian arc (Rahiman, 2006).

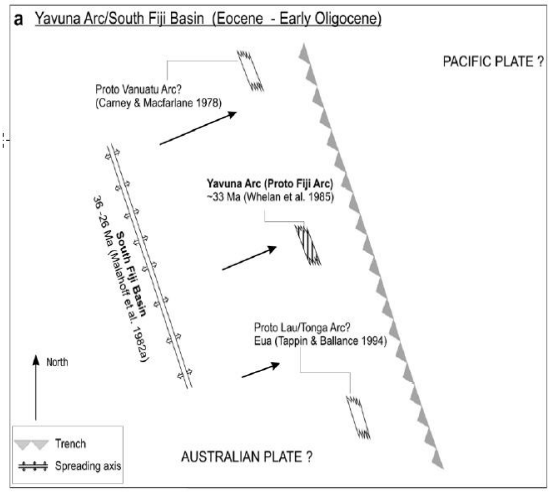

Figure 2.5: Opening of the South Fiji Basin marking the onset of Wainimala arc (Rahiman, 2006).

This opening of the South Fiji Basin (Figure 2.5) was accompanied by swarming of dolerite dyke intrusion with periods of uplift and normal faulting. Following these, southwest and westward directed subduction of the Pacific plate under the Australian plate instigated a

period of volcanic activity along the rifted southwestward margin of the Yavuna Block and resulting in the development a new volcanic arc comprising the Waimala Group (Figure 2.4). During this period, the proto-arc (also known as Melanesian arc) was composed of the ancestral Solomon, Vanuatu, Fiji Platform (FP)/Lau, Tonga and Kermadec-Colville arc segments along the Tonga-Kermadec Trench and the now relict Vityas Trench: this marks sites of former subduction zone (Hamburger, 1986) and lying north of Fiji's present position (Rahiman, 2006) (Figure 2.3).

2.2.2 Wainimala Group (WG)

The WG, constituting a fore-arc basinal and arc assemblage (Rodda, 1994), was unconformably formed on the proto-arc basement (i.e. angular unconformity) with the youngest magmatic rock range from 10 to 14 Ma (Rahiman, 2006). During this period (Up until the middle-Late Miocene), the Melanesian arc prevailed (Hamburger, 1986) with the Pacific Plated being subducted from the east along the Tonga-Vitiaz trench (Webb, 1999). The submarine rocks of the group (predominantly found in the western and eastern part of Fiji), consist of intrusive and extrusive basic to acidic lava flows (dacite, basalt and andesite) some of which were later deformed by greenshicst facies regional metamorphism (Rodda, 1994), fragmental rocks (volcanic breccia and conglomerate), argillites and pelagic limestone.

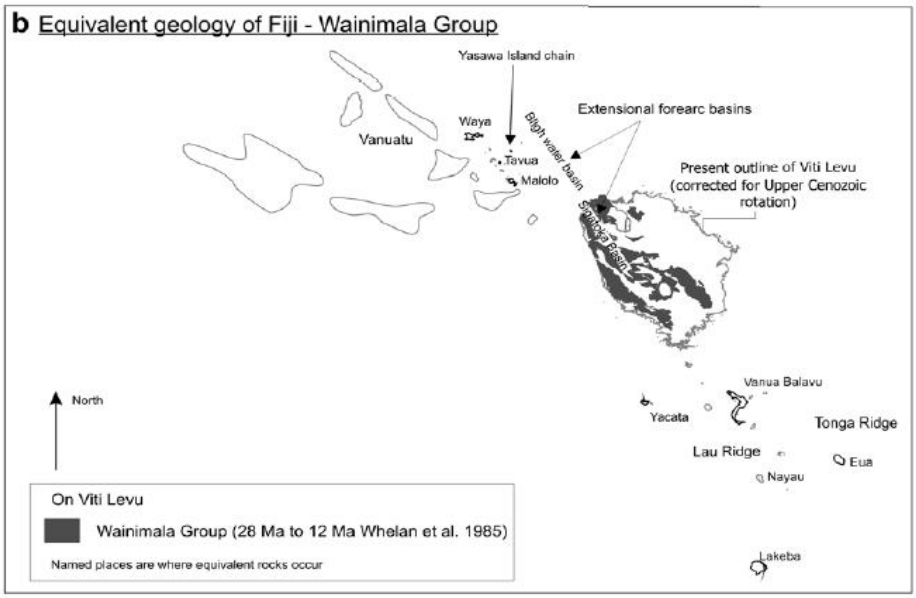

Figure 2.6: position of ancestral forearc-intraarc Sigatoka Basin and the Bligh Water Basin during the formation of the Wainimala Arc.

The basinal assemblage in this Wainimala arc was interpreted to be deposited in a fault-controlled (half-graben) fore-arc and intra-arc Sigatoka basin, composed of an uplifted Wainimala arc block from a downthrown (hanging wall) Yavuna block on the north (Hathway & Colley, 1994): these were related to the crustal thinning and extension related to the opening of the South Fiji Basin. Webb (1999) documented that the southern (arcward) migration of the former depositional environment and the formation of Early Miocene to Middle Miocene Limestone can be attributed to emergence as a result of isostatic uplift due to crustal thickening in the accretionary wedge and under-plating, which could have resulted in the erosion of Wainimala arc and associated reef/platforms. Further, the deposition of carbonate coincided with an increase in epiclastic sediment yield to the forearc, indicating increased emergence, which brought larger submerged areas into the photic zone, and erosion of the arc (Hathway, 1995). Of the numerous Wainimala Group members, the Tari Formation and Qalimare Limestone are of special interest due to their existence in the study areas.

2.2.3 Colo Plutonic Group (CPG)

This plutonic group or suite occur in an elongate belt from southwest Viti Levu with compositions ranging from olivine-augite gabbro through quartz gabbro to tonatile (Rodda, 1994) and Rahiman (2006) summarized several events during this period including:

- widespread plutonism occurring in an elongated E-W belt southern Viti Levu from 12-7 Ma, referred to as the Colo Plutonic Suite – the Colo Orogeny, and
- brittle and ductile deformation, with the formation of anticlinorium encapsulating the plutonic belt (Figures 2.7 & 2.8) and deformation in rocks post dating the Colo Orogeny, notably those on the Tuva Group in southwest Viti Levu.

These plutonic intrusions and associated deformations and volcanic eruption episodes marked the break-up and/or fragmentation of the ancient Melanesian arc into series of ridge and arc systems during the Middle to Late Miocene. Having concentrated around the SW Viti Levu, this orogeny is responsible to widespread contact metamorphism around the area, particularly the WG.

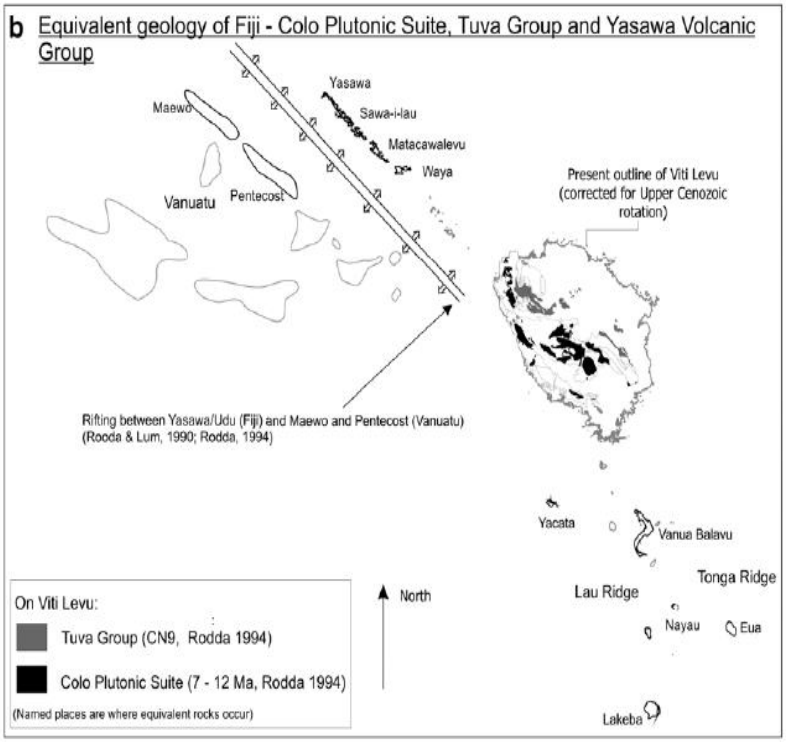

Figure 2.7: location of Colo Plutonic suite and younger units prior to rotation (Rahiman, 2006).

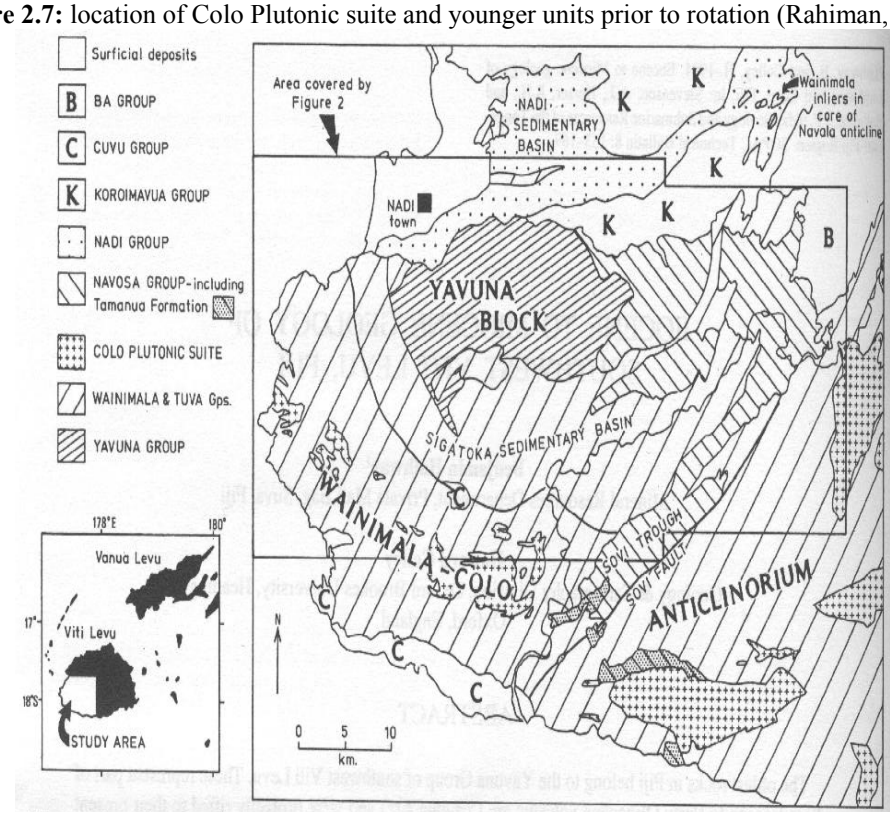

Figure 2.8: distribution of Wainimala Group, orientation of anticlinorium on Southwest Viti Levu (Hathway & Colley, 1994).

2.2.4 Tuva Sedimentary Group (TSG)

This middle to late Miocene and post-Colo Plutonic sedimentary group is composed of as breccias, conglomerate and sandstone with minor mudstone, strongly deformed in places and comprising the Cici Sandstone and the Takaro Conglomerate (Rodda, 1994). Hathway (1989) defined the latter as a poorly sorted weathered-unweathered matrix-supported rudite in which well-rounded to angular clasts of andesite, dacite and limestone are locked, whereas the former was defined a feldspathic lithiarinites with a conservative thickness estimate of 600m. The Tuva Group have been construed as a turbidite system in the fault-controlled the Wainimala arc. The arc's adjoining basin, the Sigatoka Basin, with its half-graben correlatives in the Tonga platform (Oligocene-Miocene in age), have been subject to several phases of normal faulting, which creating sufficient space to accommodate the deposition of minor volcaniclastic rudites, sandstone, and siltstone and hence, prevented the formation hemipelagic carbonates (Webb, 1999). The sedimentary group, having an extensive coverage on the study area, will be described further in later chapters.

2.2.5 Disruption or fragmentation of Melanesia Arc

Subduction along the Vityas arc ended as a result of collisions with Pacific plate oceanic plateau whilst the Melanesian Border Plateau collided north of Fiji with the Ontong-Java Plateau, further north near the Solomon Islands (Rahiman, 2006) and hence, the commencement of the fragmentation of Melanesian arc around the Middle-Late Miocene (Figure 2.9). This resulted to the fragmented configuration seen today, which requires separation of Vanuatu and Fiji in the western sector and polarity reversal, as well as drifting away of the Vanuatu arc segment from Fiji. Subduction polarity reversal on the Vanuatu arc resulted from continued subduction between Australian plate and Pacific Plate, whilst breakup of Melanesian arc and rifting led to opening of the North Fiji Basin (NFB).

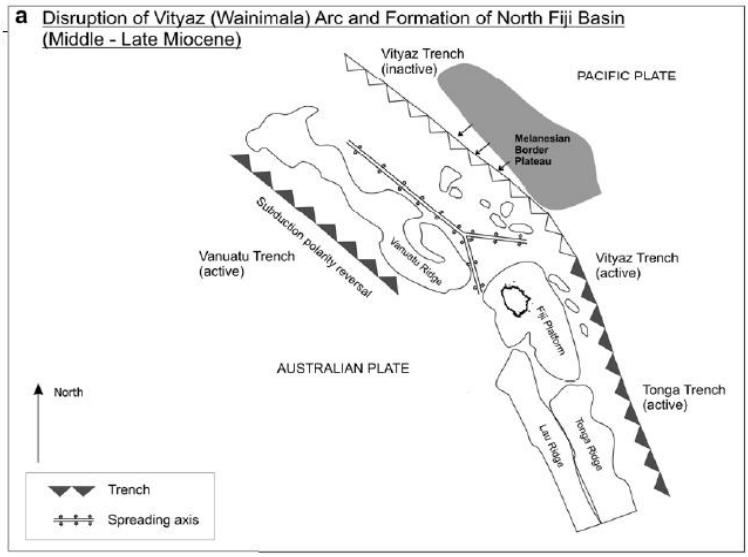

Figure 2.9: initial breakup of Melanesian arc (Rahiman, 2006).

During the fragmentation, the FP may have gone through a 30-40° anticlockwise rotation between 5.5-2.5 Ma (Webb, 1999) and during which crustal compression and shortening occurred with the emergence of the Yasawa Island group: this is clearly observed by the deformed Wainimala and Tuva Group group in SW Viti Levu. Malahoff (et.al, 1981) added that paleomagnetic analysis conducted on fifteen oriented rock samples from the Ba Volcanic Group showed an age of 2.9-7 Ma as evidences of post-Miocene rotation of the island of Viti Levu**.**

2.3 Records of climate change and eustatic fluctuation

2.3.1 Introduction

Relative sea level (RSL) are a product of changes in oceanic and crustal variables, which depend on sea surface level changes, any isostatic, glacial and tectonic changes and local coastal processes (Woodroffe & Horton (2004)). The Pacific islands have been subject to these events overtime where RSL fluctuated to which hydro-isostacy, localized and regional tectonism (i.e. forearc and backarc processes), and universal glacio-eaustatic fluctuations have been attributed (Dickinson, 2001).

2.3.2 Global and regional events

The last oscillation between glacial and interglacial conditions during the Quaternary, the Last Glacial Maximum (LGM) (between 30000 and 19000 years ago) transferred millions tones of ice in the ocean and hence, global sea level in regions, particularly in far-field locations, rose by about 130 m (Woodroffe & Horton, 2004). Thus, the return of ocean waters to the glaciations centres during the interglaciation period led to the drastic sea level drawdown. These events were also imprinted in the relatively young Pacific where terraces in the islands of Tongatapu and Eua in Tonga, which are dated back to this inter-glacial event (Dickinson, 2001). However, a substantial portion of Pacific region was still undergoing tectonic moments over Holocene, and even longer timescale, and RSL fluctuation was attributed to geoid migration (Woodroffe & Horton, 2004). During the mid-Holocene, sea level may have risen 2.1m above present 4200 cal yr BP before gradually falling to present level (Kumar, 2006). Evidences of this Holocene high sea-level stand in Vanua Levu, including the presence of higher paleonotch observed around the southeastern coast were 2.2-3.3 m above low-tide level and lower paleonotch 1.5-1.6 m above low-tide level which with encrusting corals were dated to be 6000-3400 yr before present, confirmed sea level was higher than at present (Miyata et.al., 1990). Dickinson (2001) added that paleo-shorelines in coastal ares of Viti Levu was characterized by rising paleo-beach rock (mid-Holocene age of 4000 yr BP) rising to an elevation 1.4 m above modern and with coastal beaches cut into uplifted Quartenary reef flat limestone at elevation of 1.8-2.2 m above modern shoreline notches. These fluctuations in paleoshoreline would have significant impacts in paleo-fluvial processes via the advancement and recession of base level, which in turn dictate their tendency to either degrade or aggrade the river beds.

2.3.3 Relevance to the study area

Seismic reflection survey conducted around the Sigatoka River and Navua River produced profiles construed as alluvium materials infilling deeply steeply incised country rock or bedrock and signifying low sea level between 100 to 130 m below present day sea level (Figure 2.10) (Smith, 1989).

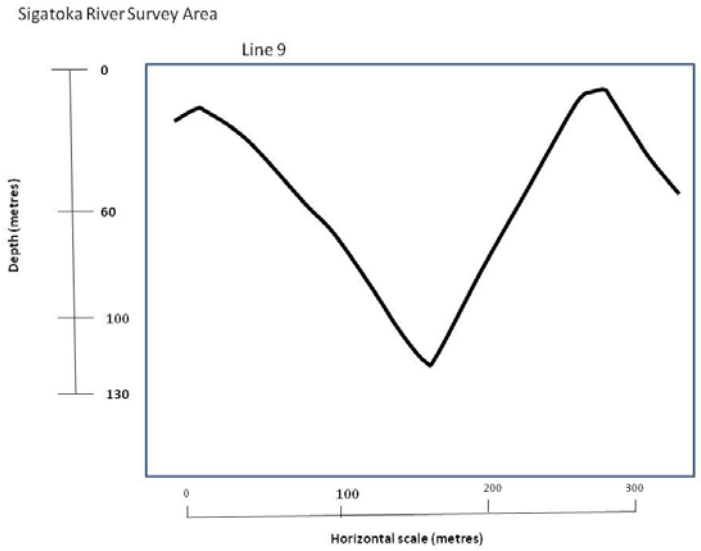

Figure 2.10: deeply incised country rock (Tari Formation) in response to interglaciation after the LGM (Smith, 1989).

Davies (1992), based on geophysical surveys and lithological samples of groundwater exploration drilling around the Sigatoka valley, commented that the alluvium deposits around the valley were episodically built above bedrock post-LGM, which was deeply incised by Sigatoka River bedrock 18 000 yr BP and during which much of the ocean was returned to the glaciations centres after LGM resulting in a massive sea level drawdown (Figure 2.11).

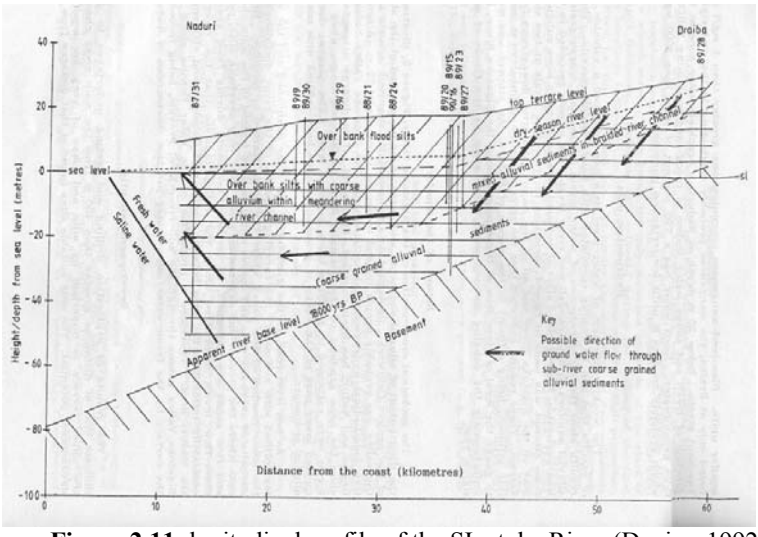

Figure 2.11: logitudinal profile of the SIgatoka River (Davies, 1992).

Again, the inception of RSL transgression post-LGM, as mentioned earlier, coupled with numerous localized paleoshoreline fluctuations from Quaternary to Recent, control the deposition and aggradation of fluvial materials along the Sigatoka River.

2.4 Geological setting of the study area

The study area is underlain by the steeply inclined and deformed Wainimala arc basinal/sedimentary group and the juxtaposed Tuva sedimentary group, with the incised valleys filled with Quaternary to Recent Alluvium deposits. Clearly, the evolution of tectonic systems controlling arc volacanism and basinal environment with episodic sedimentation and carbonate deposition together with Holocene eustatic fluctuation has dictated the deposition and formation of such a geological framework. Further, the compression and deformation instigated by the fragmentation of proto-Melanesia arc and the ensuing anti-clockwise rotation of the FP is evident in the ENE-WSW sinistral Nasovatava Fault (NF). These will be covered in detail in the next chapter.

2.5 Groundwater development & utilisation in Fiji

The following sections present the status of groundwater use and development in Fiji. This includes a history of groundwater development in Fiji and an overview of groundwater use in Fiji. These are followed by a view of the hydrogeological setting of the SV area as per the Sigatoka Valley Rural Development Project (SVRDP) results before groundwater utilization in the study area is discussed.

2.5.1 History of groundwater development, use and monitoring in Fiji

The Mineral Resources Department (MRD) and its predecessor, the Geological Survey Department (GSD), committed to a program of groundwater exploration, assessment and development since 1967 (Peach, 1988). Despite the lack of professional staffs and appropriate technology, MRD maintained its interest in groundwater development and, has since, conducted groundwater assessment and development with its own funds, together with PWD funds and

foreign aids. In 1985, the groundwater resources assessment and development unit (GRADU) was formed and operated to systematically assessing and developing groundwater resources to allow the continued development of the people of Fiji (Peach, 1988). Further, groundwater monitoring network was established by the GRADU as funded by the British Governement (1985-1990), SVRDP (1988-1991) and the Japanese Government funded North Viti Levu groundwater development project (1993-1995), where places like Yaqara, in Tavua, Vatiyaka in Ba were investigated. The Hydrology section of the Public Works Department provided funds for the installation of groundwater wells in northern and western Viti Levu whilst French Government aid project permitted the installation of numerous well in Seaqaqa, Bua and Labasa in Vanua Levu (Kumar, 1997). These resulted in the compilation of 1:250 000 Hydrogeological maps of Viti Levu and Vanua Levu and Taveuni and are described in Gale and Booth (1993). At present, despite financial challenges, groundwater monitoring is still conducted, on monthly and quarterly basis, in several wells in Dubalevu, Korotogo, Namaka, Tavarau, Yaqara, Rabulu Viti Levu and Vanua Levu (Figure 2.12).

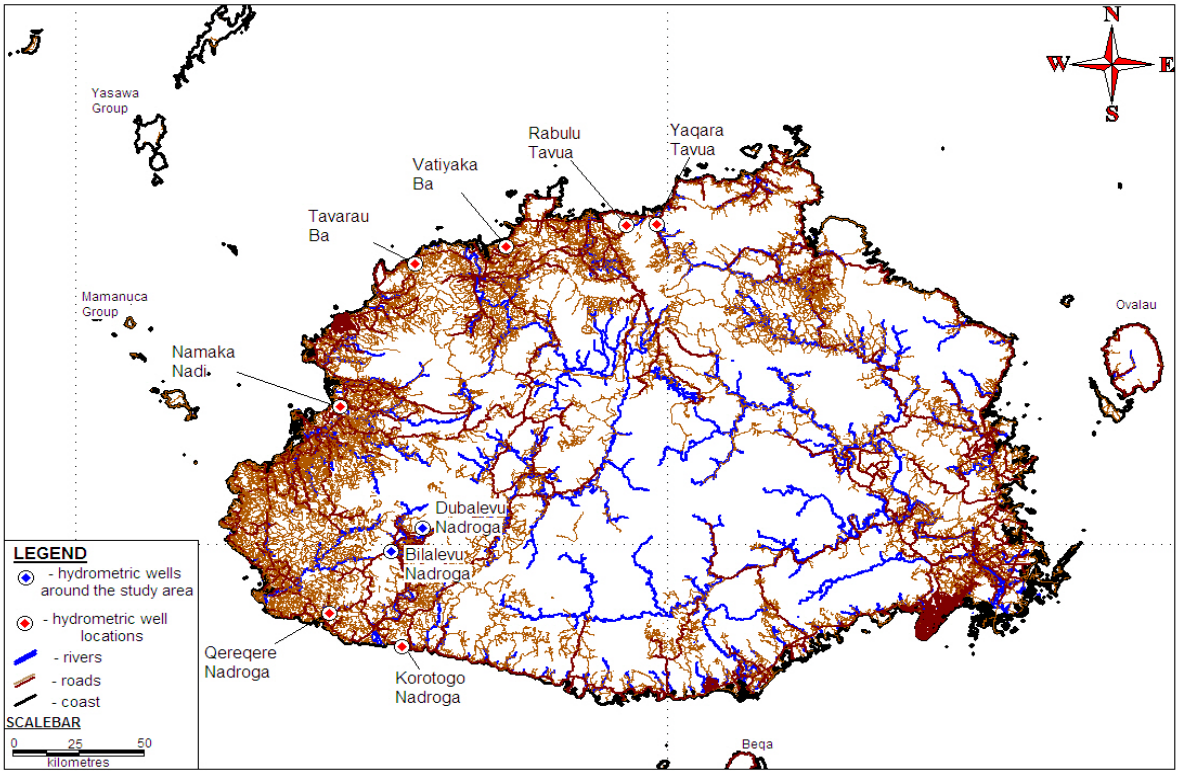

Figure 2.12: boreholes around SW and NE Viti Levu that are monitored on monthly and quarterly basis.

2.5.2 Overview of groundwater demand and use

In response to the rapid population growth and frequent extreme climatic events, particularly droughts, groundwater development projects for public water supply in Fiji had grown recently. , Government funded groundwater exploration and development, through the GRADU's annual budget allocation, has extended to villages, communities and schools on the two main islands in Fiji, as well as small islands, mainly for drinking purposes. This trend is likely to escalate in the long-term due to the frequent water-shortages and possible contamination of existing surface sources from improper landuse practices. Further, several groundwater private drilling companies (PDC) are in operation in Fiji and are responsible for the provision of groundwater sources for small community and individual-household water projects, most of which are unknown to MRD. Simultaneously, the success of "Fiji Water Brand" in the commercial bottling arena has attracted potential foreign investor to establish commercial bottling ventures and at present 4 bottling companies in operation in Viti Levu. However, MRD, being custodian of all minerals in Fiji, as stipulated in the Mining Act, have assumed control over the exploration and development of groundwater resources and have been given the mandate to provide relevant policies.

2.5.4 Hydrogeological setting of the study area

As mentioned earlier (section 1.1), the rural development project in the Sigatoka valley (SVRDP) was intended to upgrade the agricultural sector through the provision of reliable of irrigation sources, particularly during the dry season. Low-lift pump method, initially proposed to abstract water from the SR at an average rate of 9 L/s (Mr Govin Raju, Senior Agricultural Officer, Nacocolevu Agriculture Office, Sigatoka, pers.comm, April, 2010), was favoured due to its mobility. Such a distribution system will be a success to areas located within 400 m of river-bank abstraction point but a substantial portion of the targeted farmland were located beyond this distance (Figure 2.13). Hence, alluvial groundwater sources were proposed and to which a special requirement was made to permit wells having yields above 8 L/s to be constructed for irrigation purpose.

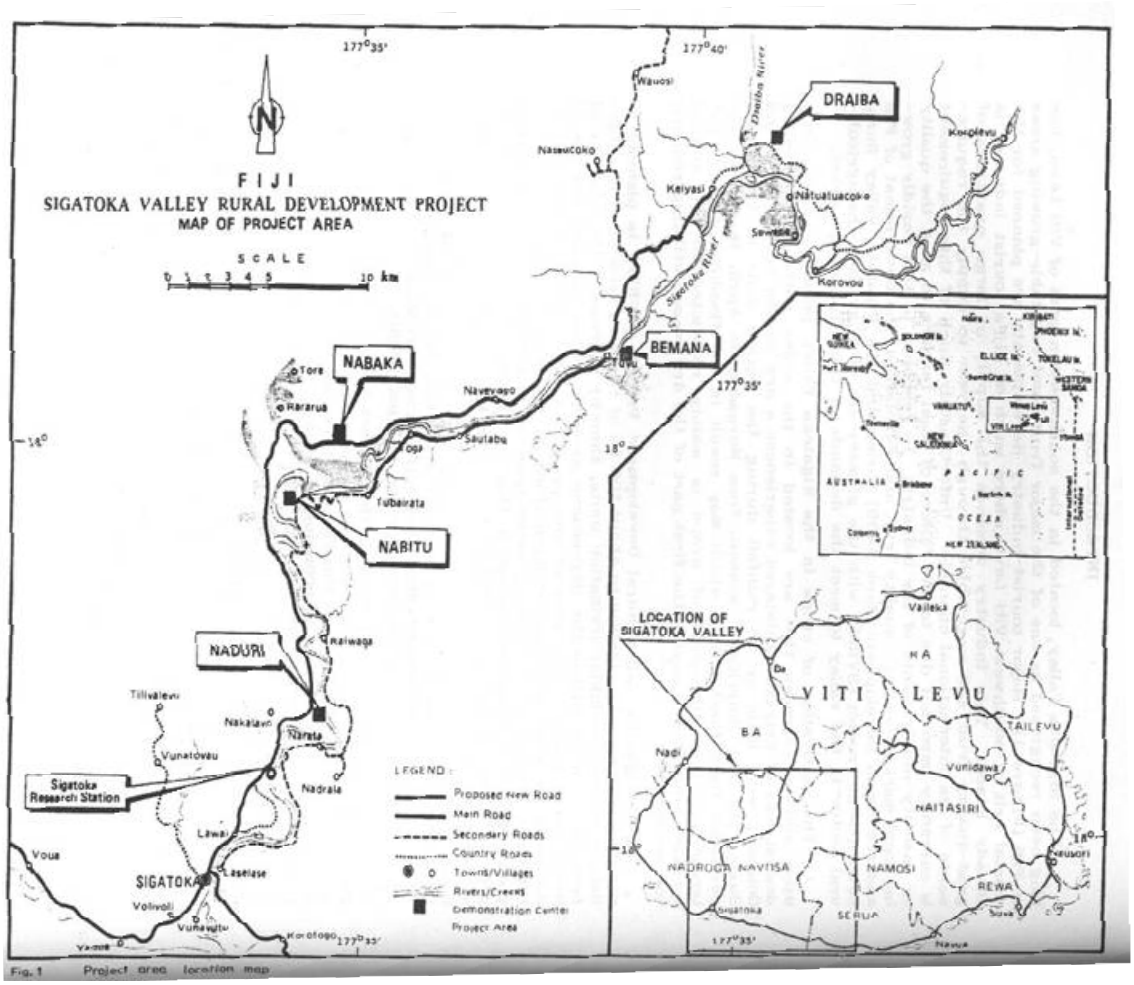

Figure 2.13: Farming areas identified as ideal for groundwater exploration (Davies, 1992).

Groundwater investigation, conducted by MRD, entailing geological, geomorphological and geophysical surveys on six identified areas, namely Draiba, Dubalevu, Nabaka, Nabitu, Bilalevu and Naduri (Figures 2.13 and 2.14), to assess the nature and groundwater potential of the alluvium deposits in the valley for irrigation purpose. Summaries and locations of the drilled wells are provided below:

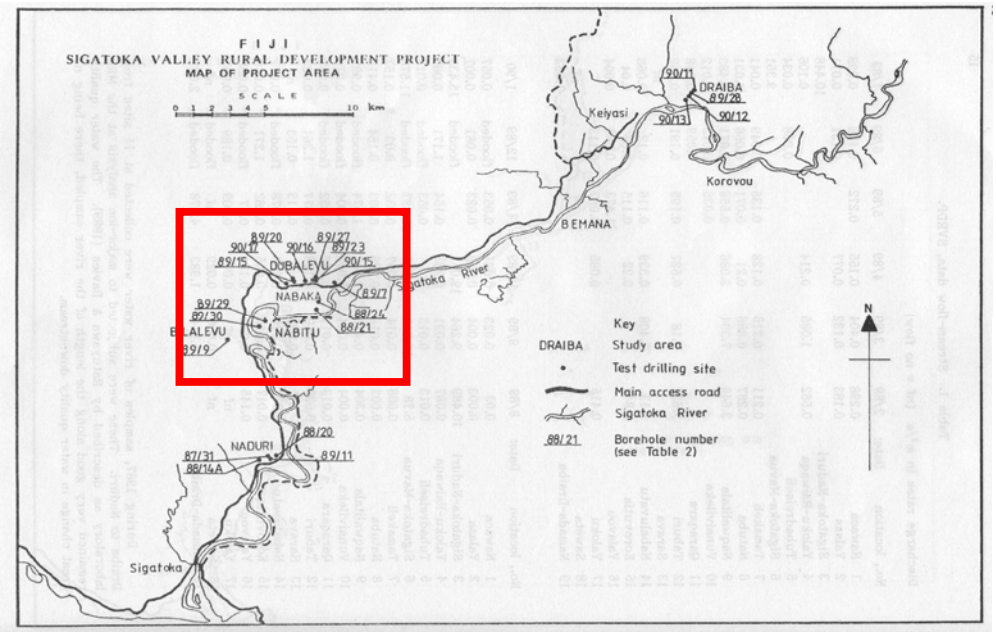

Figure 2.14: location map of wells drilled during the SVRDP project (study area denoted by the red square) (Davies, 1992).

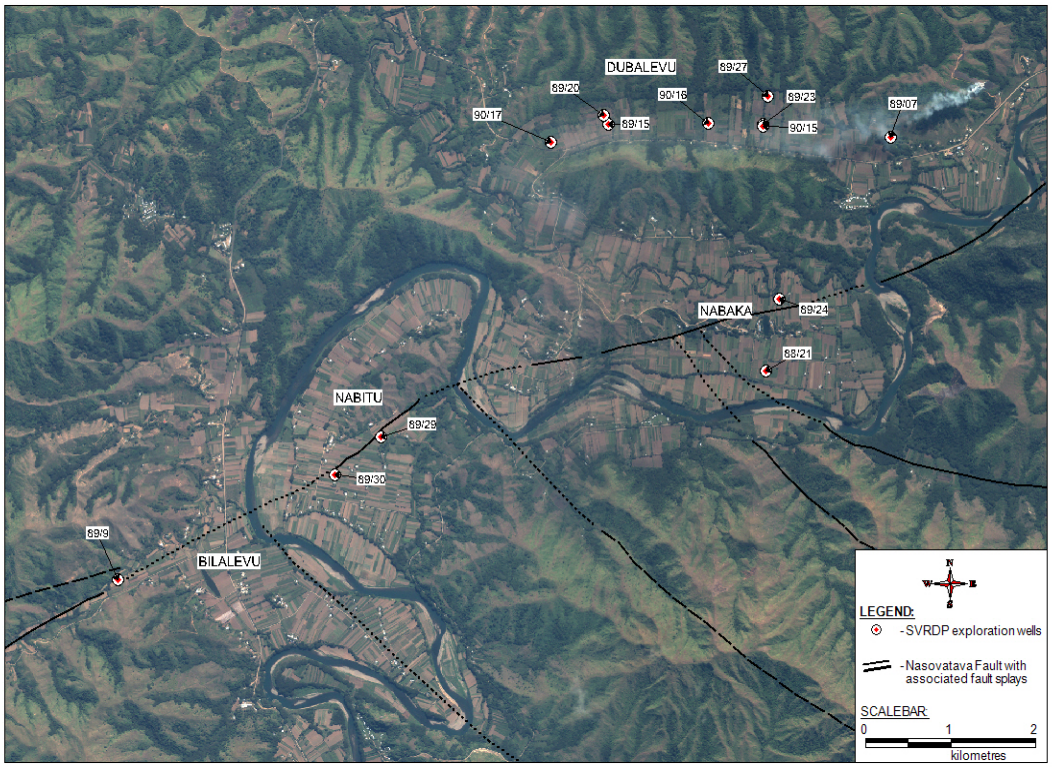

Figure 2.15: location of SVRDP exploration wells around the study area.

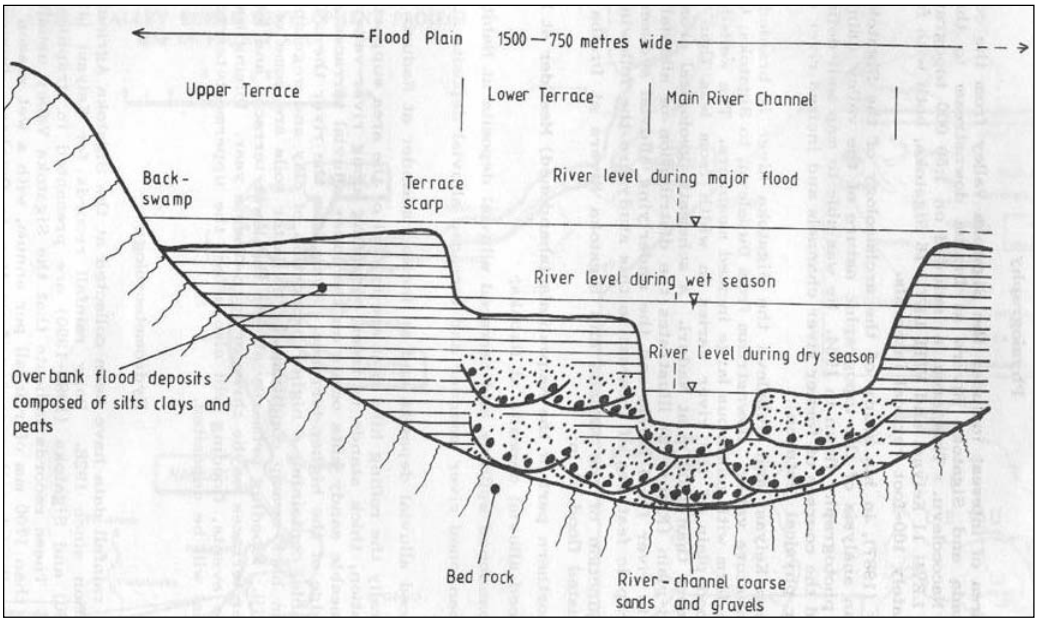

Figure 2.16: tentative model of sediment deposition following bedrock incision in response to eustatic fluctuation and as consequent, the SR may have shifted on numerous occasions, hence, deposition and distribution of unconsolidated gravels will vary over space (Davies, 1992).

The project was concluded with the drilling and evaluation of 21 exploration groundwater wells and 7 of which (Dubalevu (4), Naduri (1), Draiba (2)) meeting irrigation scheme requirement (Table 2.1). As per project intention, the hydrogeological classification of the valley was dominated by QRA deposits, comprising unconsolidated coarse gravels and fan outwash gravels, medium to coarse sands with minor silt, which were unevenly distributed as controlled by episodic migration of the Sigatoka River (Figure 2.16). The underlying Wainimala, Tuva and Navosa Sedimentary Groups were deemed low productivity systems, whilst the WSW-ENE sinistral fault zone investigation at Bilalevu was inconclusive as borehole 89/9 recorded negligible yield (Figure 2.15 and Table 2.1). Further, it was recommended that the QRA aquifer systems show potential for water supply development for domestic needs, to the benefit of all rural communities within the Sigatoka valley (Davies, 1992)

Location	Naduri	Bilalevu	Nabitu	Nabaka	Dubalevu	Draiba
Number of exploration wells drilled	4	1	2	2	8	4
Well Number(s) (depth(m))	87/31 (54) 88/14 (56.5) 88/20 (64) 89/11 (60)	89/9 (60)	89/29 (20) 89/30 (37)	88/21 (36) 88/24 (40)	89/7 (21) 89/15 (42) 89/20 (23) 89/23 (32.5) 89/27 (28) 90/15 (40) 90/16 (45) 90/17 (45)	89/28 (36) 90/11 (20) 90/12 (60) 90/13 (28)
Number production well(s)	1	-	-	-	4	2
Well Number(s)	89/11	-	-	-	89/15 90/15 90/16 90/17	89/28 90/13
Aquifer system(s)	medium-coarse sand (QRA)	(1)QRA systems underlain by (2) weathered Takaro Conglomerate (TSG)	Overbank silt (QRA) underlain by Weathered Dakadaka Basalt (WG)	Overbank silt (QRA) underlain by weathered Takaro Conglomerate (TSG)	Coarse sand and gravels (QRA) underlain by Cici Sandstone (TSG)	Fan outwash gravels (QRA) underlain by Navosa Sedimentary Group (NSG)
Q (L/s) & T (m^2/day)	12 L/s & 650 m^2/day	(1) 2.2 L/s & 23.1 m^2/day (2) 3 L/s & 16 m^2/day	2 L/s & 33 m^2/day		20 L/s & 600 m^2/day	20 L/s & 1400 m^2/day
Hydrochemistry type	$Na(HCO_3)$	$Ca(HCO_3)_2$	$Ca(HCO_3)_2$	$Ca(HCO_3)_2$	$Ca(HCO_3)_2$	$Ca(HCO_3)_2$

Table 2.1: summary of SVRDP exploration wells and hydrogeological characteristics with the main aquifer investigated include Quaternary-Recent Alluvium (QRA), Tuva Sedimentary Group (TSG), Wainimala Group (WG) and Navosa Sedimentary Group (NSG) (Davies, 1992).

2.5.5 Intensification of groundwater use/exploitation - the study area

As mentioned above, several of wells were drilled in the Dubalevu, Nabaka, Nabitu and Bilalevu area (Figure 2.15). Four wells in Dubalevu were deemed favourable for the irrigation scheme and are currently in operation for sprinkler irrigation system, while farmers are forced to also use these wells for domestic use during prolonged dry seasons (the other wells around the Dubalevu area were continuously monitored in the above-mentioned hydrometric scheme (Section 2.5.1)). Wells 88/24 and 89/29 located in Nabaka and Nabitu, respectively, are currently used for domestic water supply by Mr Janmin Jai and Mr Anil Prasad, respectively, whilst the other SVRD wells were abandoned due to either low yield or poor water quality (Figure 2.17). To date, farmers in the Bilalevu, Nabitu and Nabaka are using the mobile low lift-pumps to operate the sprinkler irrigation system, which utilizes the Sigatoka River (Figures 2.18-2.21).

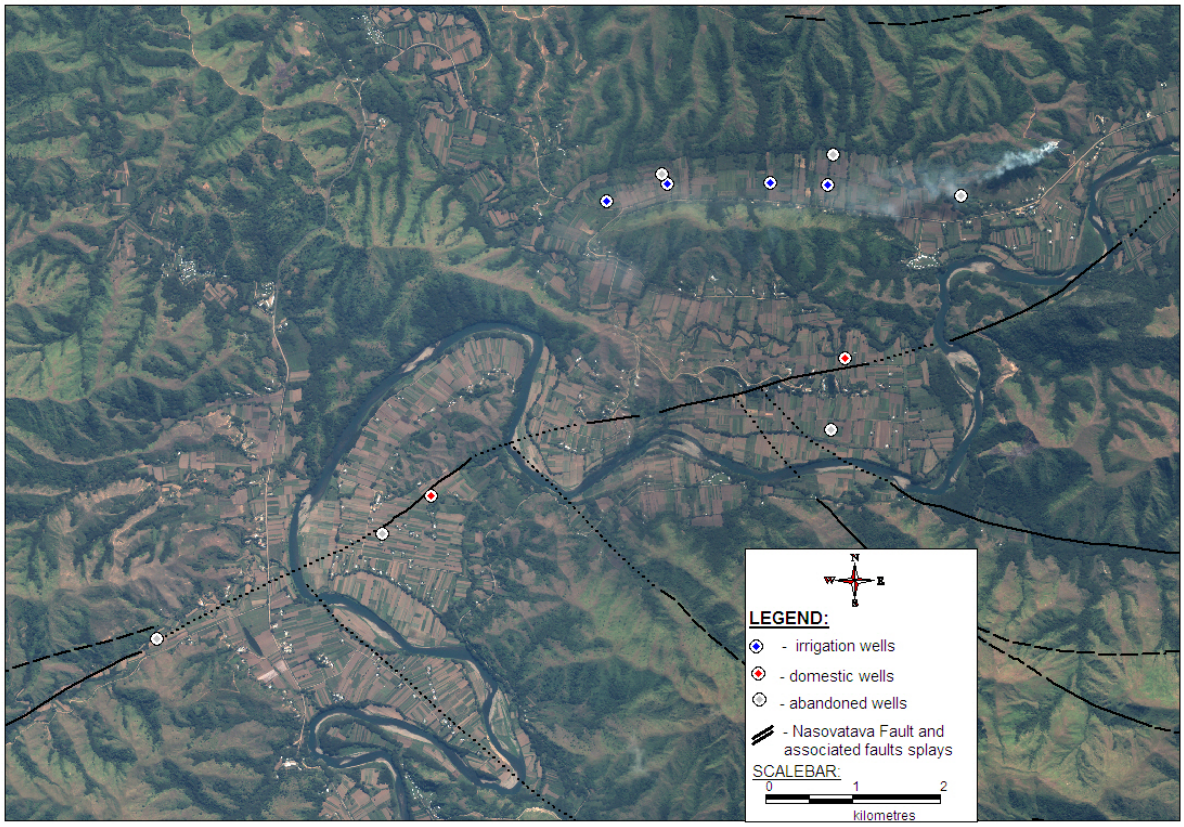

Figure 2.17: location of SVRDP wells within the study areas: irrigation wells, wells now used for domestic water supply and abandoned wells.

Figure 2.18: low-lift pump abstracting water from the Sigatoka River at 9 L/s.

Figure 2.20: irrigation water abstracted from SR and distributed to farmers through polythene hose.

Figure 2.19: Sprinkler-irrigation scheme operating in Bilalevu.

Figure 2.21: Sprinkler system used in an egg plant field in Bilalevu.

Following the success of the SVRDP, a number of privately drilled wells (PDW) were installed in the Bilalevu area. The continual growth in farming community and extreme climatic conditions, such the 1998 drought event, resulted in the accelerated groundwater exploration demand for community and domestic water supply. Consequently, approximately 25 wells, all of which are 4 " in diameter and drilled by private drilling companies, namely Nagan Drilling and Western Drilling, have been drilled within the study area.

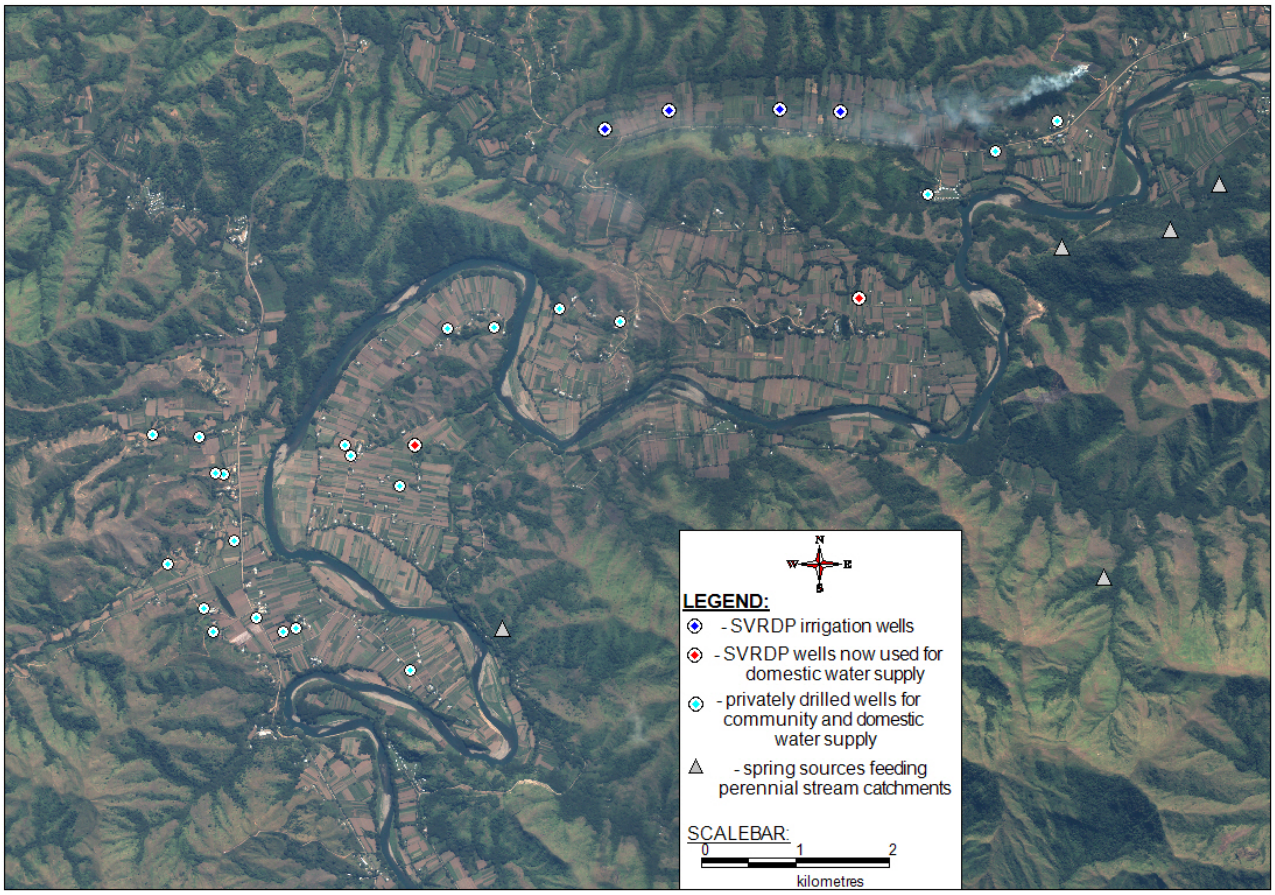

Figure 2.22: existing SVRDP and private wells, as well as springs around the study area as of November, 2010.

Most of these private wells, drilled for community water projects, have been co-funded by the Ministry of Multi-Ethinic Affairs (MMEA), whilst some are funded and owned by individual households (Figure 2.22). These private wells were drilled without the knowledge of MRD and attempts to obtain well logs from private companies proved futile. Several adjacent villages, namely Jubairata and Rararua utilize private wells for drinking purposes, whereas Toga, Vunarewa, Dreke, Narewa and Narata, utilize the

springs and perennial stream-catchments for portable purposes (Figure 2.22). These springs and stream catchments, occurring in the highly fractured local sedimentary units, are sites of groundwater discharge and hence, signifies the intensification of groundwater use in the area, as well as demonstrating the hydrogeological potential of the underlying basement. Details of current groundwater abstraction rates of these private wells, depths and groundwater use will be covered in later chapters in relation to groundwater recharge estimation.

2.6 Status of groundwater policies & legislation

The FG neither has a policy nor a legislation to warrant the sound protection and sustainable management of groundwater resources. Peach (1988) enumerated several longstanding issues (and still prevalent today) hampering the progress of groundwater development and management in Fiji such as:

- no clear, coordinated national water policy culminating in the uncoordinated efforts of many different agencies, government and private, in the attempt to develop water resources, and
- absence of groundwater legislation meaning that there can be no effective conservative of groundwater and protection of the resource from improper and unsustainable use.

2.6.1 Existing water legislations

To date, there are numerous existing legislations that deal with various aspects of surface water and **NO** legal reference to groundwater. These existing legislations, including the River and Streams Act, Mining Act, Irrigation Act, Water Supply Act and Environment Management Act, have varying roles and controls in the utilization, allocation and management of surface water resources, with minor emphasis on groundwater quality management in response to mining activities. The Fiji Government has, recently, taken numerous steps towards the formulation and enactment of groundwater legislation. In August, 2002 at a preparatory meeting to the Kyoto 3rd World Water Forum, Pacific Island leaders agreed to a Pacific Regional Plan on Sustainable Water Management so as to strengthen their commitment to the 2001 United Nations Millennium Goal. Subsequently, the FG initiated the design, development and documentation of the "Fiji Islands Water Policy": this responsibility was handed to the MRD and is currently in draft stage (Rao & Dau, 2004). This policy recognized that prior to 1874, ownership of land

and water resources in Fiji was vested with tribal chiefs. This ownership, currently having two different legal opinions (Figure 2.23), was affected when chiefs ceded Fiji to Her Majesty Queen Victoria in October, 1874, which permit the colonial administration make laws that transferred the control of land and other resources from local control (Rao & Dau, 2004).

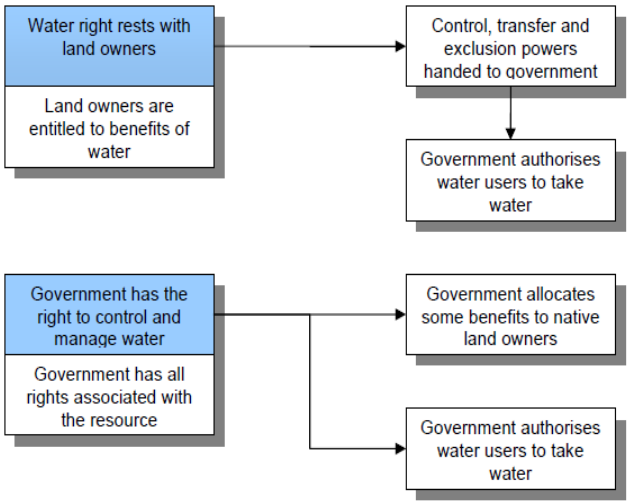

Figure 2.23: two legal opinions on right to use water (Water Policy Services Pty Ltd, 2006).

This draft policy, again, recognizes the absence of national legal framework and the need to protect water resources for environmental sustainability with continuing support needed for capacity building. The FG, though this policy, aims to clarify its legal status in being the custodian of all water resources, and recognizes that groundwater should be declared a mineral as defined in the Mining Act, although its susceptibility to pollution will necessitate special protection mechanism that do not apply to minerals (Water Policy Services, 2006). Further, the right to the flow, the use and management control of both surface water and groundwater is to be vested with the Government, which will exercise the national water management on behalf of the public of Fiji. This "2004 Draft Water Policy", upon which future surface and groundwater management, allocation and exploitation acts were to be based, was never endorsed by Cabinet and needed further consultations. Recently, changes have been made to include both water resources management and sanitation.

2.6.2 Pilot Study

In 2006, the European Union (EU) funded a Fiji pilot study for the Programme for Water Governance (PfWG) with the intention to progress water resources management (WRM) at the national level in Fiji (Water Policy Services Pty Ltd, 2006). The study recognizes loopholes in the current water resources management set-up (Figure 2.24) and recommended the introduction of Integrated Water Resources Management (IWRM) and developments of specific responsibilities for WRM. It was recognized that pollution control, an aspect of WRM, is adequately covered by the Ministry of Environment (MoE), whilst other aspects, namely the allocation of water resources among all users, flood management, riverine controls and activities for water body protection as neglected (Water Policy Services Pty Ltd, 2006).

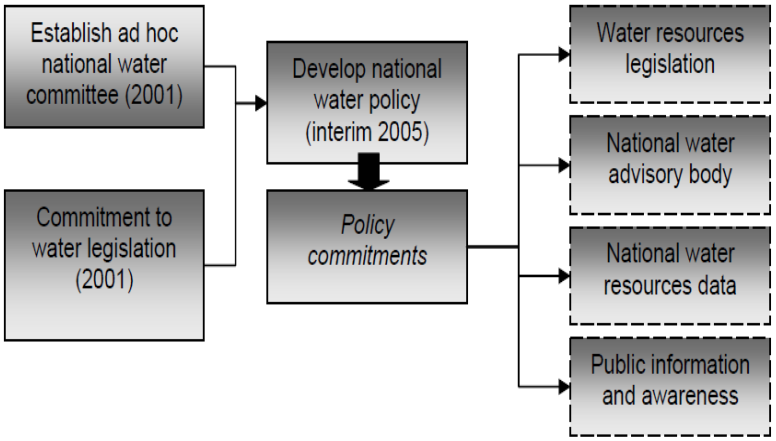

Figure 2.24: current water-related structure in Fiji Government.

Currently, some aspects of water resources management have been undertaken in a fragmented manner by either ad-hoc activities or default by various government departments, namely Department of Metereological Services (DMS), Land and Water Resources Management (LWRM) Division of the Ministry of Agriculture, Hydrology Office of Public Works Department and MRD without adequate legislative backing. Hence, the need to develop a water resources department with regulatory power was recommended, as well as the implementation of IWRM. The function of this department was suggested to ensure the protection and sustainable development of water resources, without conflicting MoE's role of regulating wastewater discharge and environmental protection, with the equitable allocation and management of surface and groundwater likely to be addressed through:

- identification of volumes of water available and sustainable limits for various water users or types of water use;
- characterization or available water and flow conditions;
- statement or rules for ensuring flow for environmental and aesthetic values/benefits, and
- drawdown levels are determined and at which water abstraction should be limited;
- volumes of water various users may take and the rates at which water may be abstracted in known;
- various technical criteria such as minimum distance between bores for different users; and
- statement of priorities among water user in circumstances of low flow or water scarcity with rules and penalties for breaching these guidelines.

2.7 Stable Isotope Hydrology

2.7.1 Introduction

Isotope geochemistry is concerned with the measurement and interpretation of the variation of isotope composition that occur in of elements of same atomic number but different atomic weight due to varying numbers of neutron in the nucleus (Fetter, 2001). Stable isotopes are non-radioactive whilst radioactive isotopes undergo radioactive decays forming new elements and may even form stable isotope products, known as radiogenic isotopes. In hydrology, stable isotopes of hydrogen (H), oxygen (O), carbon (C), nitrogen (N) and sulphur (S) are commonly used to study processes that affect surface and groundwater whereas radioactive isotopes can be used to ascertain groundwater age. Although errors associated with chemical-extraction procedures continue to be limiting factor in isotope analysis (Faure & Mensing, 2005), stable isotopes are gaining widespread recognition in the hydrology and geochemistry discipline.

2.7.2 Background of application in hydrology

Stable isotopes, in this study using hydrogen and oxygen isotope, is focused on the fractionation or separation of isotopes into light and heavy pairs caused by flux processes (e.g. condensation, evaporation, temperature changes) and controlled by difference in atomic mass and differences in their abundance in nature (Table 2.2).

Isotope	Abundance (%)	Mass (amu)
^{1}H	99.985	1.007825
^{2}H	0.015	2.014
^{16}O	99.762	15.994915
^{17}O	0.038	16.999131
^{18}O	0.2	17.99916

Table 2.2: mass and abundances of H and O stable isotopes (Faure & Mensing, 2005).

Light isotopes, more abundant in nature (Table 2.2), have greater translational velocities, more reactive and have greater vibration frequency than heavy isotopes. Light isotopes also form chemical bonds with high degree of valency whilst heavy isotopes form stable molecular compounds and preferentially held in strong bonds (O'Brien, 2010).These control their behavior through a phase or across phase boundaries in processes, such as evaporation and diffusion. For example, light isotope can preferentially diffuse out of a system leaving a reservoir to be enriched in heavy isotopes. However, any substitution or replacement of light and heavy during these processes will not change the gross chemical properties of these elements or compounds but will have subtle changes chemical and physical differences in mass attendants as governed by the differences mentioned earlier (Sharp, 2007). In this study, H and O isotopes (the most abundant in the earth's crust) are analysed in a number of different water sources and detail of which will be covered in the later chapters. Table 2.2 shows that H has two stables isotope whereas O has three meaning there are nine possible combinations of these isotope that make stable water molecules with $H_2{}^{16}O$ dominating the abundance in the Hydrosphere (Table 2.3). Henceforth, H^1 or protium and H^2 or deuterium will be referred to as H and D, respectively.

Isotope	Abundance (%)
$H_2{}^{16}O$	99.73098
$H_2{}^{18}O$	0.199978
$H_2{}^{17}O$	0.037888
$HD^{16}O$	0.031446
$HD^{18}O$	0.0000006
$HD^{17}O$	0.0000001
$D_2{}^{16}O$	0.00000002
$D_2{}^{17}O$	0.00000000001
$D_2{}^{18}O$	0.00000000005

Table 2.3: average natural abundances of the nine (9) isotopologues of water vapor (Sharp, 2007).

The isotope ratios of H and O are measured by mass spectrometry and expressed relatively to standard mean ocean water (SMOW), conventionally plotted as meteoric water line (MWL) and derived by:

$$\delta D\ (‰) = 8\delta^{18}O + 10$$

This is due the near-linear relation between majority of waters D and ^{18}O and reinforcing that all waters are of meteoric origin and is used to reduce systematic errors in measurement made on different mass spectrometer. D and ^{18}O are therefore expressed in terms of a parameter called delta δ and through:

$$\delta^{18}O\ (‰) = [((^{18}O/^{16}O_{\ sample}) - (^{18}O/^{16}O_{\ standard})) / (^{18}O/^{16}O_{\ standard})] \times 1000$$

$$\delta D\ (‰) = [((D/H_{\ sample}) - (D/H_{\ standard}) / (D/H_{\ standard})] \times 1000$$

Isotope composition variability of $H^{16}O$ and $D^{18}O$, as mentioned earlier, will show the enrichment (depletion) of heavy isotopes with respect to processes of precipitation, condensation and water-rock interaction. For instance, due to the Rayleigh fractionation, condensation and precipitation of air mass is common occur in windward and high altitude areas and cause heavy isotopes to preferentially diffuse out of the vapor phase and fall as rain (Sharp, 2007), and hence, water vapor moving into and precipitating as rain in the leeward side will be depleted in $\delta^{18}O$. Further, processes of water-rock interaction and mixing with magmatic waters can cause $\delta^{18}O$ to be release into solution and hence, groundwater or geothermal waters can enriched with the heavy isotopes (Figure 2.25)

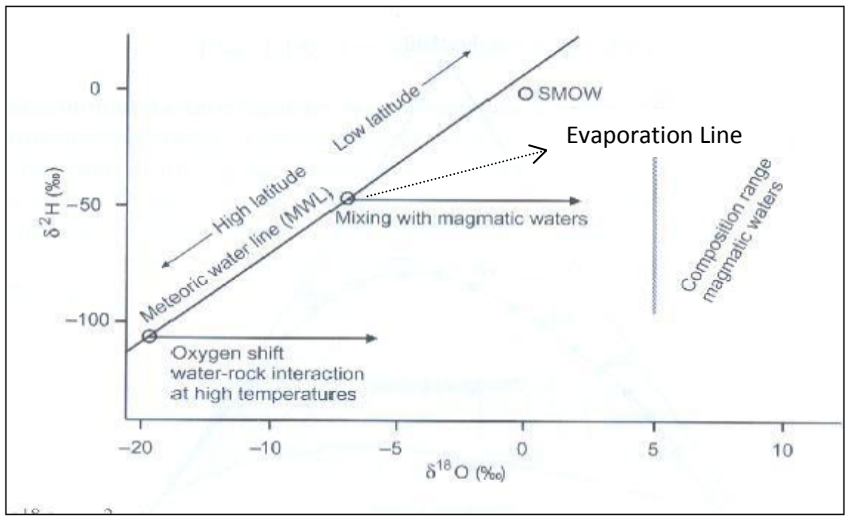

Figure 2.25: isotopic composition of water in relation to MWL and oxygen shifts driven by either water-rock interaction or mixing with magmatic waters (O'Brien, 2010).

2.7.3 Previous Isotope Study in Fiji

A study was conducted around the islands of Viti Levu and Vanua Levu tin the late 1970's to determine the origin of thermal waters and the characteristics of geothermal activity. Cox and Hulston (1980) documented the investigation and results of thermal and other waters in Fiji, which entailed the sampling

of 79 water sources, including thermal springs, hand-dug wells, rainwater and streams from the two mail islands of Fiji (Figures 2.26 & 2.27).

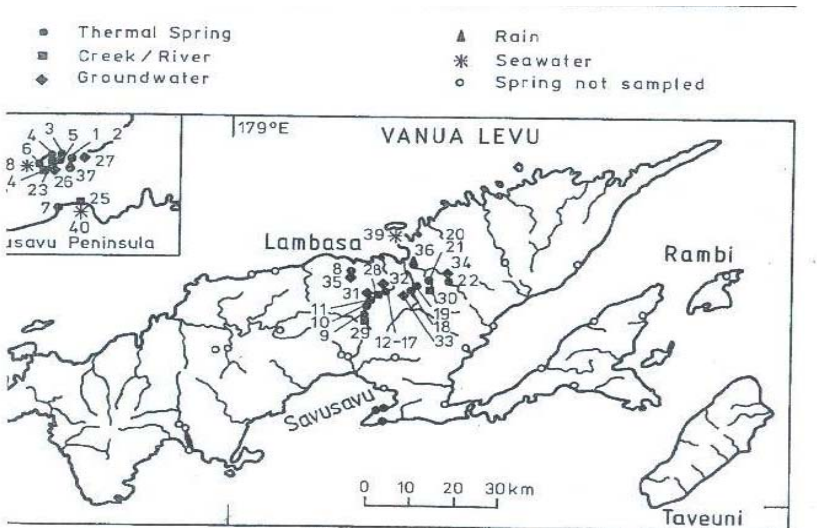

Figure 2.26: sample location around Vanua Levu (Cox & Hulston, 1980).

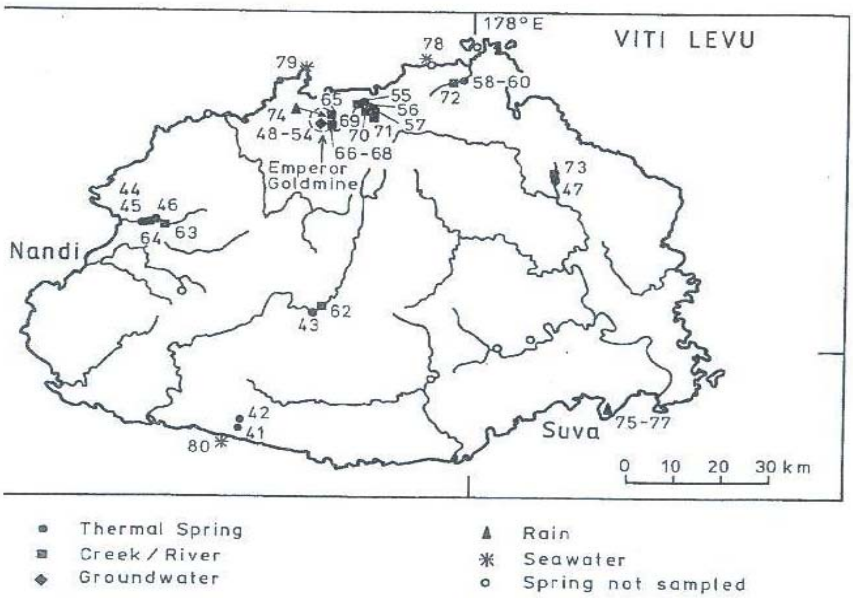

Figure 2.27: sample location around Viti Levu (Cox & Hulston, 1980).

These samples water analysed on $^{18}O/^{16}O$ and D/H ratios and chloride concentration. $^{18}O/D$ characteristics and composition were related to a best linear approximation of WML for the Fiji waters such that:

$$\delta D = 8\delta^{18}O + 13$$

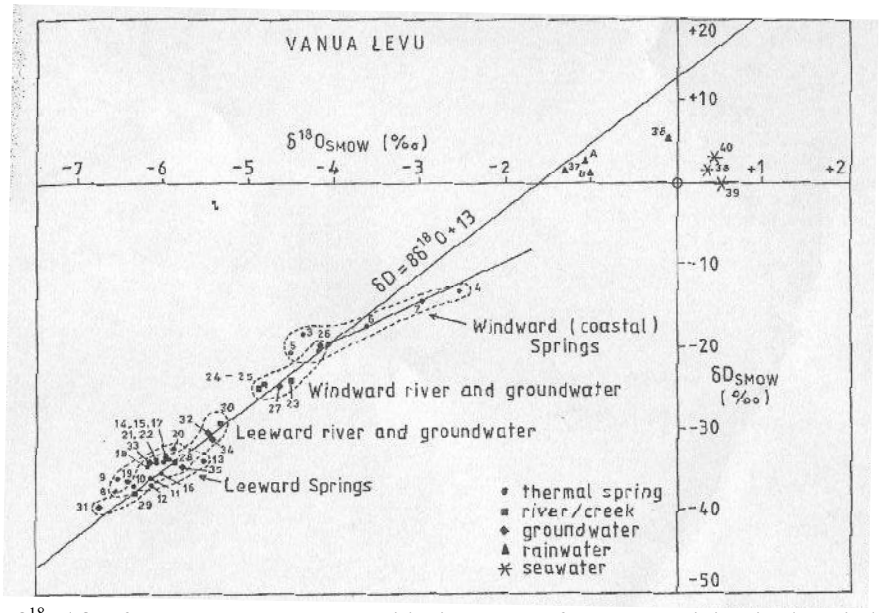

Figure 2.28: $\delta^{18}O$/ δD for Vanua Levu waters with signatures of seawater mixing in the windward thermal waters along a line with a slope of about 4.5 (Cox & Hulston, 1980).

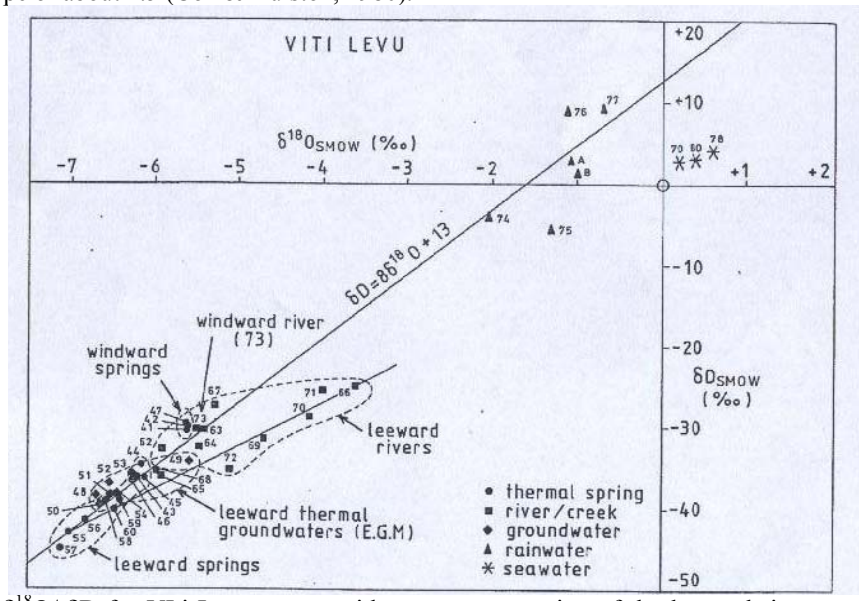

Figure 2.29: $\delta^{18}O$/ δD for VIti Levu waters with strong evaporation of the leeward river water as shown by a line with a slope of about 5 (Cox & Hulston, 1980).

It was then concluded that Fiji thermal waters are of meteoric origin and their stable isotope composition is similar to the surface and shallow groundwater. Significant differences were attributed to mixing of other water (fresh groundwater, saline groundwater or sea water – particularly sites adjacent to the coast) (Figures 2.28 & 2.29). The overall isotopic data showed that most sample geothermal systems were

dominated by low temperature with no signatures (except Savusavu ≈ 150° C) of oxygen enrichment caused by high temperature rock-water interactions. The δD compositions of meteoric and thermal waters reflect the windward and leeward climatic conditions with an increasing depletion of deuterium in the leeward areas. Further, the difference in isotopic compositions in precipitation at different localities is attributed to temperature variations, different amounts of rainfall and seasonal changes in the wind direction (Cox & Hulston, 1980).

2.8 Conclusion & Synthesis

- The regional geology of the SW Viti Levu, Fiji is composed of Eocene to Recent arc and basinal assemblages and carbonate aprons formation (Wainimala Group), a period of plutonic intrusion (Colo Plutonic Group) and followed deposition and lithification of sediments (coupled with submarine mass wasting) (Tuva Sedimentary Group), periods of widespread displacements and deformation triggering further volcanism, with eustatic and base level fluctuations likely to control the aggdration of Quaternary-Recent Alluvium deposits onto incised bedrock.
- The study area, dominated by the highly deformed and juxtaposed Waimala and Tuva sedimentary groups, is dissected by the sinistral Nasovatava Fault, to which the deformation and displacements in the basement units is attributed and, with synchronous eustatic fluctuations, controlled the deposition of alluvial materials in the incised valleys.
- Groundwater use and exploitation around the Fiji islands has grown and resulting in the formation of the GRADU and has since been committed in the systematic development of groundwater for the benefit of wider communities and this is evident in the previous aquifer classifications of Fiji.
- Groundwater resources use and demand in the study area, as characterized by the rapid growth of PDW together with villages relying on springs and perennial stream chatchments, is exceedingly high and will be serious concern during water deficit periods and may jeopardize the long-term sustainability of groundwater
- Despite several water-related legislations and numerous recent water-resources studies, the Fiji Government has **NO** legal framework to warrant the sustainable management and protection of groundwater resources.

- Isotope hydrology looks at the fractionation or separation into light and heavy pairs of stable isotope that occurs in fluxes, such as evaporation and condensation, and driven by the atomic mass and their abundance in nature. Previous studies in Fiji showed the dominance of meteoric waters in most of the sampled water bodies with minor differences attributed to mixing with saline and fresh groundwater.
- In summation, the tectonic and geological evolution of the southwest Viti Levu, together with eustatic fluctuation, have varying influences on the groundwater potential of the study area as substantiated by the previous rural development project in the Sigatoka Valley (SVRDP). One, however, may wonder if there are potential fractured units underlying the alluvium deposits (QRA) and if so, how would these fractured systems vary in terms of chemical and isotopic composition in relation to the origin and complexity of groundwater systems, as well as to previous studies. With the current growth on groundwater abstraction on the study area, it is critical that groundwater recharge and sustainability are established upon which the need for proper groundwater allocation and management legislative frameworks will be linked.

Chapter 3: Field investigation, methods and results

3.1 Engineering geology and geomorphological classification

3.1.1 Introduction

The field area is located in the middle Sigatoka valley, from Dubalevu to Bilalevu, and covers both sides of the Sigatoka River (SR). The major geological units observed, include the Tari Formation (TF) and the Qalimare Limetone (QL) of the Oligocene-Middle Miocene Wainimala Group (WG), juxtaposed Cici Sandstone (CS) and Takaro Conglomerate/Rudite (TCR) of the Late Miocene Tuva Sedimentary Group (TSG), and Quaternary to Recent Alluvium (QRA) deposits infilling the incised valleys (Figures 3.12 & 3.13) (Hathway, 1989 &Hathway and Colley, 1994). This section presents the lithological and engineering geology descriptions of the units based on the surface geomorphological mapping.

3.1.2 Methodology

Geological units were described/defined based on rock outcrop observations, although most geological contacts were obscured by thick vegetation cover and surface deposits. Surface outcrops were accessed by either vehicles or foot traverses through the hilly landscape to validate previously mapped units with geological nomenculture based on previous geological mapping around the Southwest Viti Levu region by Hathway (1989). Engineering geological classifications were also conducted based on Pettinga & Bell (1983) and NZ Geotechnical Society (2005) guidelines.

3.1.3 RESULTS

3.1.3.1 Geological units

3.1.3.1.1 WG

This group of rocks, dated Upper Oligocene to Middle Miocene (Hathway & Colley, 1994) and composed of the TF and the QL, is ubiquitous around the SSW-SSE of the study area and south of the ENE-WSW NF (Figure 3.13). The group had been interpreted as ungraded deposits of high density flows with minor stratified tops and carbonate debris apron deposited in deep water, respectively (Hathway, 1989 & Hathway, 1995).

3.1.3.1.1.1 TF

This Upper Oligocene to Middle Miocene formation, approximately 50 m in thickness and classified as polymict volcaniclastic rudites, limestone and lava (Hathway & Colley, 1994), appeared as moderately thin-thickly bedded and interbedded dark-brown argillite, grey-bluish grey sandstone, bluish grey to light grey dacite and dacitic tuff, light grey andesitic lava flows (abundant in quartz amygdales), and creamy claystone that is well indurated (Figures 3.1-3.3). The moderate-steeply inclined unit (46-83°N and 26-35°NW) appeared unweathered-moderately weathered, extremely-moderately strong, highly fractured (subvertical and sub-perpendicular to bedding orientation) with close spacing, narrow apertures, rough surfaces and with moderate to high persistence.

Figure 3.1: well indurated, extremely strong brown argillite composite of the TF (highly fractured with slickensided surface) observed at Bilalevu (Localiity 1, Figure 3.12).

Figure 3.2: moderately weathered interbedded argillite and dacitic tuff of the TF observed at Vunarewa (Locality 34, Figure 3.12).

Figure 3.3: Extremely strong, fine to massive fabric, creamy claystone, well indurated, around Mavua (moderately incline (20-25°) towards the NW) (observed at localities 17 & 18, Figure 3.12).

3.1.3.1.1.2 QL

This Lower to Middle Miocene Platform unit was observed as a white to creamy, massive to crudely bedded, limestone body dominated by cavernous weathering and moderate-highly fractured systems with sub-angular to sub-rounded volcaniclastics included (Figures 3.4-3.6). The limestone unit, 200-300 m in thickness, represents the upthrusted component of the sinistral NF that protrudes the landscape as a north-facing ENE-WSW trending escarpment (NE of the study area) and extends for around 1 km towards the North (Figure 3.7). The unweathered-slightly weathered and extremely strong unit is moderately-highly fractured, as characterized by high persistence and wide-very wide apertures that is widely spaced. The QL steep and rugged terrain is covered thick vegetation cover, and flanked by scree and talus slopes comprising limestone cobbles and boulders and suggesting active hillslope processes.

Figure 3.4: cavernous weathering processes active in the Limestone unit.

Figure 3.5: sub-rounded andesite included in a massively bedded, white and extremely strong QL around locality 32 (Figure 3.12). Note book is 10cm×16.5cm.

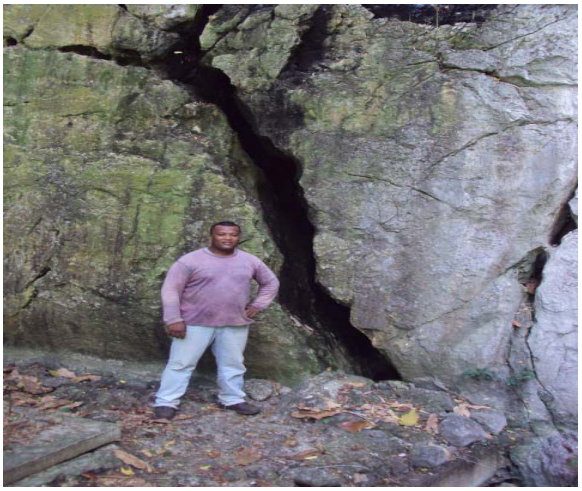

Figure 3.6: Highly fractured QL (wide aperture and high persistence) and from which the Matanitavuni (Q3) spring discharges (locality 33, Figure 3.12).

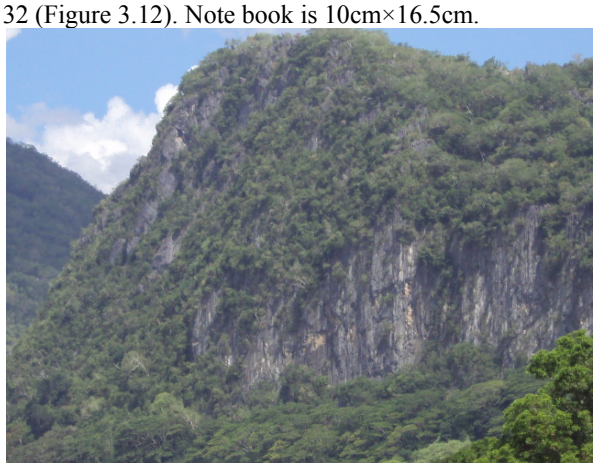

Figure 3.7: north-facing QL escarpment protruding the NE corner of the study area and extending for around 1 km towards the NE.

3.1.3.1.2 TSG

This sedimentary group, interpreted as Late Miocene turbidite system in the Sigatoka Sedimentary Basin in age and ubiquitous around the WSW-ENE of the study area (Figure 3.13), is composed of the CS and TCR that were deposited during the erosion of the post-Colo and Wainimala arc (Sections 2.2.2 & 2.2.3) that supplied abundant epiclastic material to the Sigatoka Basin.

3.1.3.1.2.1 CS

This feldspathetic litharenites unit, interpreted as a 600 m thick Late Miocene turbidite system (Hathway, 1989), was observed as a bluish grey to grey, fine-medium grained, well indurated, thickly bedded and interbedded sandstone, mudstone and siltstone (Figure 3.8). The unweathered-slightly weathered and extremely strong-moderately strong unit is ubiquitous around the N-NNW of the field area (Localities 16, 21-23, 39-42, Figures 3.12 & 3.13), and exhibited moderately-highly fractured systems (subvertical and sub-perpendicular to bedding orientations) (Figure 3.9), with low to moderate persistence and tight to narrow apertures (with quartz and calcite infill). The inclination of the unit varies from moderately inclined (24-26° SE) to steeply-inclined (40-47° SSE) and suggesting tectonic shortening overtime.

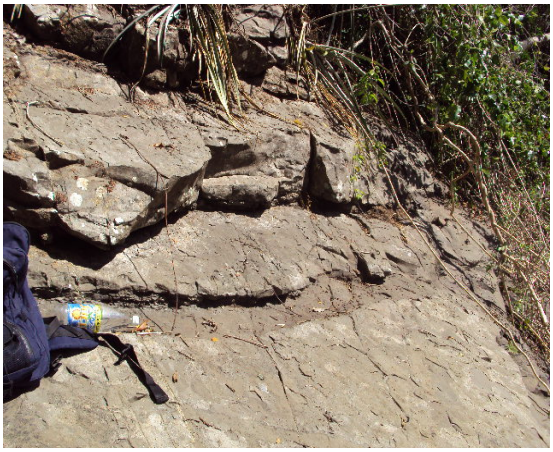

Figure 3.8: Moderately thick-thickly and steeply inclined CS around Rararua village (locality 21, Figure 3.12).

Figure 3.9: subvertical fractures with closely spaced and moderately wide aperture in the CS around locality 16 (Figure 3.12).

3.1.3.1.2.2 TCR

Outcropping at the hills N-NW Bilalevu and around Nabaka (localities 10-13, 15, 27, 35 and Figures 3.12 & 3.13) , the Late Miocene high density mass flow conglomerate and rudites (and post CS formation) is thickly bedded and massive with dark grey matrix supported framework comprising fine silt and medium-coarse sandy matrix locking sub-angular to sub-rounded andesite, dacite, tonalite and limestone clasts. The unwerathered-moderately weathered and very strong unit is highly fractured, closely spaced with narrow aperture (filled with quartz) and showing moderate-high persistence. The unit is exhibits moderate inclination (20-28° SE).

Figure 3.10: outcropping TCR NW of Bilalevu (locality 13, Figure 3.12) showing sub-angular to sub-rounded andesitic and dacitic clasts locked in sandstone matrix.

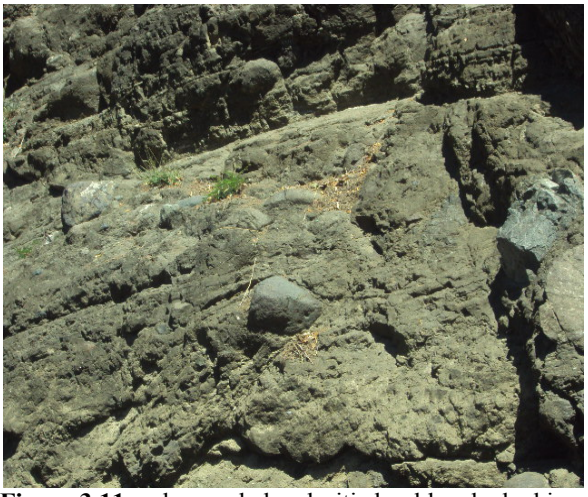

Figure 3.11: sub-rounded andesitic boulders locked in sandstone matrix of the TRC around the Nabaka area (locality 27, Figure 3.12).

3.1.3.1.3 QRA

This alluvium unit, comprising materials transported and deposited by the Sigatoka River in response to Quaternary and Recent eustatic fluctuations, appeared to be around 25 m in thickness and composed of yellowish sandy silt with gravel beds comprising medium-coarse, sub-angular to sub-rounded, pebbles in Bilalevu. In Dubalevu, the distribution and extent of alluvial deposits is marked by the E-W trending abandoned meander bounded by the north and south facing steeply inclined sandstone hills. The alluvium materials are composed of flood overbank deposits on the east, whilst the western end is dominated by unconsolidated sandy gravels as validated by the drilling of wells 89/15, 90/15 and 90/16 during the Sigatoka Valley Rural Development Project (Davies, 1992).

3.1.3.2 Spring mapping

Five springs were investigated: three occur around the fractured QL in the Toga area, namely Koro-i-Ra (Q1), Nacule (Q2) and Matanitavuni (Q3), and two occur in the fractured TF at Vunarewa and Mavua, namely Mataukaba (V1) and Navala (M1), respectively (sites 31-33, 34, 36 in Figure 3.12) . Discharge in all but one spring responded rapidly to rainfall events, with Q2 recording constant flow throughout the year, suggesting that Q2 is recharged by both proximal and distal sources controlled by the persistence and connectivity of its fracture system. The other springs, although also occurring along fractured conduits, are controlled by fluctuations in the local water table responding rapidly to rainfall events and hence, a proximal recharge source. Q2 spring discharges approximately 2.2 L/s whilst the other springs recorded discharge rates of 0.1 – 10 L/s depending on the frequency/intensity of rainfall events.

3.1.3.3 Relevant geomorphic expressions

Several geomorphic markers helped constraint the surface processes that shaped the Sigatoka Valley. These include:

- two Quaternary to Recent terraces along the Sigatoka River course may also include buried river channels (potential groundwater sources) (Figure 3.13);
- two abandoned lakes (also called oxbow lakes) observed in (1) Nabaka and (2) Bilalevu representing areas of either groundwater recharge or groundwater discharge (Figure 3.13); and
- uplifted QL and steeply inclined CS proving deformations and displacements relative to the NF fault and its associated shear zones or fault splays, which may also be responsible for the initial development of fracture systems observed in the mapped geological units.

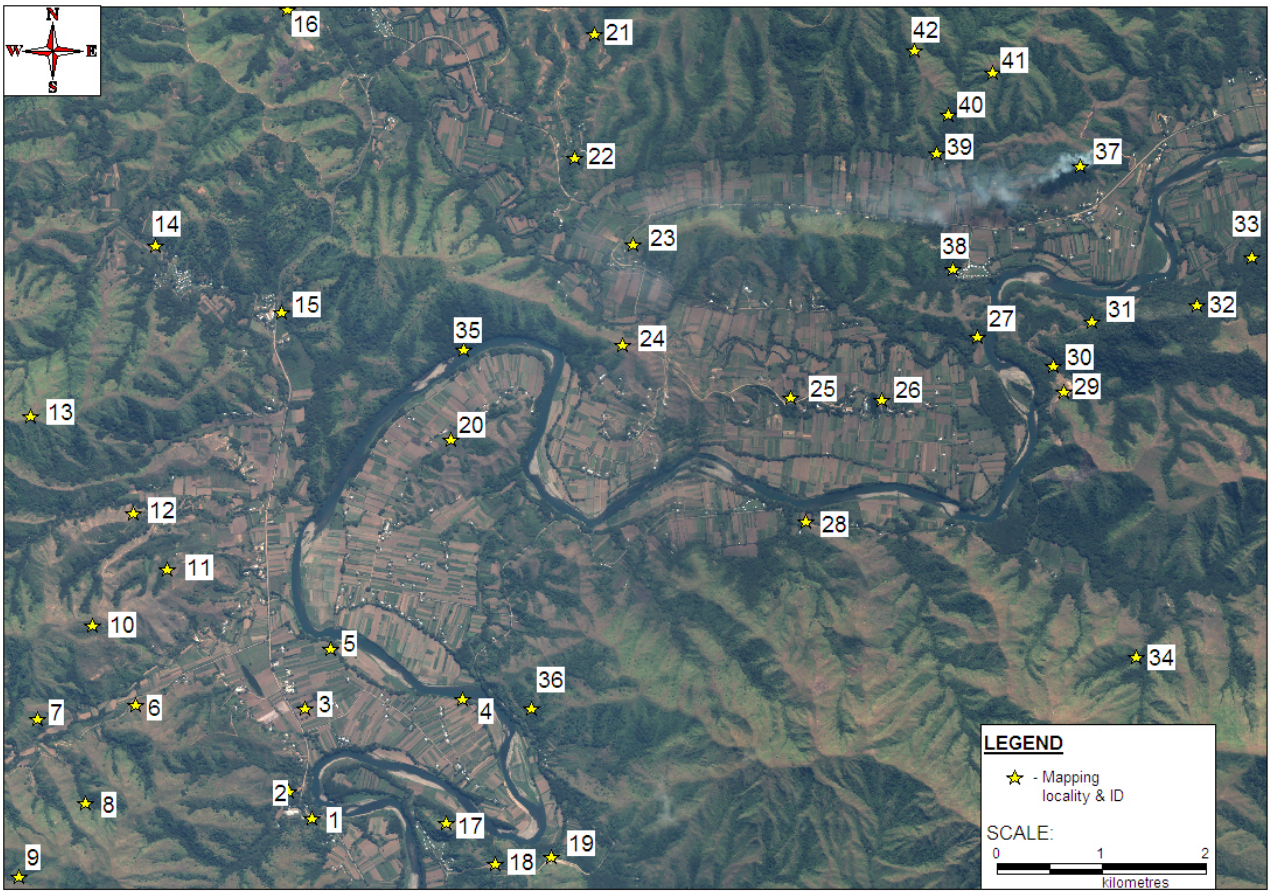

Figure 3.12: location map of surface outcrops locations within the study area. Summary of the mapped localities are presented in Appendix C.

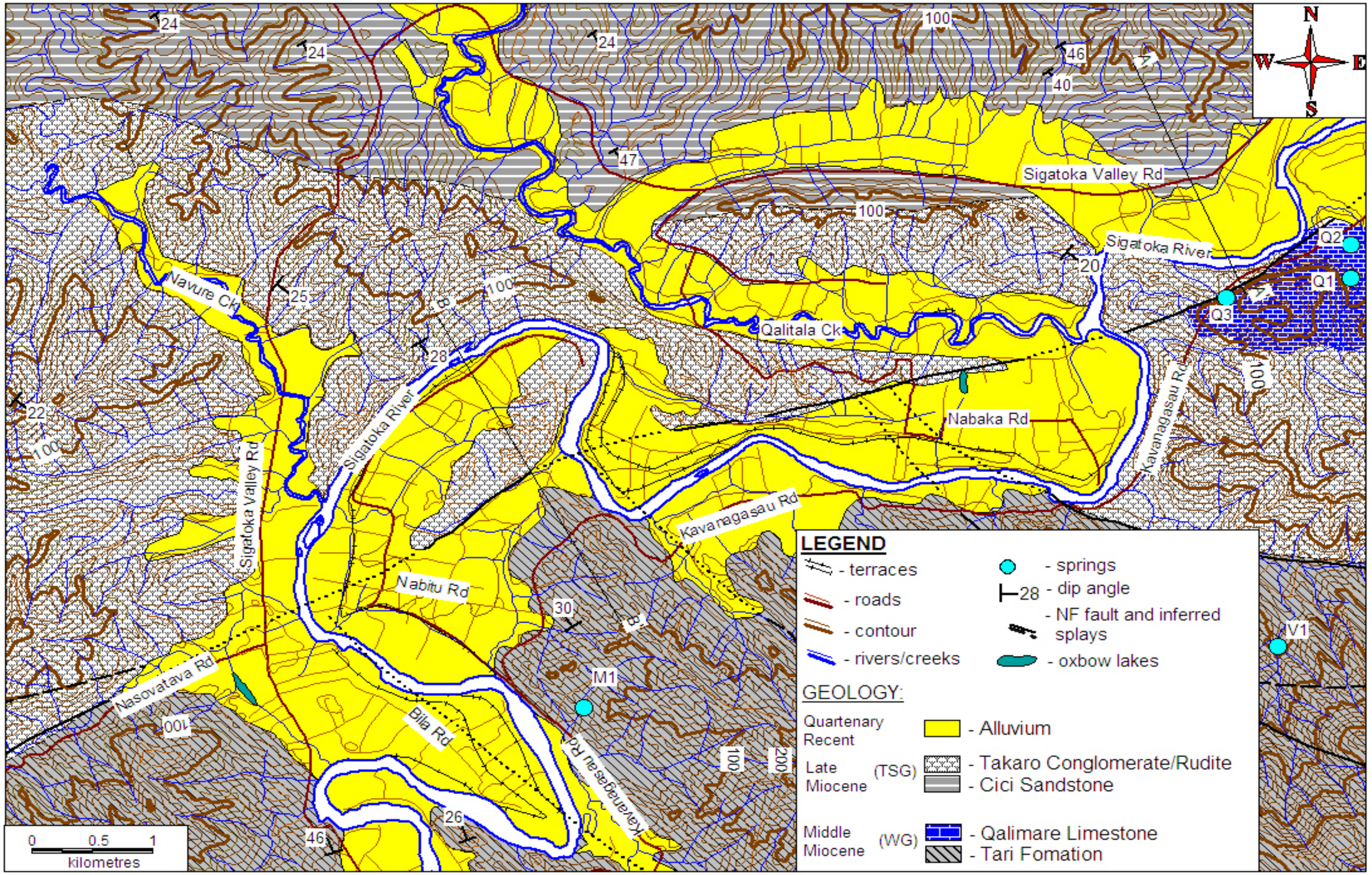

Figure 3.13: geological and geomorphological map of the study area showing Oligocene to Middle Miocene Tari Formation and Qalimare Limestone, Late Miocene Cici Sandstone and Takaro Conglomerate/Rudite and Quarternary to Recent alluvium, imprints of tectonic processes via the sinistral Nasovatava Fault (and its inferred splays), with a several geomorphic features, namely terraces, spring and oxbow lakes.

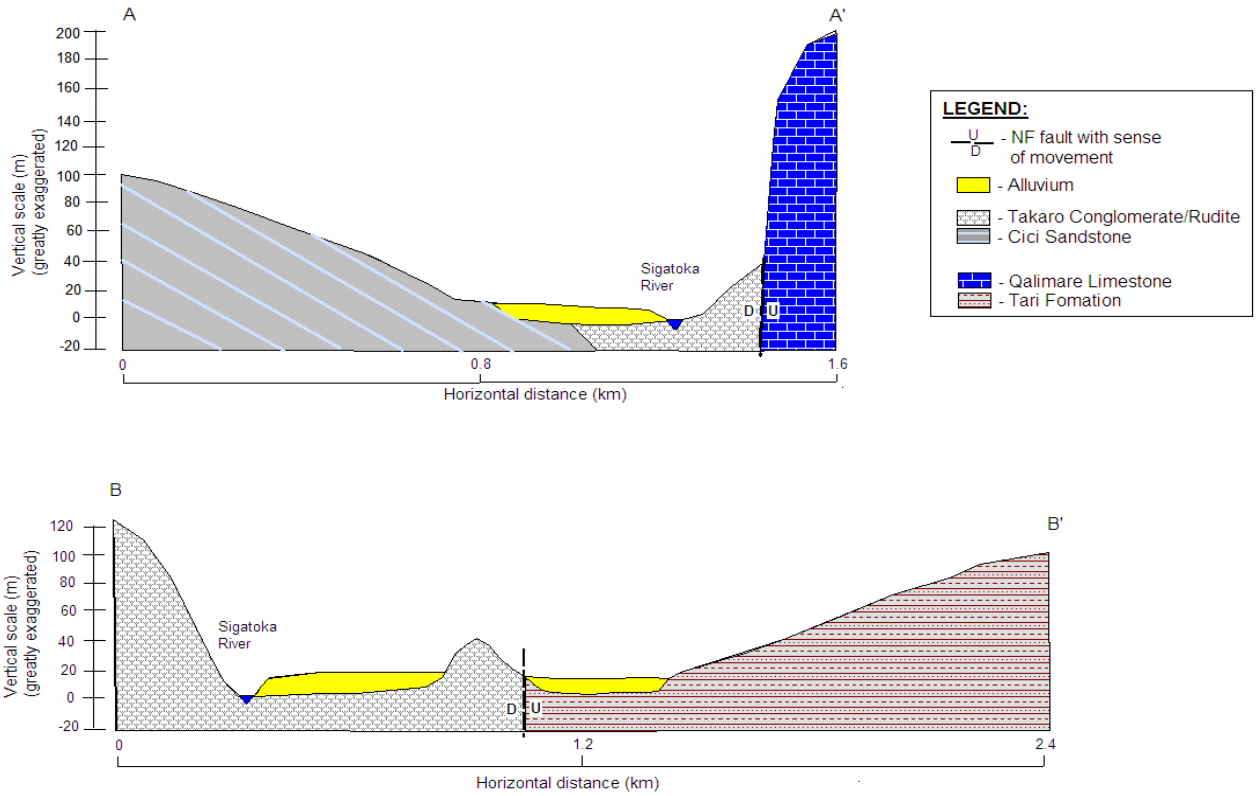

Figure 3.14: geological cross-sections at A-A' and B-B' showing the influence of the sinistral NF in dissecting the study area and may be responsible for the development moderate-high fracture systems observed in the mapped units.

3.1.4 SUMMARY

The above geological classifications and maps provide three contributions to the physical hydrogeology of the study area. First, the local sedimentary units represent either a low-negligible permeability basement or a fractured with moderate-high permeability basement governed by the fracture dimensions at depths. Second, the alluvial materials will be composed by either surficial silt-dominated confining units or unconsolidated sandy gravels representing buried river channels. Third, the presence of moderate-high fracture systems within the local sedimentary units, the uplifted Qalimare Limestone and the presence and close proximity of ENE-WSW trending sinistral fault (with its associated fault splays) suggest moderate-intense tectonic-induced shearing, which could create preferential groundwater storage and flow.

3.2 Geophysical survey

3.2.1 Introduction

The application of geophysics in hydrogeology is favoured due to its intrinsically non-invasive and non-destructive nature (Nobes, 1996) and its ability to produce high resolution subsurface models. In this research, two geophysical survey methods, namely electrical resistivity (ER) and electromagnetic (EM) methods, were used with the following objectives:

- to show water table depth, determine maximum thickness and spatial extent of Quaternary-Recent alluvium (QRA) materials;
- to estimate depth to bedrock;
- to identify subsurface anomalous structural features, such as folds, fracture density and faults, which are propitious for groundwater flow and storage; and
- to select potential drill sites

The following sections outline the methodologies and results obtained from these surveys. Details of site conditions, survey designs and background information of electromagnetic and resistivity methods, as well as field raw data are presented in Appendix D.

3.2.2 Methodology

Site reconnaissance, with the aid of API and surface geological mapping, permitted the selection of the subjective survey areas in Dubalevu, Tubakeli and Bila Rd (Figure 3.15). Borehole logs and water levels measurements data of existing boreholes were measured, using Solinist TLC depth probe, and were recorded beforehand (Tables 3.2 & 3.3). The geophysical surveys were conducted several days after Tropical Cyclone Mick (TCM), which caused widespread flash flooding around the area. Two geophysical survey systems were used, namely EM34-3 Geonics and Supersting Avi Ip, with one (l) line of each method used in Dubalevu, two (2) EM and three (3) ER lines were laid in Tubakeli while both methods were run twice in Bila Rd (Figure 3.16 & 3.17). The EM equipment, comprising transmitter and receiver coils, was used in the horizontal coplanar coil orientation (also called vertical dipole (VD)) and in the vertical coplanar coil

orientation (also called horizontal dipole (HD)) (Figures 3.18 and 3.19). Two conductivity readings were generated and recorded at each site. The VD measures subsurface voluminous conductivity to a maximum depth of 1.5 times the coil separation whilst the HD gives conductivity to a maximum depth of 0.75 times the coil separation (Table 3.1). Reading stations were marked at 5 m intervals. Survey lines were laid such that either two or three different coil separations, namely 10 m, 20 m and 40 m, were used and during which VD and HD measurements were recorded manually on field data sheets (Figure 3.18) and subsequently stored in Microsoft Office Excel format. Due to the presence of several cultural features around the study areas, the raw data were deemed noisy (Dr David Nobes, University of Canterbury, pers.comm, 2010) (Appendix 3.2). The data quality was improved through the process of convolution and using the 5-point running mean tapering formula (Dr David Nobes, University of Canterbury, pers.comm, 2010) given by:

$$\text{Conductivity at reading } X_{(i)} = (X_{(i-2)}+2*X_{(i-1)}+3*X_{(i)}+2*X_{(i+1)}+X_{(i+2)})/9$$

The ER equipment (Figure 3.20), powered by two 12V batteries (Figure 3.21), was designed and set-up such that the ER lines ran either perpendicular or parallel to the EM lines. In-built programs of Schlumberger and dipole-dipole strong gradient (DDSG) arrays were selected and initialised prior to the survey. Procedures, such as adequate grounding of steels pegs and contact resistance test, were followed prior to the start of survey. The Supersting Avi Ip equipment has an estimated resolution of 0.25 times the length of the survey line and all of the survey lines were around 280 m in length. The measured resistivity values were recorded in the Supersting Avi Ip equipment and downloaded into a desktop PC using the dongle provided. Survey raw data were then loaded into EarthImager 3.2 where the raw data were converted through in-built algorithms, before using an inversion process to produce subsurface models/profiles.

3.2.3 Results

The following sections will show location maps of survey areas, measured groundwater level, DDSG electrical resistivity profiles, as well as HD and VD electromagnetic responses.

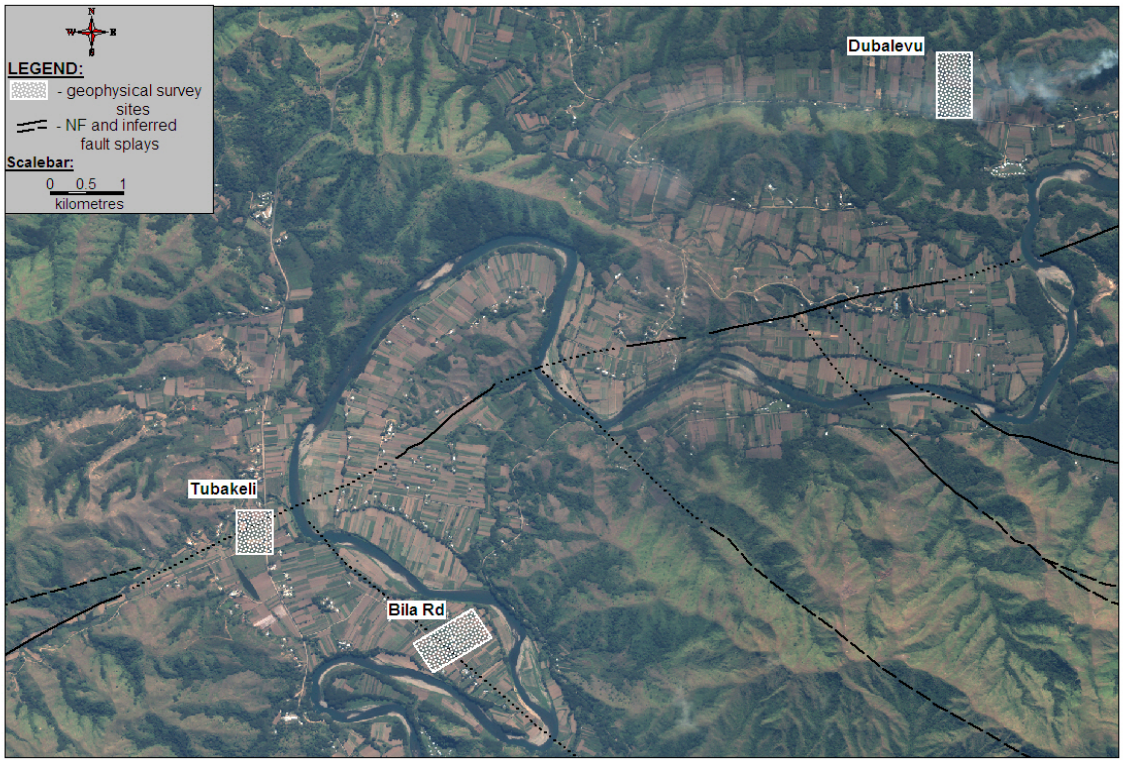

Figure 3.15: location map of geophysical surveys areas that were selected to explore the presence of fractured or shear zones related to the inferred structural features at Tubakeli and Bila Rd and the continuity of the gravel aquifer, as well as any fractured bedrock system, in Dubalevu.

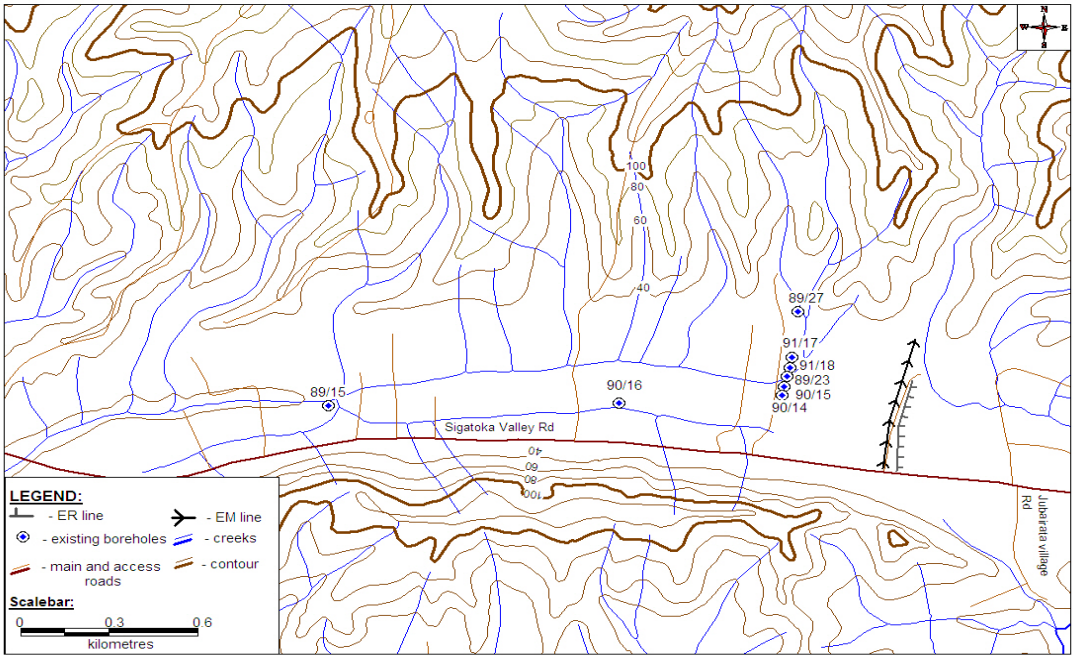

Figure 3.16: location map of geophysical lines on the E-W trending abandoned meander at Dubalevu with the adjacent existing boreholes which were measured for a priori (Table 3.2). Note that boreholes 90/15, 90/16 and 89/15 are irrigation sources drilled into unconsolidated sandy gravel during the SVRDP (see section 2.5.3). This survey permitted the assessment of extent of this gravel aquifer to the western end of the abandoned meander.

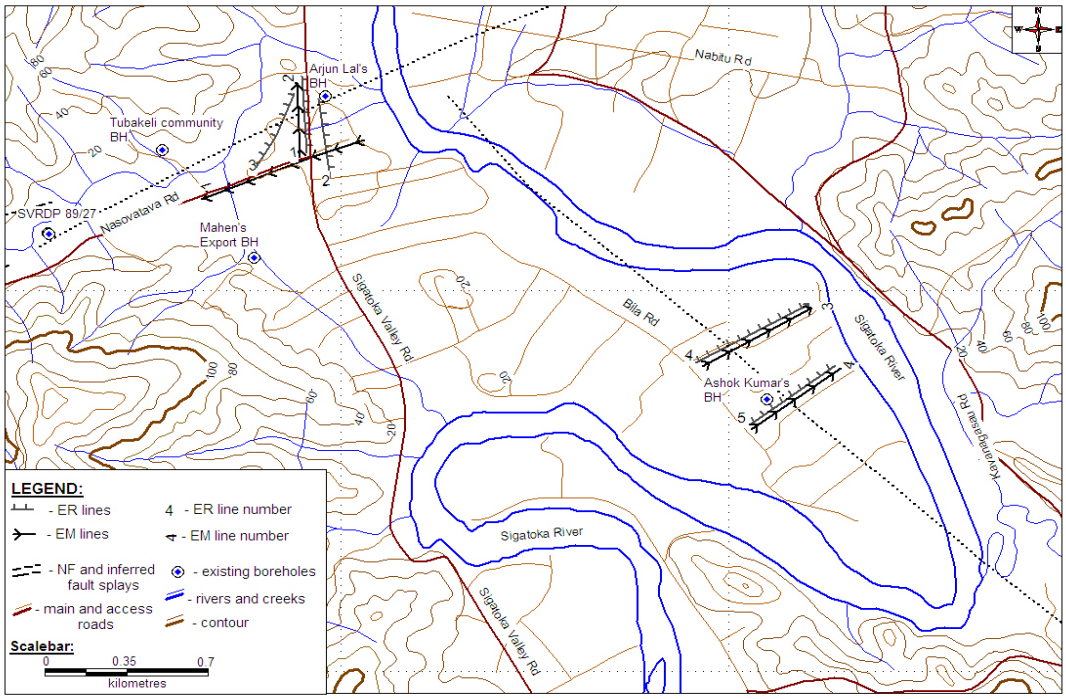

Figure 3.17: location map of geophysical lines at Tubakeli and Bila Rd with adjacent existing boreholes that were measured for a priori (Table 3.3). Note that the surveys lines were oriented either along or perpendicular to the sinistral fault and its inferred splays to investigate of possibility of high fracture density of shear zones related to these structural features.

Intercoil Spacing (m)	HD	VD
10	7.5	1.5
20	15	30
40	30	60

Table 3.1 exploration depths for EM34-3 at various inter coil spacings (McNeill, 1980).

Borehole	Depth (m)	SWL (m bgl)	EC (mS/m)	Temperature (°C)
89/27	28	2.22	13.5	26.1
91/17	26.59	4.4	26.4	26.1
91/18	21.9	5.19	127.2	26.2
89/23	19.41	5.37	26.9	26.6
90/15	48	6.21	21.3	26.7
90/14	32.69	5.31	21.1	27

Table 3.2: water level measured in meters below ground level (m bgl) on nearby wells in Dubalevu using TLC Solinist depth probe that measures water level, temperature and conductivity.

Borehole owner	Depth (m bgl)	SWL	EC (mS/m)	Temperature (°C)
Tubakeli Community BH	40	3.59	38	28.5
Arjun BH	15.4	9.15	47	26.9
Mahen 's Export BH	40	3.6	65	25.7
Ashok Kumar BH	20	12	25	25
Manoj Kumar	39	9.5	28.5	26.7

Table 3.3: water level measured in meters below ground level (m bgl) on nearby wells in Tubakeli and Bila rd using Solinist depth probe.

Figure 3.18: EM34-3 receiver coil on a horizontal coplanar arrangement (also called vertical dipole (VD)) with the readings manually recoded on a data sheet.

Figure 3.19: EM34-4 transmitter coil in a vertical coplanar arrangement (also called horizontal dipole (HD)).

Figure 3.20: Electrical resistivity equipment, Supersting Avi Ip.

Figure 3.21: two 12V batteries used as power sources for ER survey.

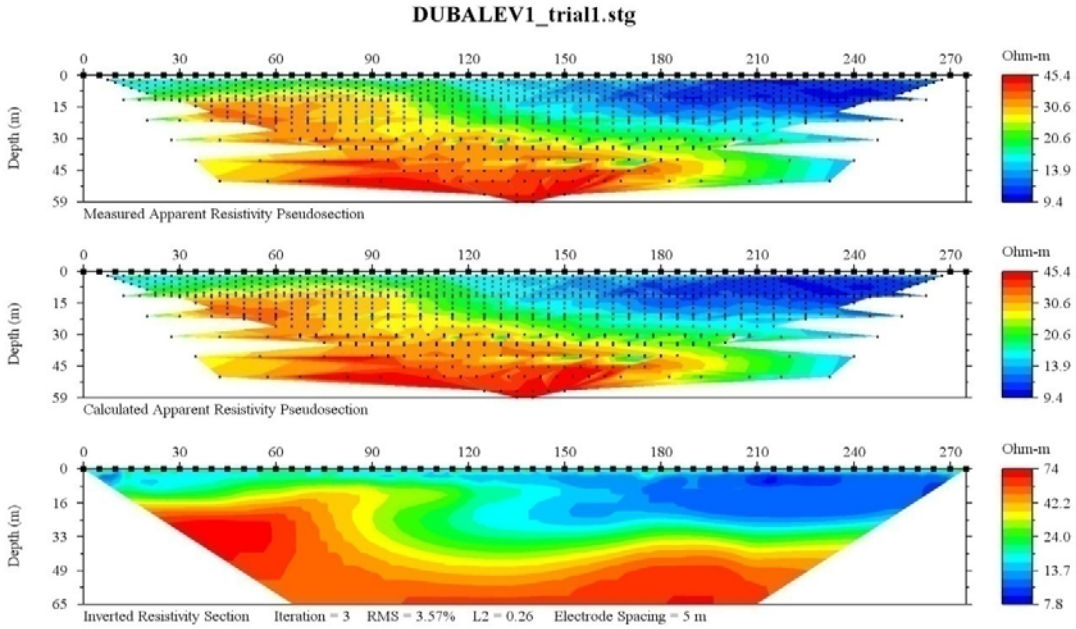

Figure 3.22: DDSG resistivity profile of Dubalevu a with very high resistivity zone at depth (possibly indicating deformed bedrock (CS) with a bedrock high between 30-90 m ER positions before an increasing depth to around 26-33 m depths after 90-100 m ER positions. The zone of very low resistivity may represent QRA flood overbank deposits that is saturated from TCM rainfall.

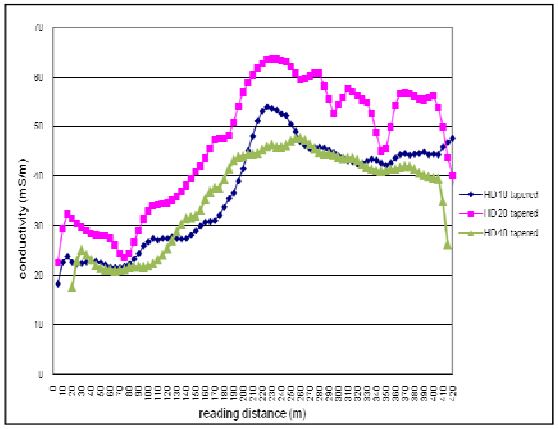

Figure 3.23: Dubalevu HD showing a uniform increase in EM responses beyond 100 m reading positions suggesting increasing thickness of QRA, increasing depth to bedrock and possibily increasing fracture densities (possible water sources).

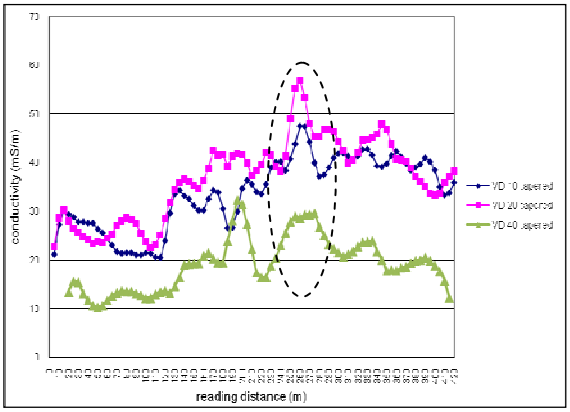

Figure 3.24: Dubalevu VD show a noisy dataset with uniform peak responses between 240-280 m reading positions and suggesting possible fracture zone at 15-60m depth.

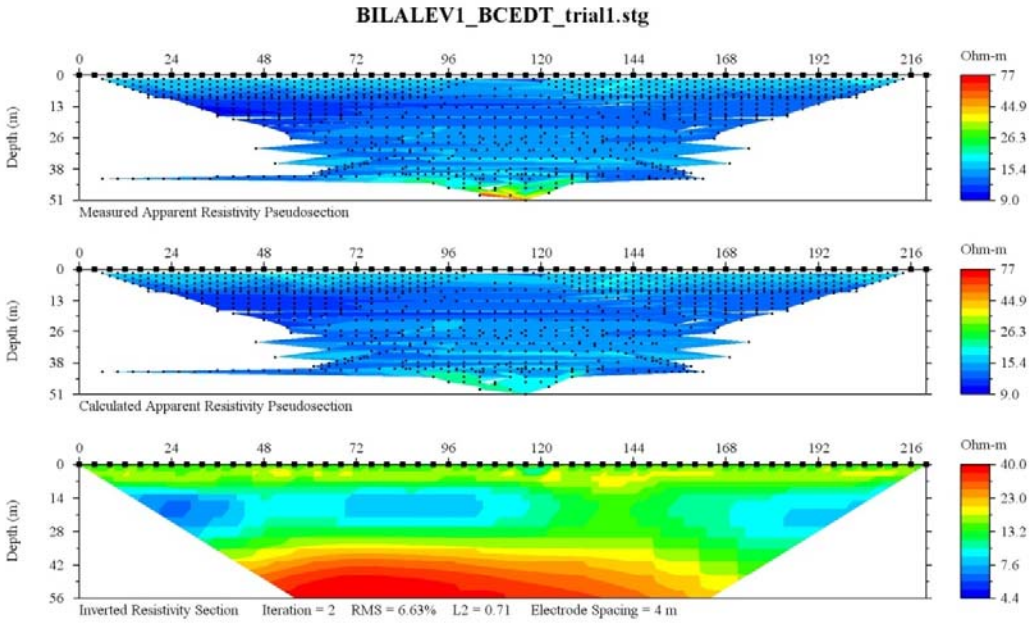

Figure 3.25: DDSG profile of line 1 at Tubakeli, Bilalevu showing an erroneous ER profile, as characterized by a field dataset dominated by very low resistivity values and subsequently inverted to a stratified profile; this was attributed to improperly connected electric cables.

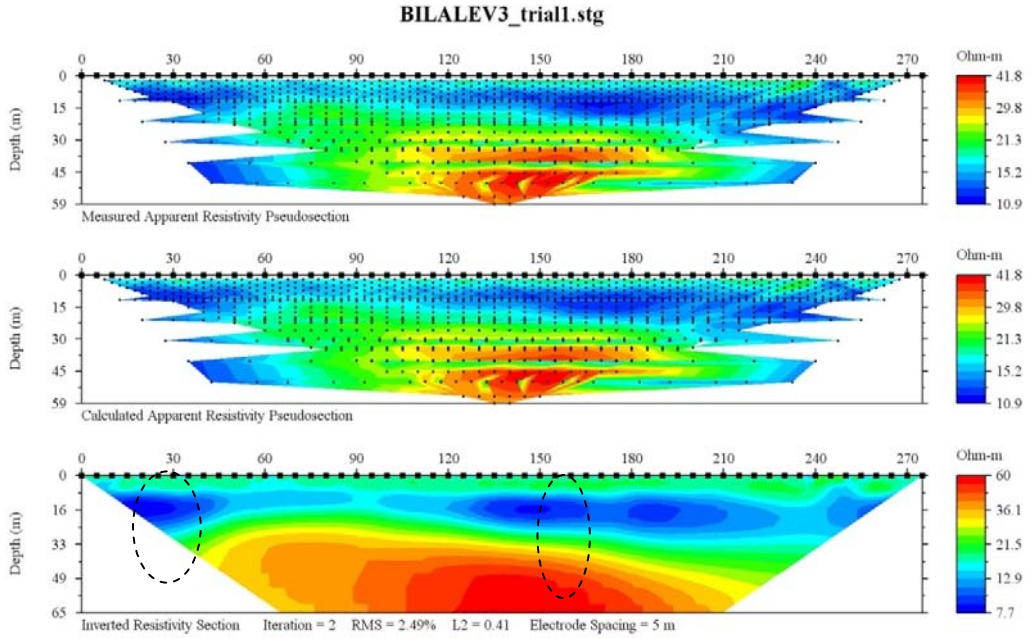

Figure 3.26: DDSG profile of line 2 at Tubakeli, Bilalevu showing high resolution ER profile of TCR bedrock with potential drill sites (denoted by dashed ovals) on Mr Hari Chand's farm.

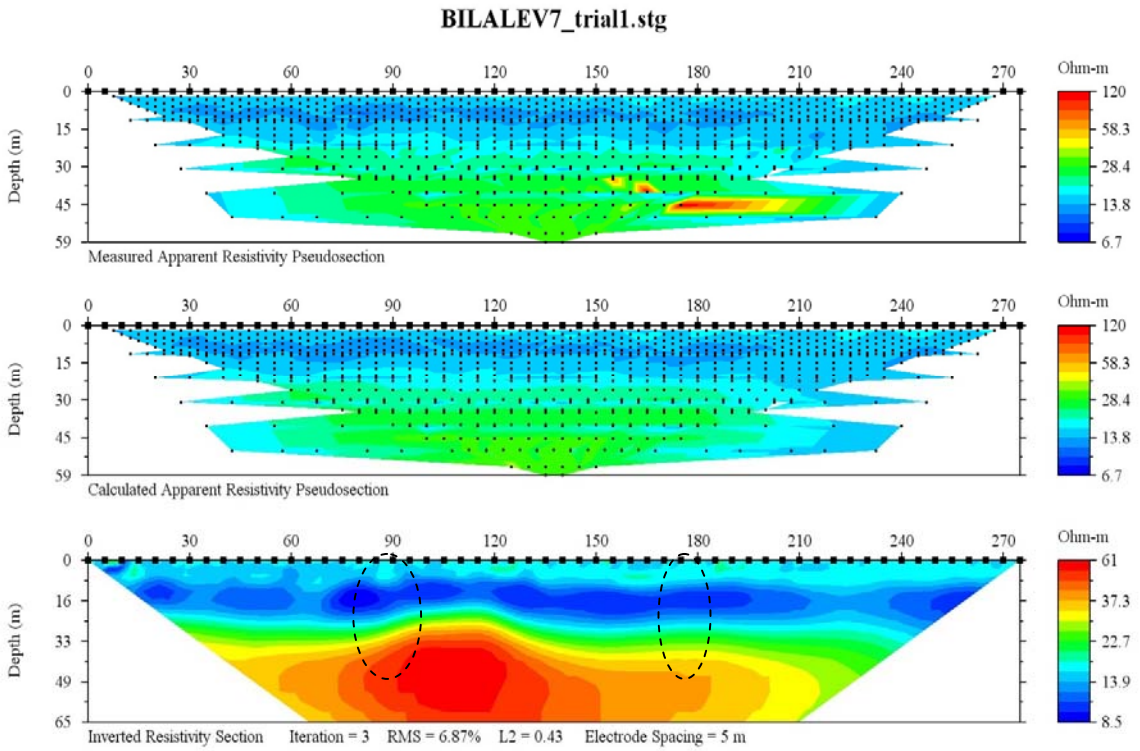

Figure 3.27: DDSG profile at line 3 at at Mr Umesh and Mr Sanjay's farm in Tubakeli showing a zone high resisity from 40-65 m depths (possibly bedrock) and surrounded intermediate resistive zone, suggesting weathered or fractured compositied. Areas low resistivity may indicated saturated overbank flood deposits. The dashed oval represent areas of possibile fractured systems as shown by 20-m VD peaks and hence, potential drill sites.

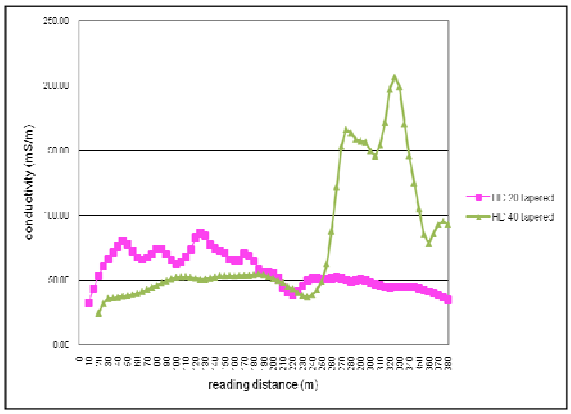

Figure 3.28: EM line 1 HD reponse at Tubakeli showing high anamolously high readings from 40-m separation suggetsing a fractured or sheared zone at around 30 m depth.

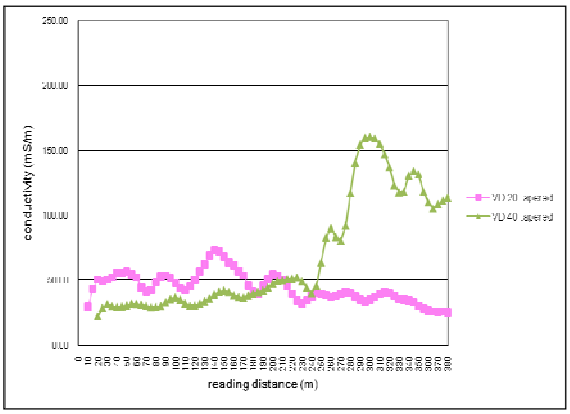

Figure 3.29: EM line 1 VD at Tubakeli consistenly showing anamolously high 40-m separation response and sugesting fractured basement.

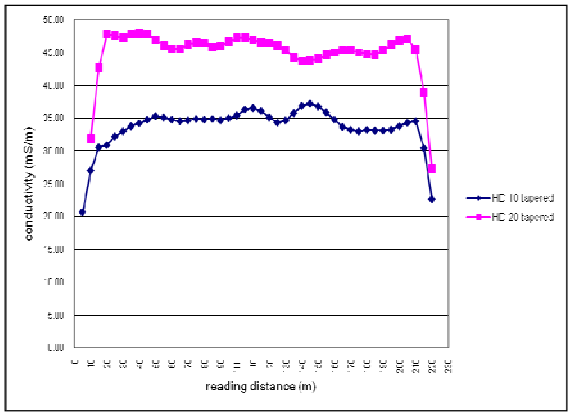

Figure 3.30: EM line 2 HD at Tubakeli showing relatively uniform and higher 20-m separation response sugest slight altered porosity at around 15 m depth. The lower 10-m response may suggest homogeneoeous material to 7.5 m depth (possibly overbank flood deposits).

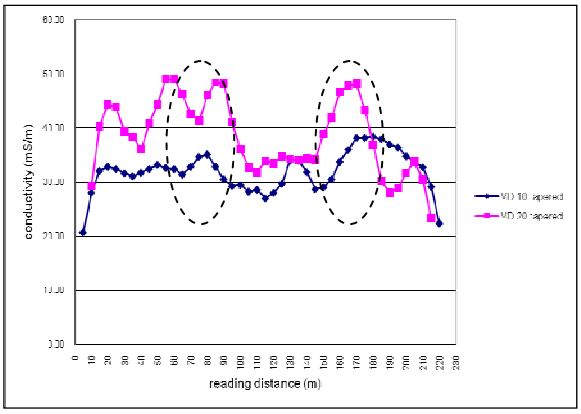

Figure 3.31: EM line 2 VD at Tubakeli showing fluctuating responses of 20-m separation and suggests presense of possibile fractured system around 35 m depth between 60-100 m and 150-180 m EM positions. Hence, two potential drill sites have been selected as denoted by dashed oval.

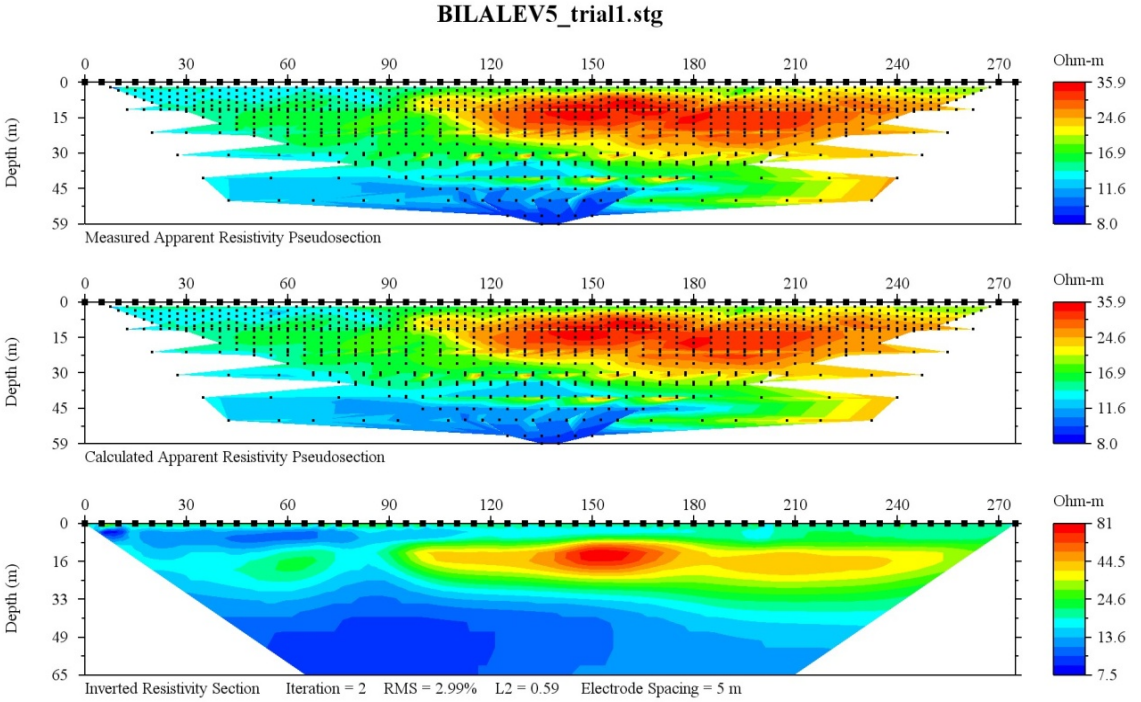

Figure 3.32: ER profile at Ashok Kumar's farm, Bila Rd, Bilalevu showing low resistive bedrock suggesting highly sheared or fractured basement unit between 60-90 m ER position with a band of with a zone of high resistivity, which may indicated a buried gravel bar.

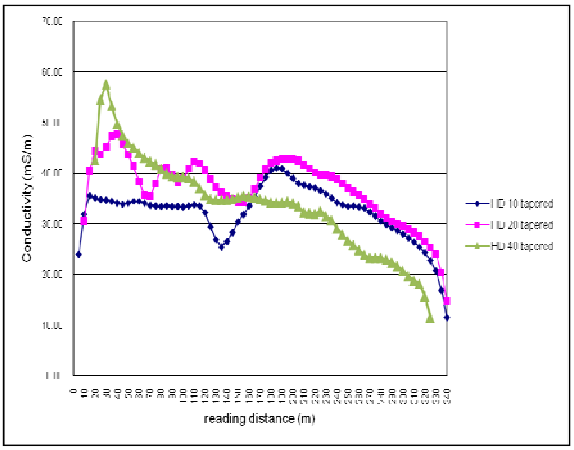

Figure 3.33: EM line 3 HD at Ashok Kumar BIla Rd, Bilalevu showing anamolously high 40-m and 20-m separation reponses in the first 60 m of EM positions suggesting fractured bedrock between 15-35 m whilst the decreasing response beyond 190 m represents the influence of buried highly resistive gavel band inferred by the ER profile.

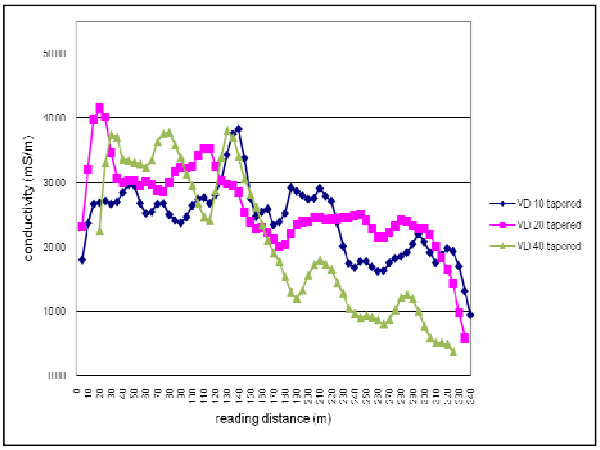

Figure 3.34: EM line 3 VD at Ashok, Kumar BIla Rd, Bilalevu showing a noisy dataset with relatively high 40-m and 20-m separation reponses in the first 100 m of EM positions suggesting fractured bedrock between 35-60 m whilst the decreasing response beyond 120 m represents the influence of buried highly resistive gavel band shown on the ER profile.

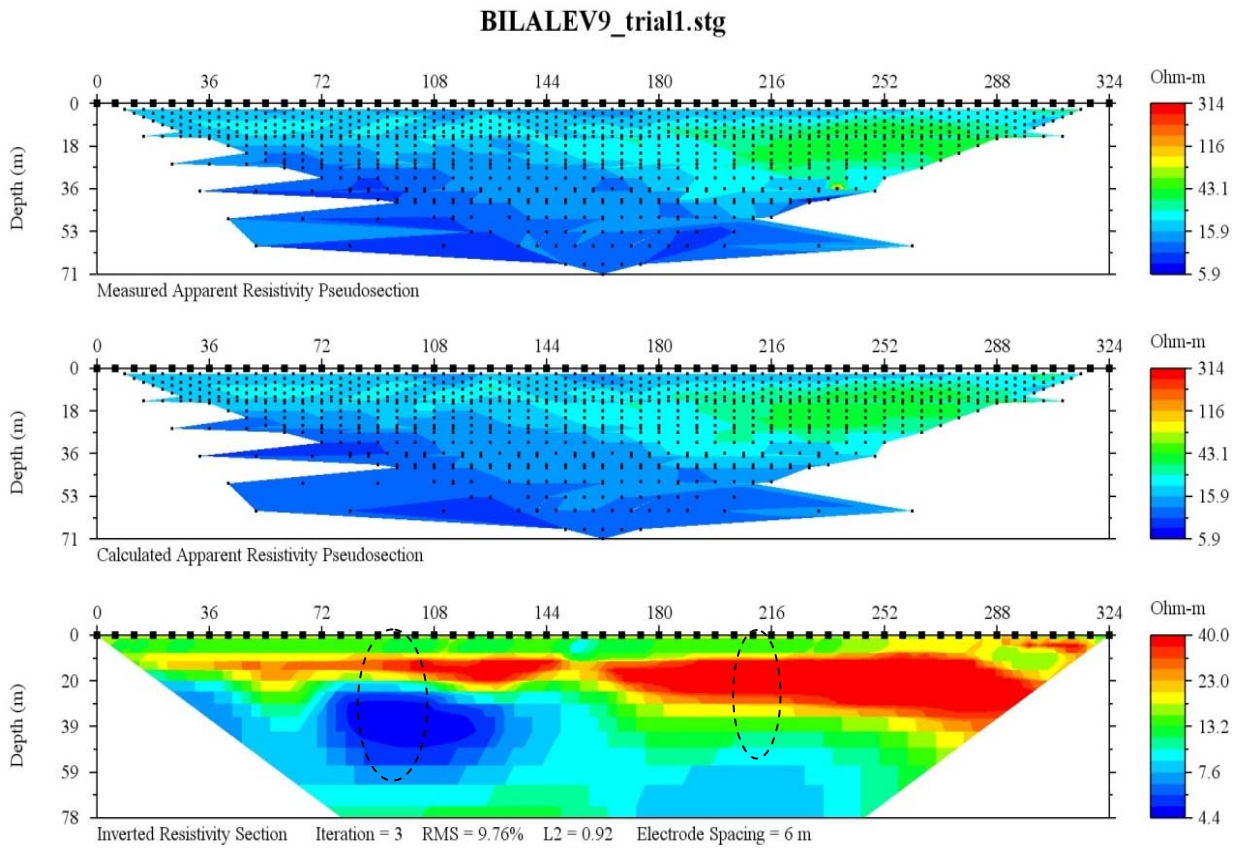

Figure 3.35: DDGS line 5 profile at Sugar Ram's farm at Bila Rd showing a possible sheared bedrock at 28-48 m depths between 72-110 m ER positions together with an inferred gravel bar characterised by very resistive zone around 10-20 m depths. Hence, two potential drill sites have been selected as denoted by dashed oval.

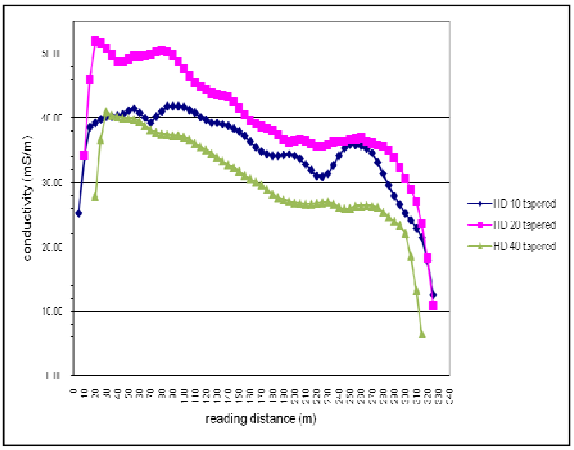

Figure 3.36: EM line 4 HD at Sugar Ram's farm, Bila Rd,Bilalevu showings a relatively high response of 20-m separation suggesting altered porosity at 15m depths whilst the decreasing responses of all coil separations towards the end suggests the influence of the buried gravels bar in attenuating the emmitted signals.

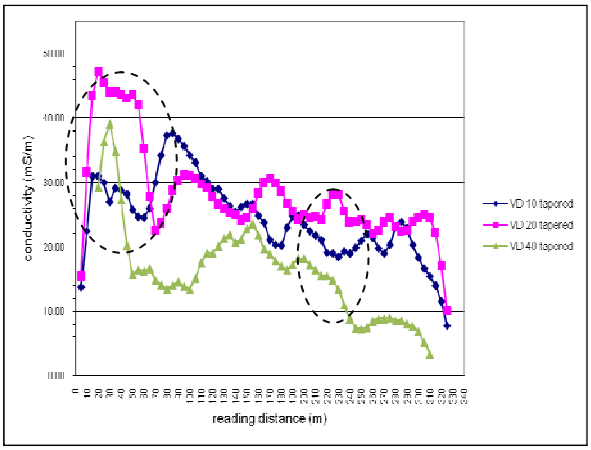

Figure 3.37: EM line 4 VD at Sugar Ram's farm, Bila Rd showing a noisy dataset with higher response of 20-m and 40-m separations supporting the the presence the sheared bedrock betwwen 35-60 m depth, while the decreasing trend towards towards the end of the line suggests the influence of the inferred gravel bar attenuating all the emitted electric currrent and hence, inducing low EM response for all coil separation. Two potential drill sites, denoted by dashed ovals, have been selected.

The above geophysical data and interpretations make three the contributions to the physical hydrogeology of the study area. First, the surficial low resistivity bands at Dubalevu and Tubakeli suggest 5-10 m silt-dominated alluvium, whilst the anomalously high resistivity band observed at Bila Rd, suggested a sandy gravel unit (potentially a buried river channel) between 10-20 m (a potential groundwater source). Second, the undulating and slightly weathered sedimentary basements are very well represented in the Dubalevu and Tubakeli ER profiles between 15-60m depth, whilst the anomalously low resistivity response in the Bila Rd basement suggest highly sheared or fractured unit at 30-60 m depth. Third, the fluctuating EM responses in all survey area, particularly with 20-m and 40-m separations, suggest that presence of fractured basements, and potential groundwater sources, in places between 30-60 m depth. Fourth, the above estimated fractured zones, particularly in Tubakeli and Bila Rd, are likely to be related to the sinistral ENE-WSW fault and its associated shear zone, which is believed to be propagating along Bila Rd and hence, suggesting the influence of structural controls on hydrogeological conditions.

3.3 Permeability test

3.3.1 Introduction

The "Falling head" method, suitable for testing the hydraulic conductivity (K) of fine grained soils, namely silts and clays (Mr David Bell, Senior Lecturer, University of Canterbury, pers.comm., 2009), was conducted on soil samples from Dubalevu and Bilalevu (previously classified in Chapter 1) to determine:

- K of the capping soil; and
- the rate of vertical recharge via infiltration from meteoric and irrigation water

3.3.2 Methodology

Soil samples were collected insitu after mud pits of a several drill holes, namely10/07, 10/12 and 10/15, were dug (Figure 3.38). The permeater cell was carefully driven onto the 2 m × 1 m × 1 m mud pit wall to procure the samples. Samples were trimmed on both sides of the cells before adequate compaction, using compaction hammer, was applied to prevent having air spaces and leakages on the sides. Wire gauze was placed on both sides of the permeater cell before it was placed in the cage and was clamped evenly to the top by a clamping plate. The top inlet of the permeater cell was connected to a stand pipe, which in turn was connected to a storage tank. The permeater was immersed in to bucket of water to assist de-airing: a discharge outlet was made on the side of the bucket slightly above the top of permeater cell to which the bucket was filled. The sample was saturated (through the standpipe water from the storage tank) for 24 hours. The top inlet of permeater was closed using a pinch clip before the standpipe was filled to a suitable level, disconnected from the storage tank and placed at a known height. The initial level of the standpipe (h_0) was recorded before the timer started upon the release of the pinch clip and the instantaneous change in head (h) was measured at different times.

The formula used to determine K of the tested sample is

$$K = (a/A)\times(L/t)\times\ln\{h_0/h\} \text{ or } K = 2.3\ (a/A)\times(L/t)\times\log_{10}\{h_0/h\}$$

where K = hydraulic conductivity (m/s)

a = standpipe area (m^2)

A = sample cross sectional area (m^2)

L = sample thickness or height (m)

h_0 = initial head above top of sample (m)

h = measured head during or at the end of test (m)

t = elapsed time from h_0 to h (sec)

3.3.3 Results

Site	Hydraulic conductivity (K) (m/s^{-1})
Dubalevu	7.8×10^{-8}
Tubakeli	2.2×10^{-7}
Bila Rd	4.3×10^{-8}

Table 3.4: measured K using the WF26010 Falling Head permeability cell showing low K values and suggesting relatively slow infiltration from meteoric and imported waters through the vadoze zone (test results area shown in Appendix E).

The above result makes a major contribution to the physical hydrogeology of the Middle Sigatoka Valley. The low permeability values suggest that infiltration of meteoric and irrigation water through the silt-dominated soil and vadoze zone will be relatively slow.

3.4 Groundwater drilling, development and evaluation

3.4.1 Introduction

This section denotes the methods and results of groundwater drilling, development (through construction and flushing) and hydrogeologic pumping test assessments.

3.4.2 Methodology

3.4.2.1 Groundwater drilling

The objectives of the groundwater drilling were to:

- validate the inferences of geophysical surveys;
- assess lithological samples in relation to surface geological units; and
- determine the depth and thickness of aquifers (if any).

Borehole depths were targeted to either completely or partially penetrate the inferred alluvial and fractured sedimentary units. The drilling of nine boreholes within the Dubalevu and Bilalevu areas was conducted through the mud-rotary circulation method (Figure 3.38). Boreholes were targeted for 203 cm outside diameter (OD) to permit the use of maximum possible pump size and leaving adequate allowance for the depth probes during the evaluation stages. However, inadequate supply of 203 cm plain and slotted piping resulted in the drilling only one 203 cm OD borehole, namely 10/07, with the rest of the boreholes wells drilled to 152 cm OD. Drilled cuttings were collected at one meter intervals and washed for lithological description. Geological contrasts, including abrupt changes in lithological properties, were noted relative to possible groundwater occurrence and movement. Several disadvantages were encountered with the drilling methods including:

- samples contamination by mud such that the presence of fine materials were difficult to recognize;
- distorted representation of drill cutting samples due to the high level of mixing from sediments and samples from layers above the drilled depth; and
- tendency of drilling mud to infiltrate the investigate aquifer systems causing difficulty to remove deeply infiltrated mud during well development (Davies, 1989).

3.4.2.2 Well construction and development

Wells were constructed/developed to ensure the longevity and stability of the boreholes. Locally purchased plain and 3 mm slotted PVC pipes were used before adequate gravel packing was applied to act as groundwater filters. Cement grouting was applied on the top 2 m of every borehole to avoid the infiltration of storm water into the boreholes before borehole caps were installed for well protection. All boreholes were adequately purged (Figure 3.42) through compressed air, together with the use of surging and jetting tools, to clean well screens, permit the settling of gravels outside the screens and to ensure that low groundwater turbidity is maintained prior to the evaluation stage During the flushing stages, well potential estimates were determined in order to select the most appropriate pump-size for subsequent groundwater evaluation (Table.3.5).

3.4.2.3 Aquifer evaluation via pumping tests

This was conducted on six of the nine recently installed wells with the following objectives:

- to calculate the aquifer properties, namely transmissivitiy (T), storativity (S) and hydraulic conductivity (K); and
- to establish the potential of the aquifer and permit the collection of chemical and isotope samples.

A mono-pump, powered by Lister-Petter engine, with a maximum capacity of 11 L/s, was used to evaluate wells 10/07 and 10/12 (Figures 3.43 & 3.44). Boreholes 10/08 and 10/13 were evaluated using a 1 L/s pump due to their low well potential estimate, whilst a 3 L/s Grunfos submersible pump was used to 10/14 and 10/15 (Figure 3.45). The pumps were lowered down to the middle of the inferred aquifer to capture maximum aquifer flow. Step drawdown tests were conducted on boreholes 10/08 and 10/13 to select the ideal discharge rate to be used during the long-term test, while the unavailability of a suitable sized pump for 10/14 and 10/15, as well as the difficulties of the inserting and retrieving the depth-probes (due to the vibration of mono-pump column pipes) into 10/07 and 10/11 prevented the step-drawdown analysis. Hence, these boreholes were analysed for long-term constant-rate tests (as per well estimate in Table 3.5), whilst the nearest available boreholes (10/10 and 10/12, respectively) were monitored full-time for drawdown and recovery responses. Solinist depth probes, stop watches and a 14 L bucket and a 200 L drum were used to

measure pre-pumping static water levels together with depth to water table and discharge during the pumping tests (Figures 3.46 & 3.47). Aquifer parameters (T, K and S) were estimated by either the Theiss curve-matching method or the Cooper-Jacob straight-line approximation or both, depending on the availability of an observation well.

3.4.2.4 Groundwater monitoring

Groundwater levels were monitored during two periods, namely 31/08/10 and 02/10/10 (Tables 3.7 & 3.8). In each period water levels were measured for a number of wells in Dubalevu and Bilalevu to generate the potentiometric surfaces in these two areas. Water level measurements, taken at the top of PVC pipe casing, were taken using a Solinist TLC model dipper and measurements were taken before PDW in Bilalevu were pumped for drinking purposes with all irrigation sources in Dubalevu not currently used due to pump problems. Locations and elevation data of the wells were captured using Garmin76 GPS device for GIS use. Water levels measured from the two monitoring periods were imported into Golden Software Surfer 9.0 to create contour surfaces, which, in turn, were exported in a compatible format to be used for GIS purpose in MapInfo10.0.

3.3.3 Results

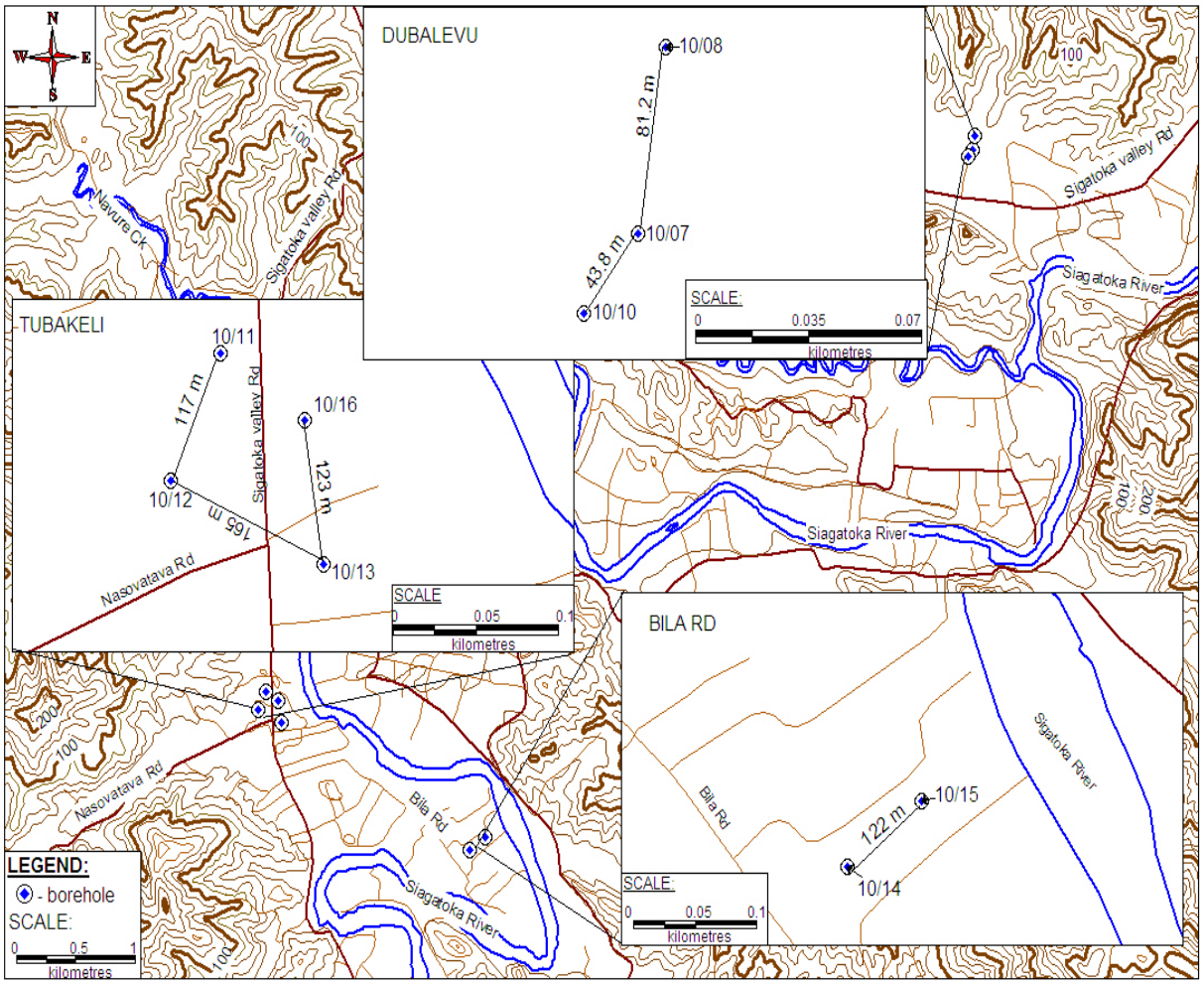

Figure 3.38: Location of boreholes with unique numbers (depth): three (3) in Dubalevu (10/07 (34 m), 10/08 (28 m) and 10/10 (36 m)), Tubakeli (10/11 (41 m), 10/12 (43 m). 10/13 (31 m) and 10/16) and Bila Rd (10/14 (60 m) and 10/15 (35 m)).

Well Number	Location	Depth (m)	Outside diameter (mm)	Aquifer thickness (m)	Estimated Flow (L/s)
10/07	Dubalevu	34	203	10	6-7
10/08	Dubalevu	28	152	5	0.3-0.5
10/10	Dubalevu	36	152	11	-
10/11	Tubakel	41	152	3	3-4
10/12	Tubakeli	43	152	5	4-5
10/13	Tubakeli	30	152	3	0.4-0.6
10/14	Bila Rd	60	152	5	3-4
10/15	Bila Rd	35	152	6	1.8-2
10/16	Tubakeli	31	152	1	0.05-0.1

Table 3.5: summary of drilled wells around the Dubalevu, Tubakeli and Bila Rd areas with the well potential estimates attained from well flushing. Note that the estimated aquifer thicknesses are estimated from zones of concentrated geological contrasts as per well lithological log (Individual well logs are shown in Appendix F).

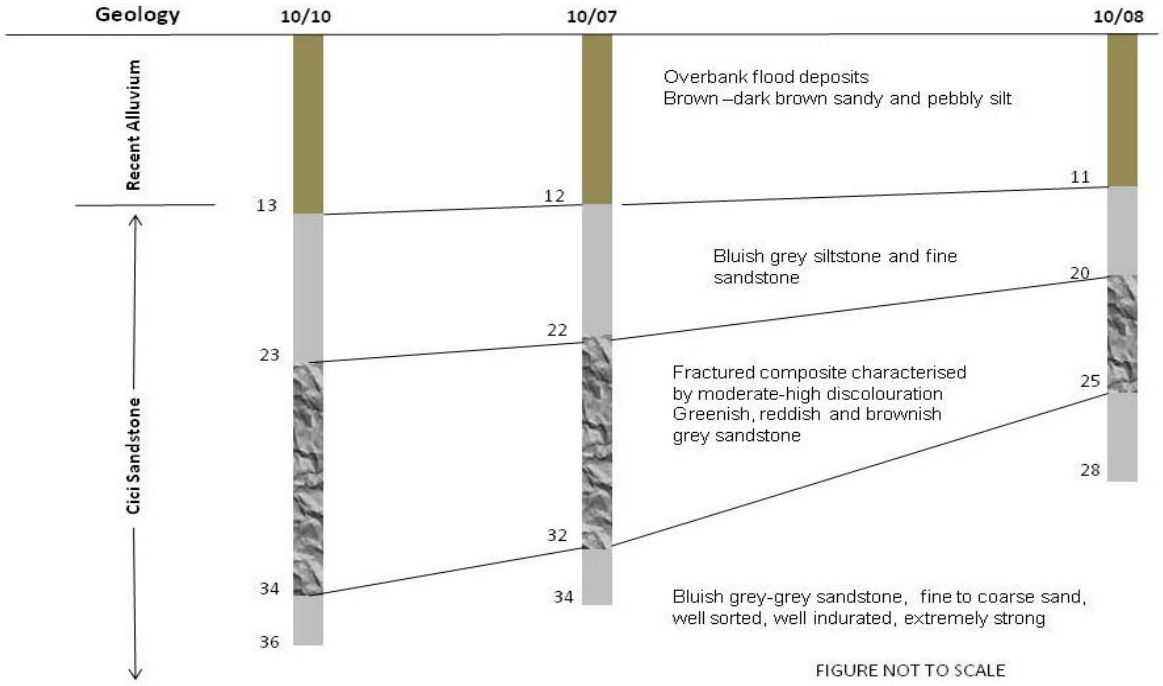

Figure 3.39: Dubalevu stratigraphic logs showing an 11-13 m thick surficial confining unit, composed of flood overbank deposits, overlying an intermediate confining unit of fresh interbedded siltstone and sandstone of around 10 m thickness and underlain by the fracture composite of the CS with 5-11 m thickness (Individual well logs are shown in Appendix F).

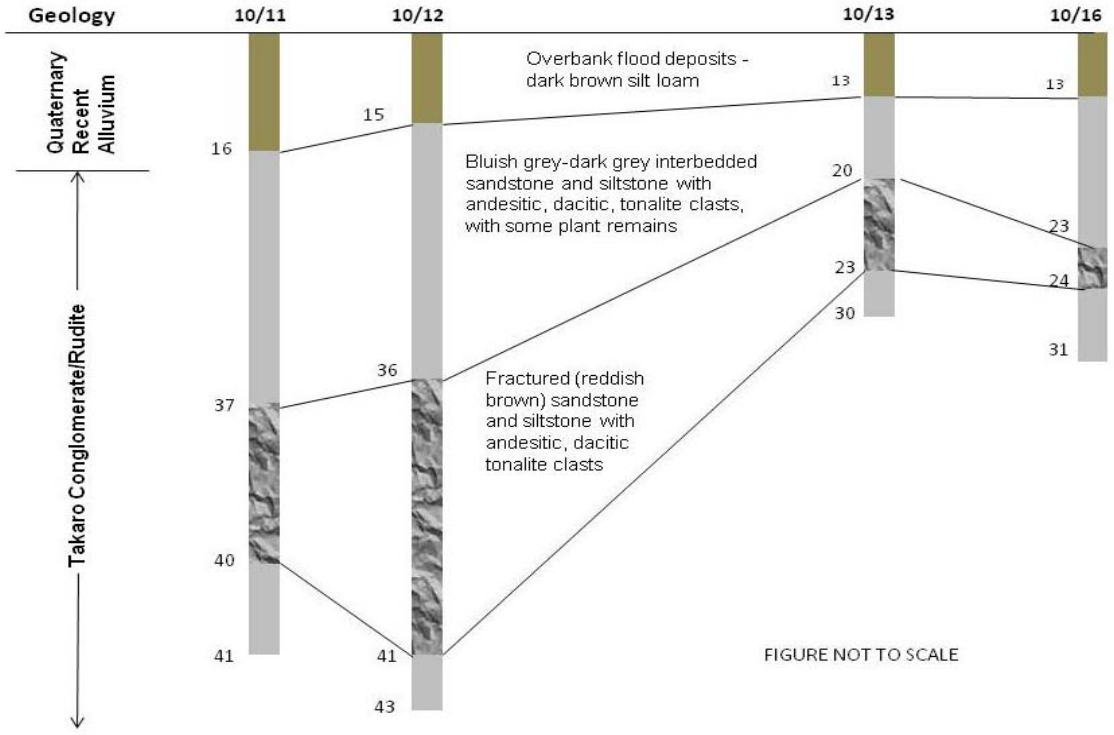

Figure 3.40: Tubakeli stratigraphic logs showing surficial confining unit, composed of flood overbank deposits overlying intermediate confining unit of fresh interbedded siltstone and sandstone and, in turn, underlain by the fracture composite of the TCR.

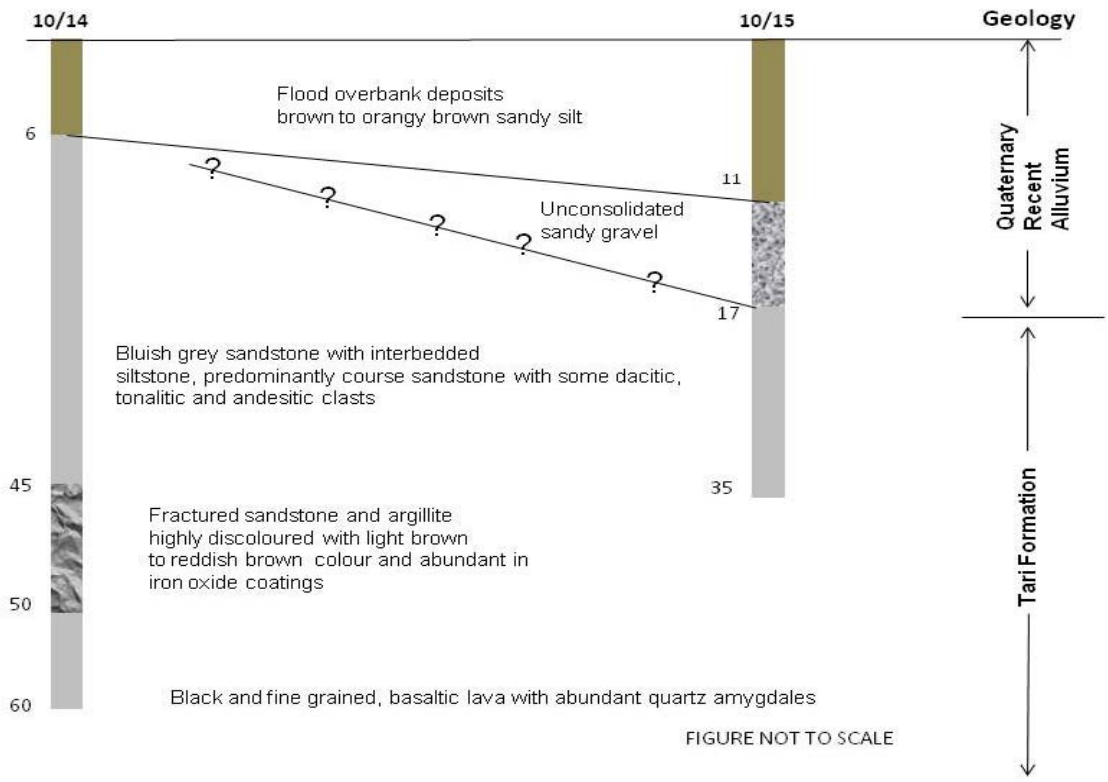

Figure 3.41: Bila Rd stratigraphic logs showing the surficial confining unit, composed of flood overbank deposits, a 6 m thick alluvial aquifers, comprising unconsolidated sandy gravels, which in turn are underlain by an intermediate confining unit and the fractured composite of the TF that is penetrated between 45 and 50 m in 10/4. (Individual well logs are shown in Appendix F).

Figure 3.42: well flushing of BH 10/13 at Tubakeli, Bilalevu.

Figure 3.43: installation of mono-pump in BH 10/07 at Dubalevu by MRD's drill crewmen.

Figure 3.44: test-running the mono-pump prior to constant rate test. Step-drawdown tests were not conducted at 10/07 and 10/12 due to the vibration of column pipes and preventing the free insertion and retrieval of depth probes. Hence, 10/10 and 10/11 were monitored for drawdown and recovery analysis.

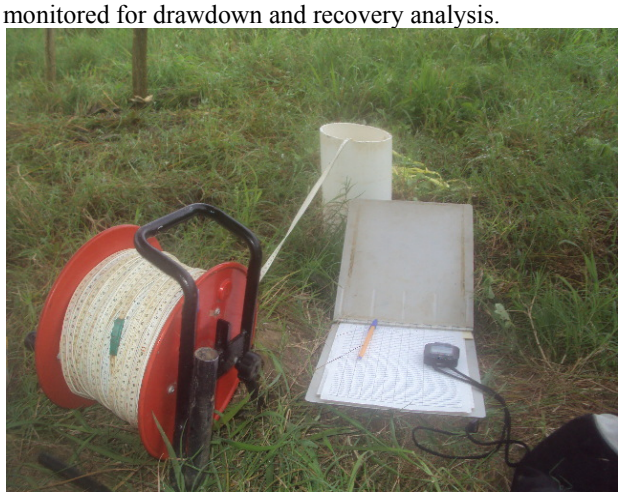

Figure 3.46: TLC Solinist depth probe with stop watch, and data sheet on which drawdown and recovery data are recorded during the observation of 10/11 in response to the constant-rate pumping at 10/12.

Figure 3.45: assembling electrical submersible pump and accessories before lowering into the borehole 10/14, Bila Rd, Bilalevu.

Figure 3.47: using the volumetric method through filling up a 200 L drum and a timer, to determine the mono-pump discharge rate. Variability in discharge rate was common due to human errors and mechanical responses of pump impellers, due to kinked canvass hose and moderate suspended materials at suction level.

Pumping well (pw)	10/07	10/08	10/12	10/13	10/14	10/15
Observation well	10/10	10/07	10/11	10/12	10/15	-
Pump setting depth	30	23	36	29	47	30
Distance to pwl (m)	43.8	81.2	117	165	122	-
Q (L/s)	10.6	0.57	5	0.9	1.4	1.85
Test duration (mins)	1140	575	1320	920	1230	920
T (m^2/d^{-1})	8.2–29.1	1.14-5.22	19.3-53.5	10.4-21.8	23.3-74	1338.4-1949.5
S	2.3×10^{-4}	4.3×10^{-4}	6.7×10^{-4}	8.9×10^{-4}	1.7×10^{-3}	-
	4×10^{-4}	-	8.6×10^{-6}	-	-	-
K (m/d^{-1})	0.82-2.9	0.23-0.69	4.3-11.9	2.6-5.5	4.7-13.5	223.1-324.9

Table 3.6: summary of aquifer parameters derived from constant-rate pumping and recovery tests data.(Results of all tests is shown in Appendix G) Hydraulic conductivity (K) calculation for attained using the average aquifer thickness of pumping and observation wells. Storativity, where (h_0 –h) and t were derived from W(u) = 1 and 1/u = 1 match point, was only calculated from drawdown recorded in the available observation wells whilst the two estimates for 10/10 and 10/11 represent drawdown and recovery as they monitored full-time for drawdown and recovery analysis . BH 10/12 showing a significantly lower aquifer response during the recovery analysis suggesting that the aquifer was pumped beyond its capacity and hence, recharge is low. The pumping of 10/15 did not induce drawdown at 10/14 suggesting abundant recharge from the adjacent Sigatoka River, supported by high T and K values. Hence, the estimation of S through the use of Theiss match-curve was not made.

Name	31/08/10 water Level (m)	02/10/10 water level (m)
10/07	6.82	7.48
10/08	7.32	8.19
90/15	9.51	10.35
90/16	9.1	9.89
89/15	7.55	8.11
10/10	6.42	7.26
89/27	7.57	8.25
91/17	8.98	9.85
91/18	9.28	10.17
89/23	9.34	10.29
91/15	10.24	11.1
91/14	10.01	10.9

Table 3.7: groundwater level measured at Dubalevu. Wells 10/07, 10/08, and 10/10 are recently drilled and have not been used; 89/15/, 90/15 and 90/16 are unused irrigation sources due to non-operational mono-pumps and the others are monitoring bores. The measurements show a decline in groundwater head from August to October, which can be attributed to reduction in groundwater recharge due to low rainfall in the dry period and suggests the sensitivity of the aquifer to climatic variability.

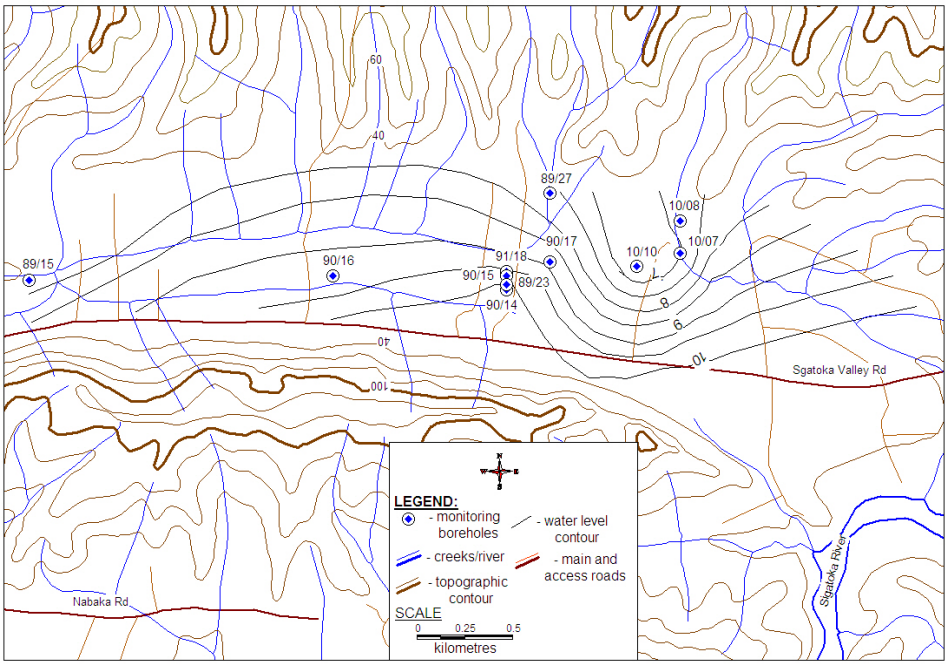

Figure 3.48: Dubalevu water level contour derived from the average of the two measurement periods and showing a NW-SE flow direction towards the Sigatoka River.

Site	31/08/10 water level (m)	02/10/10 water level (m)
10/11	8.37	8.35
10/16	8.4	8.45
10/14	11.4	11.39
10/15	11.45	11.92
Arjun Lal residence	8.5	8.52
Tubakeli Water Project	4.17	5.32
10/12	6.02	6.19
10/13	8.32	8.07
Mahen's Export	5.64	6.13
Manoj Kumar	11.42	11.35
Ashok Kumar	12.42	12

Table 3.8: groundwater level measured at Bilalevu. Five private wells, currently used for drinking purposes were monitored with measurements taken before daily pumping started to avoid any pumping effect. Wells 10/11 – 10/16 are recently drilled and have not been used. The readings showed minor fluctuations in water level from August to October. These variable responses can be attributed to complexity of groundwater flow conditions and proximity to some local recharge sources.

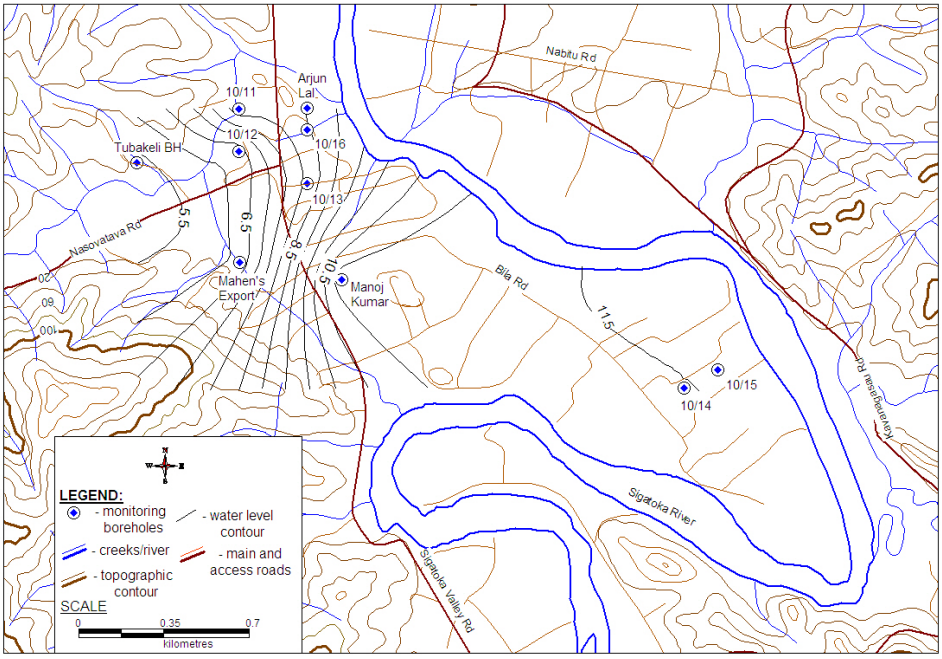

Figure 3.49: Bilalevu water level contour, taken from the averages of the two monitoring periods, showing WNW-ESE flow direction towards the Sigatoka River.

The results and interpretations presented in this section make four major contributions to the physical hydrogeology of the Middle Sigatoka Valley. First, the groundwater drilling permitted the exploration of four major hydrogeological units. These include namely surficial (silt-dominated confining units, alluvial aquifer system (unconsolidated sandy gavels), intermediate confining unit (unweathered sedimentary units) and fractured sedimentary basement. Second, pumping tests showed variable flow and storage capacities of the investigated geological units governed by primary and secondary porosities, preferential flows, heterogeneity of groundwater systems, and limited recharge. Third, the flow of groundwater towards the Sigatoka River, in both the monitored areas, suggests that river flow is composed of groundwater discharge. Fourth, the decline of groundwater level in most of the monitored wells in the two dry season months suggest that groundwater is responding to climatic conditions and hence, a relatively shallow groundwater system.

3.5 Water chemical sampling and analysis

3.5.1 Introduction

The chemical composition of groundwater is a function of bedrock composition, flow conditions and aquifer residence time (Andreo & Carrasco, 1999). This section presents the methodology and results of chemical samples collected from the study area in an effort to:

- determine the hydrochemical facies present in the study area;
- evaluate surface and groundwater interaction; and
- determine the spatial variability of groundwater chemistry and its possible causes.

3.5.2 Methodology

Forty-seven water collection sites within the study area, including groundwater, creek, river, oxbow lakes and springs, were sampled (with duplicates) from September 2009 to January 2011 for chemical analyses. Oxbow lakes, creeks, rivers, were sampled on the surface whilst springs were sampled at either discharge points or dams (Figures 3.52 & 3.54). Groundwater pumps were run to adequately purge boreholes and to allow the collection of aquifer water (Figure 3.53). Sampling site locations were determined using a Garmin 76 GPS device, whilst physico-chemical parameters, namely temperature, pH, salinity and electrical conductivity (EC) were measured using a HORIBA multi-meter probe (Figure 3.51). Samples, filled in 1 L screw-cap plastic bottles (Figure 3.54), having properly labeled and stored, were submitted to the MRD's geochemical laboratory for dissolved ionic concentration, pH, electrical conductivity, total dissolved solutes (TDS), total hardness (TH) determinations. Major ions, including calcium, magnesium, sodium, potassium, bicarbonate, sulfate and chloride, were analysed at MRD's geochemical laboratory through various analytical procedures, including titration, filtration, and colometric determination methods, adopted from the "2005 Standard for analyzing water and wastewater" (Raksha Rani, Chemist, MRD, pers.comm, 2011 Chemist, Mineral Resources Department). The results, having ionic charge balance error of less than 10% (deemed a satisfactory for hydrochemistry interpretation (Hiscock, 2005)), were input into Microsoft Excel

spreadsheets, which were later used to produce piper plots, stiff plots, contour surfaces and variability maps (Golden Software Surfer 9.0, USGS GW_chart, and MapInfo 10.0).

3.5.3 RESULTS

Site, Location	Depth (m)	Location	Source	ID	pH	EC (µS/cm)	Salinity (%)	Temp (°C)
Tubakeli Project	35	B	GW	B1	7.1-7.3	367-410	0.01	27-27.2
Tore Project	37	B	GW	B2	6.9-7.4	369-419	0.01	27-27.2
Manoj Kumar	39	B	GW	B3	7.5	465	0.01	27.1
Waiwai Project	23	B	GW	B4	6.9-7.1	440-473	0.01	27-27.2
Tavuto Project	47	B	GW	B5	6.9-7.3	510-514	0.02	26-26.8
Bulatale Store	40	B	GW	B6	6.8-7.4	282-393	0.01	27.5-29.1
Shiu Shankar	40	B	GW	B7	6.8-7.3	350-383	0.01	26.8-28.3
Ashok Kumar	20	B	GW	B8	5.9-6.6	201-254	0	27.5-27.6
Mahen's Export	40	B	GW	B9	7-7.2	578-638	0.02	28.5-30
Shiu Prasad	43	B	GW	B10	7.1-7.2	343-421	0.01	26.2
Sunil Prasad	45	B	GW	B11	7.5-8	381	0.01	27.2
Arjun Lal	20	B	GW	B12	6.7	279	0.01	29.5
SVHS	30	B	GW	B13	Nm	Nm	Nm	Nm
Oxbow Lake	0	B	OL	B14	7.3-7.7	31-136	0	26.8-30
Bilalevu Meander	0	B	Rr	B15	6.9-7.9	113-184	0	26.7-31.4
BH 10/12	43	B	GW	B16	7.5-8.5	240-280	0.01	25.5-27.1
BH 10/13	30	B	GW	B17	7.6-7.9	380-403	0.01	26-27
BH 10/14	60	B	GW	B18	7-6-8.1	370-385	0.01	26.6-28
BH 10/15	35	B	GW	B19	6.4-8	288-300	0.01	27.5-28
Ami Chand	60	D	GW	D1	6.3-7.8	350-389	0.01	27-28
BH 90/15	40	D	GW	D2	6.1-6.9	243-294	0-0.01	26.2-26.6
BH 90/16	45	D	GW	D3	6.1-7.2	260-279	0.01	26.2-30.7
BH 89/15	43	D	GW	D4	6.6-6.9	315-341	0.01	26.6-27.5
BH 10/07	34	D	GW	D5	7.1-7.7	243-248	0	25-26.3
BH 10/08	26	D	GW	D6	6.1-6.8	224-299	0.01	25-26
Jubairata village	38	D	GW	D7	7.3	404	0.01	28.7
MPI Station	40	D	GW	D8	6.8-7.5	363-396	0.01	27-28.2
Raunitogo meander	0	D	Rr	D9	7.34	189	0	28.1
Jubairata meander	0	D	Rr	D10	7.2-7.4	150-212	0	27-27.8
Nakavika settlement	26	Na	GW	Na1	6.8-7.5	394-407	0.01	26.5-27.2
Qalitala Creek	0	Na	Ck	Na2	7.1-7.4	147-171	0	27.1
Oxbow Lake	0	Na	OL	Na3	7.2-7.5	63-82	0	27.8-32
Janmin Jay	40	Na	GW	Na4	6.5-7.8	257-327	0.01	27-30.7
Paras Ram	18	S	GW	S1	7.3-7.6	304-310	0.01	27.8-28
Hari Chand	40	S	GW	S2	6.4-7.1	580-592	0.02-0.03	27-27.5
Nabitu Community	27	Nb	GW	Nb1	6.9-7.6	397-477	0.01	27.1-28.6
Kamal Kishor	40	Nb	GW	Nb2	6.9-8.3	400-653	0.01-0.02	27.5-27.9
Pramend Singh	25	Nb	GW	Nb3	6.7-7.1	293-388	0.01	27.2-28.2
Nabitu Primary Sch	30	Nb	GW	Nb4	7.1-7.4	406-421	0.01	27.2
Anil Prasad	40	Nb	GW	Nb5	6.5-7.2	182-187	0	27.5-28
Ram Deo	37	Nb	GW	Nb6	7.12	301	0.01	27.6
Koroira Spring	0	Q	SP	Q1	7.7-8.5	250-256	0	23.4-24.1
Nacule Spring	0	Q	SP	Q2	7.1-7.4	310-315	0.01	25.3-25.6
Matanitavuni Spring	0	Q	SP	Q3	7.15	390	0.01	24.9

Mataukaba Spring	0	V	SP	V1	7.7	229	0	25
Navala Spring	0	M	SP	M1	7.5-7.6	355-392	0.01	24.1-25.5

Table 3.9: sampled water sources (groundwater (GW), oxbow lakes (OL), creeks (Ck), river (Rr) and springs (SP)) from Bilalevu (B), Dubalevu (D), Nabaka (Na), Siminilaya (S), Nabitu (Nb), Qalimare (Q), Vunarewa and Mavua (M) with unique ID. Physical water properties were measured using Horiba multi-meter probe. Sigatoka Valley High School (SVHS), drilled in 2008, was neither samples nor measured (Nm) for physical parameters but chemical results from pumping tests will be used.

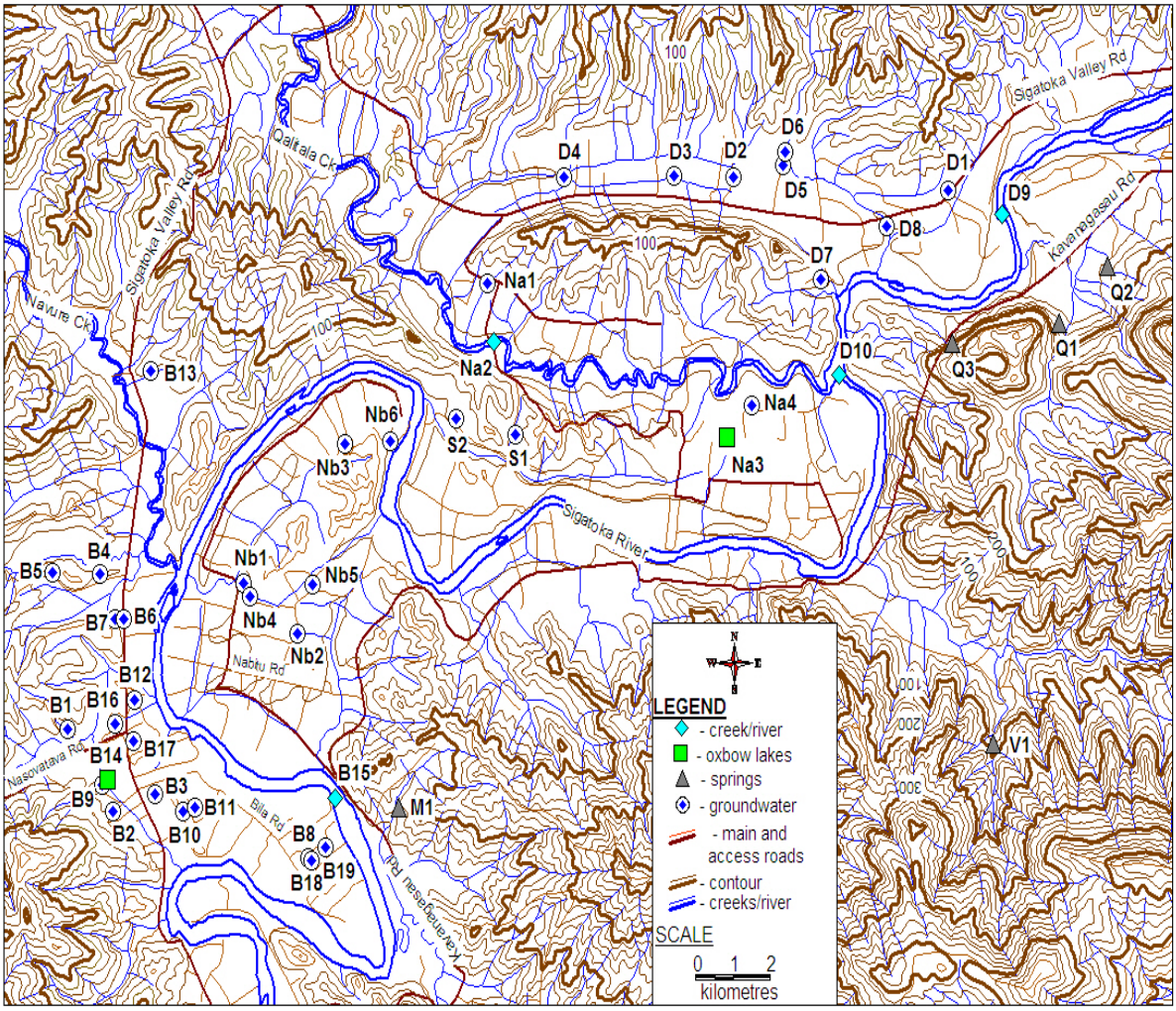

Figure 3.50: Location of map of chemical sampling sites with Site ID. Details of the sites and physical water parameters are shown in Table 3.9.

Figure 3.51: measuring water physical parameters using multi-meter Horiba at an oxbow lake, Nabaka (Site ID: Na3, Figure 3.50).

Figure 3.52: sample collection at Raunitogo meander, Sigatoka River (Site ID: D9, Figure 3.50).

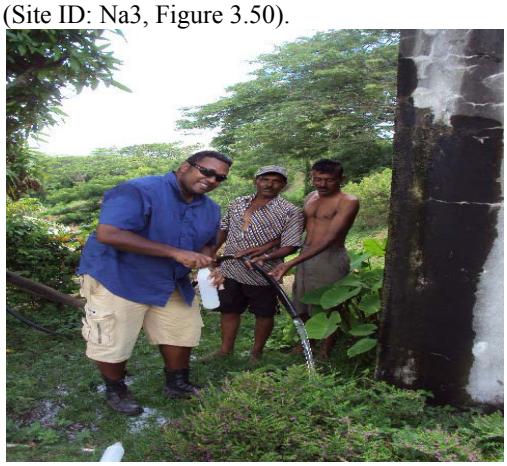

Figure 3.53: sample collection at Pramend Singh's borehole, Nabitu after adequately purging the borehole (Site ID: Nb3, Figure 3.50).

Figure 3.54: sample collection at Navala Spring, Mavua using 1 L plastic bottle (Site ID: M1, Figure 3.50).

Location	Natadola Harbour	Natadola Harbour
Region	SW Viti Levu	SW Viti Levu
Season	Wet	Dry
pH	5.4625	5.24
HCO_3^- (mg/L)	0.9475	1.2275
Ca^{2+} (mg/L)	0.1725	0.0925
Cl^- (mg/L)	1.2275	1.775
EC (µS/cm)	6.85	9.6
Fe^{2+} (mg/L)	0.035	0.0275
Mg^{2+} (mg/L)	0.065	0.065
Mn^{2+} (mg/L)	0.02	0.0275
K^+ (mg/L)	0.11	0.1925
Si (mg/L)	0.065	0.06
Na^+ (mg/L)	0.63	0.9375
SO_4^{2-} (mg/L)	0.735	0.7725

Table 3.10: chemistry of bulk precipitation measured at Natadola Harbour, SW Viti Levu (Waterloo et al., 1997). The average Cl^- of 1.5 will be used to assess the variability in Cl^- content of 2 rainwater samples collected whilst the average pH of 5.35 can be used as a reference to assess the evolution of groundwater from slightly acidic (<7), base (7) to alkaline (>7) as controlled by complexity of flow and variability in bicarbonate exchanges.

Site ID	Nb1	Nb2	Nb3	Nb4	Nb5	Nb6	Q1	Q2	Q3	V1	M1
pH	7.3	7.1	7.0	7.2	6.6	6.9	8.0	7.2	7.2	8.5	8.1
HCO_3^- (mg/l)	333.9	335.4	266.1	341.6	127.0	220.6	203.9	262.8	263.3	187.1	329.4
CO_3^{2-} (mg/l)	0.0	0.0	0.0	0.0	0.0	0.0	0.0	0.0	0.0	0.0	0.0
Ca^{2+} (mg/l)	79.0	91.1	61.9	73.2	23.9	57.0	59.5	78.6	75.8	47.2	66.6
Cl^- (mg/l)	15.4	6.9	10.9	8.4	5.3	18.8	4.4	4.4	5.0	1.3	2.4
EC (µS/cm)	561.8	525.5	449.8	531.5	220.8	401.5	323.0	404.0	407.0	296.0	481.0
Fe^{2+} (mg/l)	0.0	0.0	0.0	0.0	0.0	0.0	0.0	0.0	0.0	0.0	0.0
Mg^{2+} (mg/l)	11.3	7.3	8.6	14.4	7.5	7.7	3.5	3.6	3.6	4.5	16.2
Mn^{2+} (mg/l)	0.0	0.0	0.0	0.0	0.0	0.0	0.0	0.0	0.0	0.0	0.0
K^+ (mg/l)	0.9	0.7	0.6	1.0	0.4	0.5	0.4	0.4	0.9	0.8	0.6
SiO_2(mg/l)	31.6	43.9	34.5	34.0	40.7	40.2	17.4	19.2	22.9	28.9	32.6
Na^+ (mg/l)	29.8	16.4	23.5	30.0	12.7	29.4	12.6	9.7	12.8	21.0	24.0
SO_4^{2-} (mg/l)	8.5	1.3	3.5	0.0	0.5	6.5	0.0	0.0	0.0	0.0	0.0
TH	243.8	257.5	190.3	242.0	90.8	173.5	163.0	211.5	204.0	136.0	233.0
TDS	347.3	325.3	278.3	329.0	136.5	247.5	200.0	250.0	252.0	183.0	298.0

Table 3.11: chemical results from water sources in Nabitu (Nb), Qalimare (Q), Vunarewa (V) and Mavua (M). Nb5, drilled to 40 m and adjacent to numerous groundwater sources, and recording relatively low pH, EC and HCO_3 suggests direction recharge from surface sources (having similar compositions to D9 and D10) as controlled by fractures systems that is hydraulically connected to the Sigatoka River. (Individual results are provided in Appendix I).

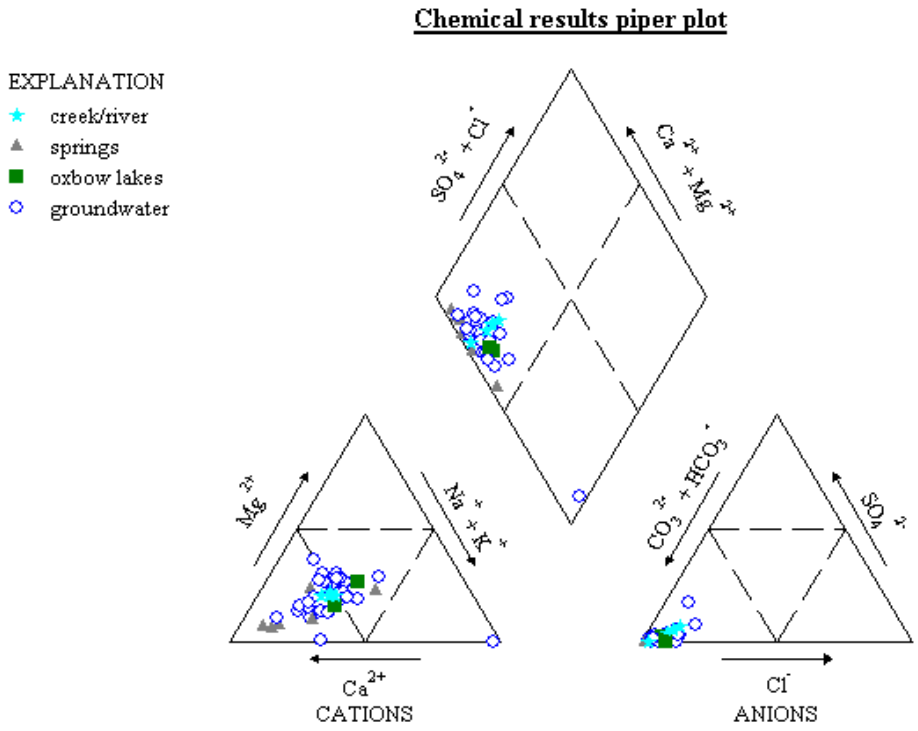

Figure 3.55: piper plots of collected chemical samples (generated in USGS GW_chart program). The samples are dominated by $Ca(HCO_3)_2$ type water, suggesting dissolution of calcite in the sedimentary units, with a number of samples occupying the "non-dominant type" zone, suggesting mixing from different cations sources at depths. One (1) sample, B5, showed $Na(HCO_3)_2$ type water with anomalously high Na^+ concentration and suggests longer residence and limited recharge and hence, accelerating cation exchange through the saturation and precipitation of Ca^{2+} minerals and dissolution of Na^+.

Site ID	D1	D2	D3	D4	D5	D6	D7	D8	D9	D10	Na1	Na2	Na3	Na4	S1	S2
pH	7.6	6.7	7.0	6.9	7.3	7.4	7.5	7.1	8.0	7.8	7.8	7.4	7.3	7.0	7.9	7.3
HCO_3^- (mg/l)	298.9	186.7	209.1	263.3	197.2	250.1	305.0	286.7	134.3	140.3	235.9	127.5	57.3	228.8	247.1	377.8
CO_3^{2-} (mg/l)	0.0	0.7	0.0	0.0	0.0	0.0	0.0	0.0	0.0	0.0	0.0	0.0	0.0	0.0	0.0	0.0
Ca^{2+} (mg/l)	47.6	33.5	37.9	45.5	39.1	42.5	76.6	45.2	25.3	26.8	38.7	24.8	11.9	43.2	49.0	74.7
Cl^- (mg/l)	9.9	3.3	4.7	3.7	10.4	4.0	9.3	9.5	10.2	8.4	13.3	2.4	3.1	7.8	3.1	24.9
EC (µS/cm)	452.3	289.3	317.8	379.3	338.0	383.5	536.0	314.7	249.0	252.0	390.7	207.4	99.9	387.0	394.0	764.0
Fe^{2+}(mg/l)	0.0	0.0	0.0	0.0	0.0	0.0	0.0	0.0	0.0	0.0	0.0	0.0	0.0	0.0	0.0	0.0
Mg^{2+} (mg/l)	14.1	10.9	11.5	13.9	11.4	7.3	9.1	18.2	6.0	6.1	13.7	5.4	2.1	11.0	6.2	7.3
Mn^{2+} (mg/l)	6.0	0.0	0.1	0.1	0.0	0.0	0.0	0.0	0.0	0.0	0.2	0.0	0.0	0.2	0.0	0.0
K^+ (mg/l)	0.8	0.4	1.5	1.3	0.4	0.6	1.1	0.9	1.8	1.9	0.3	1.1	3.6	1.3	0.9	0.7
SiO_2(mg/l)	27.6	40.8	49.3	43.5	31.2	29.5	34.8	28.4	21.8	22.4	26.1	21.2	8.8	39.6	30.0	32.8
Na^+ (mg/l)	27.3	14.2	15.0	18.6	19.1	26.1	23.4	28.2	15.2	14.4	29.1	11.1	5.7	24.1	23.7	32.1
SO_4^{2-} (mg/l)	2.8	0.7	0.0	0.9	3.3	0.5	5.0	1.7	9.0	7.0	4.3	0.0	0.0	2.0	3.0	6.5
TH	190.7	128.7	141.8	170.8	144.7	136.5	229.0	187.7	88.0	92.0	153.0	84.5	38.5	153.5	148.0	244.0
TDS	280.0	188.0	203.8	243.0	209.0	237.5	332.0	291.0	154	156	128.3	128.3	61	244.0	244	474

Table 3.12: chemical results from Dubalevu (D), Nabaka (Na) and Siminilaya (S) showing dominant $Ca(HCO_3)_2$ type water and relatively variable Na^+ and Mg^+ concentration suggesting variable sources such as dolomite and halite. S2 showed elevated Cl^-, with both S2 and Na4 recording enriched Na^+, suggest proximity to some sources of $NaCl^-$. (individual results are provided in Appendix I).

Site ID	B1	B2	B3	B4	B5	B6	B7	B8	B9	B10	B11	B12	B13	B14	B15	B16	B17	B18	B19
pH	7.7	7.5	7.5	7.5	7.6	6.6	7.7	6.7	7.1	7.1	7.1	6.7	6.8	7.5	7.5	7.6	7.3	7.1	6.6
HCO_3^-(mg/l)	298.9	292.8	284.7	338.6	368.0	220.6	262.2	151.5	374.1	310.4	258.0	201.3	233.8	98.2	115.9	201.3	334.5	277.6	215.5
CO_3^{2-} (mg/l)	0.0	0.0	0.0	0.0	0.0	0.0	0.0	0.0	0.0	0.0	0.0	0.0	0.0	0.0	0.0	0.0	0.0	0.0	0.0
Ca^{2+} (mg/l)	56.8	53.8	55.5	76.7	3.6	42.8	53.4	31.5	68.8	45.2	49.7	37.7	40.3	13.9	24.4	37.0	55.3	32.2	43.2
Cl^- (mg/l)	8.0	11.1	35.9	9.5	17.5	14.7	14.4	8.0	25.5	7.4	12.1	4.0	10.3	4.4	6.2	15.1	7.5	23.9	17.4
EC (µS/cm)	461.0	466.0	583.5	547.0	593.0	413.3	464.0	287.5	746	496	457.8	350	371.3	163.0	213.6	353.3	508.0	492.5	390.0
Fe^{2+} (mg/l)	0.0	0.0	0.0	0.0	0.0	0.0	0.0	0.1	0.0	0.0	0.0	0.0	0.3	0.0	0.1	0.0	0.0	0.0	0.0
Mg^{2+}(mg/l)	8.0	13.4	20.3	12.6	0.2	11.8	8.0	9.8	26.2	12.1	17.9	11.6	11.5	5.7	6.1	8.5	13.7	18.1	19.0
Mn^{2+} (mg/l)	0.0	0.0	0.0	0.0	0.0	0.0	0.0	0.0	0.0	0.0	0.0	0.2	0.5	0.0	0.0	0.2	0.6	1.3	0.5
K^+ (mg/l)	1.0	0.5	0.5	1.1	0.5	0.9	1.3	1.0	0.5	0.5	0.3	0.9	0.6	2.0	1.5	0.8	0.6	1.4	1.1
SiO_2(mg/l)	29.9	39.9	45.7	27.6	23.2	28.3	25.0	50.2	47.9	41.5	58.1	51.7	31.3	20.8	27.9	25.7	29.7	53.4	50.9
Na^+ (mg/l)	34.4	31.5	35.6	27.5	156.3	29.8	31.6	15.0	46.7	45.1	21.6	15	30.8	12.7	13.3	27.9	44.4	48.5	12.3
SO_4^{2-} (mg/l)	2.0	2.0	21.0	1.5	5.0	6.5	3.0	5.5	68.0	7.3	6.5	2.0	0.0	2.1	3.5	10.0	4.5	0.5	6.7
TH	175.0	189.0	222.0	243.0	255.5	155.8	166.0	119.0	279.0	162.7	197.8	142	176.3	58.0	85.8	127.0	194.5	155.0	186.0
TDS	265.0	288.0	361.5	338.5	367.5	255.5	287.5	178.3	461.5	307	283.5	216	263.0	101.0	132.2	218.3	314.5	305.0	241.7

Table 3.13: chemical results from different water sources within the Bilalevu (B) area dominated by $Ca(HCO_3)_2$ type water except for B5 and B18, which record $Na(HCO_3)_2$ type groundwater. Elevated Cl^- B3, B9 and B18 suggest proximity to sources of chloride, such as halide or ionically enriched connate groundwater whilst the high SO_4in B9 and 16 may represent the dissolution of gypsum along these groundwater flow paths(Individual results are provided in Appendix I).

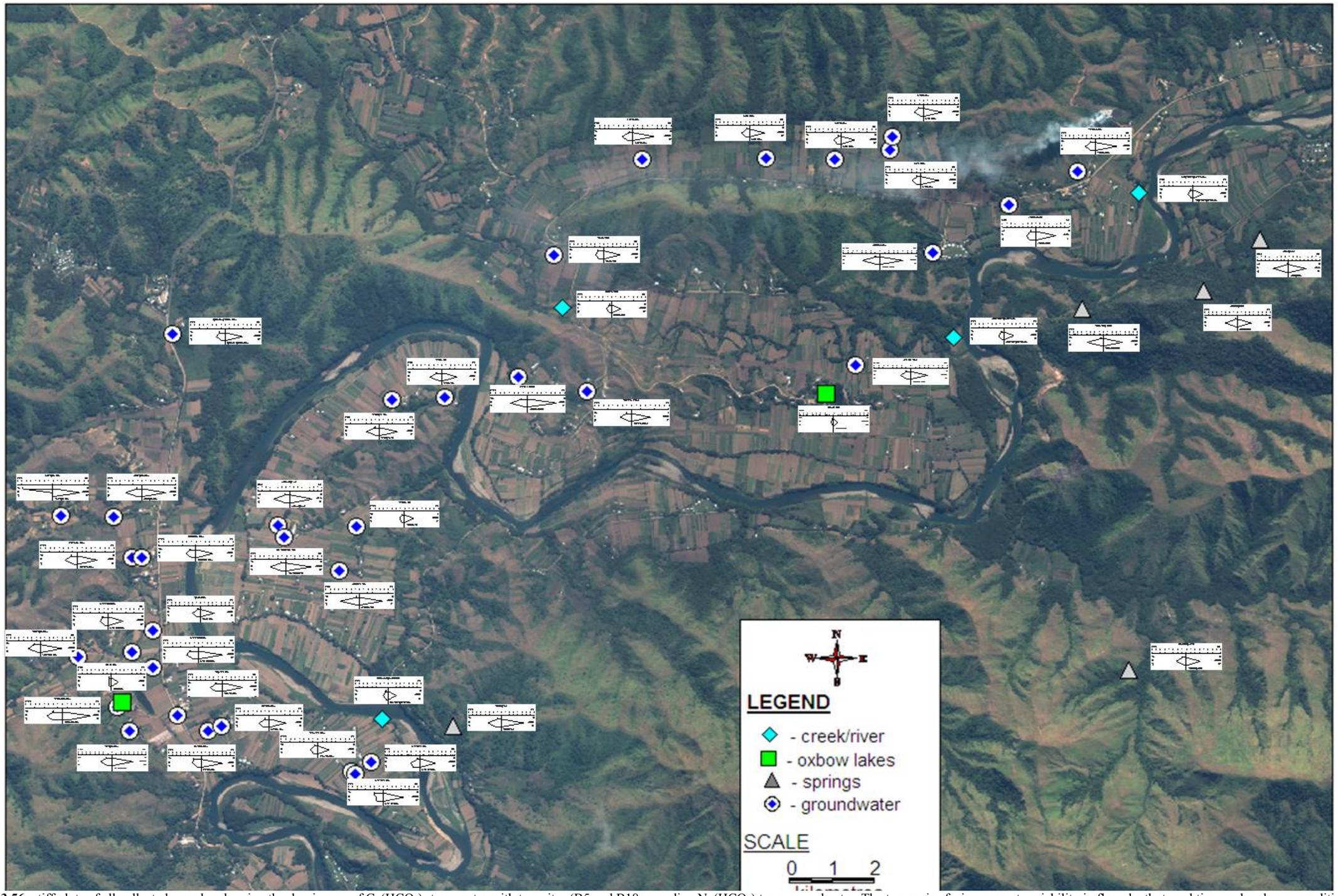

Figure 3.56: stiff plots of all collected samples showing the dominance of $Ca(HCO_3)_2$ type water with two sites (B5 and B18 recording $Na(HCO_3)$ type groundwater, The two major facies suggest variability in flow depth, travel time and recharge conditions with $Ca(HCO_3)_2$ suggesting rapid and shallow flow system with adequate flushing and recharge whilst $Na(HCO_3)$ type suggesting a deeper system and limited recharge.

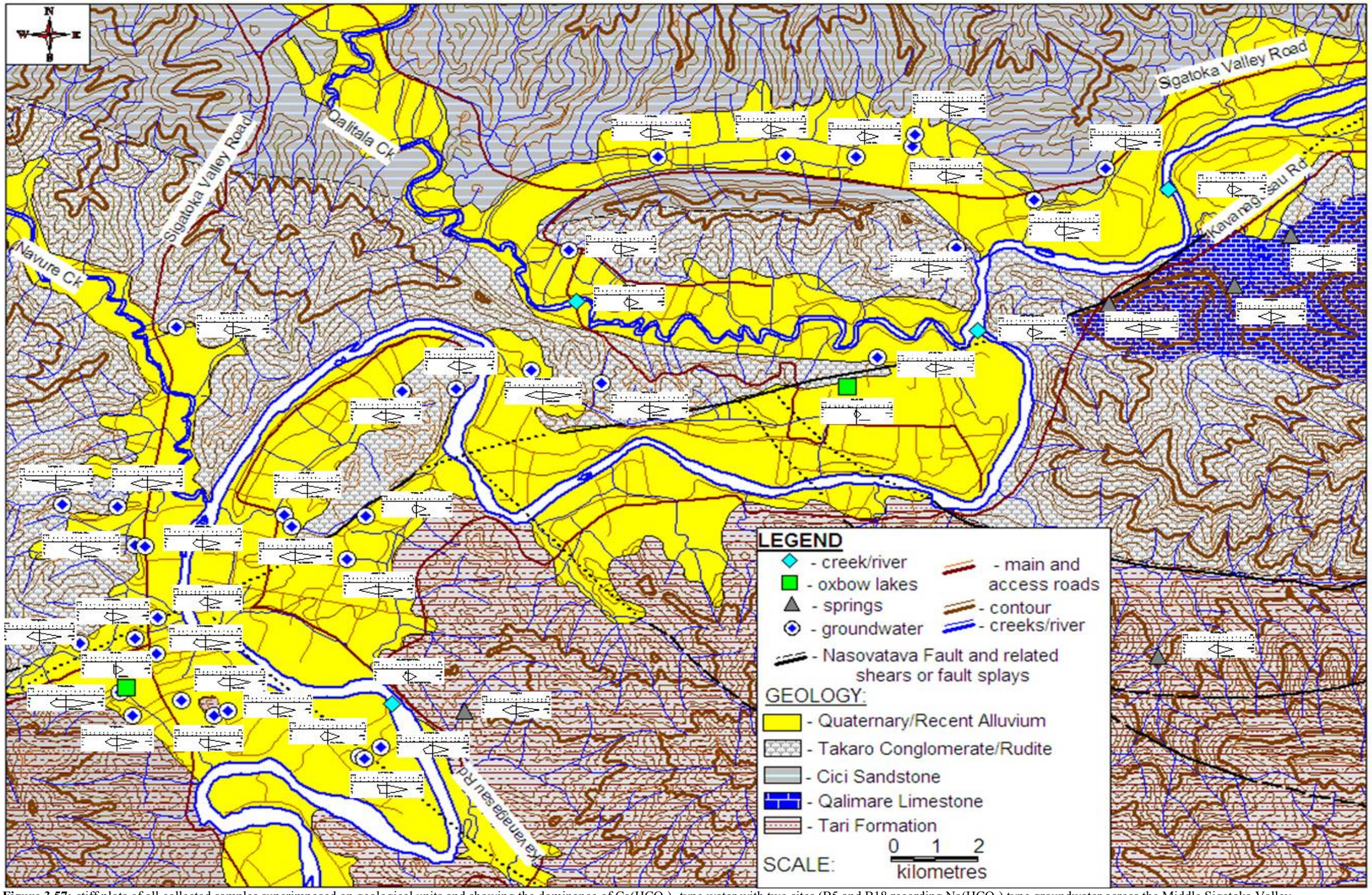

Figure 3.57: stiff plots of all collected samples superimposed on geological units and showing the dominance of $Ca(HCO_3)_2$ type water with two sites (B5 and B18 recording $Na(HCO_3)$ type groundwater across the Middle Sigatoka Valley.

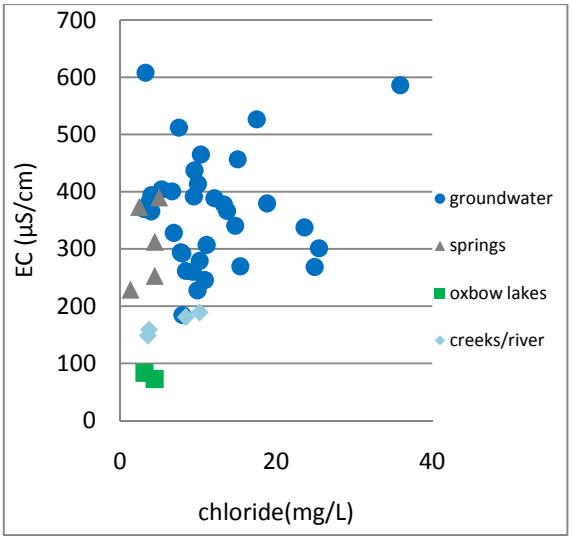

Figure 3.58: plot of chloride (mg/L) vs electrical conductivity (µS/cm) showing highly variable trend.

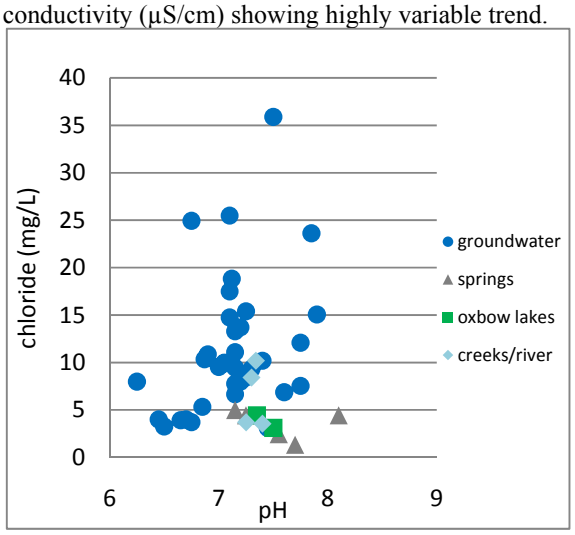

Figure 3.60: plot of pH vs chloride (mg/L) suggesting highly variability of sources of chloride, mixing of water sources, possibly through different interconnected flow paths, hence, proves complexity of groundwater flow systems.

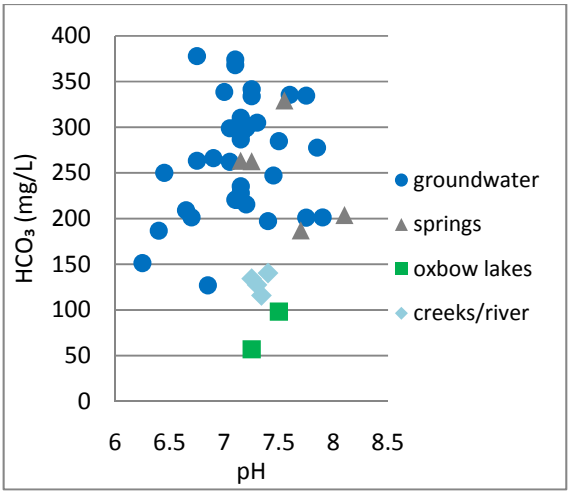

Figure 3.59: plot of pH vs HCO_3 (mg/L) showing highly variable trend suggesting variable flow paths, controlling varying HCO_3 exchange rates and driving the evoloution of slightly acidic rainwater (pH of 5.35, Table 3.5.2) towards alkaline state.

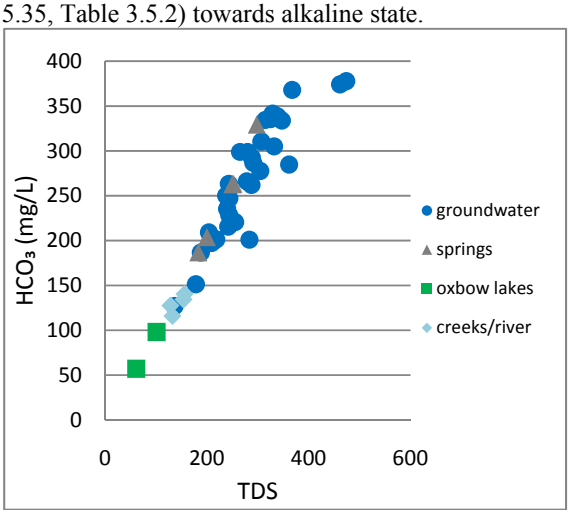

Figure 3.61: plot of TDS vs HCO_3 (mg/L) showing linear relationship and suggesting TDS and HCO_3 will depend travel and residence, which will drive cation exchanges and ionic enrichment.

The above results and interpretations make two major contributions to the hydrochemistry in the study area. First, the catchment is composed of two major hydrochemical facies, namely $Ca(HCO_3)_2$ and $Na(HCO_3)$, and suggesting two major flow systems. $Ca(HCO_3)_2$ type waters represent shallow flow systems, rapid calcite weathering from the local sedimentary units and abundant meteoric recharge and/or flushing. $Na(HCO_3)$ type waters of relatively deep groundwater sources with more limited recharge rates and ionic (Na^+) enrichment. Second, the highly variable trends in the HCO_3 vs pH, EC vs chloride, TDS vs HCO_3 and pH vs chloride plots suggest the complexity and heterogeneity of groundwater systems as governed by variable recharge rates, HCO_3 enrichment, and proximity to some chloride sources.

3.6 Stable isotope analysis

3.6.1 Introduction

Stable hydrogen and oxygen isotopic analyses were conducted to evaluate the potential to trace waters of different compositions through the study area. These data were used to specifically determine:

(1) if groundwater is derived from either dispersion of rapid flowing and isotopically depleted rain-derived recharge, or from slow isotopically enriched flows through fractured bedrock areal sources, and
(2) if groundwater represent mixed meteoric and heavy isotope enriched connate water derived from basement or magmatic sources.

3.6.2 Methodology

Samples (and duplicates) were collected in air-tight 35 and 100 ml plastic vials with screw caps. Creeks, rivers and oxbow lakes were sampled at the surface whilst springs were sampled at discharge points (Figures 3.63 & 3.64). Groundwater pumps were run to purge boreholes and to permit the sampling of aquifer waters. Rainwater collectors were used to also sample rainfall in the study area, as well as in the windward area, namely Suva. Caution was taken during sample collection to keep suspended materials at minimal level to comply with NZMAF water importation guidelines after which samples were properly labeled and stored. Samples, at University of Canterbury's MAF laboratory, were extracted into 3ml screw-cap vials and properly labeled (Figures 3.65 & 3.66) before each sample was analysed three times using a Thermo Scientific Temperature conversion elemental analyser (TC/EA) to determine O^{18}/ O^{16} and H^2/H^1 ratios. The TC/EA reactor is held at 1420°C and the gas chromatography column is held at 40°C with a continuous flow of ~110 ml/min of 99.9999% helium (i.e. Ultra-high purity helium). The TC/EA is connected to a Thermo Scientific Delta V Plus isotope ratio mass spectrometer (IRMS) via a Thermo Scientific ConFlo III gas distribution system. Measurement accuracy was determined through analysis of two international certified reference waters, SMOW2 and SLAP2. Measured isotopic compositions were recorded in a Microsoft Excel

spreadsheet and the average value of each triplicate sample analysis, and its corresponding duplicate, was calculated to get a realistic representation of isotopic composition, before linked to GPS-surveyed locational attributes. These were loaded into Golden Software Surfer 9.0 to generate contour surfaces and exported into compatible formats that permit its superimposition onto MapInfo 10.0 Fiji GIS system. For ease of referencing and consistency, the site IDs used for chemical sampling (refer to Table 3.9) are also used here.

3.6.3 Results

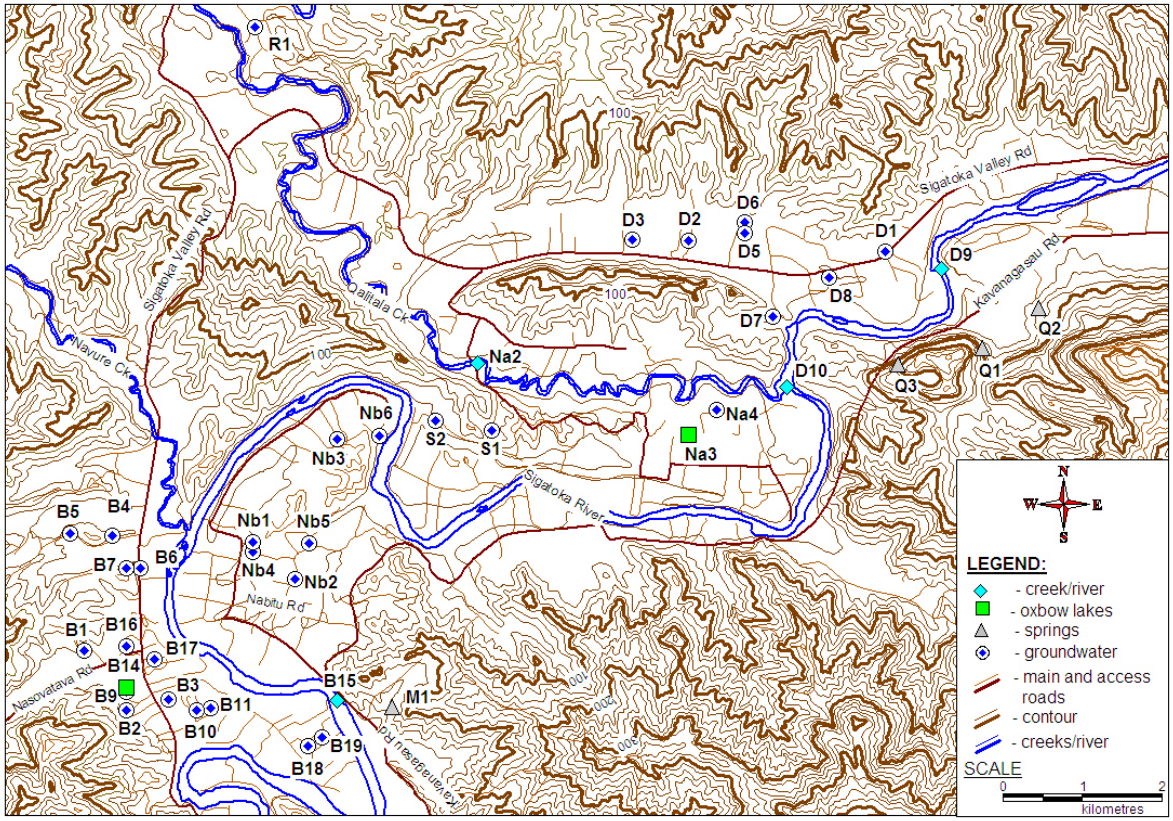

Figure 3.62 location map of isotope sampling sites with sample ID (same as chemical sampling site ID (Table 3.9). Note that D5, B16 and B19 were sampled twice (Table 3.14) whilst a number of samples were discarded due to suspended materials above NZMAF guidelines.

Figure 3.63: sample collection at Koro-i-Ra spring, a fractured spring of the Qalimare Limestone (site Q1, Figure 3.62).

Figure 3.64: Sigatoka River sample collection at the Bilalevu meander (site B15, Figure 3.62).

Figure 3.65: isotope samples, yellow capped 100 ml plastic vials, extracted into 3ml plastic vials.

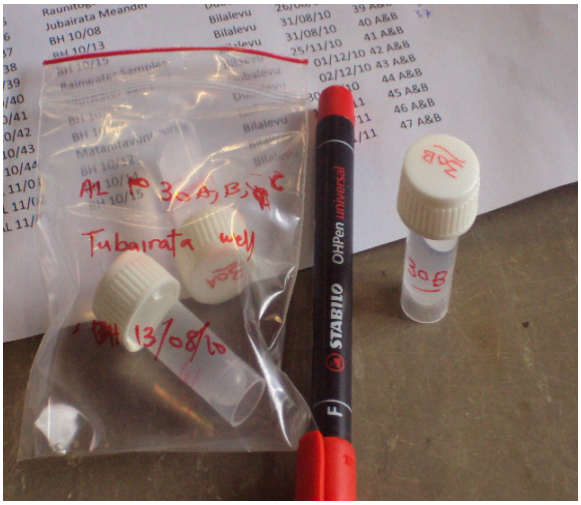

Figure 3.66: labeled 3ml sample cells ready to be taken to the isotope laboratory for δD and $\delta^{18}O$ analysis.

Site	Location	Collection date	SampleID	SOURCE	δD(‰)	$\delta^{18}O$(‰)	d-excess
Kamal Kishor	Nabitu	18/05/2010	Nb2	GW	-19.80	-1.60	-7.04
Anil Prasad	Nabitu	16/06/2010	Nb5	GW	-22.85	-2.93	0.61
Ram Deo	Nabitu	18/05/2010	Nb6	GW	-23.93	-3.02	0.19
Pramend Singh	Nabitu	18/05/2010	Nb3	GW	-18.72	-1.47	-7.00
Nabitu Indian School	Nabitu	16/06/2010	Nb4	GW	-18.17	-1.25	-8.19
Nabitu Community	Nabitu	16/06/2010	Nb1	GW	-16.21	-0.67	-10.84
Sunil Prasad	Bilalevu	16/06/2010	B11	GW	-15.62	0.08	-16.26
Ami Chand	Dubalevu	16/06/2010	D1	GW	-22.25	-2.80	0.18
MPI Station	Dubalevu	16/06/2010	D8	GW	-20.67	-2.23	-2.79
90/15	Dubalevu	16/06/2010	D2	GW	-24.16	-3.20	1.46
90/16	Dubalevu	16/06/2010	D3	GW	-22.57	-2.68	-1.16
Bulatale Store	Bilalevu	16/06/2010	B6	GW	-22.68	-1.20	-13.05
Shiu Shankar	Bilalevu	16/06/2010	B7	GW	-17.26	-0.55	-12.89
Tubakeli	Bilalevu	16/06/2010	B1	GW	-20.47	-1.57	-7.88
Koroira Spring	Qalimare	16/06/2010	Q1	SP	-21.39	-1.29	-11.06
Nacule Spring	Qalimare	16/06/2010	Q2	SP	-18.99	-0.74	-13.05
Navala Spring	Mavua	16/06/2010	M1	SP	-19.81	-0.16	-18.50
Sigatoka River	Bilalevu	16/06/2010	B15	ck/rv	-22.38	-2.46	-2.71
Hari Chandra	Nabaka	21/06/2010	S2	GW	-21.30	-2.59	-0.61
Paras Ram	Siminilaya	21/06/2010	S1	GW	-22.45	-2.15	-5.27
Janmin Jai	Nabaka	21/06/2010	Na4	GW	-23.70	-2.65	-2.52
Oxbow Lake	Nabaka	21/06/2010	Na3	OL	-18.84	0.38	-21.86
Qalitala Creek	Nabaka	21/06/2010	Na2	ck/rv	-15.89	-0.47	-12.09
Rararua Village	Rukuruku	21/06/2010	R1	GW	-19.71	-1.92	-4.34
Oxbow Lake	Bilalevu	22/06/2010	B14	OL	-10.56	0.63	-15.58
Mahen's Export	Bilalevu	22/06/2010	B9	GW	-20.06	-2.47	-0.32
Tore Project	Bilalevu	22/06/2010	B2	GW	-20.09	-1.97	-4.36
Rainwater Samples	Suva	13/07/2010	Rn1	Rn	8.64	0.16	7.40
10/12	Bilalevu	14/07/2010	B16	GW	-31.99	-4.07	0.56
Jubairata BH	Dubalevu	13/08/2010	D7	GW	-30.17	-3.43	-2.72
Manoj Kumar BH	Bilalevu	14/08/2010	B3	GW	-27.35	-3.82	3.18
Tavuto	Bilalevu	17/08/2010	B5	GW	-30.53	-4.42	4.84
Waiwai	Bilalevu	17/08/2010	B4	GW	2.36	-0.29	4.64
Shiu Prasad	Bilalevu	19/08/2010	B10	GW	-27.75	-4.01	4.34
10/13	Bilalevu	26/08/2010	B17	GW	-31.50	-4.23	2.33
10/15	Bilalevu	31/08/2010	B19	GW	-31.96	-4.18	1.47
Rainwater	Bilalevu	31/08/2010	Rn2	Rn	-28.90	-4.58	7.75
10/08	Dubalevu	17/09/2010	D6	GW	-31.76	-4.99	8.13
Raunitogo Meander	Dubalevu	17/09/2010	D9	ck/rv	-32.88	-5.17	8.46
Jubairata Meander	Dubalevu	17/09/2010	D10	ck/rv	-28.62	-4.32	5.94
Rainwater	Bilalevu	25/11/2010	Rn3	Rn	8.76	1.20	-0.83
10/07	Dubalevu	1/12/2010	D5	GW	-33.48	-5.12	7.49
10/07	Dubalevu	1/12/2010	D5	GW	-35.71	-5.62	9.22
Matanitavuni Spring	Qalimare	30/12/2010	Q3	SP	-36.57	-5.96	11.14
10/12	Bilalevu	16/01/2011	B16	GW	-35.96	-5.43	7.51
10/14	Bilalevu	19/01/2011	B18	GW	-35.44	-5.71	10.28
10/15	Bilalevu	21/01/2011	B19	GW	-35.66	-5.60	9.11

Table 3.14: δO^{18}(‰) and δD (‰) composition of sampled groundwater (GW), springs (SP), creek and river (ck/rv), oxbow lakes (OL) and rainfall (Rn) representing the average of samples and their corresponding duplicates with deuterium excess (d-excess) showing the variability of atmospheric conditions upon which isotope fractionation occurred (Sharp, 2007). Groundwater, with a range of -5.7 to 0.08 ‰ δO^{18} and suggesting meteoric waters flushing through the groundwater systems with variable influences of evaporation. 10/07 (D5),

showing two samples, was sampled in the 1st hour and 16th hour of long-term pumping tests. 10/12 and 10/15 (B16 & B19) were both samples during the well development and pumping test and hence, showed two samples. Rain sample (Rn1) was collected on the windward site of Viti Levu, near Suva, whilst Rn2 and Rn3 were collected at the study area(Bilalevu), in the dry and wet season, respectively.

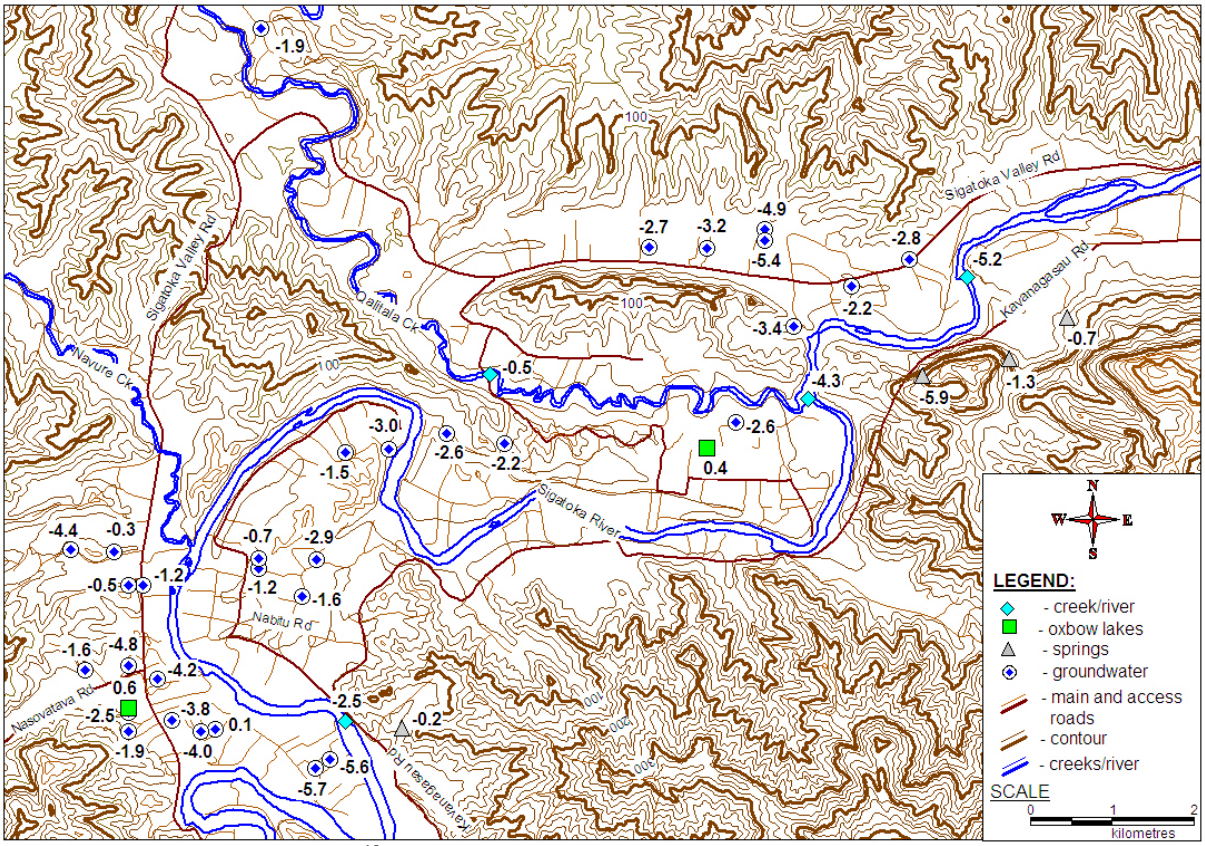

Figure 3.67: spatial variability $\delta^{18}O$ (‰) in the study area showing variable influences of evaporation on variable water sources with notable enrichment of both oxbow lakes (Na3 and B14) as well as in B11 (groundwater). NB: sites D5 and B19, having sampled twice (Table 3.14), show averages of the samples.

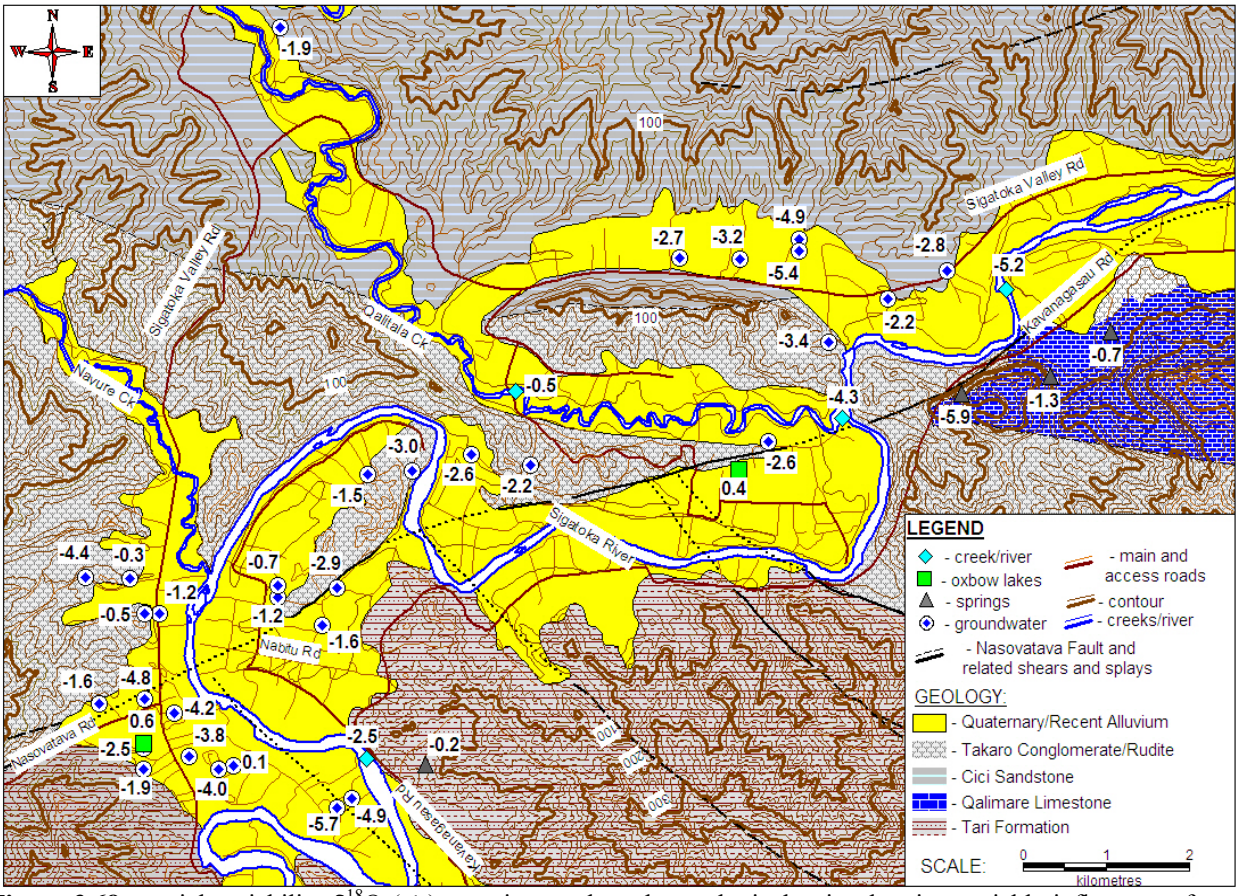

Figure 3.68: spatial variability $\delta^{18}O$ (‰) superimposed on the geological units showing variable influences of evaporation on variable water sources and aquifers with notable enrichment of both oxbow lakes (Na3 and B14) as well as in B11 (groundwater). NB: sites D5 and B19, having sampled twice (Table 3.14), show averages of the samples.

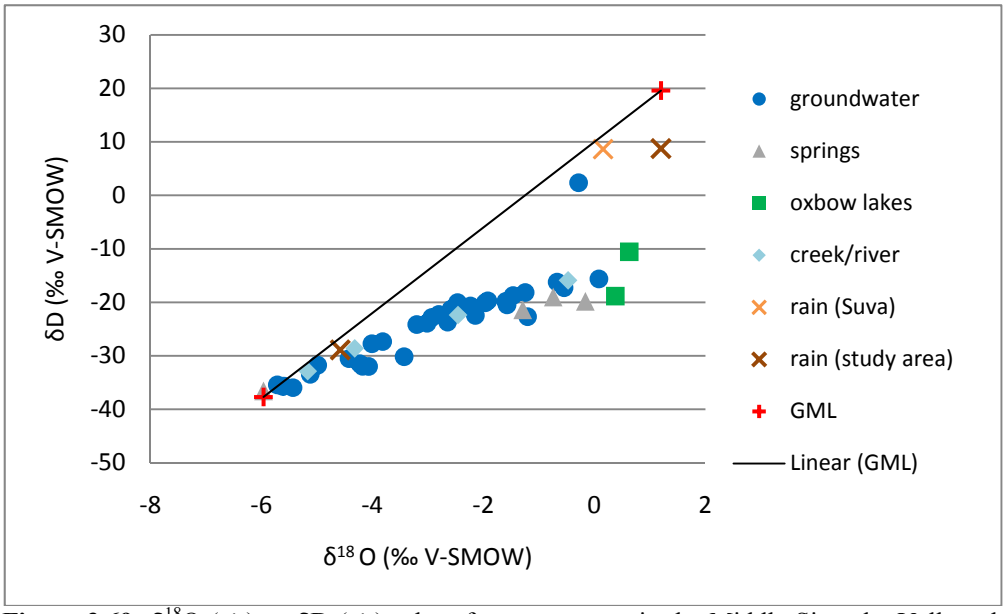

Figure 3.69: $\delta^{18}O$ (‰) vs δD (‰) plot of water sources in the Middle Sigatoka Valley plotting on a LMWL slope of 4.3 in relation to the GMWL of relation $\delta D = 8\times(\delta^{18}O) + 10$.

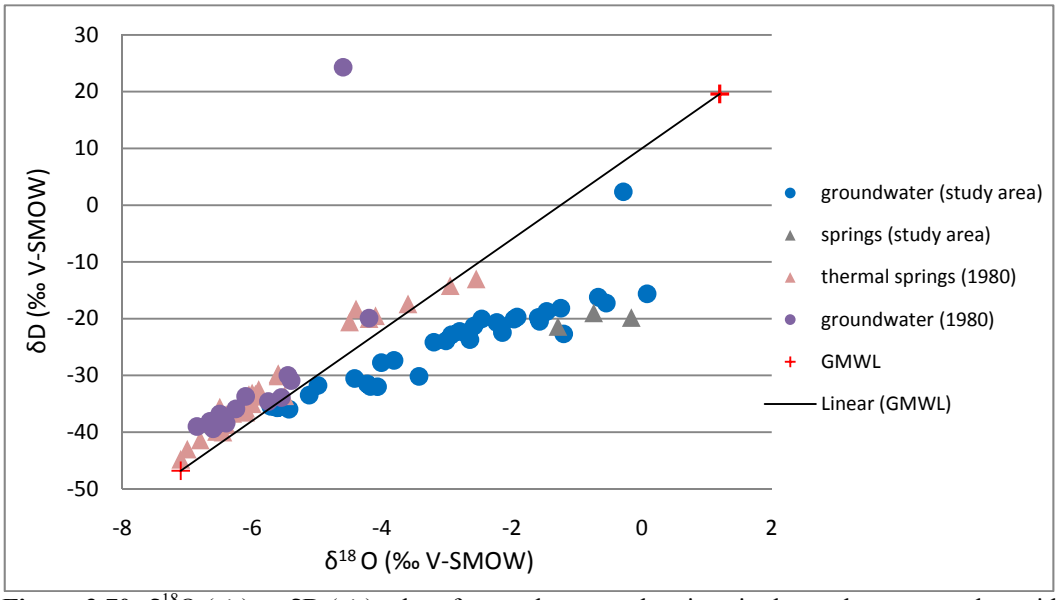

Figure 3.70: $\delta^{18}O$ (‰) vs δD (‰) plot of groundwater and springs in the study area together with groundwater and springs data documented in Cox and Hulston (1980)in relation to GML of relation δD(‰) = 8 $\delta^{18}O$ (‰) + 10.Clearly, the more negative isotope values are plotted close to the GMWL, suggesting recent meteoric waters whilst variable influences of evaporation is causing a more positive linear trend that is falling away from the GMWL with a sloe of 4.34 for the Middle Sigatoka Valley samples in relation to a slope of around 6.5 for 1980 data.

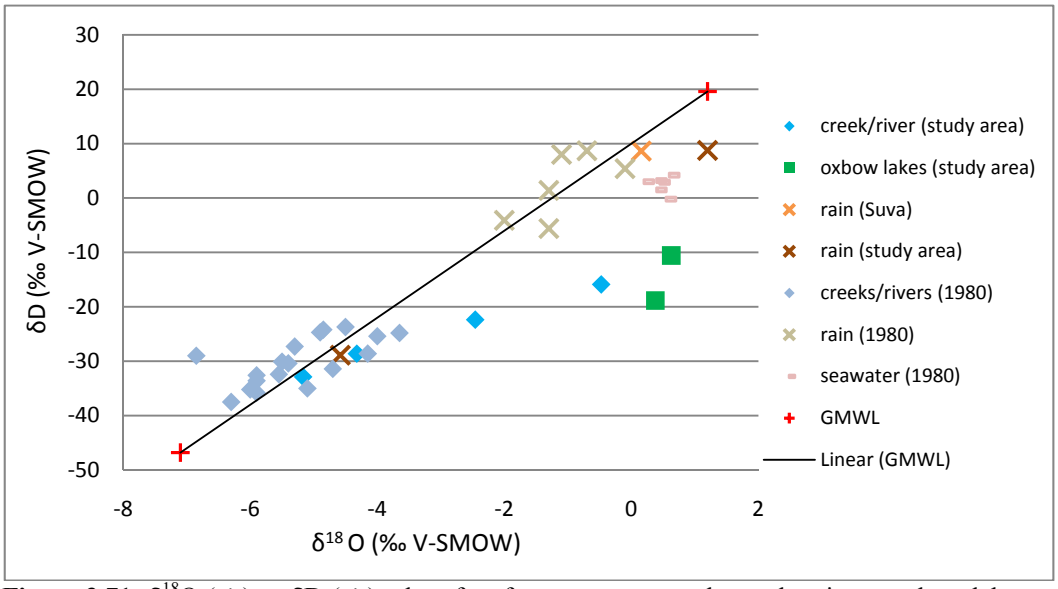

Figure 3.71: $\delta^{18}O$ (‰) vs δD (‰) plot of surface sources, namely creeks, rivers, oxbow lakes and rain for this research, and surface sources sampled in 1980 (Cox & Hulson, 1980) in relation to GMWL of relation δD(‰) = 8 $\delta^{18}O$ (‰) + 10. The water resources in the study area plot along the leeward side evaporation line of slope 4.34, while the windward sources fall on or close to the GML. Variability in isotopic composition of rainwater collected in the study area (Rn2 and Rn3) suggest isotopically depleted waters precipitating (possibly from higher altitude clouds) during dry season (due to high evaporation and low humidity) whilst isotropic enrichment in the wet season can be attributed to Rayleigh isotopic effect causing the preferential precipitation of heavy isotopes (Sharp, 2007). Rainwater samples, Rn1 and Rn3, showed similar isotopic signature and suggests variable atmospheric conditions.

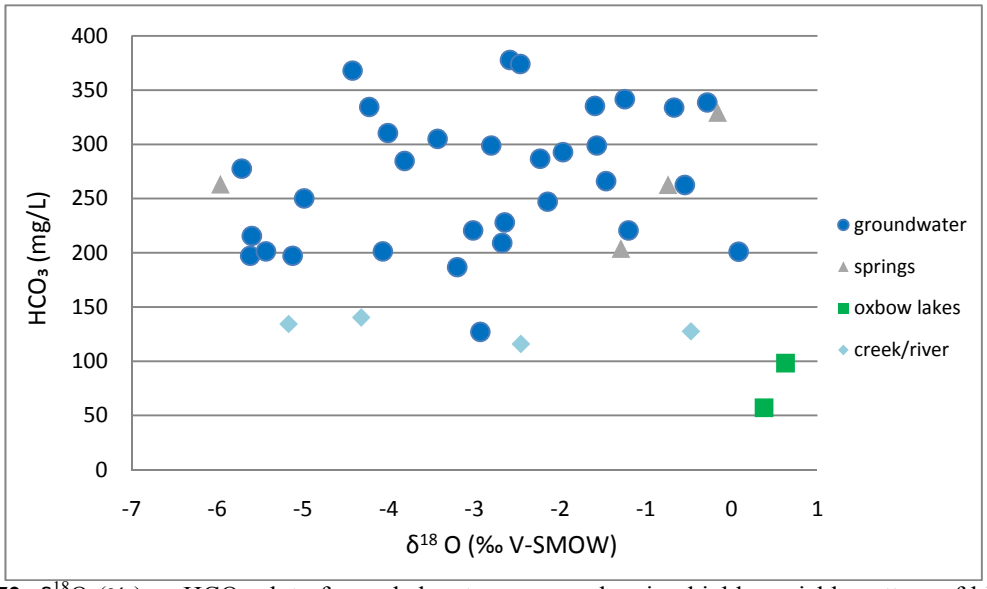

Figure 3.72: $\delta^{18}O$ (‰) vs HCO_3 plot of sampled water sources showing highly variable pattern of bicarbonate exchange with respect to depletion or enrichment of $\delta^{18}O$.

The above results and interpretations make four major contributions to the hydrochemistry of the study area. First, the linear trend of predominantly negative and relatively positive isotopic compositions, along a local meteoric water line (LMWL) of slope 4.3, suggest that water resources are meteoric in origin with variable modifications by evaporation and mixing with other residual evaporated waters in surface and groundwater storage. Second, the comparative analysis of the study area with the previous isotopic survey data collected in Vanua Levu and Viti Levu showed similarities in more negative isotopic characteristics with a number of previously sampled leeward sources plotting close the study area data, which suggests similar atmospheric conditions. Third, the Sigatoka catchment showed lower LMWL slope in relation to the 1980 LMWL, which can be attributed to the valley's leeward and more arid climatic conditions. Fourth, the highly variable HCO_3 and $\delta^{18}O$ plot suggests variable bicarbonate enrichment sand variable modifications from evaporation occurring at different water sources, particularly in groundwater sources, and hence, signifies the complexity and heterogeneity of subsurface flow systems.

3.7 Chloride concentration test

3.7.1 Introduction

This section presents the methodology and results of chloride concentration test conducted on collected isotope samples to determine the spatial variability of chloride in the sampled water sources.

3.7.2 Methodology

Following the extraction of 3ml isotope samples (Section 3.6), the remaining sampled waters, were analysed for chloride concentration. Two (2) 20 ml screw-cap plastic cells, namely blank and sample, were filled with 10 ml of sample waters. The blank cell was closed and ready for testing while different chloride tablets were added into sample cell. One (1) RT-120 chloride acidifying tablet was added and mixed to dissolve in the sample cell before one (1) RT-121 Chloride tablet was added (without crushing or mixing) and allowed to disintegrate for 2 minutes to produce a murky solution (Figure 3.73). Both the blank and sample cells were then slotted in the "Model 975 MP Analyst" from Orbecco-Hellige (Figure 3.74): a portable micro-processor based water analysis system was used to read the chloride concentration in mg/L . Test 34 was selected in the equipment whilst the filter was set to 528 nm as per test procedure manual. Both the blank and samples cells were slotted into the Analyst reader for Cl^- concentration measurement.

3.7.3 Results

Figure 3.73: remaining sample (left) and blank (right) cells after chloride tablets have been added in the sample cell producing murky colour.

Figure 3.74: the Model 975 MP Analyst with a blank (right) and sample (left with cloudy appearance) cells ready to be slotted for Cl^- concentration measurement (mg/L).

Site	SiteID	δD(‰)	$\delta^{18}O$(‰)	d-excess (‰)	Cl^- (mg/L)
Kamal Kishor BH	Nb2	-19.81	-1.60	-7.04	7.12
Anil Prasad BH	Nb5	-22.85	-2.93	0.61	4.28
Ram Deo BH	Nb6	-23.93	-3.02	0.20	12.64
Pramend Singh BH	Nb3	-18.73	-1.47	-7.01	13.10
Nabitu Indian School BH	Nb4	-18.17	-1.25	-8.19	7.26
Nabitu Community BH	Nb1	-16.21	-0.67	-10.84	7.98
Sunil Prasad BH	B11	-15.62	0.08	-16.26	10.62
Ami Chand BH	D1	-22.26	-2.81	0.18	7.02
MPI Station BH	D8	-20.67	-2.23	-2.79	5.66
90/15	D2	-24.16	-3.20	1.46	3.00
90/16	D3	-22.57	-2.68	-1.16	3.14
Bulatale Store BH	B6	-22.69	-1.20	-13.05	10.62
Shiu Shankar BH	B7	-17.26	-0.55	-12.89	8.80
Tubakeli BH	B1	-20.47	-1.57	-7.88	4.85
Koroira Spring	Q1	-21.39	-1.29	-11.06	3.45
Nacule Spring	Q2	-18.99	-0.74	-13.05	3.32
Navala Spring	M1	-19.81	-0.16	-18.50	1.58
Bilalevu Meander	B15	-22.38	-2.46	-2.72	4.36
Hari Chandra BH	S2	-21.30	-2.59	-0.61	34.77
Paras Ram BH	S1	-22.45	-2.15	-5.27	2.32
Jamin Jay BH	Na4	-23.70	-2.65	-2.52	5.02
Oxbow Lake	Na3	-18.84	0.38	-21.86	2.69
Qalitala Creek	Na2	-15.89	-0.48	-12.09	2.45
Rararua Village BH	R1	-19.71	-1.92	-4.34	9.67
Oxbow Lake	B14	-10.56	0.63	-15.58	5.69
Mahen's Export BH	B9	-20.06	-2.47	-0.32	31.14
Tore Project BH	B2	-20.09	-1.97	-4.36	13.57
Rainwater Samples	Rn1	8.64	0.16	7.40	5.11
BH 10/12	B16	-31.99	-4.07	0.56	5.51
Jubairata BH	D7	-30.17	-3.43	-2.72	8.20
Manoj Kumar BH	B3	-27.35	-3.82	3.18	31.13
Tavuto BH	B5	-30.53	-4.42	4.84	11.23
Waiwai BH	B4	2.36	-0.29	4.64	2.91
Shiu Prasad BH	B10	-27.75	-4.01	4.34	5.17
BH 10/13	B17	-31.50	-4.23	2.33	6.50
BH 10/15	B19	-31.96	-4.18	1.47	7.86
Rainwater Samples	Rn2	-28.90	-4.58	7.75	1.06
BH 10/08	D6	-31.76	-4.99	8.14	1.08
Raunitogo Meander	D9	-32.88	-5.17	8.46	8.54
Jubairata Meander	D10	-28.62	-4.32	5.94	7.19
Rainwater Samples	Rn3	8.76	1.20	-0.83	5.84
BH 10/07	D5	-33.48	-5.12	7.49	2.40
BH 10/07	D5	-35.71	-5.62	9.22	2.21
Matanitavuni Spring	Q3	-36.57	-5.96	11.14	2.17
BH 10/12	B16	-35.96	-5.43	7.51	4.84
BH 10/14	B18	-35.44	-5.72	10.28	18.26
BH 10/15	B19	-35.66	-5.60	9.11	3.98

Table 3.15: chloride concentration (mg/L) of collected isotope samples. The results, dominated by low [Cl^-] (1.02-18.3 mg/L), suggest either recharge-induced dilution or short travel paths preventing accumulation of [Cl^-]. Elevated [Cl^-] at three (3) sites (with >30 mg/L concentration), suggesting proximity to some chloride sources. The low chloride (<40 mg/L) concentration, together with isotopically depleted water, suggests that all sampled water sources are mainly meteoric in origin. D5, collected the 1st and 16th hour of pumping tests, showed variable [Cl^-]. The variability in [Cl^-] in the Bilalevu rainwater samples, Rn2 and Rn3, collected in dry and wet seasons, suggest the variable source of solute, probably caused by difference in precipitation altitude in the seasons. Similar [Cl^-] concentration between rainwater collected in Rn1 (windward area) and Rn3 suggests similar atmospheric conditions.

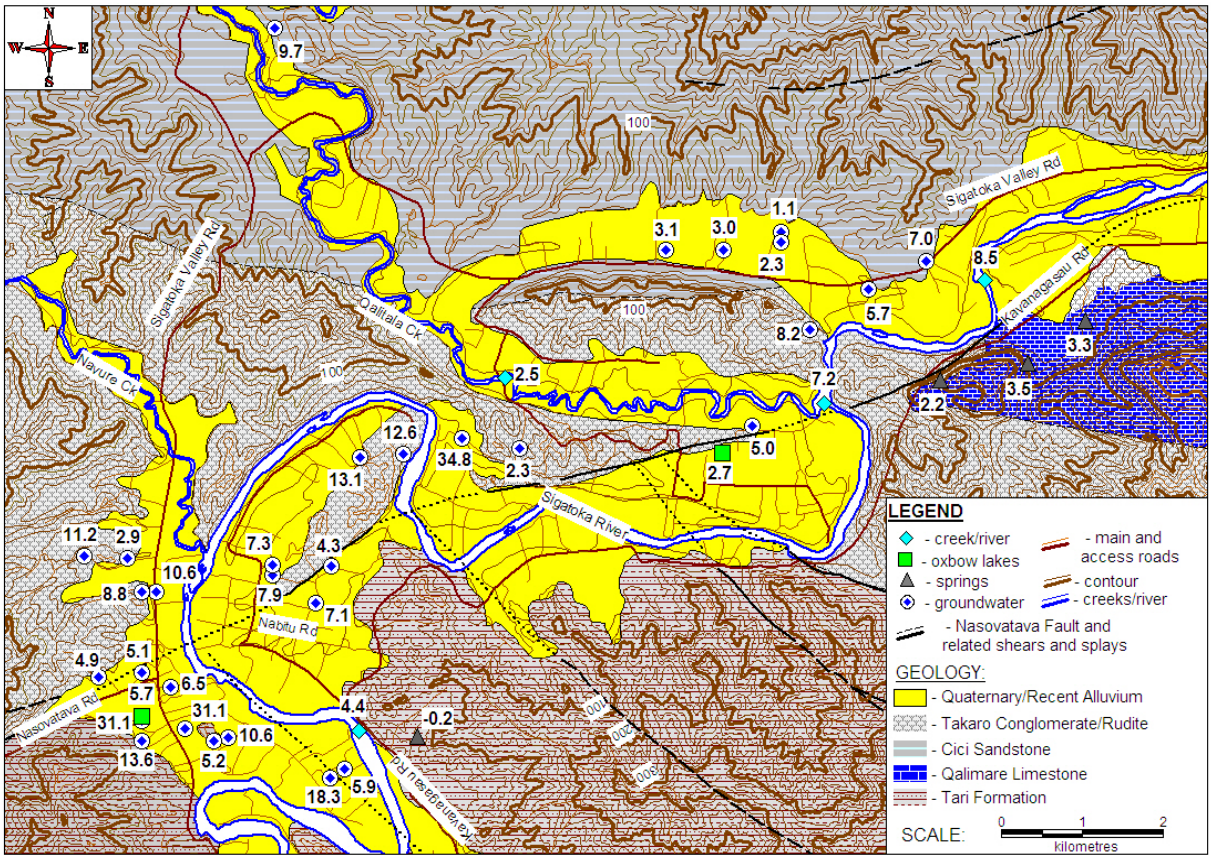

Figure 3.75: chloride spatial variability superimposed on geological units showing predominantly low [Cl^-] (1-18 mg/L) with three areas of elevated concentration and suggesting proximity of some [Cl^-] sources. The dominant low [Cl^-], together with the isotopically depleted compositions, suggests abundant meteoric recharge-induced dilution.

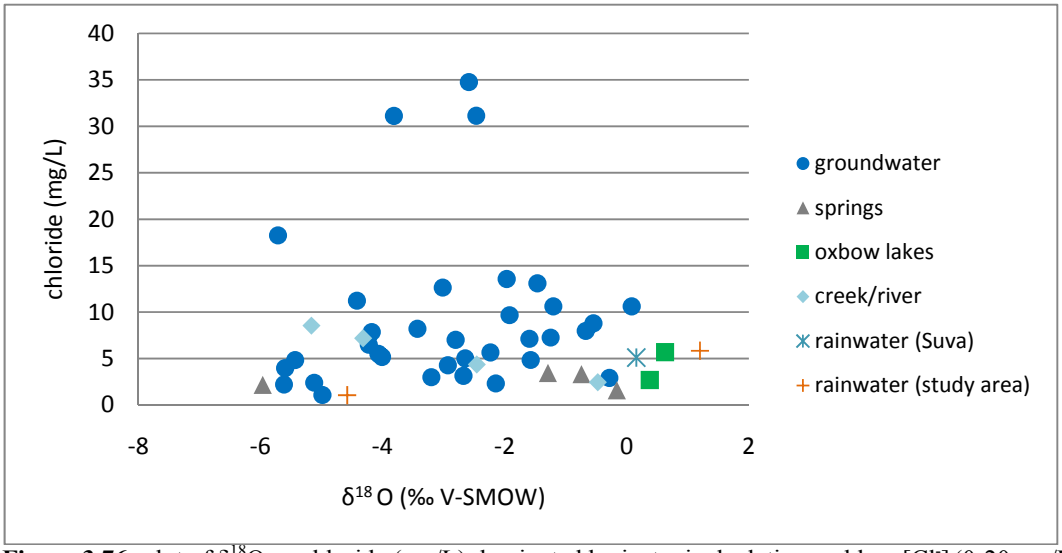

Figure 3.76: plot of $\delta^{18}O$ vs chloride (mg/L) dominated by isotopic depletion and low [Cl^-] (0-20 mg/L) suggests minimal accumulation of [Cl^-] along flow paths suggesting either short recharge to discharge (R→D)travel path or abundant and rapid recharge-induced dilution. Elevated [Cl^-] in sites S2, B3 and B9, suggest proximity to some chloride sources. [Cl^-] variability in rainwater measured in the study area (sample Rn2 and Rn suggest different sources of air

masses and solutes with the dry season rain event (R2) likely to be sourced from high altitude airmass from a distal source that may have lost most of its chloride before reaching the study area whereas the wet season rainfall event (Rn3) may represent low altitude airmass that is saturated with solutes from a nearby source (local) . Similar isotopic compositions and [Cl^-] of Rn1 and Rn3 suggest similar sources of solute and atmospheric conditions of precipitation.

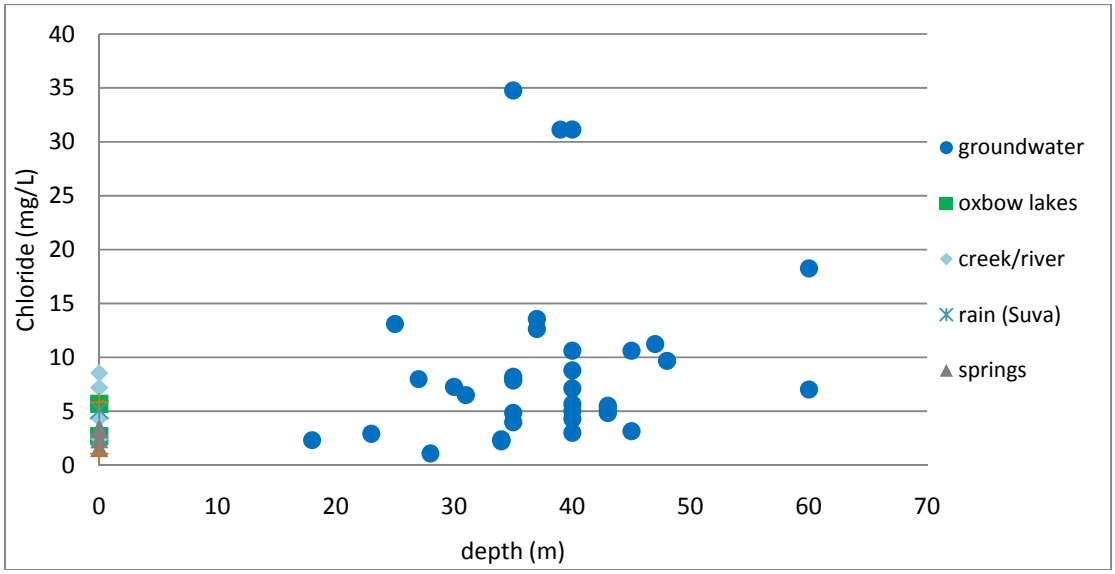

Figure 3.77: plot pf depth of water source vs chloride concentration showing highly scattered data, particularly for groundwater sources, suggesting variability of [Cl^-] sources with depth. Low chloride concentrration suggests either short R→D travel path or reachrge-induced dilution whilst slight elevated [Cl^-] measurements may suggest proximity to [Cl^-] sources, such as halite and ionically enriched connate groundwater.

The results and interpretation make four contributions to the hydrochemistry of the Middle Sigatoka Valley. First, the predominant low chloride suggests abundant meteoric recharge to cause adequate dilution of the water sources as supported by the relatively negative isotope characteristic. Second, the low chloride concentration eliminates the possibility of magmatic mixing in the investigated hydrogeological system. Third, the highly variable low chloride and depth source, particularly with groundwater, suggest that shallow flow system and short travel time to prevent chloride accumulation. Fourth, the chloride variability and isotopic composition of the sampled rain events can be attributed kinetic and Rayleigh isotopic fractionation prevalent in the different seasonal climatic conditions, as well as the proximity of the solute sources in the air mass.

3.8 Groundwater recharge

3.7.1 Introduction

The growing demand and use of groundwater resources, particularly during the dry season, represents a major human impact that may jeopardize the safety, equitable allocation and sustainability of groundwater resources. This section presents the methodology and results of a water resources inventory, including physical and chemical mass balance models to:

- determine groundwater recharge rate; and
- establish sustainability of groundwater resource.

3.7.2 Methodology

Owners and pump attendants of privately drilled wells (within the 40 km^2 study area) interviewed for well details, including depth, abstraction rate, duration to establish the amount of groundwater abstraction for drinking and irrigation purposes (Table 3.16). The Ministry of Agriculture's irrigation profile was reviewed for irrigation data using low-lift pumps for sprinkler irrigation systems within the study area (Table 3.17) whilst the long-term rainfall and evapotranspiration of the Sigatoka area was documented in Hawaiian Agronomics International Inc (1984). Runoff studies in the SW Viti Levu, conducted in forested and grassland range from 2.7-5.5% of rainfall, was estimated at 4.1% of total rainfall (Waterloo et.al., 2007). The calculation of the water balance is made upon the following assumptions:

- groundwater abstraction during the wet season is solely for drinking purpose whilst it is utilized for both irrigation and drinking purposes in the dry season;
- irrigation is only conducted during dry months; and

With the available data, the physical water balance is calculated through the equation:

$$R = P - (ET+Ru+GA) \text{ (for wet season)}$$

$$R = (P + I) - (ET+Ru+GA) \text{ (for dry season)}$$

where R is recharge (m^3/month), P is precipitation (m^3/month), I is irrigation (m^3/month), ET is evapotranspiration (m^3/month), Ru is runoff (m), GA is groundwater abstraction (m^3/month).

Chloride mass balance (CMB) equation, applicable for alluvial aquifers to determine recharge (Kresse & Clark, 2008), was also used through the following formula:

$$R = P * Cp/Cgw$$

where R is recharge (m/month), P is precipitation (m/month), Cp is chloride concentration in precipitation (mg/L), and Cgw is chloride concentration in groundwater (mg/L).

Chloride concentrations of two rainfall samples collected at Bilalevu were measured through chloride concentration test (Chapter 3.7). The dry season rainfall event was sampled on August 31st, 2010 whilst the wet season rainfall event was collected on November 25th, 2010. For the alluvial aquifers, chloride concentration of three sites sampled in both the climatic seasons, namely D3, D4 and B8, was used. Well B8, penetrating a silty sand aquifer at Bilalevu, was sampled on October 6th, 2009 and while both D3 and D4, occurring in unconsolidated sandy gravels at Dubalevu, were sampled September 1st, 2009 during the dry period. All these aquifers were sampled on January 28th, 2010 during the wet season (refer to Figures 3.5.1 and 3.6.1 for the locations of these alluvial aquifers).

3.7.3 Results

Ownner	Year Drilled	Depth (m)	Location	Project	Q (l/s)	Daily Abstraction (hrs)	Purpose	Number of Families/students
Tubakeli Project BH	1995	35	B	CWS	1 L/s	8	D	17
Tore Project BH	1999	37	B	CSW	1 L/s	7	D	15
Manoj Kumar BH	1995	39	B	CSW	1 L/s	4	D	4
Waiwai Project BH	1998	23	B	CSW	1 L/s	6	D	6
Tavuto Project BH	1998	47	B	CSW	1 L/s	6	D	8
Bulatale Store BH	1995	40	B	ISW	1 L/s	5	D	1
Shiu Shankar BH	2007	40	B	CSW	1 L/s	6	D	12
Ashok Kumar BH	2005	20	B	ISW	1 L/s	3	D	1
Mahen's Export BH	1995	40	B	ISW	1 L/s	4	D	1
Shiu Prasad BH	2005	43	B	ISW	1 L/s	1	D	1
Sunil Prasad BH	2005	45	B	CSW	1 L/s	8	D	20
Ami Chand BH	2005	60	D	CSW	2 L/s	6	D	17
BH 90/15	1991	40	D	SVRD	2 L/s	4	Ir	7
BH 90/16	1991	45	D	SVRD	3 L/s	4	Ir	7
BH 89/15	1991	42	D	SVRD	2 L/s	4	Ir	7
Jubairata village BH	2005	38	D	CSW	1 L/s	6	D	30
MPI station BH	2005	40	D	IWS	1 L/s	3	D	2
Janmin Jay BH	1989	40	Na	SVRD	1 L.s	3	D	2
Nabitu Community Project BH	2005	27	Nb	CSW	1.5 L/s	6	D	35
Kamal Kishor BH	2005	40	Nb	CSW	1 L/s	8	D	35
Pramend Singh BH	2006	25	Nb	CSW	1 L/s	6	D	14
Nabitu Primary School BH	1998	30	Nb	CSW	1 L/s	4	D	50
Anil Kumar BH	1989	40	Nb	SVRD	1 L/s	4	D	3
Ram Deo BH	2004	37	Nb	ISW	1 L/s	3	D	1
Rararua village BH	1998	48	R	CSW	1.5 L/s	5	D	30
Anil Kumar BH	2004	35	S	CSW	1 L/s	5	D	5
Hari Chand BH	2010	35	S	CSW	1 L/s	5	D	6
Paras Ram BH	1998	18	S	CSW	1 L/s	6	D	13
Nakavika settlement BH	2010	26	Na	GRADU	0.4 L/s	10	D	10

Table 3.16: summary of drinking (D) and irrigation (Ir) groundwater sources (year drilled and depth), with variable discharge rates (Q) and pumping duration, in Bilalevu (B), Dubalevu (D), Nabaka (Na), Sminilaya (S), Nabitu (Nb). ISW and CSW denotes individual water supply and community water supply projects, respectively whilst SVRDP and GRADU projects are funded government. In the calculation of physical water balance, 26 groundwater sources are accounted for groundwater abstraction during the wet season with an average discharge rate and pumping duration of 1.06 L/s and 5.15 hrs whilst 1.19 L/s and 4.93 hrs was used to account for drinking and irrigation abstraction from 29 groundwater sources in the dry season.

Location	Number of farmers	Currently operating low lift pumps
Dubalevu	3	1
Nabaka	7	2
Siminilaya	14	3
Nabitu	16	3
Vunarewa	9	2
Bilalevu	25	3
Total	74	14

Table 3.17: currently used low-lift pumps used for sprinkler irrigation scheme and operated at an average abstraction rate of 9 L/s for approximately 6 hours/day during prolonged dry periods (Source: Sigatoka Research Station Irrigation Profile, 2004).

Parameters	Wet season	Dry season
Land area (m^2)	40000000	40000000
Precipitation (m/month)	0.223	0.089
Evapotranspiration (m/month)	0.138	0.098
Total Precipitation (m^3/month)	8920000	3560000
Total Evapotranspiration (m^3/month)	5520000	3920000
Total runoff (m^3/month) (assuming 4.1 % of P)	365720	145960
Total number of Groundwater sources	26	29
Average pumping rate (L/s)	1.06	1.19
Average daily abstraction duration (hrs)	5.15	4.93
Daily groundwater abstraction (m^3/day)	510.96	612.48
Total groundwater abstraction (m^3/month)	15328.87	18374.50
Total number of low lift pump	-	14
average pumping rate (L/s)	-	9
average pumping duration (hrs)	-	6
Daily low-lift pump abstraction (m^3/day)		2721.6
Low-lift pump abstraction (m^3/month)	-	81648
Total number of groundwater irrigation source	-	3
average pumping rate (L/s)	-	2.3
average abstraction duration (hrs)	-	3
Daily groundwater abstraction		74.52
Groundwater irrigation (m^3/month)	-	2235.6
Total irrigation (m^3/month)	-	83883.6
Total Recharge (m^3/month)	3018951.13	-440450.90
Total Recharge (m/month)	0.08	-0.01

Table 3.18: physical water balance recharge calculation showing 0.08 m/month in the wet season (which is a 36% of monthly rainfall) and a recharge deficit of -0.01 m/month (details of the calculations are shown in Appendix H).

Season	Wet	Dry
Precipitation (m/month)	0.223	0.89
Chloride (mg/L)		
Rain	5.84	1.06
B8	6.65	9.75
D4	2.22	5.98
D3	3.99	4.43
Recharge (m/month)		
B8	0.19	0.10
D4	0.58	0.16
D3	0.33	0.21

Table 3.19: groundwater recharge estimate of 0.19 – 0.59 m/m^{-1} in the wet season and 0.1 – 0.21 m/m^{-1} in the dry season. Chloride concentration represent 31/08/10 and 25/11/10 rainfall events whist alluvial aquifers samples from wells B8, D4 and D3 were collected in September/October 2009 and January 2010 (refer to sample AL09/03, AL09/04, AL 09/10, AL10/06, AL10/10, and AL10/11 in Appendix I). Chloride concentration is higher in dry season due to evaporation-induced Cl^- enrichment whist abundant recharge-induced dilution is observed during the wet season. B8, drilled in to a silty sand aquifer, recorded slight lower recharge as opposed to D3 and D4, which occur in unconsolidated sandy gravels.

The above physical and chemical models make three contributions to the groundwater recharge mechanisms at the study area. First, two major recharge mechanisms can be established. The fractured sedimentary units, from which most of the drinking wells are sourced, are recharged by rainfall that is flowing through preferential pathways in the fractured systems, whilst alluvial aquifers are recharged by leakage of adjacent surface sources that is rapidly dispersing through unconsolidated macro-pores. Second, rainfall recharge, through physical model, is constrained by climatic variability as shown by the recharge surplus and negative replenishment in the wet and dry seasons, respectively. Third, the sustained recharge rates, estimated from the chemical model, suggest that the hydraulic connectivity of the alluvial systems to the surfaces water sources will warrant continued recharge. The fluctuating recharge rates in the wet and dry season are likely to be related to seasonally variable surface flow conditions.

4.0 DISCUSSION

This chapter examines and integrates the results, presented in chapter 3, in an attempt to define and classify the underlying hydrogeological system present in the Middle Sigatoka Valley (MSV). The following sections include a discussion of the interpretation of geophysical data, physical hydrogeology, hydrochemical facies identification and groundwater recharge estimates from mass balance modeling.

4.1 Interpretation of the geophysical data

Geophysical survey results demonstrate high resolution vertical and lateral variability in geophysical properties, namely electrical resistivity and electro-magnetism. Thus, suggesting heterogeneity in the physical and chemical properties of the geological and hydrogeological materials. The dipole-dipole strong gradient (DDSG) array profiles generated a detailed dataset in relation to the smoothed Schlumberger profiles (Appendix 2.1). The electromagnetic (EM) results, presented as a tapered 5-point running mean, showed features of high lateral and vertical variability in electromagnetic properties. Most of this variance is supported by the electrical resistivity (ER) models. The following sections will focus on the DDSG and tapered EM data and analyze these results as per these pre-survey objectives:

- to show water table depth, determine maximum thickness and spatial extent of alluvium materials;
- to estimate depth to bedrock;
- to identify subsurface anomalous structural features, such as folds, fracture density and faults, which are propitious for groundwater flow and storage; and
- to select potential drill sites.

4.11 Depth to water table, thickness and infilling behavior of alluvium materials

Overall, delineation of water table (Tables 3.2 & 3.3) was difficult in all survey areas due to the saturation of the capping soil from high rainfall associated with Tropical Cyclone Mick (TCM)

whilst the infilling alluvium appears to be constrained by either deformed, uplifted or incised bedrock. As shown below in Figure 4.1, fluvial deposits at Dubalevu are characterized by low resistivities and are ~3-8 m thickness in the first 100 line positions. These units increase in thickness, to ~10-16 m, beyond 120 m survey line position. No buried river gravels, that would be expressed as a high resistivity zone within the low resistivity zone (i.e. between 0-16 m depths), was observed. These results suggest that the Dubalevu survey area is dominated by overbank deposits of relatively uniform grain size and composition.

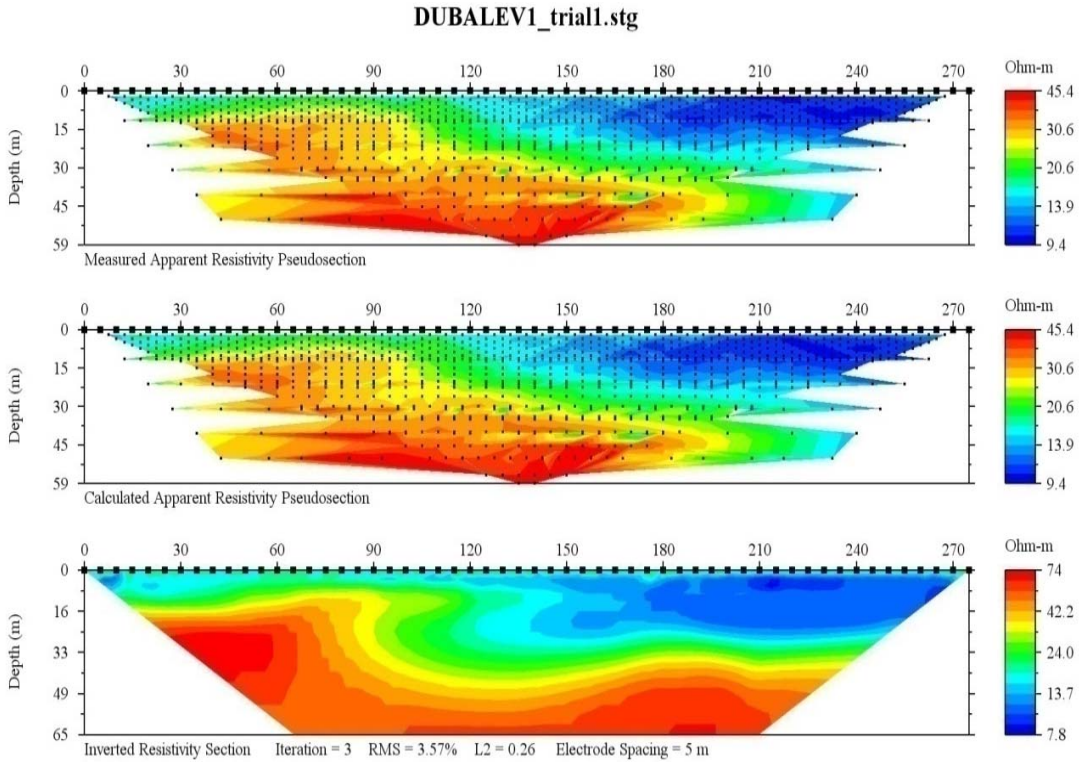

Figure 4.1: resistivity (DDSG array) profile at Dubalevu.

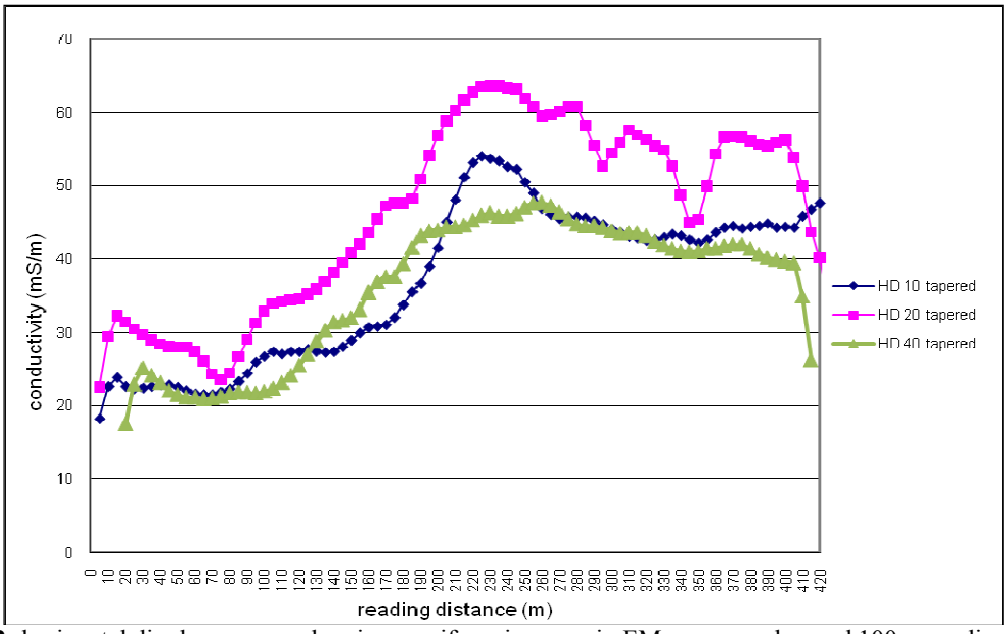

Figure 4.2: horizontal dipole response showing a uniform increase in EM responses beyond 100 m reading positions at Dubalevu.

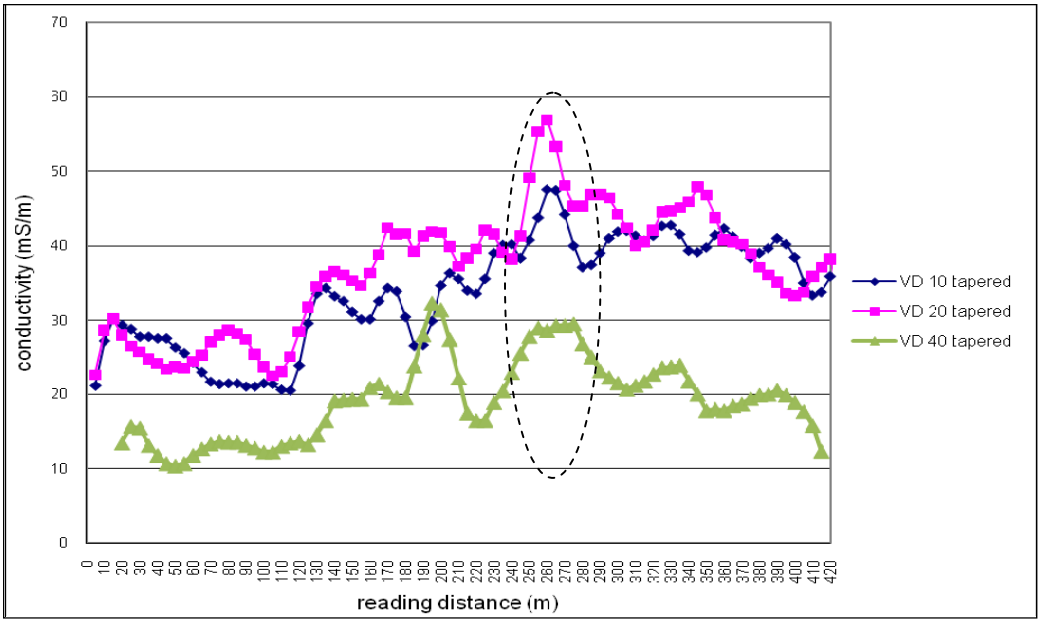

Figure 4.3: vertical dipole response at Dubalevu show a noisy dataset with uniform peak responses between 240-280 m reading positions

An increase in conductivity responses, in Figures 4.2 and 4.3, beyond 100 m EM line positions results from the increasing thickness of saturated alluvium estimated at 7.5-15 m thickness as shown from 10-m coil separation responses in this area. The relatively low horizontal dipole (HD) response is indicative of compact and dry overbank silt whereas the high vertical dipole

(VD) response, due to its deeper depth penetration (Table 3.1), is likely to be caused by increased pore spaces and water content and may represent either pebbly silts or weathered basement at 15 m depth

At Tubakeli, the resistivity profile shown below (Figure 4.4) exhibited an extensive and low-intermediate resistivity layer around 4-7 m depth suggesting flood overbank materials, namely silt and fine sand dominate the shallow subsurface. A low resistivity zone ~8-20 m depths, together with patches of very low response between 0-30 m and 150-180 m resistivity line positions, could represent either saturated overbank materials from excess infiltration from the cyclone event or weathered bedrock. The saturated overbank interpretation is supported by relatively uniform 10-m horizontal and vertical dipole responses (Figures 4.4 and 4.5), suggesting fine and compact materials.

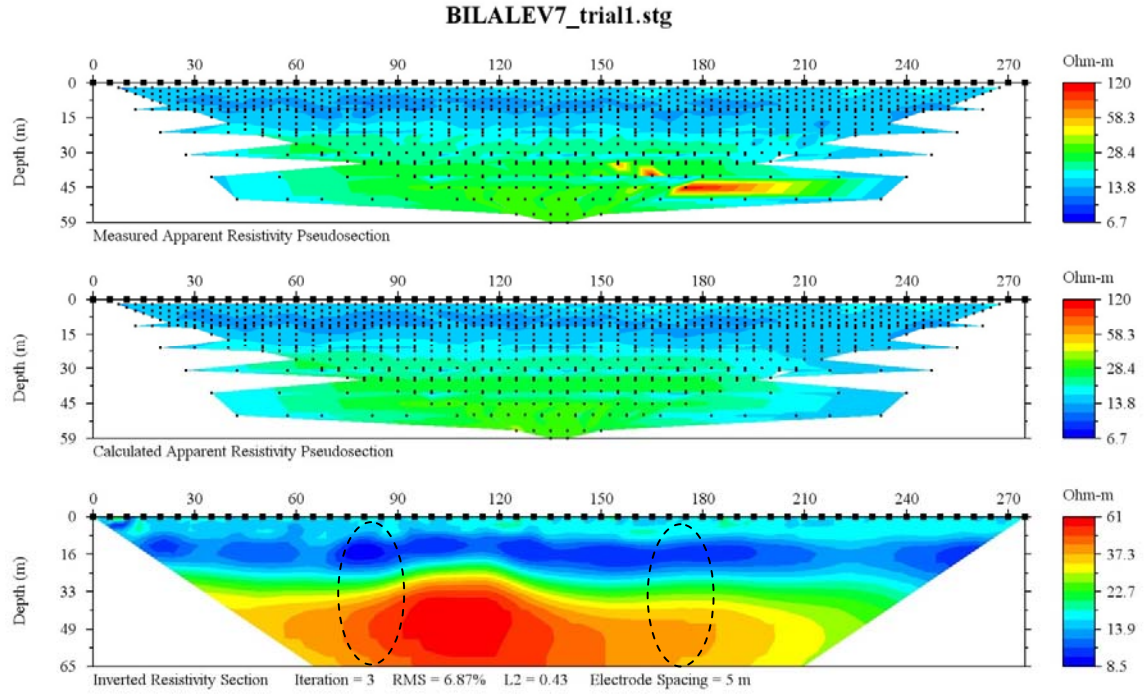

Figure 4.4: resistivity (DDSG array) from Tubakeli showing zone high resisity from 40-65 m depths (possibly bedrock) and surrounded intermediate resistive zone, suggesting weathered or fractured compositied. Areas low resistivity may indicated saturated overbank flood deposits. The dashed oval represent areas of possibile fractured systems as shown by 20-m VD peaks at Figure 4.5.

.

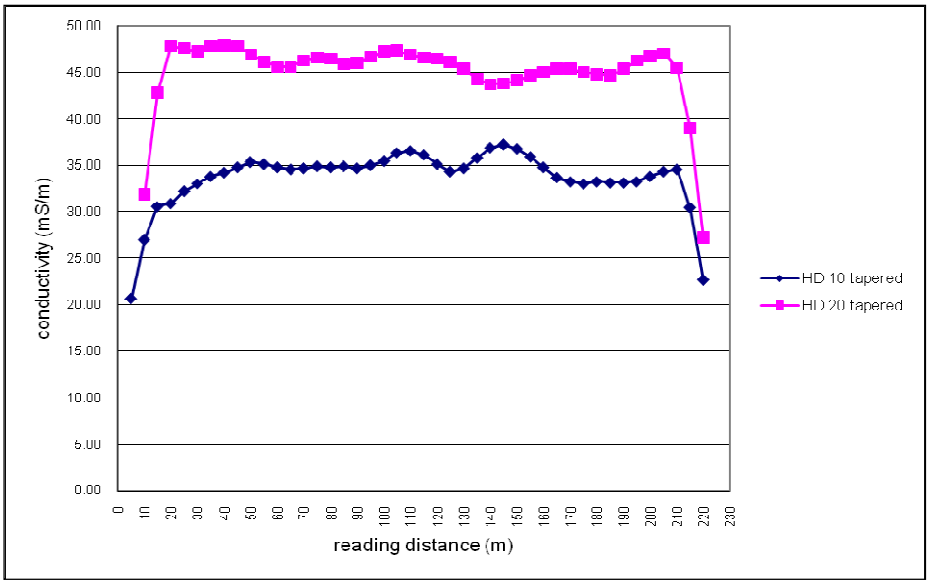

Figure 4.5: EM line 2 horizontal dipole response at Tubakeli showing relatively uniform response in both coil separations with a higher 20-m separation response sugest slight altered porosity at around 15 m depth.

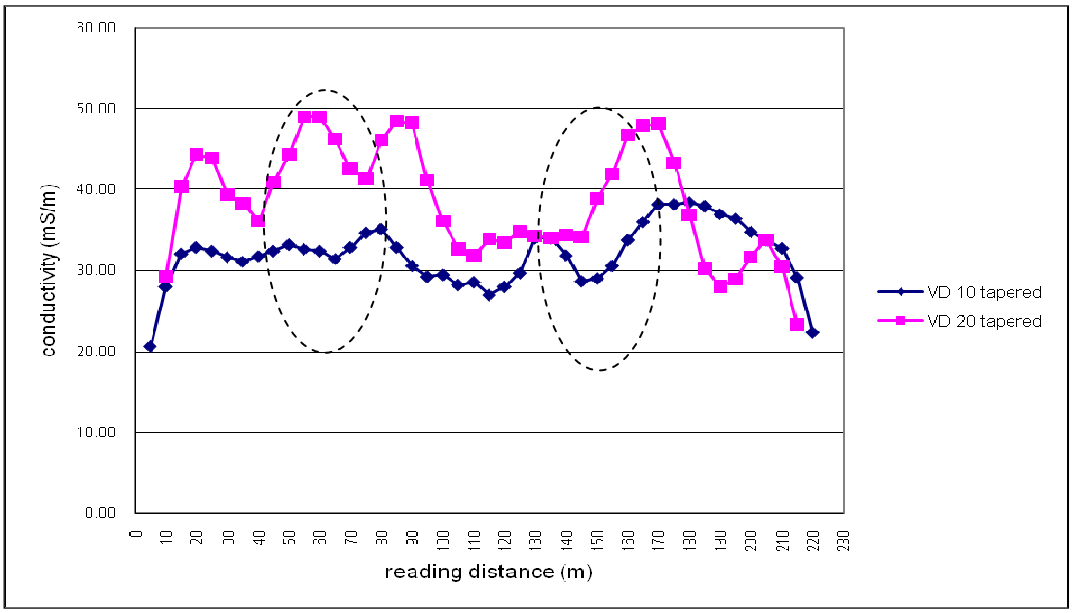

Figure 4.6: EM line 2 vertical dipole response at Tubakeli showing fluctuating responses of 20-m separation and suggests presense of possibile fractured system around 35 m depth between 60-100 m and 150-180 m EM positions.

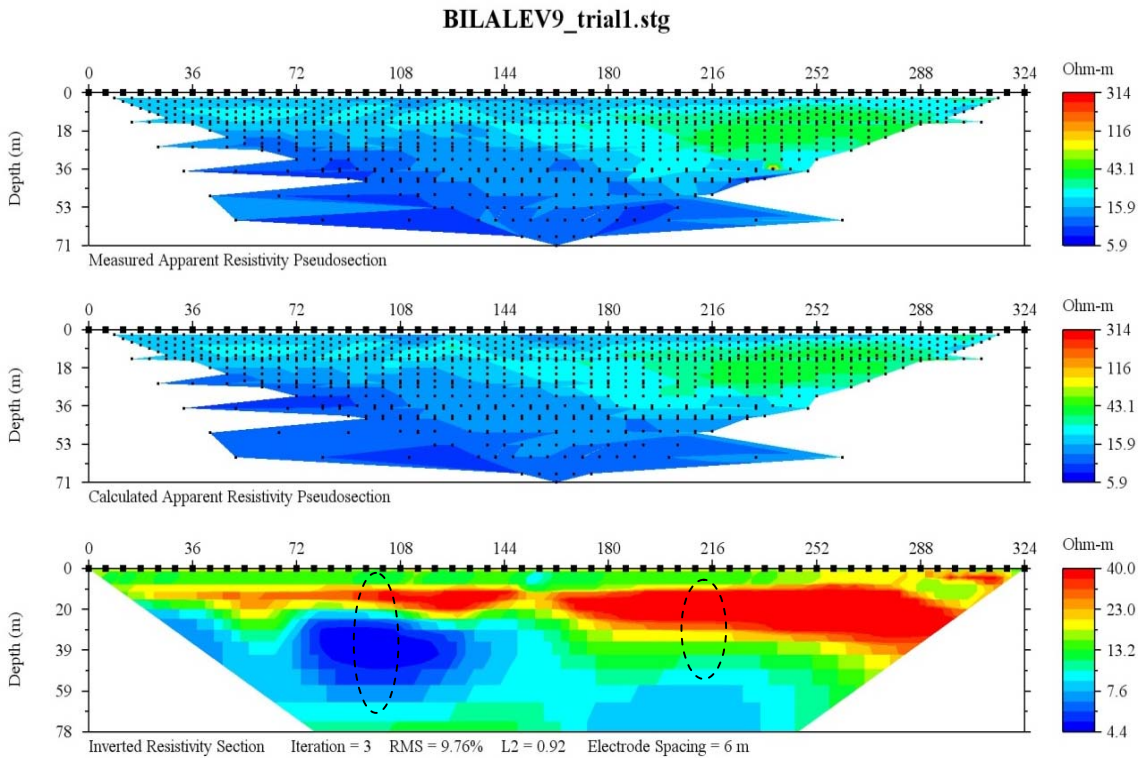

Figure 4.7: resistivity profile at Sugar Ram's farm at Bila Rd showing a possible sheared bedrock at 28-48 m depths between 72-110 m ER positions together with an inferred gravel bar characterised by very resistive zone around 10-20 m depths.

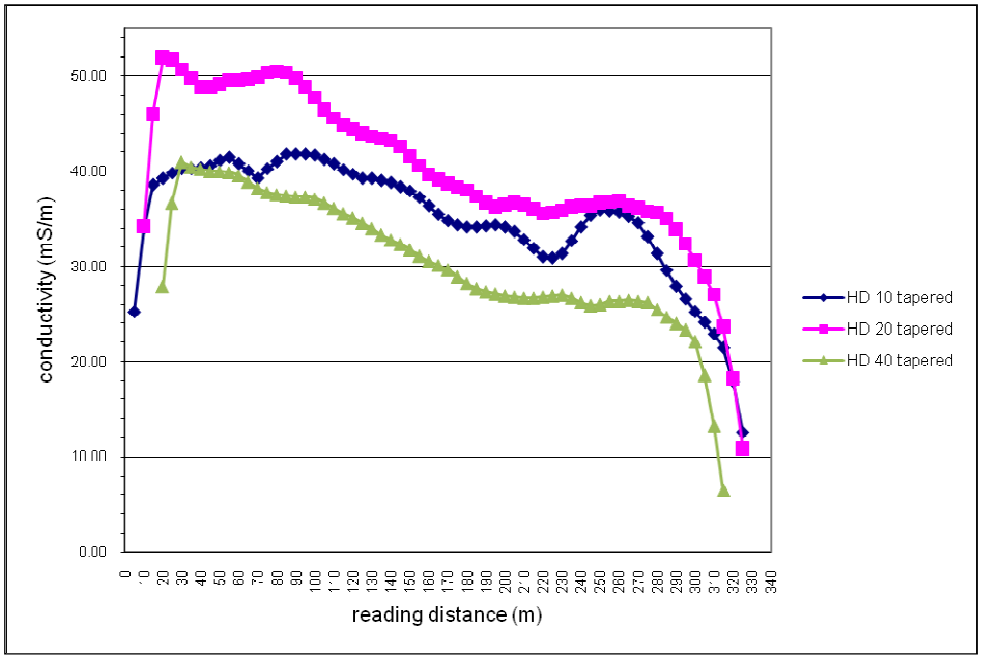

Figure 4.8: horizontal dipole EM response at Bila Rd,Bilalevu showings a relatively high response of 20-m separation suggesting altered porosity at 15m depths whilst the decreasing responses of all coil separations towards the end suggests the influence of the buried gravels bar in attenuating the emmitted signals.

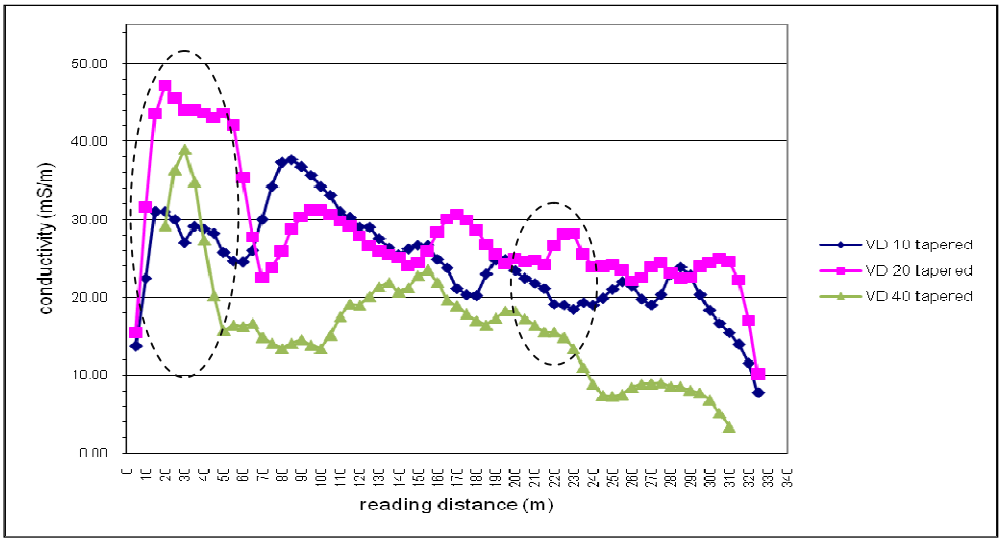

Figure 4.9: vertical dipole EM response at Bila Rd showing a noisy dataset with higher response of 20-m and 40-m separations supporting the the presence the sheared bedrock betwwen 35-60 m depth, while the decreasing trend towards towards the end of the line suggests the influence of the inferred gravel bar attenuating all the emitted electric currrent and hence, inducing low EM response for all coil separation. Two potential drill sites, denoted by dashed ovals, have been selected.

At Bila Rd (Figure 4.7), the top 0-8m depths appears as a low resistivity zone and suggests saturated flood overbank silts and fine sand from TCM excess rain. This is, again, supported by 10-m HD showing low response in the first 120 m positions, suggesting silty materials at around 7.5 m depth. Resistivity profiles from around 100 m ER line positions show a distinct band of high resistivity (> 30 ohm-m) with a maximum thickness of around 8-10 m between positions 100 – 300 m (10–20 m depth) and tapers to around 3 m between 70-90 m (10-13 m depth). This could represent an unconsolidated gravel bar, potentially a buried paleo-Sigatoka River course, that is hydraulically connected to the present river course and hence, could be a favorable groundwater source. Electromagnetic responses support this hydraulic connectivity interpretation (Figures 4.8 & 4.9) with a decreasing trend towards the river where the resistive gravel bar yields low responses between 120-340 survey positions.

4.12 Depth to bedrock

Figure 4.1 clearly shows the depth to the deformed Cici Sandstone (CS) at Dubalevu, characterized by the undulating basement with high resistivity (29-74 ohm-m) and a weathered-mantle (moderate resistivity of 20-29 ohm-m). A bedrock high, probably at 8-15 m depth, is

represented by high ER and low EM responses within the first 100 m positions (Figures 4.2 & 4.3). An increasing depth to bedrock is noticeable in the resistivity profiles from 100-270 m ER line positions and is supported by a gradual increase in conductivity responses from 100 m EM position for all coil separations and orientations. These can be attributed to either increasing depth to bedrock or increasing thickness of saturated alluvium or both. At Tubakeli, the depth to the Takaro Conglomerate/Rudite (TCR) can be estimated at 20-23 m with a low dip towards North. Figure 4.4 showed bedrock as heterogeneous with a high-intermediate resistivity core, around 100-180 m and 90-150 m ER line positions, which may indicate fresh TCR and capped by weathered or fractured composites. The latter is likely to have altered porosity and be conducive for groundwater storage and movement. The 10-m VD and HD results, together with 20-m HD response (Figures 4.5 & 4.6), showed relatively uniform response, suggesting the presence of either compact silts or fresh bedrock between 7.5-15m depths, whereas 20-m VD, with fluctuating response, may indicate fractured bedrock around 35 m depth. At Bila Rd, Figure 4.7 showed the Tari Formation (TF) to be 20-23 m in depth, whilst this depth gradually increases to around 28-30 towards the river. The increasing depth to bedrock could be attributed to bedrock incision of paleo-SR (section 2.3) upon which the fluvial materials were deposited.

4.13Possibility of fault/fractured zone

At Dubalevu, the uniform peak in vertical dipole readings (Figure 4.3) in all coil separations between positions 220-280 m may represent the presence of a possible fault/fracture zone between 15-60 m depth. This may induce preferential groundwater flow and hence, increasing EM values. In Tubakeli, Figures 4.10 and 4.11 (below) showed anomalously high horizontal and vertical dipole responses from 40-m coil separation between 240-380 m, in relation to 20-m coil separation response, and thus, suggesting the presence of a fault and/or fractured zone occurring at 30-60 m depth.

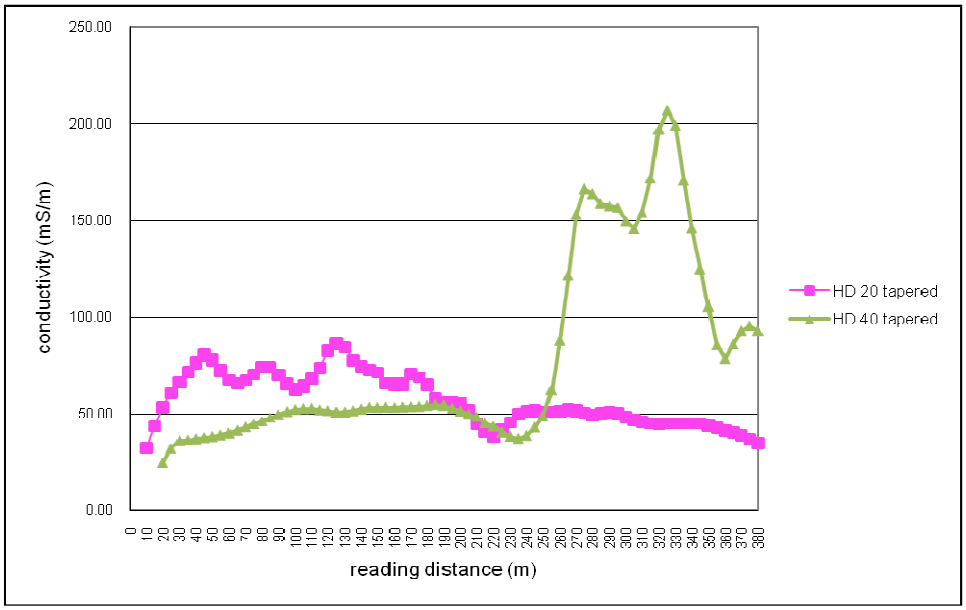

Figure 4.10: EM line 1 horizontal dipole at Tubakeli showing high anamolously high readings from 40-m separation suggetsing a fractured or sheared zone at around 30 m depth.

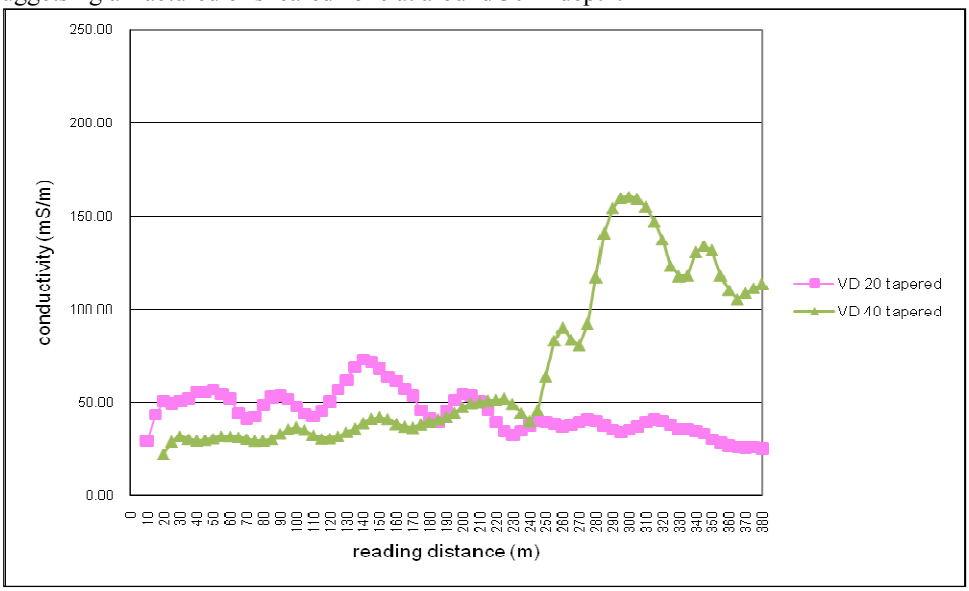

Figure 4.11: EM line 1 verical dipole response at Tubakeli consistenly showing anamolously high 40-m separation response and sugesting fractured basement around 60 m.

This interpretation of anomalous EM response (Figures 4.10 and 4.11), together with the fluctuating 20-m VD response (Figure 4.6), suggests fractured conglomerate and rudite unit around 35m depth. Further, the proximity of Tubakeli to the sinistral Nasovatava Fault (NF) (Figures 3.15 & 3.17) suggests the possibility of localized fractured composites, which could be

potential sources of extractable groundwater. At Bila Rd, the anomalously low ER (Figure 4.7) and high EM responses (Figures 4.8 & 4.9) at 0-100 m ER line-positions likely represent a highly fractured Tari Formation, possibly related to the inferred fault splay of the sinistral fault, which is believed to have propagated along Bila Rd (Figures 3.15 and 3.17). The Nasovatava Fault may create an environment conducive for groundwater flow and storage due to the secondary porosity and permeability produced by fracturing.

4.14Potential drill sites

At Dubalevu, the presence of a possible highly fractured bedrock, as characterized by high vertical dipole responses in all coil separations (Figure 4.3), presents a good opportunity for groundwater exploration and evaluation. Hence, at least two potential groundwater wells will be drilled between 240-280 m EM positions and to a depth range of 20-40 m. At Tubakeli, despite showing stratified ER profiles, the EM responses from Figures 4.6 and 4.11 suggest the occurrence of sheared or fractured basement. Hence, four (4) drill sites have been selected from three adjacent farms to explore the presence of this inferred fractured zone between 30-40 m depths. At Bila Rd, two possible drill sites have been selected at Sugar Ram's farm (Figures 4.7 & 4.9): (1) between 90-100 m ER positions and drilled to 60 m depth to investigate the inferred sheared or fracture zone and (2) between 190-210 m ER positions and drilled to a depth of 35 m to fully penetrate the inferred gravel bar.

In summary, the electrical resistivity and electromagnetic geophysical methods yielded high resolution subsurface models for estimating thickness and extend of overbank and gravelly alluvium deposits, depth to sedimentary bedrock and showing anomalous features denoting possible shear/fracture zones. These subsurface features have guided the selection of drill sites to further explore the physical and chemical conditions of the hydrogeological systems underlying the middle Sigatoka valley.

4.2 Physical Hydrogeology

The groundwater drilling and evaluation stages validated several geophysical survey inferences and proved that groundwater flow patterns are related to lithologic and hydraulic properties of the heterogeneous/complex geological systems (Tihansky, 2005). The following sections will discuss the major hydrogeological groups, namely surficial confining layer system, alluvial aquifer, intermediate confining layer and fractured basement system, before the heterogeneity of the hydraulic properties, structural influences, limited recharge and groundwater flow will be covered.

4.2.1 Hydrogeological framework

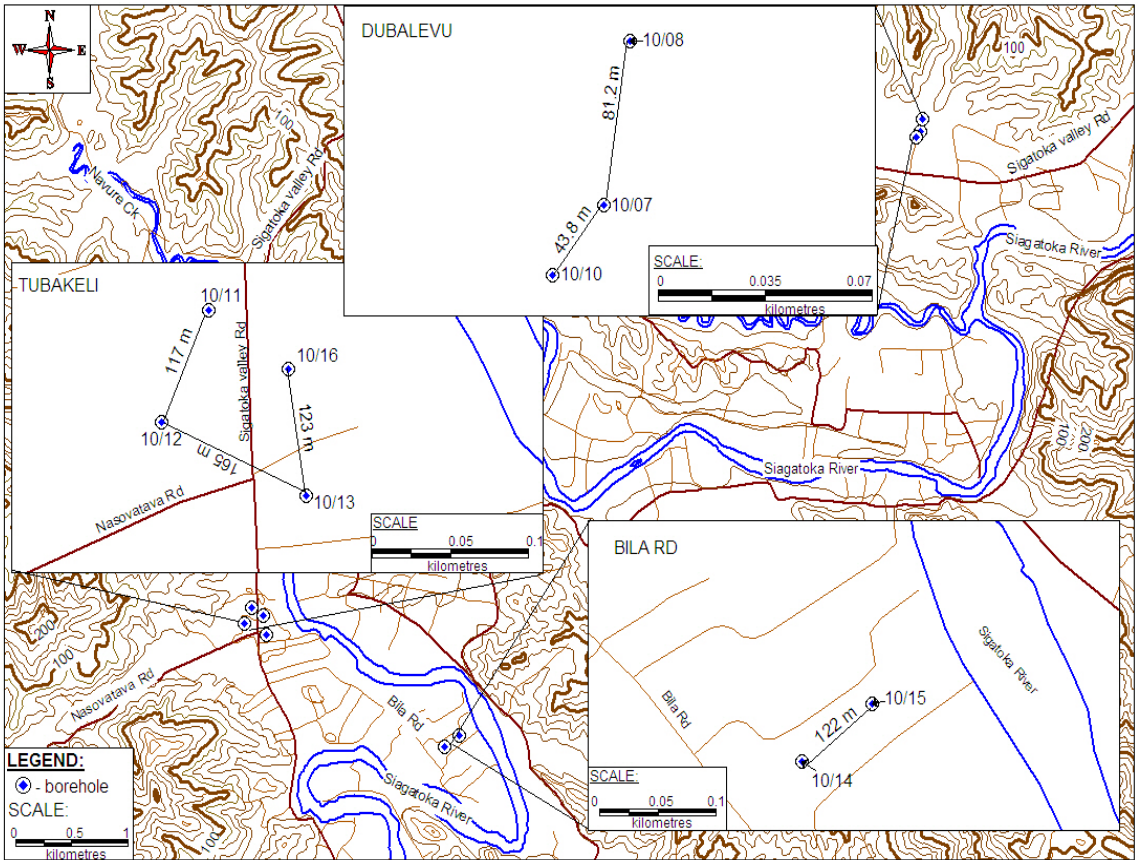

Figure 4.12: Location of boreholes with within the study area (details of the wells are provided in Section 3.4.3).

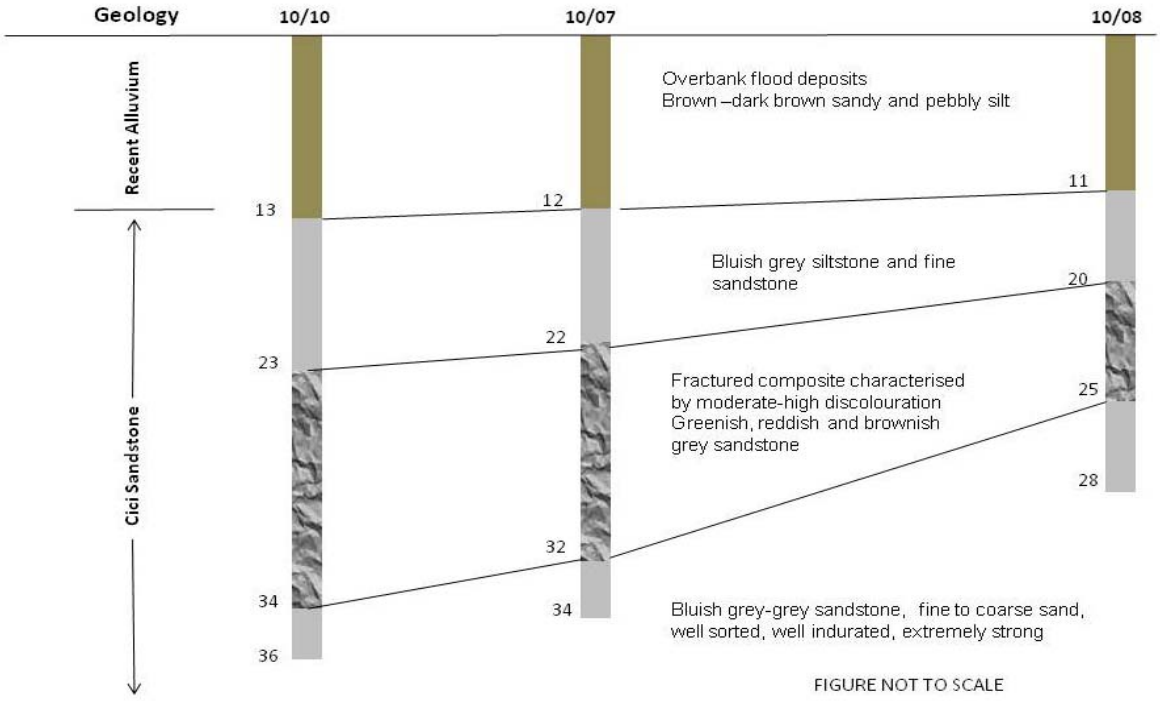

Figure 4.13: hydrostratigrahic log of Dubalevu wells penetrating the surficial confining layer, intermediate confining layer and the fractured composite of the Cici Sandstone.

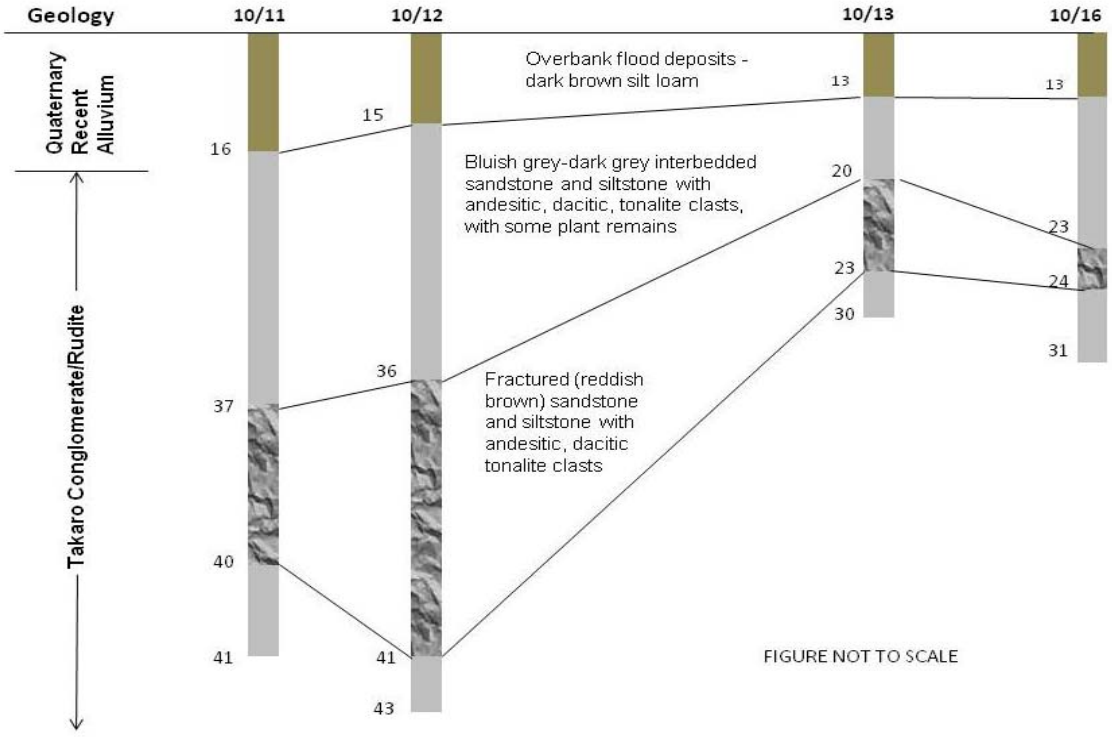

Figure 4.14:hydrostratigrahic log of Tubakeli wells penetrating the surficial confining layer, intermediate confining layer and the fractured composite of the Takaro Conglomerate/Rudite.

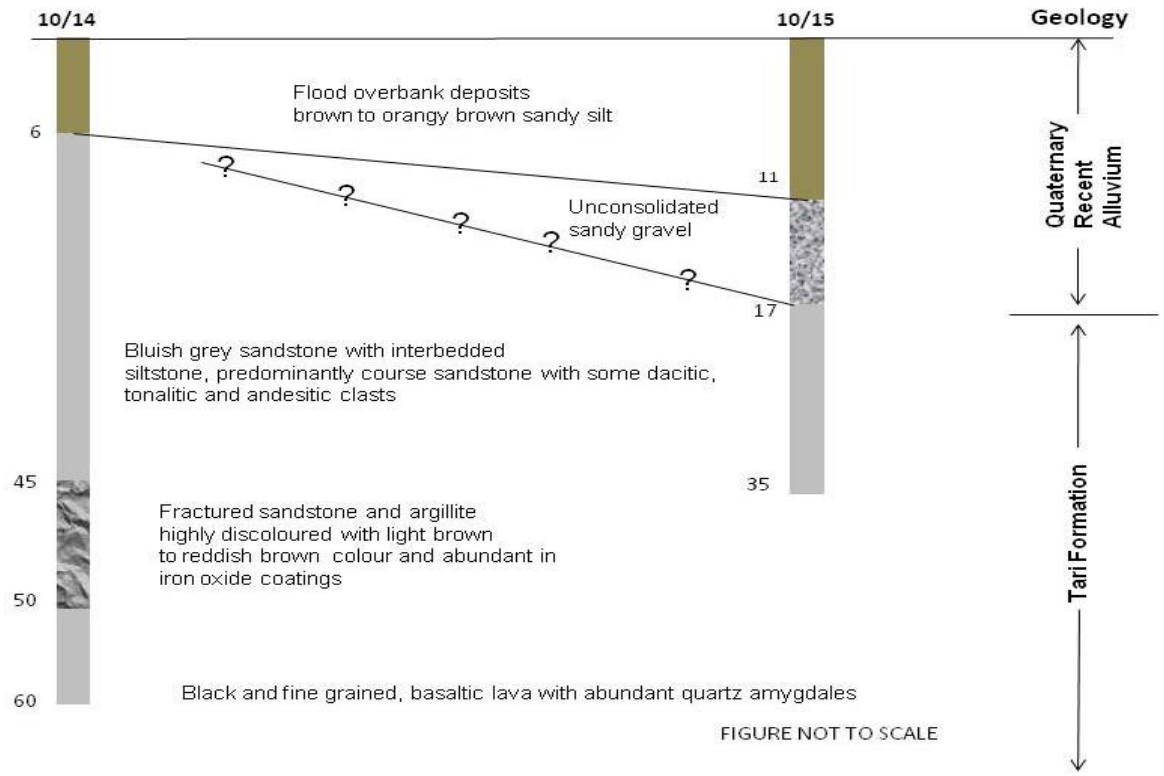

Figure 4.15: hydrostratigrahic log of Bila Rd wells penetrating the surficial confining layer, unconsolidated alluvial system, and the intermediate confining layer and fractured composite of the Tari Formation.

Site	Hydraulic conductivity (K) (m/s^{-1})
Dubalevu	3.6×10^{-8}
Tubakeli	2.4×10^{-7}
Bila Rd	4.9×10^{-8}

Table 4.1: measured K using the WF26010 Falling Head permeability cell

Pumping well (pw)	**10/07**	**10/08**	**10/12**	**10/13**	**10/14**	**10/15**
Observation well	10/10	10/07	10/11	10/12	10/15	-
Pump setting depth	30	23	36	29	47	30
Distance to pwl (m)	43.8	81.2	117	165	122	-
Q (L/s)	10.6	0.57	5	0.9	1.4	1.85
Test duration (mins)	1140	575	1320	920	1230	920
T (m^2/d^{-1})	8.2–29.1	1.14-5.22	19.3-53.5	10.4-21.8	23.3-74	1338.4-1949.5
S	2.3×10^{-4} 4×10^{-4}	4.3×10^{-4}	6.7×10^{-4} 8.6×10^{-6}	8.9×10^{-4}	1.7×10^{-3}	
K (m/d^{-1})	0.82-2.9	0.23-0.69	4.3-11.9	2.6-5.5	4.7-13.5	223.1-324.9

Table 4.2: estimated aquifer properties form constant-rate pumping tests.

4.2.11Surficial confining layer (SCL)

The surficial confining layer is present as flood-overbank deposits and completely weathered colluvium composed of sandy silt and stily loam soil. At Dubalevu, the dark brown, moist-dry, fine grained and non-plastic SCL unit has an average thickness of 10 m and average conductivity (K) value of 7.8×10^{-8} m/s (falling head test estimation - Table 4.1). At Tubakeli and Bila Rd, the brown to light brown sandy silt and silty loam SCL is approximately 11 m thick and recorded the K values of 2.2×10^{-7} and 4.3×10^{-8} m/s, respectively. These low K values suggest infiltration of meteoric and irrigation waters are relatively slow throughout the SCL and vadoze zone.

4.2.12 Alluvial aquifer system (AAS)

The alluvial aquifer system includes unconsolidated sandy gravel deposits penetrated between 11 and 17 m at 10/15 in Bilalevu (Figure 4.17) and the previously drilled Sigatoka Rural Development Project (SVRDP) wells 89/15, 90/15 and 90/16 in Dubalevu with an average depth and aquifer thickness of 40 and 20 m respectively (Davies, 1992). The AAS is composed of sub-angular to sub-rounded, poorly sorted (well graded), medium-coarse gravels (derived from andesite, sandstone, basalt and tonalite) with fine sand. At Dubalevu, the alluvium was estimated at 600 m^2/d^{-1} T and 30 m/d^{-1} K. At Bila Rd, the 6 m thickness gravel bed penetrated at borehole 10/15 yielded a T of 1644 m^2/d^{-1} and a K value of 274.8 m/d^{-1} (Table 4.2 & Figure 4.13) The high hydraulic properties are attributed to preferential flows along macro-pores in well graded and unconsolidated sediments and close proximity of the recharge source, the Sigatoka River (Figure 4.12). Further, low observed drawdown suggest that the pump's maximum output is much less than the well's yielding capacity and hence, the test does not prove boreholes safe yield and the effect of pumping on adjacent sources (Twort et.al., 2000).

4.2.13 Intermediate confining system (ICS)

The intermediate confining system refers to the low permeability layer (aquitard) that overlies the fractured basement unit and receives direct (diffuse) recharge from either silt-dominated soil

or alluvial system. In Dubalevu, this unit underlies the SCL and is characterized by the fresh and interbedded bluish grey to grey siltstone and sandstone between 11-23 m (Figure 4.13). At Tubakeli, the unit is composed of fresh siltstone and sandstone matrix supported (dacitie, andesite and tonalite) conglomerate and rudite that was variably penetrated at 13-37 m depths (Figure 4.14). Around Bila Rd, the confining unit is composed of fresh interbedded argillite and bluish grey coarse sandstone at with some andesitic and dacitic clasts, variably penetrated at 6-10 m depths and with the thickness of 31 m (Figure 4.15) The unit is likely to be leaking due to the drawdown observed at 10/15 in response to 10/14 pumping and permitting the calculation of storativity (Table 4.2).

4.2.14 Fractured basement system (FBS)

The fractured basement system at Dubalevu was variably penetrated in wells 10/07, 10/8 and 10/10 between 21 and 34 m depth ranges. The FBS is comprised moderate-highly fractured Cici Sandstone (Figure 4.13). This variable thickness contributed to the variable T, S and K average values of 18.7 m^2/d^{-1}, 3.15×10^{-4}, 1.86 m/d^{-1} for well 10/07 and 3.18 m^2/d^{-1}, 4.3×10^{-4}, 0.46 m/d^{-1} determined for well 10/08 (Table 4.2). At Tubakeli, the FBS is composed of fractured conglomerate and rudite, characterized by moderate fracture development and highly discoloured sandstone matrix locking dacite, andesite and tonalite clasts, with variable thickness between 1 to 6 m thickness. There, this unit exhibits an average transmissivity, storativity and conductivity values of 36.4 m^2/d^{-1}, 3.4×10^{-4} and 8.1 m/d^{-1} at well 10/12 and 16.1 $m2/d^{-1}$, 8.9×10^{-4} and 4.1 m/d^{-1} at well 10/13.(Figure 4.14 and Table 4.2). At Bila Rd, the FBS is composed of the weathered Tari Formation penetrated between 45-50 m and showing highly discoloured sandstone with abundant iron oxide coatings with an estimate T, S and K values of 48.7 m^2/d^{-1}, 1.7×10^{-3} and 9.1 m/d^{-1}, respectively (Figure 4.15).

4.2.2 Heterogeneity and structural influence

The variable distribution of geological materials, particularly in the alluvial and fractured basement systems, suggests that the groundwater systems are physically heterogenous. The distribution and extent of the sandy gravel in Bilalevu and Dubalevu is limited to the reaches of

historical and present Sigatoka River courses (as detected by the resistivity profiles) with groundwater flow governed by the variable distribution and connectivity of macro-pores, grading of unconsolidated sediments and proximity to recharge source (Kresse & Clark, 2008). This variability is illustrated by the widely ranging hydraulic properties of Dubalevu and Bilalevu unconsolidated alluvial materials, as described above (Section 4.2.12) with the Bilalevu alluvial system shows high yield due to its proximity to the present Sigatoka River (Figure 4.12). Groundwater flow in fractured sedimentary units is constrained by the dimension and distribution of the fractures, aperture and persistence (Cook, 2003). Thus, preferential flow is expected to be concentrated on areas of higher fracture density, aperture and persistence, but the opposite is also true. This is best illustrated by the variable hydraulic properties in the fractured basement under various stress conditions (Table 4.2).

Further, the presence of fractured systems 20-50 m depth in the local sedimentary units signifies the influences of historic tectonic deformation and displacement processes, such as the ENE-WSW trending Nasovatava Fault and its associate shears or fault splays, in controlling the development of fractures and joint systems (secondary porosity) in the sedimentary basement. These, together with precipitation overtime, cause selective dissolution of carbonate minerals causing fracture expansion and enhancing preferential flow (Fetter, 2001) and hence, create an environment conducive for appreciable groundwater storage and flow.

4.2.3 Limited recharge

All but one tested borehole showed limited groundwater recharge defined as continued drawdown during constant rate pumping. Pumping of wells 10/07 and 10/08 at Dubalevu showed continued drawdown of the FBS during the test period in response to the differential pumping rates of 10.6 and 0.57 L/s, respectively. The varying aquifer responses (Table 4.2) could be attributed to the variable thickness, density and dimensions of the FBS, as well as limited recharge (Figure 3.39). At Tubakeli, the pumping of boreholes 10/13 and 10/12 at 0.9 and 5 L/s, respectively, recorded continued drawdown indicative of limited recharge. Borehole 10/12 generated significantly different storativity values of 6.7×10^{-4} during drawdown and 8.6×10^{-6} during recovery. This variability suggests the aquifer was stressed beyond its potential and

hence, shows limited recharge as governed by the variability of thickness, density and dimensions of the FBS (Figure 3.40). At Bila Rd, borehole 10/14, recording a higher storage coefficient of 1.7×10^{-3}, which may suggest either a highly sheared zone with altered porosity and enhanced storage capacity or a proximal recharge source (through vertical down leakage) from the overlying ICS as drawdown was observed at borehole 10/15 with SR being the source. Again, the continued drawdown, although minimal, observed at borehole 10/15 indicated the growth of a cone of depression and thus, limited recharge. However, 10/15 showed little drawdown response to the 1.85 L/s long-term pumping and no drawdown observed at 10/14. This suggests well 10/15 was receiving abundant recharge from an adjacent source, in this case the Sigatoka River, and hence, the cone of depression did extend towards well 10/14 (Figure 4.12).

4.2.4 Groundwater flow direction from periodical monitoring

Figures 4.16 and 4.17 showed the average potentiometric surface that is oriented towards the Sigatoka River and suggests that river flow is composed of groundwater discharge.

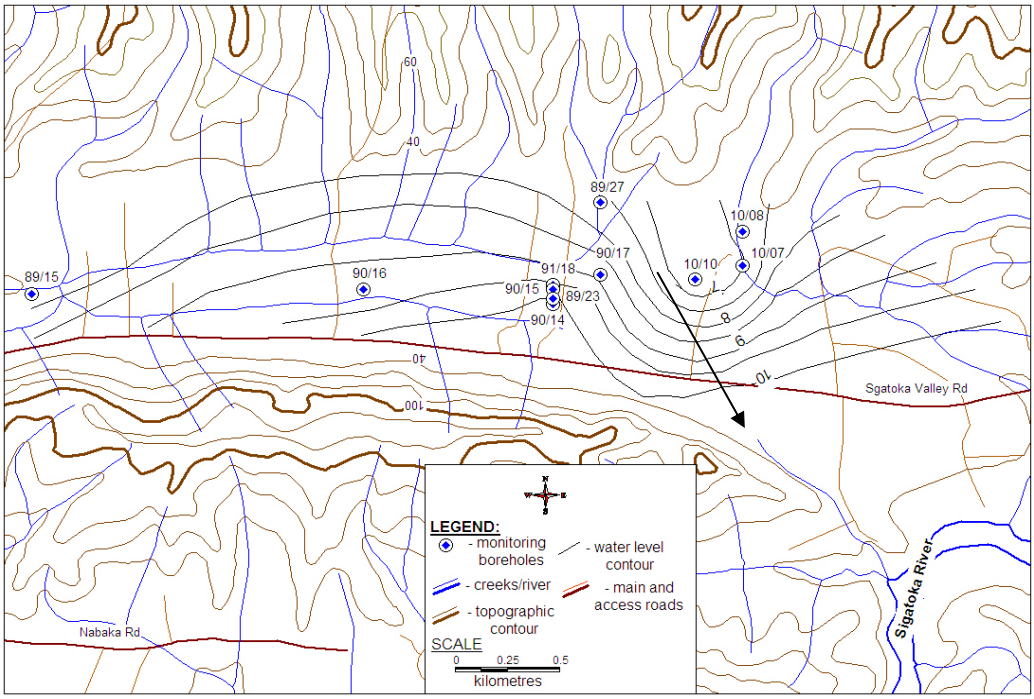

Figure 4.16: Dubalevu water level contour derived from the average of the two measurement periods and showing a NW-SE flow direction to the Sigatoka River.

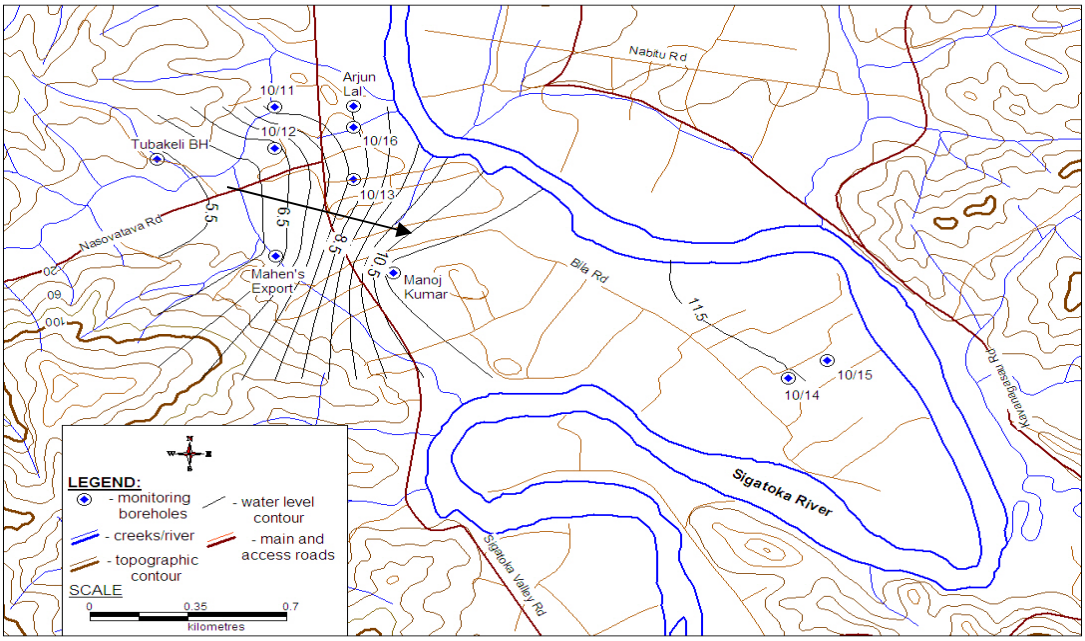

Figure 4.17: Bilalevu water level contour, taken from the averages of the two monitoring periods, showing WNW-ESE flow direction towards the Sigatoka River.

Groundwater in Dubalevu flows in a NW→SE direction whilst a WSW→ESW flow direction was recorded in Bilalevu. This flow pattern is a function of recharge conditions and the spatial variation of hydraulic properties of the aquifer system (Tihansky, 2005). However, the overall decline in water levels in most of the monitored wells (Tables 3.7 and 3.8), suggests that the groundwater system, comprising alluvial and fractured systems, is responding moderately to climatic variations, such as the reduced recharge induced by the dry condition (August and October). These findings suggest that the underlying hydrogeological system is dominated by a shallow aquifer system that receives rainfall-recharge through either fracture-induced preferential flows or unconsolidated macro-pores in the alluvium.

In summary, the physical hydrogeological framework is capped by surficial alluvium systems of silt-dominated confining unit and an unconsolidated sandy gravels aquifer, and underlain by intermediate confining and fractures systems of the local sedimentary units. Variable aquifer parameters estimates, from the pumping tests, are owed to the differing distribution and connectivity of macro-pores and preferential flow paths, heterogeneity of groundwater systems and variable recharge, whilst regional groundwater flow pattern in the valley appear to be oriented towards the Sigatoka River.

4.3 Hydrochemistry

This section first interprets the hydrochemistry of the study area using chemical and isotopic principles. Second, this section considers the observed variability of the chemical and isotopic results in relation to the heterogeneity and complexity of local hydrogeological system and hydrological cycle.

4.31 Hydrochemical classification:

Aqueous geochemical compositions (Tables 3.11-3.13 and Figures 4.18 and 4.20) indicate that the Middle Sigatoka Valley (MSV) waters include two major facies, namely $Ca(HCO_3)_2$ and $Na^+(HCO_3)$ type waters. The latter was observed in deep groundwater sources, drilled to 47-60m, while the former was observed in shallow sources penetrated at 20-45 m. The dominant $Ca(HCO_3)_2$ type water can be attributed to rainfall-derived sources, with enrichments in organic carbon due to soil respiration (Wallick, 1981) ultimately causing dissolution of carbonate minerals present in the local sedimentary units (Figure 4.20), most of which are derived from Qalimare Limestone during the Late Miocene (Hathway, 1995). Figure 4.18, below, showed the dominance of $Ca(HCO_3)_2$ type waters whilst a number of samples occupy the 'no-dominant cations' boundary suggesting mixed sources from halite (NaCl) and dolomite ($CaMgCO_3$) weathering. The $Ca(HCO_3)_2$ type water sources, therefore, suggest rapid and shallow flow systems dispersing through either alluvial or fractured systems (including springs) with moderate-high transmissivity and conductivity (Table 3.6).

However, two sites, namely B5 and B18 (Table 3.13 and Figures 4.18 & 4.20), showed $Na(HCO_3)$ type waters, which suggest a deeper groundwater source, consisting of sodium enriched connate groundwater, and more limited recharge rates. Well B5, drilled to 47 m depth, showed the depletion of calcium and magnesium in relation to most $Ca(HCO_3)_2$ type sources and the enrichment of Na^+. These data suggest the precipitation of dolomite as a secondary mineral and the associated ionic exchange of Ca^{2+} and Na^+ as shown by an anomalously high Na^+ concentration of 156 mg/L in relation to $Ca(HCO_3)_2$ (Hiscock, 2005).

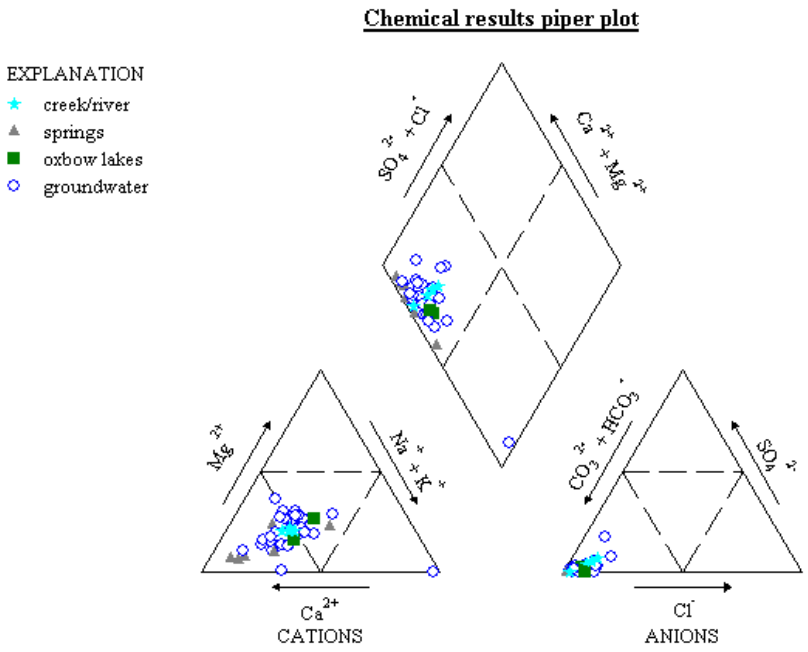

Figure 4.18: piper plots of all sampled water sources in the study area.

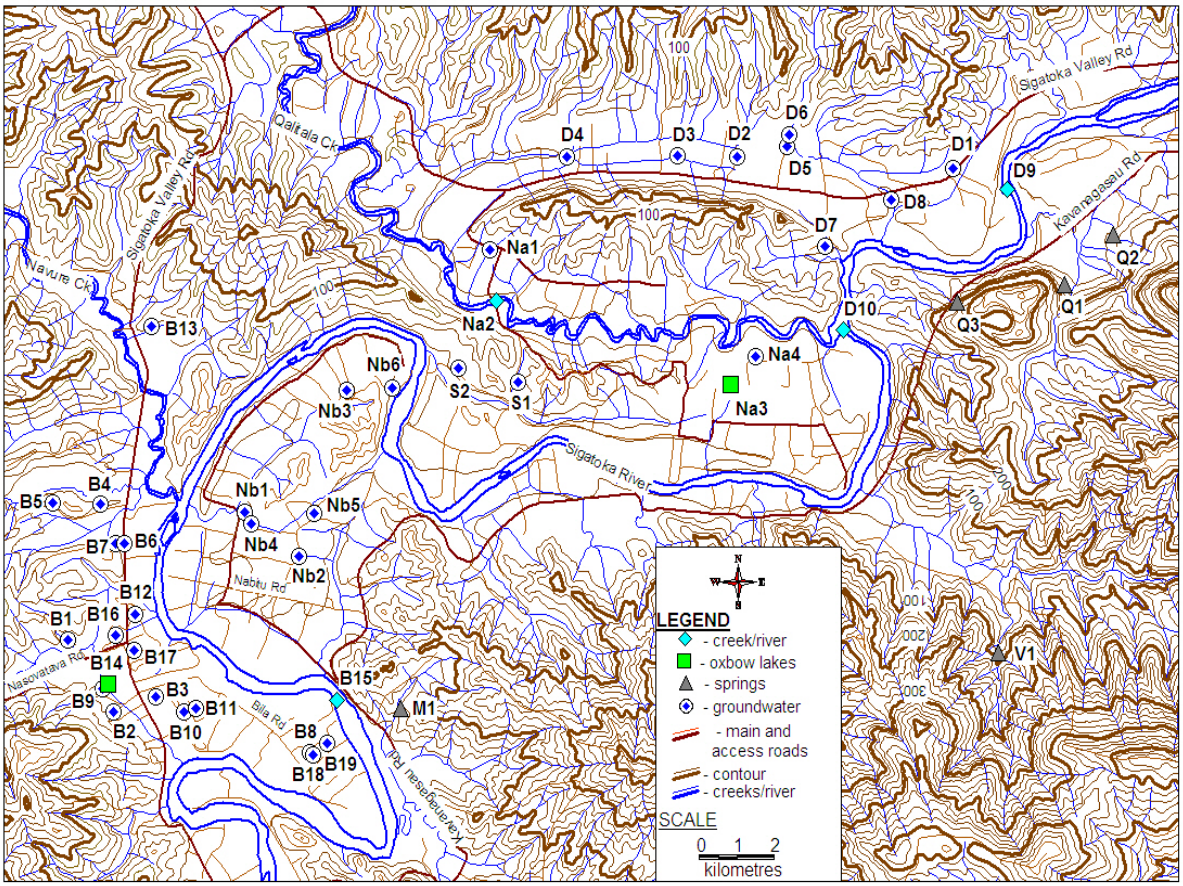

Figure 4.19: Location of map of chemical sampling sites with unique site ID.

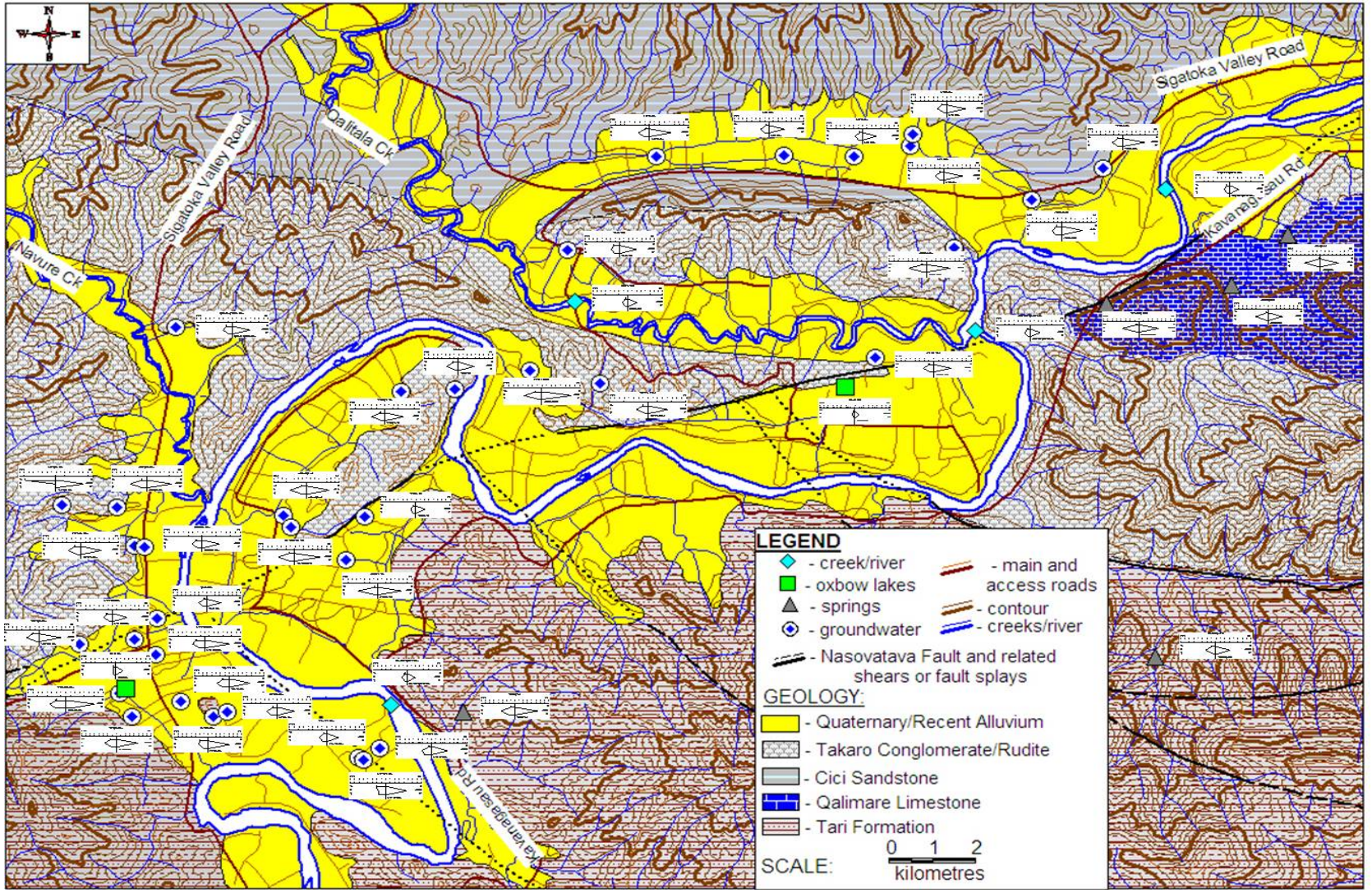

Figure 4.20: stiff plots of all collected samples superimposed on geological units and showing the dominance of $Ca(HCO_3)_2$ type water with two sites (B5 and B18 recording $Na(HCO_3)$ type groundwater across the Middle Sigatoka Valley.

The sample from bore B18, 60 m depth, showed a slightly higher [Na^+] as opposed to Ca^{2+} (relative to well B5) and in relation to well B19 suggests mixing between shallow and deep sources. The elevated Na^+ can be attributed to upward flow of connate groundwater or dissolution of evaporates, such as halite, that is mixing with [Ca^{2+}] of shallower source. The drawdown response of site B19 (located near the river) in relation B18 pumping (Figure 3.38 & Table 3.6) confirms mixing from a shallow [Ca^{2+}] source, likely from either the adjacent alluvial system or the Sigatoka River.

n summary, the chemical dataset suggest two flow systems exist in the middle Sigatoka Valley:

(1) shallow system of $Ca(HCO_3)_2$ type water dominated by rapid carbonate weathering and adequate meteoric recharge; and

(2) deeper system of $Na^+(HCO_3)$ type water dominated by connate groundwater with some mixing.

4.32 Isotopic composition – source of water resources

The stable isotopic composition of study area waters (Table 3.14),range between -5.71 to 0.08 ‰ $\delta^{18}O$ and -35.95 to 2.35 ‰ δD for groundwater, -5.96 to -0.16 ‰ $\delta^{18}O$ and -36.57 to -18.98 ‰ δD for springs, -5.17 to -0.47 ‰ $\delta^{18}O$ and -32.88 to -5.89 ‰ δD for creek/rivers sources, 0.38 to 0.63 ‰ $\delta^{18}O$ and -18.84 to -10.55 ‰ δD for oxbow lakes, and -4.58 to 1.19 ‰ $\delta^{18}O$ and -28.89 to 8.76 ‰ δD for rainwater. Figure 4.1below, a plot of δD vs $\delta^{18}O$, reveals the relatively negative compositions, with variable enrichments of deuterium and ^{18}O, on a positively linear trend. This further shows that the groundwaters exhibit similar isotopic compositions to surface sources, most of which plot along a local meteoric water line (LMWL) of slope 4.3. This demonstrates a meteoric origin for groundwaters in the area. Meteoric waters are either flowing into and through the surfaces systems or dispersing at both variable depths and flow rates through alluvial and fractured systems (Table 4.2) with variable influences of evaporation in vadoze zone and surface environment prior to infiltration. The most negative isotopic values, plot close to the global meteoric water line (GMWL), represent rapidly flowing and/or dispersing meteoric recharge with negligible evaporative influences, whilst the more positive isotopic compositions suggest moderate-intense modification via free evaporation and/or mixing with older residual evaporated water in either surface storage, groundwater storage or infiltrating the vadoze zone.

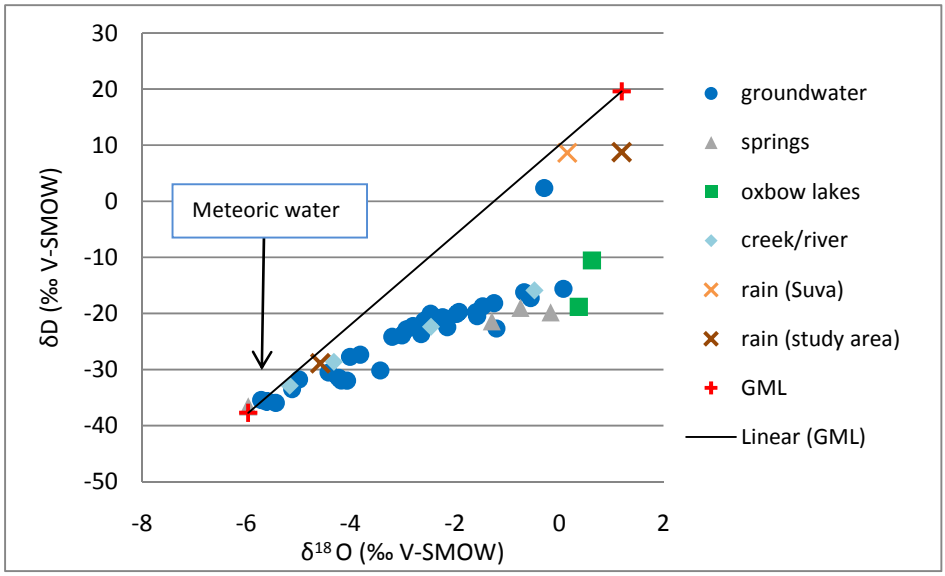

Figure 4.21: plot of $\delta^{18}O$ (‰) vs δD(‰) of sampled water sources in the study area.

This linear trend suggests that water, from headwaters (i.e. recharge zone), evolves from a relatively homogeneous meteoric source (i.e. local recharge plotted close to GMWL) to a mixture of connate groundwater and slightly enriched ^{18}O evaporated surface water infiltrating the vadoze zone (Walker & Krabbenhoft, 1998). This enrichment and mixing of groundwater is well illustrated by the enriched deuterium and more positive ^{18}O recorded in sample B11 (0.08 ‰ $\delta^{18}O$ and -15.62 ‰ δD, Table 3.14, Figures 3.67-3.68), which is possibly sourced from the mixing of evaporated connate groundwater and evaporated rainfall flushing through the fractured basement, as well as evaporated surface water infiltrating the vadoze zone.

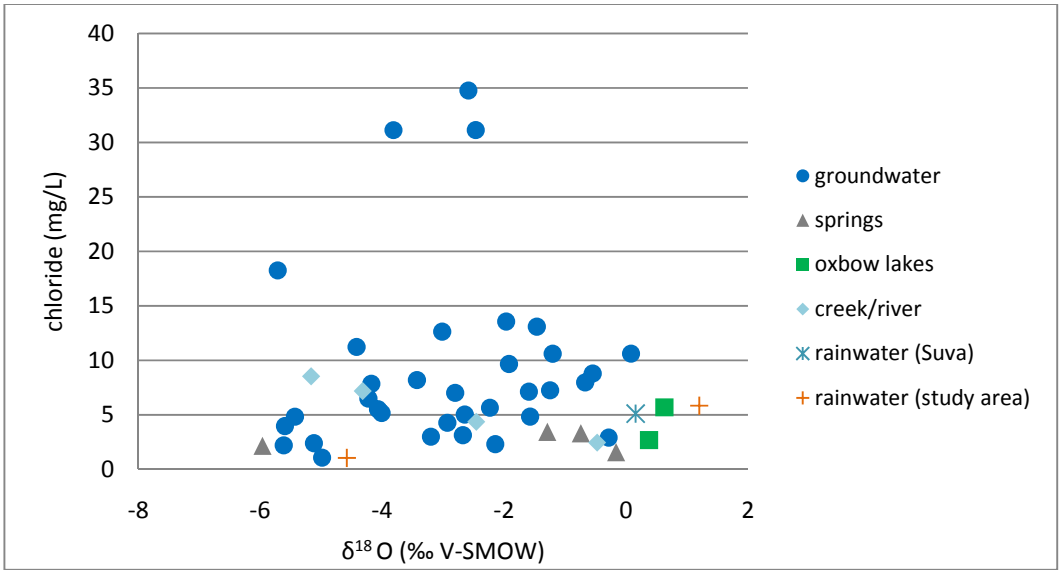

Figure 4.22: plot of $\delta^{18}O$ vs chloride (mg/L) dominated by isotopic depletion and low Cl^- (0-20 mg/L).

However, the low chloride concentration in all the sampled water sources as shown by Figure 4.22, (1.02-34.76 mg/L, Table 3.15) in relation to most of the costal and geothermal springs in Viti Levu and Vanua Levu sampled in 1980 (50-200 mg/L, Cox & Hulston, 1980), suggest that elevated chloride in valley waters via evaporation during the dry season is likely to dampened by abundant rainfall recharge-induced dilution in the wet season, hence, suggesting abundant meteoric recharge seasonally. These, together with the low temperature measured in all water sources (25.5-30.7 °C, Table 3.9) in relation to the 1980 thermal spring sources (Figure 3.70), eliminate the possibility of magmatic mixing within the study area.

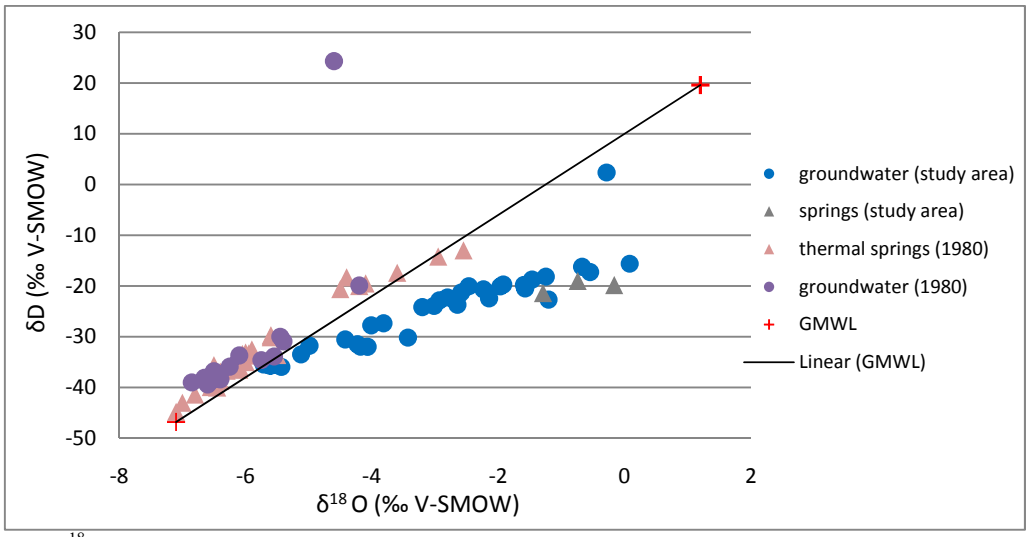

Figure 4.23: $\delta^{18}O$ (‰) vs δD (‰) plot of groundwater and springs in the study area together with groundwater and springs data documented in Cox and Hulston (1980).

Figures 4.23 and 4.24 showed the similarities and differences of the study area and Viti Levu sampled sources in the previous study conducted in 1980 (Cox & Hulston, 1980). Both the datasets exhibited LMWL of slopes < 8, which can attributed to the condensation and precipitation of vapor generated from rapid evaporation prevalent in tropical islands zone (Sharp, 2007). The plotting of more negative isotopic close to the GML and the linear trend of more positive isotopic compositions are common in both datasets.

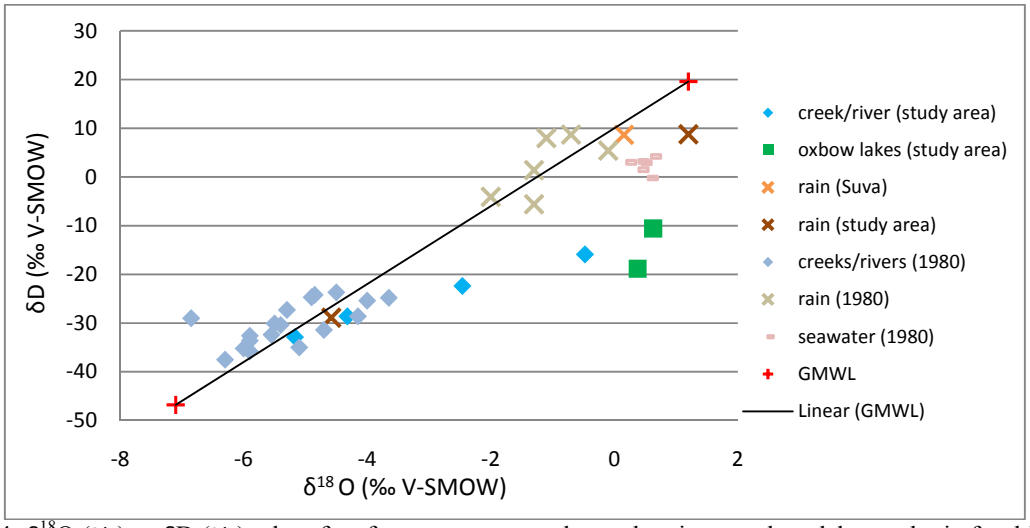

Figure 4.24: $\delta^{18}O$ (‰) vs δD (‰) plot of surface sources, namely creeks, rivers, oxbow lakes and rain for this research, and surface sources sampled in 1980.

These suggest meteoric-derived waters that are variably modified by either evaporation or mixing with other residual evaporated waters. However, the major difference is observed by the slopes of residual evaporation lines in both datasets. The 1980 data showed a LMWL slope of ~6, whilst the study area exhibited a relatively lower LMWL slope. The fact the LMWL of the study area has a slope < 4.3 suggests the influence of arid climate in the leeward area that drives the kinetic fractionation and that mixing of residual evaporated waters results in the enrichment of deuterium and ^{18}O in the liquid phase (Cox & Hulston, 1980). This enrichment is exemplified by the more positive isotopic composition recorded in both the oxbow lakes (0.4‰ and 0.6‰ $\delta^{18}O$, Table 3.14 & Figure 3.67-3.68), which can attributed to the evaporation-induced diffusional processes prevalent in lakes at low humidity (Pentecost, 2005).

4.33 Complexity of surface and groundwater systems

The heterogeneity and/or complexity of surface and groundwater flow systems and processes are illustrated by the (1) high variability in chloride concentration, (2) variable enrichment/depletion of sulfate, magnesium locally, (3) variable pH values and HCO_3, (4) variable isotopic compositions in surface flows, and (5) signatures of groundwater and surface interaction. The following section further explores these interesting geochemical patterns.

4.33.1 variability of chloride concentration (Cl^-)

Subsurface [Cl^-] sources may include saline intrusion, ionically enriched connate groundwater and evaporates weathering such as halite (Tihansky, 2005). Table 3.15 and Figure 4.22 showed that the water sources in the MSV are dominated by low [Cl^-] (1-18 mg/L): this may indicate abundant meteoric recharge-induced dilution. Numerous sites, namely S2, B9 and B3, showed slightly elevated [Cl^-] (>30 mg/L, Table 3.15), which suggests proximity to some [Cl^-] sources.

Location	Natadola Harbour	Natadola Harbour
Region	SW Viti Levu	SW Viti Levu
Season	Wet	Dry
pH	5.46	5.24
HCO_3^- (mg/L)	0.94	1.23
Ca^{2+} (mg/L)	0.17	0.09
Cl^- (mg/L)	1.22	1.8
EC (µS/cm)	6.9	9.6
Fe^{2+} (mg/L)	0.04	0.03
Mg^{2+} (mg/L)	0.07	0.07
Mn^{2+} (mg/L)	0.02	0.028
K^+ (mg/L)	0.11	0.193
Si (mg/L)	0.07	0.06
Na^+ (mg/L)	0.6	0.938
SO_4^{2-} (mg/L)	0.7	0.77

Table 4.3: bulk chemistry precipitation measured at Natadola Harbour, southwest Viti Levu showing mean chloride concentration of 1.5 mg/L (Waterloo et.al., 1997).

Type	**Location**	**SampleID**	**Collection Date**	**δD(‰)**	**δ^{18} O(‰)**	**Cl^- (mg/L)**
Rainwater	Suva	R1	13/07/10	8.64	0.16	5.11
Rainwater	Bilalevu	R2	31/08/10	-28.90	-4.58	1.06
Rainwater	Bilaevu	R3	25/11/10	8.76	1.20	5.84

Table 4.4: rainwater samples data extracted from Table 3.15

Variability in chloride was also recorded in two rain samples collected at Bilalevu (Rn2 and Rn3 - Table 4.4). Sample Rn2 (1.1 mg/L), the dry period rainfall sample, recorded similar [Cl^-] to

rainwater measured at Natadola Harbour rainfall station, southwest Viti Levu, with 1.5 mg/L (Waterloo et.al., 1997) (Table 4.3). This suggests similarity in sources of air masses and atmospheric conditions. Due to low humidity and intense evaporation common in dry period (Sharp, 2007), precipitation may have occurred at higher altitude and will be less enriched in D and ^{18}O due to Rayleigh fractionation. This is supported by negative δD and $\delta^{18}O$ values of -28.9 ‰ and -4.58 ‰, respectively, in relation to Rn1, Rn3 and 1980 rain samples (Table 4.4 and Figure 4.21 & 4.23). Sample R3 (5.8 mg/L Cl^-), collected in November, showed similar [Cl^-] to rainwater collected in the windward area, near Suva, in July, 2010 (5.1 mg/L; Table 4.4). This suggests similar sources of saturated air masses and similar atmospheric conditions (e.g. relatively high humidity) at low altitudes during the wet season. Hence, wet season rainfall will likely to experience variable amounts of Rayleigh fractionation depending on storm-track path and water recharge processes in the air parcel (Sharp, 2007). This interpretation is supported by more positive δD and $\delta^{18}O$ values of +8.76 ‰ and +1.2 ‰, respectively, in relation to R2 and some of the 1980 rain samples (Table 4.4 & Figures 4.21 & 4.23). In summary, the isotopic composition of rain is variable owing to the combined effects of Rayleigh fractionation dominant during the wet season and the seasonal amount effect known to occur in tropical regions.

4.33.2 variability in sulfate, sodium and magnesium

Elevated [SO_4^{2-}] in numerous samples, namely D9, D10, B3 and B9, suggests gypsum dissolution is occurring along numerous flow paths in the study area (Tables 3.12 and 3.13). The fact that numerous groundwater sources plot in the 'no-dominant cations' boundary (Figure 4.19), suggests mixing between end-member sources is a dominant control on groundwater chemistry. Gypsum, halite ($NaCl^-$) and dolomite ($Ca^{2+}Mg^{2+}$) dissolution at depth contributes to the complexity and heterogeneity of groundwater flow systems.

4.33.3 variability of pH values and HCO_3

The measured groundwater pH range of 6-8 (Table 3.9), in relation to rainfall pH of 5.3 measured at the southwest of Viti Levu (Waterloo et.al., 1997; Table 4.3), represents the varying evolution of meteoric-derived groundwater from acidic to neutral to mildly alkaline state. This evolution can be

attributed to variability in recharge, variable ionic exchange processes and variable concentration of aqueous CO_2.

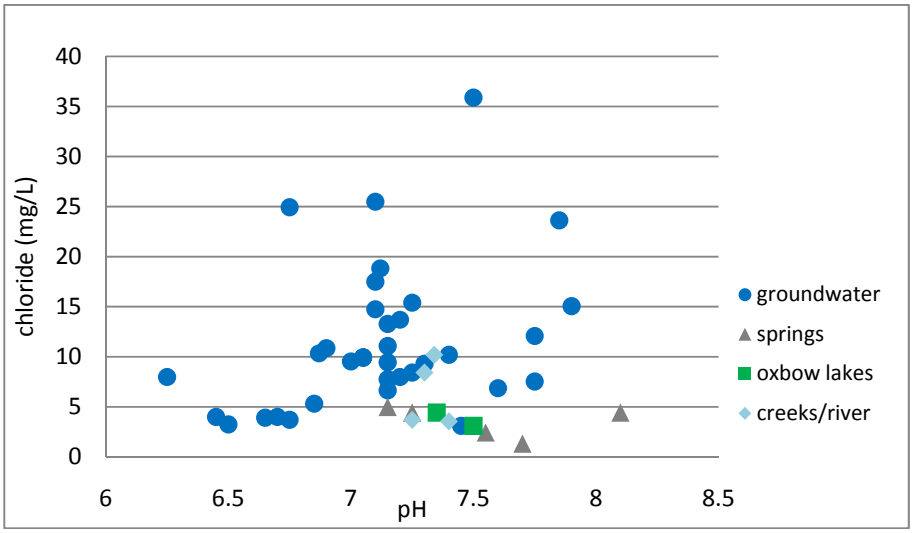

Figure 4.25: ph vs [Cl^-] (mg/L) plot of sampled water sources in the study area showing highly scattered data.

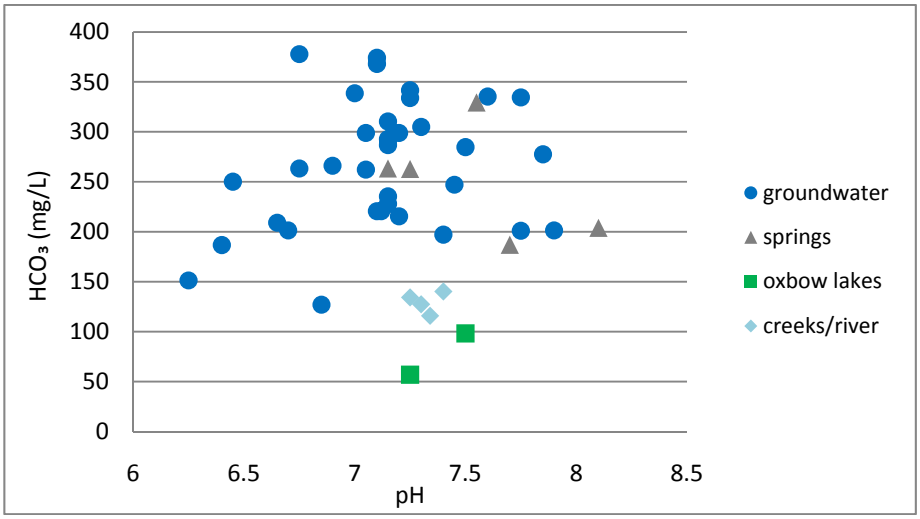

Figure 4.26: pH vs [HCO_3^-] (mg/L) plot of sampled water sources in the study area showing highly scattered data.

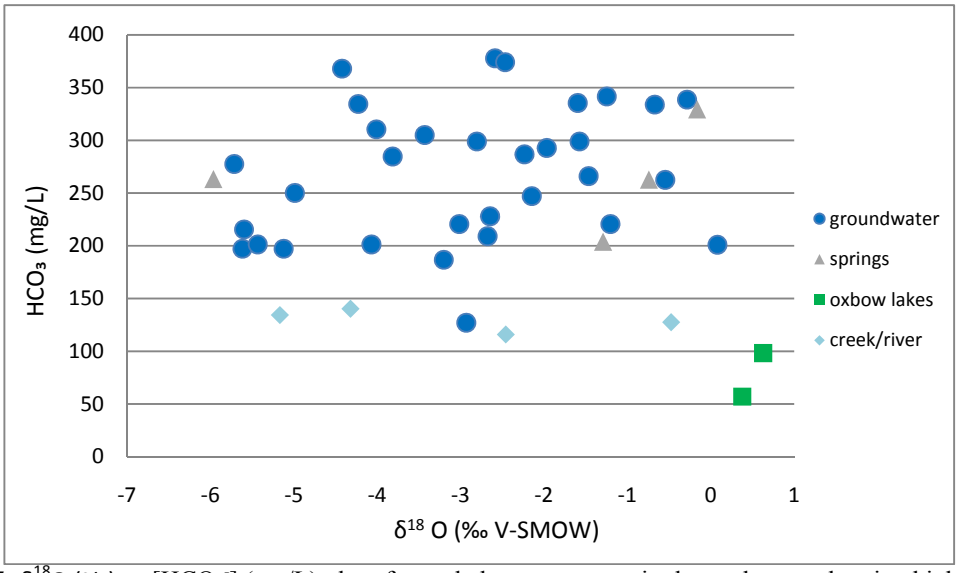

Figure 4.27: $\delta^{18}O$ (‰) vs $[HCO_3^-]$ (mg/L) plot of sampled water sources in the study area showing highly scattered relationship.

Figures 4.25 and 4.26 show a highly complex relationship between pH vs $[HCO_3^-]$ and pH vs $[Cl^-]$, further reinforcing the variable recharge, and physical and chemical processes at work in the system. The sampled springs, most of which are water table springs (section 3.1.3.2), are mildly alkaline waters (7.1-8.1, Table 3.9) attributable to rapid calcite dissolution and bicarbonate enrichment derived from the Qalimare Limestone (Figure 4.20). Figure 4.27 shows a similar, highly scattered, relationship between $\delta^{18}O$ and $[HCO_3^-]$ suggesting variable amount of evaporation on water sources in the study area and varying HCO_3 enrichment Again, these findings, reinforce the complexity of the groundwater and surface water processes that influence the local hydrogeochemistry.

4.33.4 signatures of groundwater-surface interaction

A number of groundwater samples provided evidences of groundwater-surface interaction. Sample D2 and D3 (drilled into sandy gravel to 40-45 m depths at Dubalevu) and sample B19 (drilled into silty sand in Bilalevu) and showed low EC, HCO_3 and TDS similar to creeks and river samples D9, D10 and B15 (Tables 4.5, 3.12 and 3.13).

SampleID	Location	Type	EC	TDS	HCO_3^- (mg/L)	δD(‰)	$\delta^{18}O$ (‰)	Cl^- (mg/L)
D2	Dubalevu	GW	289.3	188	186.7	-24.16	-3.20	2.9
D3	Dubalevu	GW	317.8	203.8	209.1	-22.57	-2.68	3.1
D9	Dubalevu	R	249	154	134.3	-32.88	-5.17	8.5
D10	Dubalevu	R	252	156	140.3	-28.62	-4.32	7.1
B15	Bialevu	R	213.6	132.2	115.9	-22.38	-2.46	3.9
B19	Bilalevu	GW	390	241.7	235.5	-35.66	-5.60	4.3
Nb5	Nabitu	GW	220.8	136.5	127	-22.84	-2.93	4.2

Table 4.5: groundwater (GW) and river (R) samples showing signatures of groundwater-surface water interaction.

With a low Cl^- of 2.9 and 3.1 mg/L and isotopic composition of and -3.2 and -2.7‰ $\delta^{18}O$, it is likely that these alluvial sources receive direct recharge from leakage of surface water bodies, demonstrating the connectivity of surface and groundwater systems as was earlier shown by the geophysics results. Further, well Nb5, drilled to 40m into local conglomerate and rudite unit(Table 4.5 and Figures 4.19 and 4.20) also recorded EC and TDS similar to surface samples D9 and D10, together with depleted isotopic composition of -2.9 ‰ $\delta^{18}O$ in relation to surrounding wells in Nabitu (sites Nb1, Nb2 and Nb4on Figures 3.67 and 3.68), represents either leakage and mixing through the conglomerate unit or direct recharge from the SR possibly through preferential flow through fractured systems, and hence, reinforcing the complexity in flow conditions.

In summary, aqueous geochemistry of the Middle Sigatoka Valley is composed of:

- $Ca(HCO_3)$ type waters of shallow flow systems receiving abundant meteoric recharge with few deep flow systems showing $Na(HCO_3)$ type waters and limited recharge;
- Meteoric derived waters, defined by a linear trend of stable δD and $\delta^{18}O$ isotopes along a LMWL of slope 4.3, that is either flowing into and through the surfaces systems or dispersing at both variable depths and flow rates through alluvial and fractured systems with variable influences of evaporation in vadoze zone and surface environment prior to infiltration; and
- Highly complex interactions between seasonally variable hydrological conditions, surface water bodies and heterogeneous geological systems as demonstrated by the highly variable chloride concentration, rainfall chloride and isotopic compositions, pH values, HCO_3 enrichments and elevated end-member sources along numerous groundwater flow paths.

4.4 Groundwater recharge estimation

Physical water balance (PWB) and chemical mass balance (CMB) estimates for the middle Sigatoka Valley system yield recharge estimates that differ by ~ 300 %. These differing results stem from the highly complex and temporally dynamic physical and chemical processes at work in the system. The following section presents these two models in relation to groundwater recharge in the Middle Sigatoka Valley.

4.41 Physical water balance

Parameters	Wet season	Dry season
Land area (m^2)	40000000	40000000
Precipitation (m/month)	0.223	0.089
Evapotranspiration (m/month)	0.138	0.098
Total Precipitation (m^3/month)	8920000	3560000
Total Evapotranspiration (m^3/month)	5520000	3920000
Total runoff (m^3/month) (assumed 4.1 % of P)	365720	145960
Total number of Groundwater sources	26	29
Average pumping rate (L/s)	1.06	1.19
Average daily abstraction duration (hrs)	5.15	4.93
Daily groundwater abstraction (m^3/day)	510.96	612.48
Total groundwater abstraction (m^3/month)	15328.87	18374.50
Total number of low lift pump	-	14
average pumping rate (L/s)	-	9
average pumping duration (hrs)	-	6
Daily low-lift pump abstraction (m^3/day)		2721.6
Low-lift pump abstraction (m^3/month)	-	81648
Total number of groundwater irrigation source	-	3
average pumping rate (L/s)	-	2.3
average abstraction duration (hrs)	-	3
Daily groundwater abstraction		74.52
Groundwater irrigation (m^3/month)	-	2235.6
Total irrigation (m^3/month)	-	83883.6
Total Recharge (m^3/month)	3018951.13	-440450.90
Total Recharge (m/month)	0.08	-0.01

Table 4.6: groundwater recharge estimation via physical water model.

Table 4.6 showed groundwater recharge rate of 0.08 m/month in the wet season whereas a -0.01 m/month was estimated for the dry season. Despite the limitation of the assumptions and the limited data available, the slightly higher precipitation in relation to evapotranspiration in the wet season contributed to a surplus in groundwater recharge and would result in an increase in groundwater levels and storage (Kumar, 1996). This rainfall recharge is likely to occur mainly in the fractured

sedimentary units, from which most of the drinking wells are sourced, through rapid dispersion along preferential flow paths. Conversely, the recharge deficit in the dry season is largely controlled by excess evapotranspiration in relation to precipitation. Therefore, groundwater abstraction for both drinking and irrigation during the dry season are likely to utilize non-renewable (in the dry period) groundwater storage (Water and Rivers Commission, 2002). These activities, if not properly regulated, could have adverse ecological and hydrological impacts to groundwater systems ultimately reducing streams and springs discharge. Such a result could jeopardize the availability and usability of groundwater resources in the long-term.

4.42 Chloride mass balance

Season	Wet	Dry
Precipitation (m/month)	0.223	0.89
Chloride (mg/L)		
Rain	5.84	1.06
B8	6.65	9.75
D4	2.22	5.98
D3	3.99	4.43
Recharge (m/month)		
B8	0.19	0.10
D4	0.58	0.16
D3	0.33	0.21

Table 4.7: groundwater recharge estimation using chemical mass balance model.

Table 4.7 showed an estimated recharge rate 0.2 to 0.6 m/month in the wet season. The variability in recharge rate in the selected alluvial aquifers is attributed the differences in material compositions. Well B8, drilled to 20 m depth into a silty sand aquifer in Bilalevu, recorded a lower recharge estimate possibly due to the abundance in fine materials. In constrast, wells D3 and D4, penetrated into sandy gravels, recorded a higher recharge estimate due to macro-pores and well graded sediments. The high recharge rate during the wet season suggests abundant recharge from the adjacent surface networks, including surface runoffs, interflow, throughflows and baseflow (Brassington, 2007 and Green, 1986), during the period of high flow. Hence, the alluvial aquifers recorded low [Cl^-] due to recharge-induced dilution (Kresse & Clarke, 2008). The dry season, an

anticipated recharge deficit due to low precipitation rate and high evapotranspiration, showed continued recharge of 0.1-0.2 m/m^{-1}, with impacts of high evaporation and water table decline shown by slight increases in $[Cl^-]$, Table 3.8.5. The low but sustained recharge rate may indicate a period of diminished flow from surface sources, consisting only of base flow (Brassington, 2007 and Green, 1986). These model results suggest that the hydraulic connection of alluvial aquifers to surface water bodies results in continued but seasonally variable recharge governed primarily by climatic variations.

In summary, the middle Sigatoka Valley groundwater system is recharged through meteoric recharge that is dispersing rapidly through the fractured flow paths and seasonally variable leakage, from surface water bodies, dispersing through macro-pores of alluvium deposits. The negative and low recharge rate in the dry period, together with the excess groundwater abstraction, is a serious concern due to the utilization on non-renewable groundwater storage and could have serious implications of the sustainability of groundwater in the long-term.

4.5 Conclusion & Synthesis

- The interpretation of geophysical data permitted the estimation of alluvium materials (including silt-dominated deposits and sand-gravels possibly marking buried river channels), depth to bedrock and possible shear/fracture zones at Dubalevu, Tubakeli and Bila Rd culminating in the selection of potential groundwater drill sites
- The physical hydrogeological framework is composed of
    - surficial silt-dominated layer of with conductivity (K) values of 7.8×10^{-8} m/s at Dubalevu, 2.2×10^{-7} m/s at Tubakeli and 4.3×10^{-8} m/s at Bila Rd.
    - alluvial system, of unconsolidated sandy-gravel, have an estimated transmissivity (T) and K values of 600 m^2/d^{-1} and 30 m/d^{-1} at Dubalevu and 1644 m^2/d^{-1} and 274.8 m/d for well 10/15 in Bilalevu
    - intermediate confining units of unweathered/unfractured sedimentary units
    - fractured sedimentary units of variable T, storativity (S) and K 10.9 m^2/d^{-1}, 3.7×10^{-4}, 1.16 m/d^{-1} for the fractured sandstone at Dubalevu, 26.2 m^2/d^{-1}, 6.1×10^{-4}, 6.1 m/d^{-1} for the fractured conglomerate/rudite at Tubakeli and 48.7 m^2/d^{-1}, 1.7×10^{-3}, 9.1 m/d^{-1}

for the fractured sandstone and argillite at Bila Rd as estimated during the long-term pumping at various stress conditions.

- the variable aquifer responses suggest the heterogeneity and complexity of groundwater systems and limited recharge.
- Regional groundwater is flowing towards the Sigatoka River (NW→SE and WNW→ESE in Dubalevu and Bilalevu, respectively), whilst the sensitivity of groundwater level to the climatic conditions suggest a shallow aquifer system underlying the Dubalevu and Bilalevu areas.

- Aqueous geochemistry showed that the study area include:
  - dominant $Ca(HCO_3)_2$ type waters of shallow flow systems receiving abundant meteoric recharge with few deep flow systems showing $Na(HCO_3)$ type waters and limited recharge;
  - Meteoric derived waters, defined by a linear trend of stable δD and $\delta^{18}O$ isotopes along a LMWL of slope 4.3, that is either flowing into and through the surfaces systems or dispersing at both variable depths and flow rates through alluvial and fractured systems with variable influences of evaporation in vadoze zone and surface environment prior to infiltration; and
  - Highly complex interactions between seasonally variable hydrological conditions, surface water bodies and heterogeneous geological systems as demonstrated by the highly variable chloride concentration, rainfall chloride and isotopic compositions, pH values, HCO_3 enrichments and elevated end-member sources along numerous groundwater flow paths.
- Groundwater recharge in the Middle Sigatoka Valley, through physical and chemical mass models, was estimated to be 0.08 to 0.6 m/month and -0.1 to 0.2 m/month during the wet and dry seasons, respectively. Groundwater recharge occurs through either rapid dispersion of rainfall along fractured flow paths or seasonally variable leakage from surface water bodies into alluvium macro-pores.
- In summary, groundwater resources in the study area is highly limited in recharge (due to climatic control) with highly variable and uncertain storage capacity (due to heterogeneity

and complexity of geological systems) and hence, reliable investigation procedures and technologies, together with proper protection/management strategies, will be required to ensure the reliable and accurate modeling of hydrogeological system and as well as to safeguard the availability and usability of groundwater in the long-term.

Chapter 5: Groundwater issues & sustainable management

5.0 Introduction

The following sections present the major challenges and/or issues encountered during and after this research before outlining a number of recommendations relative to the protection and sustainable management of groundwater.

5.1 Groundwater Issues/Challenges

During the course of this investigation, numerous groundwater management issues, including the (1) large uncertainties and associates costs of hydrogeological investigation, (2) unregulated groundwater abstraction and drilling, (3) equitable allocation mechanisms, (4) absence of groundwater legislations and (5) climate change, were observed in the study area. These will be discussed in the next section such that these critical aspects are intertwined with respect to the groundwater sustainability.

5.1. Groundwater Issues

5.1.1 Large uncertainties and high associated costs of hydrogeological investigation

This research demonstrates the large uncertainties of hydrogeological systems, as well as the massive associated financial cost involved. For example, a borehole, costing around $5,000-10, 000 depending on depth (Mr Jonati Railala, Mineral Resources Department, pers.comm, 2010), may only intercept a small volume of a water bearing unit. In fractured systems, the borehole is likely to intersect no fissures or bedding planes large enough to render usable water supply and vice versa (Twort et.al., 2000), as shown by the highly variable yield of boreholes located in close proximity (Figure 3.4.1 and Table 3.4.2). Secondly, geophysical surveys, a costly and time consuming exercise, require adequate site-specific surface geological knowledge, including records of existing boreholes, to generate high resolution subsurface models. These models usually entail large uncertainties that often require groundwater exploration drilling for data validation purpose, which, again, will be an added cost and hence, augments the high uncertainties and associated costs as

governed by the heterogeneity and complexity of hydrogeological conditions (section 4.2.2 and 4.3.3).

5.1.2 Unregulated groundwater drilling and abstraction

The rapid growth in the number of privately drilled wells (PDW) within the study area, most of which are penetrating the fractured basement systems (FBS), represents major the human impact on groundwater systems. Despite the heterogeneity and limited recharge in the fractured basement system (section 4.2.3), Table 3.16 showed variable groundwater abstraction, with a volume of 510-612 m^3/month. This unregulated abstraction rate is likely to exert pressure on the aquifer storage in the fractured (local) sedimentary units (from which most of these wells are sourced) in the dry season. This could lead to deterioration in groundwater quality and quantity, as well as adverse ecological and hydrological impacts on groundwater-dependant ecosystems and streams and springs discharges. To date, the excess groundwater abstraction is strongly related to unregulated drilling by private drilling companies (PDC), which is now prevalent around Fiji. As mentioned in Chapter 2.5.2, these PDW in the study area, either co-funded by community and Ministry of Multi-ethnic Affairs (MMEA) or fully funded by individual households, were virtually unknown to Mineral Resources Department (MRD) until the inception of this research. With the growth of an excessive and unregulated groundwater drilling and abstraction, the Fiji Government (FG) will need to establish a coordinated approach for interested government department, such as MRD and MMEA, whilst implementing stringent controls of the operation of PDC, through licence or permit systems, to ensure the protection and sustainable management of groundwater systems.

5.1.3 Equitable water allocation

The excess water demand and utilization in the dry season requires the establishment of an equitable allocation mechanism for competing users. The abstraction from Sigatoka River for irrigation by farmers and the excess groundwater abstraction by adjacent communities for domestic use, during the dry period, demonstrate the increasing water demand and competing uses and hence, the establishment of an equitable allocation system is necessary. These, coupled with suggestions of direct recharge from Sigatoka River into several groundwater sources (supported by chemical and

isotopic compositions (section 4.3.3)), reinforces the need for equitable allocation based on the prioritization of water uses during dry periods in relation to the sustainable limits of both groundwater and surface networks (Water Policy Services Pty Ltd, 2006). Further, considering that surface networks will be composed primarily of base flow in the dry period (Green, 1986 & Brassington, 2007), the excess abstraction could create serious adverse impacts on groundwater availability in the long-term. These could affect the availability and usability of water to groundwater-dependent ecosystems, as well as for villages and settlements in the Lower Sigatoka Valley.

5.1.4 Absence of groundwater legislations

As highlighted earlier (section 2.6), the absence of proper legislation is a primary limitation on any attempt to protect and manage groundwater in a sustainable manner. From the estimated groundwater recharge, it is clear that the current groundwater abstraction for drinking and irrigation, particularly in the dry season, requires stringent control and regulation to avoid groundwater depletion (Fetter, 2001). The climatic control on groundwater recharge and the highly uncertain and variable groundwater storage (due to the heterogeneity and complexity of groundwater systems) necessitates the design and enactment of groundwater policies and legislations that emphasise equitable groundwater allocation limits, thus contributes to groundwater protection and groundwater sustainable management.

5.1.5 Climate change

Climate change, a phenomenon predicted with large uncertainties (Singh & Kumar, 2010), may exacerbate the groundwater deterioration and depletion through prolonged dry periods and gradual decline in rainfall recharge. Hetzel et.al (2008) commented that groundwater resources and their long-term replenishment are controlled by long-term climatic conditions, while the impacts of climate change can be observed in more frequent extreme climatic conditions and decreasing groundwater level due prolonged dry periods and downscaled rainfall. In case of Fiji, long-term climatic changes could either lead to more severe dry periods causing drastic fall in meteoric recharge and groundwater level/storage or more wetter periods culminating in abundant recharge

etc. Further, deep groundwater systems are likely to have delayed response to these extreme conditions as opposed to rivers, streams, springs and shallow aquifer systems (Singh & Kumar, 2010). These enhance the vulnerability of groundwater in the study area as the investigated alluvium and fractured systems are shallow groundwater systems as proven by the physical and chemical aspects of this study. Hence, proper management strategies and policies will be urgently required to safeguard the availability and usability of groundwater resources in the long-term.

5.2 Recommendations for groundwater sustainable management

It is critical to the long-term sustainability of water resources that the Fiji Government (FG), being the custodian of all water and mineral resources under the Rivers and Stream Act, Irrigation Act and Mining Act, recognise the scarcity and vulnerability of groundwater resources (to depletion and contamination) by establishing pragmatic and legally binding strategies and mechanisms that promote groundwater protection and sustainable management in the medium to long-term. Despite the degree of uncertainty and large costs associated hydrogeological investigations (Water and Rivers Commission, 2002), the FG should take a proactive approach in groundwater management through:

1. proper characterisation and evaluation of groundwater potential geological units (at appropriate scales), based on inherent variability, extent, thickness, depth, including structural features (fracture systems and/or fault) and using appropriate technologies and methods to establish aquifer boundaries, hydraulic properties, sustainable and allocation limits based on seasonal climates of varying severities (Department of Water, 2010 & Twort et.al., 2000);
2. improving groundwater recharge quantification through improving water resources inventories, data collection at regular and short intervals, and more alluvial aquifer sampling points for both physical and chemical mass balance models;
3. strengthening groundwater monitoring networks and data archiving in conjunction with the monitoring of surface networks through stream and river gauging to determine the interaction of surface and groundwater systems and their responses to climatic conditions;

4. extensive consultation and awareness programmes with community groups and stakeholders to permit a better understanding of their roles in relation to the need to protect and manage groundwater resources in view of the predicted impacts of climate change (Department of Water, 2010);
5. integrating water resources management (IWRM) (Chapter 2.5), including ecological freshwater studies to determine groundwater dependent ecosystems and associated threshold limits in different climatic conditions and hence, necessitating refinement in allocation limits (Department of Water, 2010); and
6. establishing proper and sustainable legal framework that warrants groundwater protection and sustainable management, including the establishment of permits and licence (and penalties) to regulate and controlling the operation of PDC, as well as metering system to regulate groundwater abstraction in rural and/or areas, with emphasis on possible impacts of climate change, (Hawke, 2006 & Water and Rivers Commission, 2002).

Chapter 6: Conclusions

6.1 Thesis conclusions

This research has presented both physical and chemical characteristics of the hydrogeological system underlying the middle Sigatoka valley, Viti Levu, Fiji. The objectives of this study were to: (1) classify the groundwater resource potential of underlying geological materials; (2) determine the dominant hydrochemical facies and origin of groundwater using chemical and isotopic principles; (3) determine the recharge mechanism and rates; and (4) project the sustainability of groundwater resources. This research demonstrates:

1. The study area, underlain by the Oligocene to Middle Miocene Wainimala and Tuva sedimentary groups both of which are deformed and displaced the Nasovatava Fault and capped by Quaternary-Recent Alluvium, is subject to massive water demand and utilisation and, simultaneously, is affected by seasonal climate with pronounced wet and dry seasons from November to April and from May to October, respectively.
2. The physical hydrogeological framework is composed of a surficial confining layer of sandy silt and silt loam, alluvial aquifer systems of unconsolidated sandy gravel around the reaches of the Sigatoka, intermediate confining units of unweathered sedimentary units and fractured basement systems of moderate-highly fractured rock mass. Differing flow and storage estimates of the alluvium and fractured systems, determined from pumping tests, are governed by variable dimension and distribution of aquifer materials, limited recharge and physical heterogeneity of groundwater systems
3. The hydrogeochemistry exhibited two major facies, including (1) shallow system of $Ca(HCO_3)_2$ type water dominated by rapid carbonate weathering and adequate meteoric recharge and (2) deeper system of $Na^{+}(HCO_3)$ type water dominated by connate groundwater with some mixing. The stable hydrogen and oxygen isotopic signatures suggest that the valley waters are meteoric in origin that is either flowing into and through the surfaces systems or dispersing at both variable depths and flow rates through alluvial and fractured systems with variable influences of evaporation in vadoze zone and surface environment prior to infiltration.

4. Groundwater recharge mechanisms, include (1) meteoric recharge that is dispersing variably through fractured sedimentary units and (2) seasonally variable leakage from surface water bodies dispersing through alluvial macro-poses. The physical and chemical mass models yielded estimated recharge rates of 0.08 to 0.6 m/month and -0.1 to 0.2 m/month in the wet and dry seasons, respectively.
5. Groundwater protection and sustainable management is likely to be jeopardized by unregulated groundwater drilling by private companies, unregulated groundwater abstraction in the dry period, absence of groundwater legislations and inherent groundwater issues, namely climatic variability, highly complex and heterogeneous hydrogeological conditions.

6.2 Areas of future studies

Several areas of future study are recommended to aid and improve the characterisation of the middle Sigatoka valley hydrogeological system. These topics include:

- charaterising the fractured basement systems, namely density and dominant trend, through the use of down-the-hole geophysical logging devices;
- determining the variability in vertical hydraulic conductivity for the fractured sedimentary systems through stratified pumping tests using packer tests;
- establishing gains and losses from adjacent surface sources through stream depletion analysis, in conjunction with of base level recession curves of Sigatoka River through gauging, to determine recharge into alluvial aquifers and base flow component in different climatic conditions;
- establishing the groundwater age, through either tritium, ^{3}H, or CFC: this will be an added dimension on the sustainability of groundwater resources;
- detailed characterisation of spring sources within the Sigatoka Valley and quantification of water used by adjacent villages and/or farming settlements for drinking: this may be an added dataset for physical water budget;
- identification of recharges sources of the two oxbow lakes; and

- conduct ecological studies to determine groundwater-dependant ecosystems and their groundwater requirements, in relation to seasonal climatic variation, to permit water allocation refinement.

6.3 CONCLUDING REMARK

The replenishment and storage of groundwater in Fiji is highly limited due to dominant climatic control and highly complex/heterogeneous geological systems. Hence, proper groundwater management, including sound hydrogeological investigation and evaluation, reliable monitoring program, proper awareness and pragmatic legal mechanisms, should be established to accurately model the physical and chemical hydrogeological conditions. These are crucial and immediate concerns as climate change, landuse intensification, pollution and rapid population growth, threaten the sustainability of groundwater resources in the long-term.

References

Abdalla, O. A., 2009. Groundwater recharge/discharge in semi-arid regions interpreted from isotope and chloride concentrations in north White Nile Rift, Sudan. Hydrogeology Journal 17: 679-692

Andreo, B., Carrasco, F., 1998. Application of geochemistry and radioactivity in the hydrogeological investigation of carbonate aquifers (Sierra Blanca and Mijas, southern Spain) In: Raisewell, R (Ed)., 1999. Applied Geochemistry, 14: 283-299

Cook, P. G., 2003. A guide to regional groundwater flow in Fractured rock aquifers. CSIRO Land & Water, Glen Osmond, 99 p.

Brassington, R., 2007. Field Hydrogeology. 3rd Editon. John Wiley & Sons Ltd, Chichester

Cox, M. E., Hulston, J. R., 1980. Stable isotope study of thermal and other waters in Fiji, In: New Zealand Journal of Science, 1980, Vol. 23, 236-249.

D'amore, F., Bolognesi, L., 1994. Isotopic evidence for a magmatic contribution to fluids of the geothermal systems of Larderello, Italy and the Geysers, Califonia. Geothermics, 23: 21-32

Davies, J., 1989. Sigatoka valley rural development project – Borehole No. 88/20. Mineral Resources Department. MRD Note BP55/6

de Biran, A., 2001. The Holocene geomorphic evolution of the Sigatoka Delta, Viti Levu, Fiji Islands. Unpublished Ph.D. Thesis, Department of Geography, University of the South Pacific, Suva.

Department of Water, 2010. Murray groundwater allocation plan. Government of Western Australia. Retrived January 28, 2011 from http://www.water.wa.gov.au/PublicationStore/first/77208.pdf

Dickinson, W. R., 2001. Paleoshoreline record of relative Holocene sea-levels on Pacific islands, In: 2001. Earth Science Review 55: 191-224

Elkrai, A., Khier, O., Shu, L., Zhenchun, H., 2004. Hydrogeology of the Northern Gezira Area, Central Sudan. Journal of Spatial Hydrology. Retrieved May 4, 2011 from http://www.spatialhydrology.com/journal/paper/Hydrogeology/hydrogeology.pdf

Faure, G., Mensing, T. M., 2005. Isotope principles and application. 3rd Edition. John Wiley & Sons, Hoboken, 897 p.

Fetter, C. W., 2001. Applied hydrogeology. 4th edition. Prentice-Hall, Inc, New Jersey, 543 p.

Fookes, P. G., Baynes, F. J. & Hutchinson, J. N. 2000. Total Geological History: a model approach to the anticipation, observation and understanding of site conditions. In: GeoEng2000, an International Conference on Geotechnical & Geological Engineering, 19–24 November 2000, Melbourne, Australia. Conference Proceedings, Technomic Publishing Company Inc., Lancaster, USA, 370–460 p.

Gale, I. N., Booth, S. K., 1993. Hydrogeology of Fiji. Mineral Resources Department Hydrogeological Report 2. ISN 1011-7512. Mineral Resources Department, Suva

Gonfiantini, R., Frohlich, K., Araguas-Araguas, L., Rozanki., K., 1998. Isotopes in groundwater hydrology, In: Kendall, C., and McDonnell (Eds). Isotope tracers in catchment hydrology. Elsevier. Amsterdam, 203-246 pp

Green, S. N., 1986. Groundwater assessment in Fiji using hydrological records (Preliminary Report). Institute of Hydrology. Oxfordshire

Harrigton, N. M., Herczeg, A. L., Le Gal La Salle., 2008. Hydrological and geochemical processes controlling variations in Na^{+}-Mg^{2+}-$Cl^{-}$$SO_4^{2-}$ groundwater brines, south-eastern Australian. Chemical Geology 251: 8-19.

Hathway, B. Colley, H., 1994. Eocene to Miocene geology of southwest Viti Levu, Fiji, In: Stevenson, A. J., Herzer R, H., and Ballance, P. F. (Eds). Geology and submarine resources of the Tonga-Lau-Fiji Region. SOPAC Technical Bulletin 8: 153-169

Hathway, B., 1994. Deposition and diagenesis of of Miocene arc-fringing platform and debris-apron carbonates, southwestern Viti Levu, Fiji, In: Sedimentary 94 (1995). Elsevier Science, 187-208

Hamburger, W. M., 1986. Seismicity of the Fiji Islands and tectonics of the southwest Pacific. Unpublished Phd Thesis, Cornell University.

Hasbrouck, J & Morgan, T. 2003. Deep groundwater exploration using geophysics In SouthWest Hydrology, July/August 2003: 6-8pp.

Hawaiian Agronomics International Inc., 1984. Sigatoka Valley rural development project feasibility study - Draft final report - Volume 1. Unpublished Report for the Asian Development Bank and the Ministry of Primary Industries of Fiji, Hawaiian Agronomics International Inc., Honolulu.

Hawke, R., 2006. Improving the water allocation framework in New Zealand. Ministry of Economic Development – Occasional paper 06/09. Retrieved January 24th, 2011 from http://www.med.govt.nz/upload/40329/med-op-06-09.pdf

Hem, J. D., 1985. Study and interpretation of chemical characteristics of natural water (3rd edition): U.S Geological survey water-supply paper 2254, 263 p.

HenesseyImm & iVenture., 2003. Surftrip.com. Retrieved May 6, 2011 from http://www.surftrip.com/destinations/islands/pacific/south_pacific.html

Hetzel, F., Vaessen, V., Himmelsbach, T., Struckmeier, W., Villholth, K (Eds)., 2008. Groundwater and climate change: challenges and possibilities. Retrieved April 30, 2011 from http://www.geus.dk/program-areas/water/denmark/rapporter/groundwater_and_%20climate_change_071108.pdf

Hiscock, K. M., 2005. Hydrogeology: principles and practice. Blackwell, Malden, 389 p.

Ingraham, N. L., Caldwell, A. E., Verhagen B. T., 1998. Arid catchments, In: Kendall, C., and McDonnell (Eds). Isotope tracers in catchment hydrology. Elsevier. Amsterdam, 435-465 pp

Japan International Cooperation Agency (JICA)., 1995. The Study on Groundwater Development in North Viti Levu in the Republic of Fiji. Volume 2. Ministry of Lands, Mineral Resources and Energy, Fiji

Kresse, T, M., Clark, B. R., 2008. Occurrence, distribution, sources and trends of elevated chloride concentrations in the Mississippi Tiver Valley Alluvial Aquifer in Southeastern Arkansas: U.S. Geological Survey Scientific Investigation Report 2008-5193, 34 p.

Kumar, P. B., 1997. Groundwater monitoring in Fiji. Mineral Resources Department, MRD Note BP44/18.

Kumar, C. P. (1996). Assessment of Ground Water Potential. Proceedings, All India Seminar on Small Watershed Development, Organised by Indian Association of Hydrologists, West Bengal Regional Centre, 15 February 1996, Calcutta.

Laaksoharju, M., Gascoyne, M., Gurban, I., 2008. Understanding groundwater chemistry using mixing models. Applied Geochemistry 23: 1921-1940

Nobes, D. C., 1996. Troubled Waters: Environmental applications of electrical and electromagnetic methods. Surveys in Geophysics, 17: 393-454.

Nunn, P.D., Thaman, R., Duffy, L., Finikaso, S., Ram, N., Swamy, M., 2001. Age of a charcoal layer in fluvial sediments, Keiyasi, Sigatoka Valley, Fiji: possible indicator of a severe drought throughout the Southwest Pacific 4500–5000 years ago, In South Pacific Journal of Natural Science 19, 5–10.

McNeill, J. 1980. Electromagnetic terrain conductivity measurement at low induction numbers. Technical Note TN6, Geonics Limited, Ontario

Miyata, T., Maeda, T., Matsumoto, E., Matsushima, Y., Rodda, P., Sugimura, A., Kayanne, H., 1990. Evidence for a Holocene high sea-level stand, Vanua Levu, Fiji. QUartenary Research 33, 352-359

NZGS 2005. Field description of soil and rock – guideline for the field classification and description of soil and rock for engineering purposes. New Zealand Geotecnical Society Inc

O'Brien, J. M., (2010). Hydro-geochemical characteristics of the Ngatamariki geothermal field and comparison with the Orakei Korake thermal area, Taupo Volcanic Zone, N.Z. Unpublished MSc Thesis, Department of Geological Sciences, University of Canterbury.

Peach, D. W., 1988. Groundwater investigation and development in Fiji. Fiji Mineral Resources Department Hydrogeological Report 1. 50 pp, 5 figs.

Pentecost, A., 2005. Travertine. Springer, Berlin, 129-147 pp.

Bell, D. H., Pettinga, J. R., 1983. Presentatrion of geological data. Proc. Symposium on Engineering for Dams and Canals, Alexandra, November 1983. Proc. Tech. Groups of Institution of Professional Engineers New Zealnd. Volume 9. Issue 4 (G) 4.1-4.75

Rijkse, W. C., 1990. Soils of Sigatoka Agricultural Research Station, Viti Levu, Fiji. NZ Soil Survey Report 81, DSIR Land Resources, Lower Hutt.

Rodda, P., 1994. Geology of Fiji, In: Stevenson, A. J., Herzer R, H., and Ballance, P. F. (eds). Geology and Submarine Resources of the Tonga-Lau-Fiji Region. SOPAC Technical Bulletin 8: 131-151.

Rahiman, T. 2003. Neotectonics, seismic and tsunami hazards, Viti Levu, Fiji. Phd Thesis, Canterbury University, Christchurch.

Ruddiman, W. F., 2001. Earth's climate: past and future. W. H. Freeman and Company, New York, 440 p.

Seiler, R.D., Gat, J. R., 2007. Groundwater recharge from runoff, infilitration and percolation. Springer, Dordrecht, 159-200 p.

Sequeira, L., Mendoza, A., 2003. Geophysical methods for groundwater exploration in Octal, northern Nicaragua, In: Krasny, J., Hrkal, Z., Bruthans, J (Eds). Proceedingd of the International Conference on groundwater in fractured rocks, Prague, Zech Republic 15-19.09.2003, IHP-VI Series on Groundwater No. 7

Sharp, Z., 2007. Principles of stable isotope geochemistry. Pearson Prentice Hall, New Jersey

Selby, M., 1985. Earth's changing system – An introduction to geomorphology. Clarendon Press, Oxford, 324 p.

Singh, R. D. and C. P. Kumar., 2010. Impact of Climate Change on Groundwater Resources. Proceedings of 2nd National Ground Water Congress, 22nd March 2010, New Delhi, pp. 332-350, Retrieved April 30, 2011 from http://www.angelfire.com/nh/cpkumar/publication/CC_RDS.pdf

Taganesia, J. V., 2009. Mechanisms and remediation of cut batter failures along the Queens Rd at Wainigasau and Namuka-i-Lau, Viti Levu, Fiji Islands, Phd Thesis, Canterbury University, Christchurch.

Thornburn, P. J., Cowie, B. A., Lawrence, P. A., 1991. Effects of land development on groundwater recharge determined from non-steady chloride profiles. Journal of Hydrology, 124: 43-58

Tihansky, A. B., 2005. Effects of aquifer heterogeneity on groundwater flow and chloride concentrations in the Upper Floridan aquifer near and within an active pumping well field, West-central Florida: U. S. Geological Survey Sciwentific Investigation Report 2005-5268, 75 p.

Twort, A. C., Ratnayaka, D. D., Brandt, M. J (Editors)., 2000. Water Supply. 5th Edition. Elsevier, London: 114-154 pp.

Vereecken, H., Binley, A., Cassiani, G., Revil, A., (Editors) 2004. Applied hydrogeophysics. Springers, Dordrecht

Walker, J. F., and Krabbenhoft, D. P., 1998. Groundwater and surface-water interactions in riparian and lake-dominated systems, In: Kendall, C., and McDonnell (eds). Isotope tracers in catchment hydrology. Elsevier. Amsterdam, 467-488 pp

Wallick, E. I., 1981. Chemical evolution of groundwater in a drainage basin of Holocene age, east-central Alberta, Canada. In. Back, W., and Letolle, R. (eds), Symposium of geochemistry of groundwater – 26th International Geological Congress. Journal of Hydrology., 54: 245-283.

Water and Rivers Commission, 2002. Managing the water resources of the Gingin groundwater area, WA – Interim allocation strategy. Retrievd January 28, 2011 from http://www.water.wa.gov.au/PublicationStore/first/12903.pdf

Waterloo, M. J., Beekman, F. J., Bruijnzeel, L, A., Frumau, K. F. A., Harkema, E., Opdam, H. J., Schelleken, J., Vught, H., 1993. The impact of converting grassland to pine forest on water yield in Viti Levu, Fiji, In: Hydrology of Warm Humid Regions (1993) 216: 149-156

Waterloo, M. J., Schelleken, J., Bruijnzeel, L, A., Vuhgt, H. F., Assenberg, P. N., & Rawaqa, T.T., 1997. Chemistry of bulk precipitation in southwestern Viti Levu, Fiji, In: Journal of Tropical Ecology, 13: 427-447

Waterloo, M. J., Schelleken, J., Bruijnzeel, L, A., Rawaqa, T.T., 2007. Changes in catchment runoff after harvesting and burning of a Pinus caribea plantation in Viti Levu, Fiji. Forest ecology and management, 251: 31-44.

Webb, J. W., 1999. Geology and geomorphology of Lomawai, SW Viti Levu, Fiji. Unpublished MSc Thesis, Canterbury University.

Woodroffe, S. A., Horton, B. P., 2004. Holocene sea-level changes in the Indo-Pacific, In Journal of Asian Earth Sciences (2005) 25: 29-43

Zheng, Y., van Geen, A., Stute, M., Dhar, R., Mo, Z., Cheng, Z., Horneman, A., Gavriel, I., Simpson, H. J., Versteeg, R., Steckler, M., Grazioli-Venier, A., Goodbre, S., Shamsudduha, M., Hoque, M. A., Ahmed, K. M., 2005. Geochemical and hydrogeological contrasts between shallow and deeper aquifers in two villages of Araihazar, Bangladesh: Implication of deeper aquifer as drinking water sources. Geochimica et Cosmochimica Acta 69: 5203-5218.

APPENDICES

Appendix A: Rainfall data from Nacocolevu & Mavua Rainfall Stations

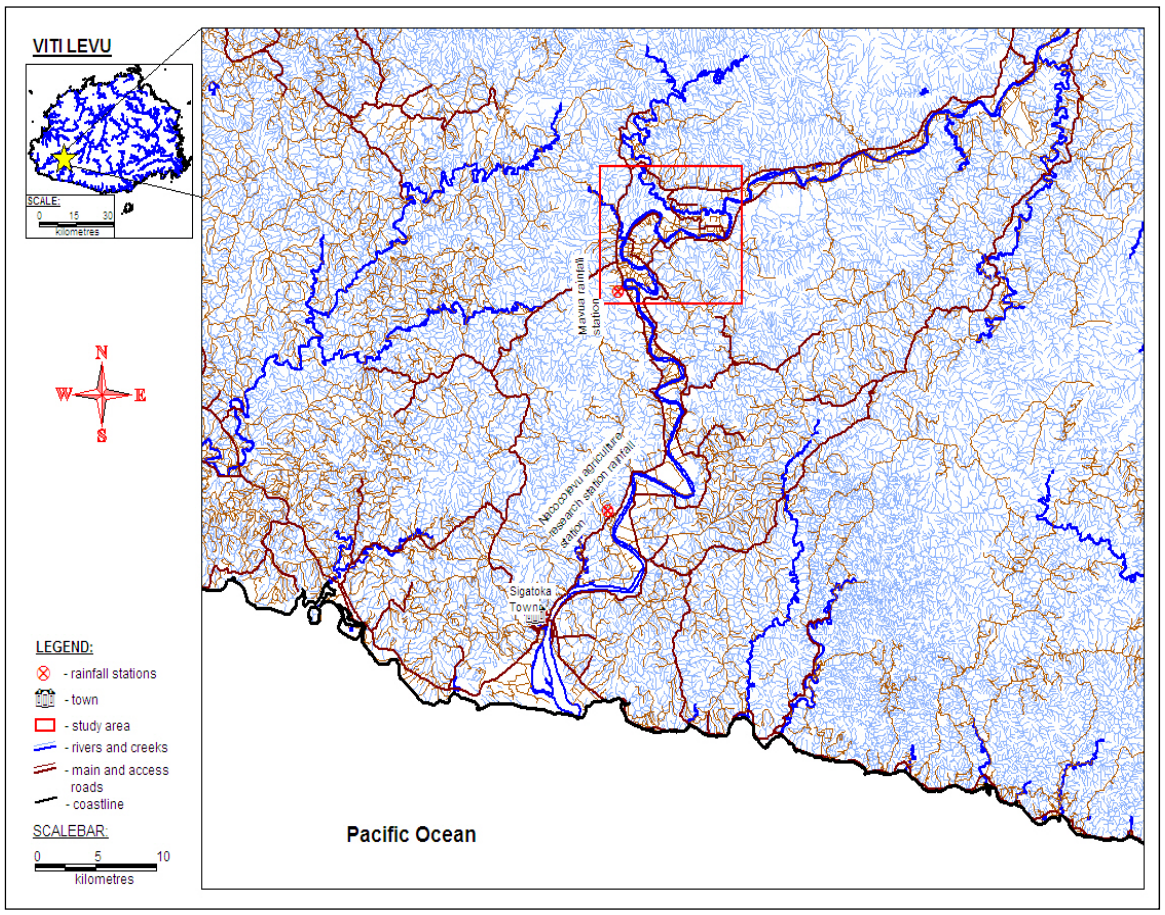

Figure 1.1: Location of Nacocolevu Agricultural Research Centre and Mavua rainfall stations

YEAR	JAN	FEB	MAR	APR	MAY	JUN	JUL	AUG	SEP	OCT	NOV	DEC
1989	476	660	186	218	409	3	95	45	104	194	46	231
1990	180	144	606	118	22	163	73	218	50	48	378	224
1991	418	348	396	231	0	0	48	57	163	216	62	17
1992	190	183	64	58	79	71	0	37	35	59	58	319
1993	519	384	365	176	217	19	22	171	50	19	182	251
1994	382	245	292	25	41	124	30	0	68	12	186	193
1995	210	121	443	148	45	19	188	18	250	22	84	76
1996	199	330	464	95	179	238	81	60	18	62	189	304
1997	297	249	257	232	129	26	81	168	136	30	69	0
1998	498	38	98	55	18	64	10	0	40	137	327	140
1999	592	662	201	391	35	150	126	115	27	73	328	377
2000	356	820	588	234	279	28	321	71	123	277	196	544
2001	364	344	28	121	65	8	104	184	15	27	32	169
2002	35	410	369	331	104	135	115	75	211	47	190	47
2003	408	165	543	119	77	9	55	87	11	57	130	330
2004	78	360	326	152	16	32	77	321	100	52	0	103
2005	172	70	298	404	0	119	93	48	84	257	316	121
2006	269	309	297	161	178	115	62	139	71	148	198	186
2007	150	66	613	146	45	0	43	63	374	177	265	190
2008	700	492	431	185	154	40	69	0	141	299	298	372
2009	1348	393	996	71	68							
mean	373	323	374	175	103	68	85	94	104	111	177	210

Table 1: Mavua monthly rainfall data FROM 1989-2009

YEAR	JAN	FEB	MAR	APR	MAY	JUN	JUL	AUG	SEP	OCT	NOV	DEC
1989	332	533	305	179	320	5	106	57	98	227	28	63
1990	153	29	333	51	13	132	80	235	72	36	269	67
1991	291	312	305	147	38	20	44	48	142	83	87	37
1992	155	86	34	49	79	50	2	31	39	64	39	----
1993	----	----	----	132	192	32	19	136	70	2	103	176
1994	321	165	109	26	32	115	41	----	62	5	146	91
1995	----	158	200	----	19	20	84	34	111	4	84	95
1996	260	130	435	32	132	196	94	29	59	61	149	139
1997	430	115	212	174	86	37	100	150	148	28	6	54
1998	199	11	98	17	31	28	55	1	29	56	205	140
1999	382	361	133	277	9	157	101	113	35	112	291	421
2000	369	324	333	300	132	30	164	98	122	190	107	385
2001	237	192	158	158	86	25	129	164	23	225	40	164
2002	303	282	225	113	59	203	69	41	190	28	103	92
2003	234	85	366	204	59	18	98	122	5	96	54	233
2004	76	363	133	172	28	171	100	254	30	28	1	129
2005	122	58	178	269	2	111	61	56	149	91	279	81
2006	200	139	110	103	140	101	76	138	75	135	138	121
2007	206	485	383	158	65	14	137	86	367	176	322	312
2008	558	325	298	166	183	85	53	28	51	108	258	
2009		321	334	123								
mean	268	219	229	144	85	78	81	96	94	88	135	156

Table 2: Nacocolevu monthly rainfall data from 1989-2009

Appendix B: List of Aerial photos and satellite image used during the preliminary stage

Area	Object	Year
Middle Sigatoka Area	Aerial photo	1967
Middle Sigatoka Area	Aerial photo	1982
Middle Sigatoka Area	Aerial photo	1994
Middle Sigatoka Area	IKONOS satellite image	2005

Appendix C: Engineering geological classification of the area and summary description of mapping localities

Soil/Rock Unit	Lithology	USC	Soil/Rock Description
Quaternary-Recent Alluvium	Silt	ML	Completely Weathered, dark brown to light brown, dry to moist, non-plastic and slightly sticky, compact, massive, fine SANDY SILT.
Quaternary Terrace Deposits - Gravels	GRAVEL	GC	Unconsolidated, unweathered, dark grey to light grey andesite-sandstone and basalt clasts, poorly sorted, sub-angular to sub-rounded course gravels with minor fine to coarse sand
Takaro Conglomerate/Rudite	Conglomerate/Rudite		Slightly weathered-unweathered, grey to bluish grey, fine to coarse fabric, moderately inclined (20-28°SE), moderately thick to massive, CONGLOMERATE/RUDITE, strong to very strong, subvertical to sub-perpendicular to bedding fractures, moderately widely spaced to closely spaced, very narrow to narrow with stepped roughness, with calcite and quarts infill and no evidence of seepage
Cici Sandstone	Sandstone		Moderately-unweathered, bluish grey-grey, fine fabric, thickly bedded (with laminations), moderately-steeply inclined (24-50° SE), SANDSTONE, sub-vertical to sub-perpendicular to bedding fracture systems, medium to high persistence, moderately widely spaced-closely spaced, tight to moderately narrow aperture (with calcite and quartz infilling) with seepage in some areas
Qalimare Lmestone	Limestone		Unweathered-slightly weathered, white to creamy, fine to massive fabric (with coarse volcaniclastics included), sub-vertical, , extremely strong to very strong, LIMESTONE, subvetical fractures, widely spaced, high persistence, wide apertures with rough walls with low-large groundwater flow (with rapid response to rainfall)
Tari Formation	ARGILLITE/SANDSTONE		Unweathered-moderately weathered, brown and bluish grey, fine-coarse fabric, strong to very strong, SANDSTONE/ARGILLITE, moderate-steeply inclined bedding which is thin to moderately thick, joints are closely to moderately wide in spacing, linear fractures perpendicular to bedding.

Table 1: Engineering geological classification of the mapped units within the study area

Number	Site Name	Ltthological decription	Dip/Dip Direction	UNIT
1	Bilalevu	bluish grey and brown, well indurated, moderately fractured, intebedded sandstone and dark brown argillite	46 NW	Tari Formation
2	Bilalevu	bluish grey and brown, well indurated, moderately fractured, intebedded sandstone and dark brown argillite	65 NW	Tari Formation

3	Bilalevu	bluish grey and brown, well indurated, moderately fractured, intebedded sandstone and dark brown argillite	80 NW	Tari Formation
4	Sigatoka River Bank, Bilalevu	~5 m thicks unconsolidated yellowish brown sandy silt with gravel bands	-	Alluvium
5	Sigatoka River Bank, Bilalevu	~5 m thick unconsolidated yellowish brown sandy silt with gravel bands	-	Alluvium
6	Bilalevu	brown, well indurated and extremely strong, argillite	-	Tari Formation
7	Bilalevu	grey, well indurated, unweathered, sandstone matrix supported rudites with dacited and andesite clasts	-	Takaro Conglomerate/Rudite
8	Bilalevu	brown, well indurated and extremely strong, argillite	-	Tari Formation
9	Bilalevu	brown, well indurated and extremely strong, argillite	85 NW	Tari Formation
10	Bilalevu	grey, well indurated, unweathered, sandstone matrix supported rudites with dacited and andesite clasts	-	Takaro Conglomerate/Rudite
11	Bilalevu	grey, well indurated, unweathered, sandstone matrix supported rudites with dacited and andesite clasts	24 SE	Takaro Conglomerate/Rudite
12	Bilalevu	grey, well indurated, unweathered, sandstone matrix supported rudites with dacited and andesite clasts	-	Takaro Conglomerate/Rudite
13	Narewa Hill, Bilalevu	grey, well indurated, unweathered, sandstone matrix supported rudites with dacited and andesite clasts	22 SE	Takaro Conglomerate/Rudite
14	Bilalevu	grey, well indurated, unweathered, sandstone matrix supported rudites with dacited and andesite clasts	-	Takaro Conglomerate/Rudite
15	Bilalevu	grey, well indurated, unweathered, sandstone matrix supported rudites with dacited and andesite clasts	25 SE	Takaro Conglomerate/Rudite
16	Along Dreke Rd	grey, well indurate, moderately fractured, interbedded sandstone and siltstone	28 SE	Cici Sandstone
17	Mavua Hill	creamy to brown, well indurated, massive, calystone and argillite	26 NW	Tari Formation
18	Roadcut , Mavua	creamy to brown, well indurated, massive, calystone and argillite	28 NW	Tari Formation
19	Roadcut, Mavua	creamy to brown, well indurated, massive, calystone and argillite	30 NW	Tari Formation
20	Nabitu Hill	yellowish brown, moderately weathered sandstone	-	Takaro Conglomerate/Rudite
21	Rararua	grey, well indurate, moderately fractured and interbedded sandstone and siltstone	24 SE	Cici Sandstone
22	Qwali Settlement	grey, well indurate, moderately fractured and interbedded sandstone and siltstone	47 SE	Cici Sandstone
23	Nakavika junction, Nabaka	grey, well indurate, moderately inclined and moderately fractured, interbedded sandstone and sitlstone	-	Cici Sandstone
24	rock outcrop on a hill at Similaya	grey, well indurated, unweathered, sandstone matrix supported rudites with dacite and andesite clasts	26 SE	Takaro Conglomerate/Rudite
25	rock outcrop near Nabaka School	grey, well indurated, unweathered, sandstone matrix supported rudites with dacite and andesite clasts	24 SE	Takaro Conglomerate/Rudite

26	rock outcrop near Oxbow Lake, Nabaka	grey, well indurated, unweathered, sandstone matrix supported rudites with dacite and andesite clasts	22 SE	Takaro Conglomerate/Rudite
27	Jubairata Meander, Dubalevu	grey, well indurated, unweathered, sandstone matrix supported rudites with dacite and andesite clasts	20 SE	Takaro Conglomerate/Rudite
28	roadcut at Vunarewa	interbedded bluish grey sandstone, dacitic tuff and argillite, moderately fractured	-	Tari Formation
29	Toga	white to creamy, well indurated, massive with volcanicalstic inclusions, fractured Limestone	subvertical	Qalimare Limestone
30	Toga	white to creamy, well indurated, massive and moderately fractured Limestone	subvertical	Qalimare Limestone
30	Toga	white to creamy, well indurated, massive with volcanicalstic inclusions, fractured Limestone	subvertical	Qalimare Limestone
31	Toga	white to creamy, well indurated, massive with volcanicalstic inclusions, fractured Limestone	subvertical	Qalimare Limestone
32	Toga	white to creamy, well indurated, massive and moderately fractured Limestone	subvertical	Qalimare Limestone
33	Toga	white to creamy, well indurated, massive with volcanicalstic inclusions, fractured Limestone	subvertical	Qalimare Limestone
34	Mataukaba, Vunarewa	interbedded argillite, sandstone and dacitic tuff	-	Tari Formation
35	Bedrock high near Sigatoka River, Nabitu	grey, well indurated, unweathered, sandstone matrix supported rudites with dacited and andesite clasts	28 SE	Takaro Conglomerate/Rudite
36	Navala, Mavua	grey, well indurated, vesicular basaltic flow with abundant quarts amygdales	-	Tari Formation
37	Ami Chand's residence	bluish grey, well-indurate, moderately fractured, thickly bedded and interbedded sandstone and siltstone	43 SE	Cici Sandstone
38	Jubaitara hill	yellowish brown, moderately weathered, moderately fractured, thickly bedded and interbedded sandstone and siltstone	35 SE	Cici Sandstone
39	Dubalevu	bluish grey, well-indurated, moderately fractured, thickly bedded and interbedded sandstone and siltstone	40 SE	Cici Sandstone
40	Dubalevu	bluish grey, well-indurated, moderately fractured, thickly bedded and interbedded sandstone and siltstone	45 SE	Cici Sandstone
41	Dubalevu	bluish grey, well-indurated, moderately fractured, thickly bedded and interbedded sandstone and siltstone	47 SE	Cici Sandstone
42	Dubalevu	bluish grey, well-indurated, moderately fractured, thickly bedded and interbedded sandstone and siltstone	46 SE	Cici Sandstone

Table 2: summary of mapping localities

APPENDIX D: Additional Geophysical Information & Results

1. Methods background information

- **Electromagnetic (EM)**

EM, regarded as an inductive technique due to the variable magnetic fields induced by the emission of variable electrical currents into the subsurface, have numerous arrangements, time-domain and frequency. In this investigation, frequeny domain EM34-3 Geonics equipment was used.

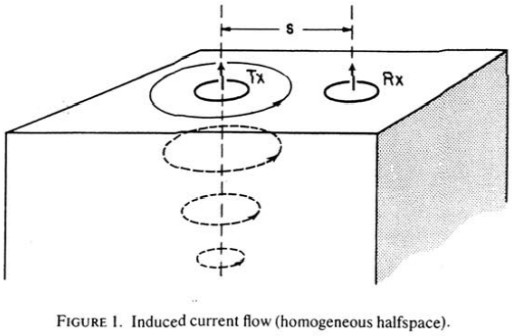

FIGURE 1. Induced current flow (homogeneous halfspace).

Figure 1: set-up of transmitter and receiver coils with alternating electric current emitted in the in the Tx

This method of enitals the emission of alternating electrical current though a transmitter coil (Tx). These time-varying currents generate a primary magnetic field and upon interaction with subsurface materials induces very small currents, generating the secondary magnetic field, which are both sensed by the receiver coil (Rx) (Figure 1) (McNeil, 1980). Hence, the secondary field depends on electrical properties of the subsurface, namely degree of saturation, conductivity of pore fluids, clay minerals and reflectors (Nobes, 1996). The strength of the secondary response is separated into two components: in-phase response, and quadrature response (Nobes, 1996). The in-phase component, identical to the signal measured by metal detectors and sometimes called the “metal detector” mode, is expressed as parts per thousand (ppt) and measures the strength of the transmitted field. In the absence of metals, the in-phase mode is generally small and highly variable, but can be sensitive to ground disturbances, particularly the presence of small amounts of metal (Nobes, 1996). The quadrature response yields a measure of the bulk electrical properties and is controlled by the particular frequency of the EM equipment. The quadrature

response, expressed as an apparent electrical conductivity and measured in mS/m, will be used in this survey in relation to delineating subsurface disturbances, which may represent a fault zone or an alluvial gravel bed.

- **Electrical Resistivity (ER)**

ER measurements of the subsurface, pioneered by the Schlumberger brothers in the 20th century (Nobes, 1996), is conducted by injecting currents through two electrodes A and B and the resulting potential through M and N. Electrical methods, comprising vertical electrical sounding (VES) and electrical profiling (EP), require galvanic ground contacts together with a resistivity equipment and an electrical power source. For this survey, VES method, mostly applied on approximately horizontal earth and due to its favorable potential of producing subsurface thicknesses with their corresponding resistivities (Ernstson & Kirsch, 2009), was used. The vertical resistivity layering is warranted by the step-wise increase in current-injecting electrode AB spacing, which, in turn, results in a deeper penetration of electric current and higher resolution of the subsurface profile. Accuracy of electrical methods are always influenced by the principle of equivalence, topographic effects and cultural noise such as power lines, metal fences and buried pipes (Nobes, 2009). ER methods are most used in smaller scale surveys mainly because the depth of penetration depends on the electrode separation and large and often impractical separations must be used to obtain large depths of penetration. However, the resultant resistivity profiles generated from these surveys represent the resistivity sum of all geologic layers above a particular sample point in the subsurface as influenced by factors mentioned above.

2. Survey site conditions

Survey sites and orientation of survey lines were selected and designed carefully to produce satisfactory subsurface profile resolution so as to achieve most of the survey objectives. It should also be noted that ER surveys were conducted several days after Tropical Cyclone Mick (TCM), which caused widespread flash flooding around the SV.

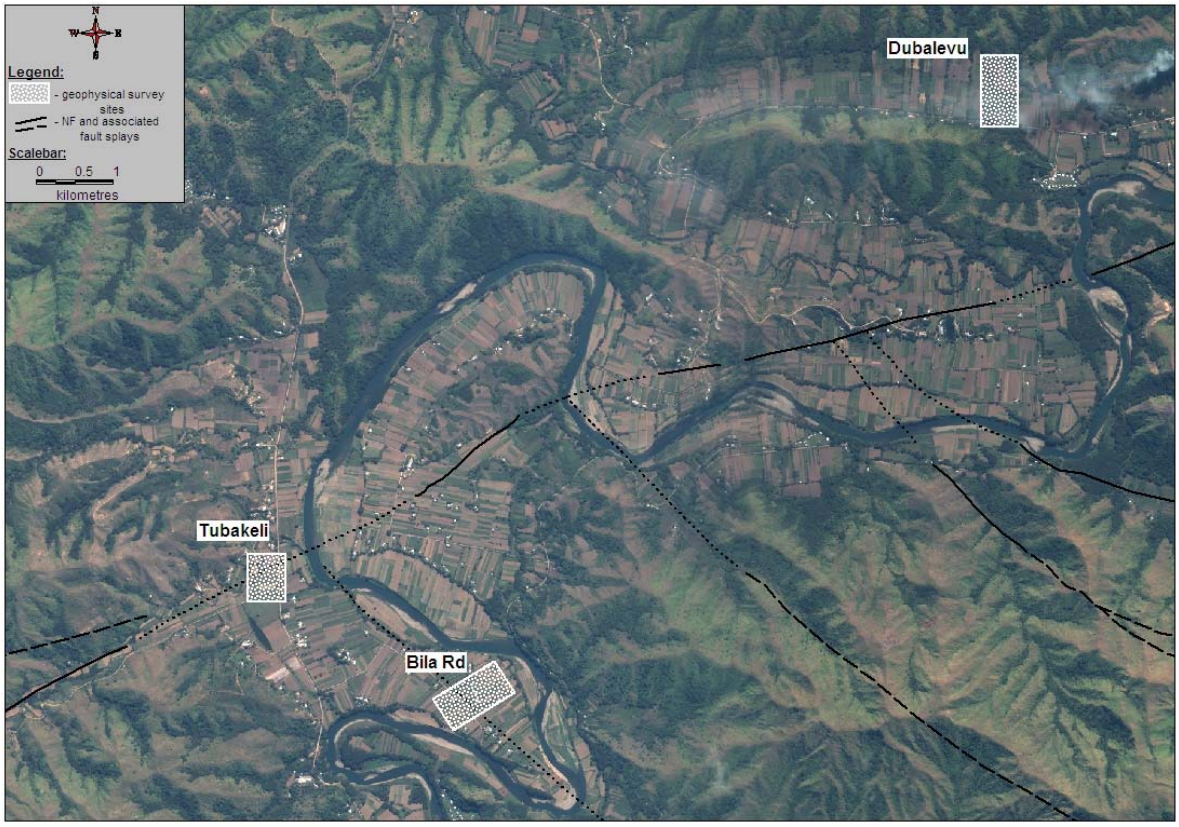

Figure 2: areas of geophysical survey as governed by the (1) E-W orientation of the abandoned meander at Dubalevu and the existence of currently used SVRD wells (2) orientation of the ENE-WSW sinistral Nasovatava fault at Tubakeli and (3) NW-SE inferred fault splay and along Bila Rd (superimposed on 1:10 000 IKONOS sateline image)

- **DUBALEVU**

Dubalevu is located on an approximately 800 m wide E-W trending incised and now-abandoned meander and bounded by the highly deformed, steeply inclined Cici Sandstone (CS). The survey was conducted on a farm, 500 m from the Tubairata Rd junction. The abandoned meander is capped by overbank materials, comprising dark brown, fine grained, non-sticky, non-plastic and well-compacted silt loam. Several existing wells (Figure 3), drilled during the SVRDP, were penetrated in series of buried river channels and the distribution of which was localized in the eastern part of the valley. This survey, however, presents an opportunity to determine the spatial extent or continuity of the QRA, particularly the buried river channels, in the western side of the valley and to establish if there are

fractured rock aquifers occurring at depth. However, SVRDP wells water levels and lithogical data from these wells were used a priori for the geophysicalsurvey and groundwater exploration drilling.

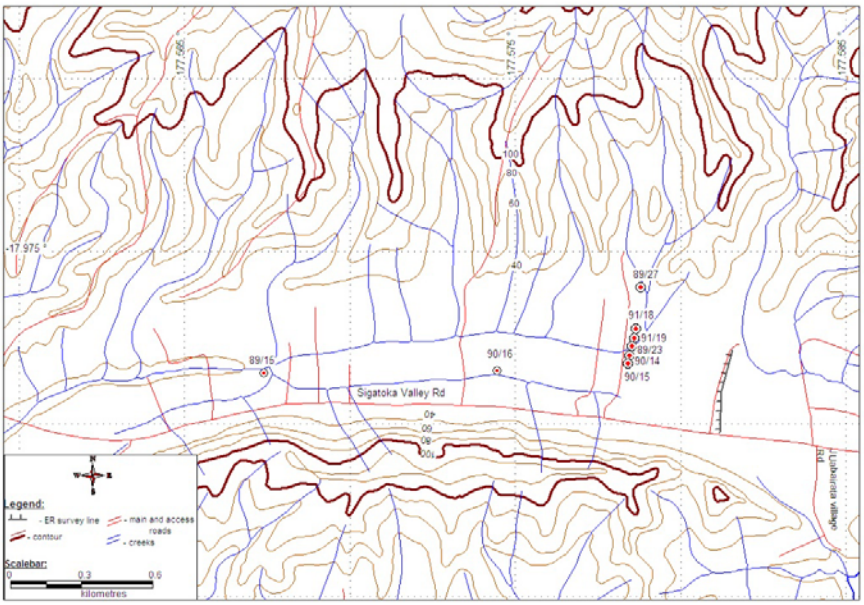

Figure 3: ER survey line – Dubalevu

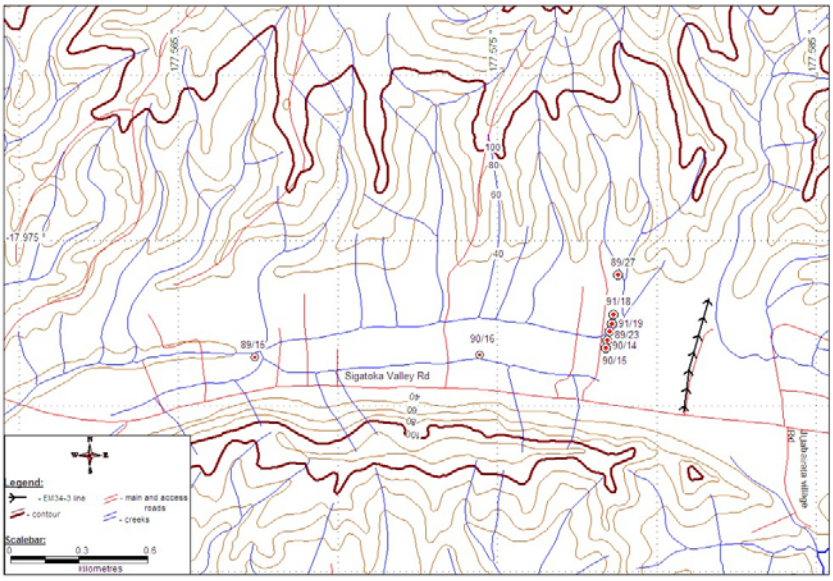

Figure 4: EM 34-3 survey line - Dubalevu

- **Bilalevu**

Survey was conducted on two separate localities, (1) at Tubakeli and (2) along Bila Rd, within the Sigatoka meander at Bilalevu. The selection of these two survey sites were to:

- explore and assess the hydrogeological potential and the variability of the two different underlying geological units, namely Takaro Rudite and Conglomerate of the TSG and Tari Formation of WG;
- identify any fault or shear zone associated with the sinistral ENE-WSE Nasovatava fault and one of its fault splays, which is inferred to have propagated perpendicular in SSE orientation along Bila Rd; and
- assess depth and thickness of the alluvial aquifer (if any) and establish the variability in subsurface materials as a possible function of continuous shifts in the ancient river systems

At Tubakeli, the survey was conducted on vegetable farms, located on alluvial terrace comprising predominantly overbank flood deposits, and underlain by the Takaro Conglomerate/Rudite (TCR). The alluvial flat, on which the two opposite farms are located, is characterized by dark brown to brown silty loam and is located adjacent to the Nasovatava Creek and an oxbow lake, and through which the ENE-WSW NF runs. Despite having eight (8) private wells around the area, only one (1) well drill-log (SVRDP well 89/27 and now abandoned due to poor quality) was available, which was inconclusive in the exploration of any fault or shear zone associated with the NF at Tubakeli. Hence, there were insufficient data to establish any geological constraint within the area and necessitating this survey. The survey lines were oriented E-W and N-S to detect perpendicular subsurface structural features (if any).

Along Bila Rd, the survey was conducted on two farms, 250 m apart, located towards the southern end of the meander and the survey lines were oriented E-W so that it could go through the inferred N-S fault splay associated with the NF. The farms are capped by light brown to dark brown silty, non plastic, slightly sticky silt loam with minor fine sand and is underlain by the Tari Formation (TF). The area has one (1) privately owned groundwater well and is drilled into unconsolidated silty sand to a depth of 20 m.

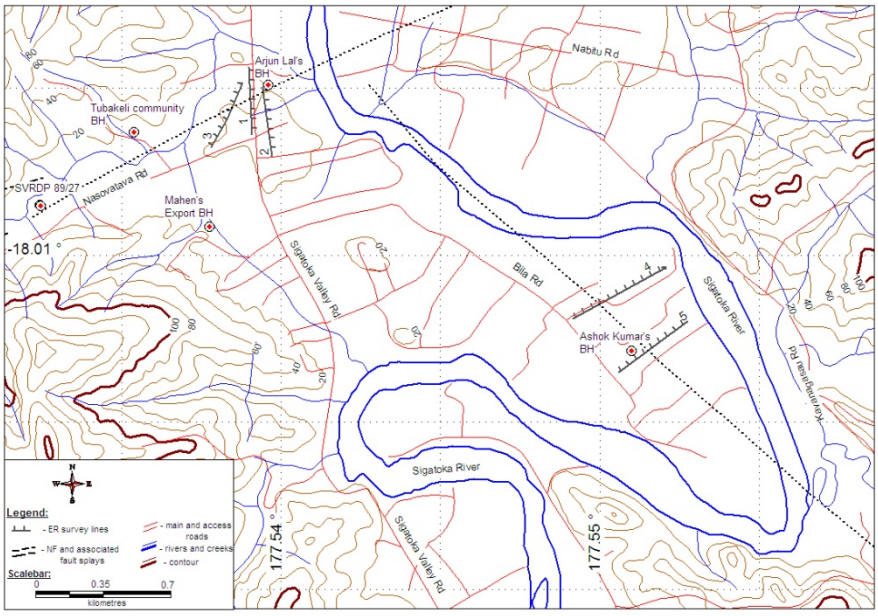

Figure 5: ER survey lines and numbers - Bilalevu

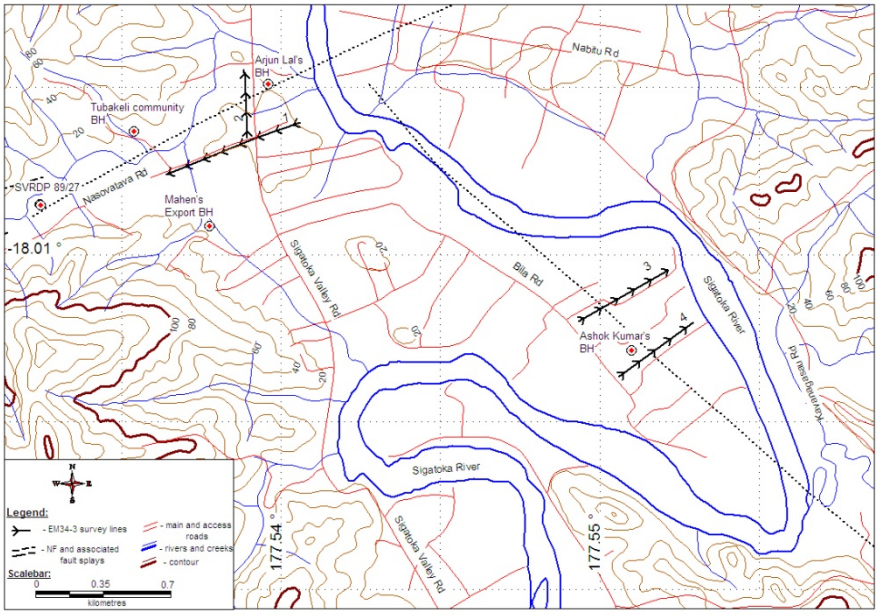

Figure 6: EM survey lines and numbers - Bilalevu

3.2.4 Survey Design, Instrumentation & Data Analysis

Prior to the survey, numerous field visits were carried out to identify the best survey areas and during which agricultural officers were consulted on areas where groundwater wells are necessary for irrigation. These visits also served to inform farmers about the project and seek land-access permission. These was followed by the measurement of standing water levels from nearby borehole, temperature and electrical conductivity using a TLC Solinist dipper to develop a priori (shown earlier in Table 3.2 & 3.3) and upon which the orientation of both

survey methods, as well as the electrode spacing of ER method, are controlled. Relatively flat areas with adequate space and minimal cultural noise were selected as shown by Figure 2. Geological reconnaissance with the assistance of aerial photo and satellite images interpretations were also conducted with the aim to understand the geological and tectonic setting of the larger landscape, with special attention given to geomorphic and structural features pertinent to groundwater occurrence (Sequeira & Mendoza, 2003). It was also critical that both the surveys were conducted under good weather conditions to ensure the safety and security of staffs, as well as the protection of costly geophysical equipment. Shown below, the electrical resistivity profiles, from both dipole-dipole strong gradient (DDSG) and Schlumberger array, and vertical and horizontal electromagnetic responses (raw and tapered) generated at Dubalevu, and Tubakeli and Bila Rd in Bilalevu.

DUBALEVU FIELD RESULTS

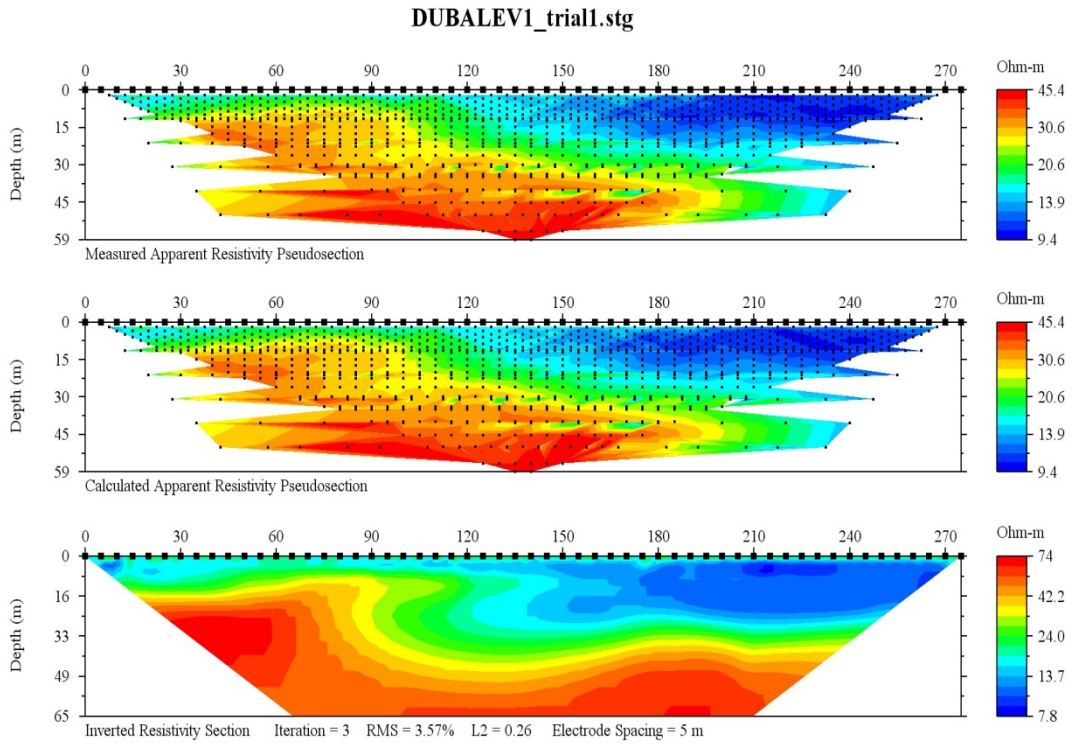

Figure 7: resistivity (Dipole-dipole strong gradient (DDSG) array) profile from Dubalevu

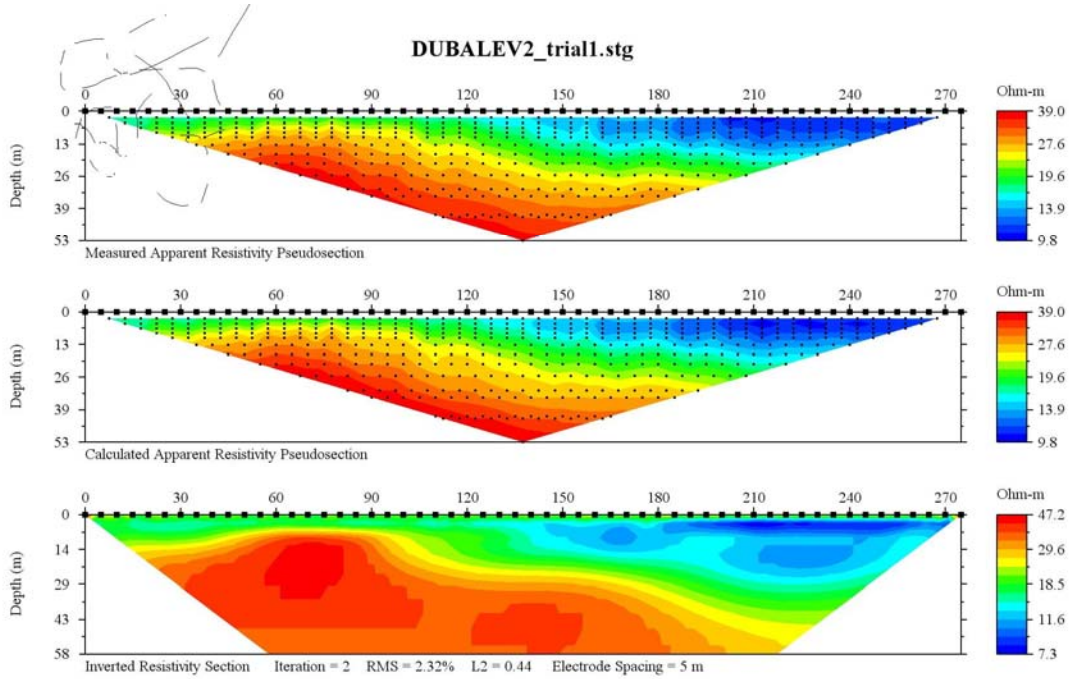

Figure 8: resistivity (Schlumberger array) profile at Dubalevu

Line number	Line 1	Site	Turaga ni Koro's farm				
Location	Dubalevu						
RX Station (m)	**Reading position (m)**	**HD 10**	**HD 10 tapered**	**HD 20**	**HD 20 tapered**	**HD 40**	**HD 40 tapered**
0	5	31	18.33				
5	10	25	22.67	35	22.56		
10	15	22	23.89	33	29.44		
15	20	23	22.67	32	32.33	27	17.56
20	25	22	22.33	32	31.44	26	22.89
25	30	22	22.44	30	30.56	25	25.11
30	35	23	22.67	30	29.78	24	24.11
35	40	23	22.89	29	29.00	24	23.11
40	45	23	22.89	28	28.44	21	22.00
45	50	23	22.56	28	28.11	21	21.44
50	55	22	22.11	28	28.00	21	21.11
55	60	21	21.67	28	28.00	22	21.11
60	65	22	21.56	28	27.44	20	20.89
65	70	21	21.56	28	26.11	21	21.00
70	75	22	21.89	23	24.33	21	21.22
75	80	22	22.33	21	23.56	22	21.67
80	85	23	23.33	24	24.44	22	21.78
85	90	24	24.44	27	26.67	22	21.78
90	95	27	26.00	29	29.11	21	21.67
95	100	26	26.78	32	31.33	22	21.89
100	105	30	27.44	33	32.89	22	22.33
105	110	25	27.11	35	34.00	23	23.11
110	115	28	27.44	34	34.22	24	24.11
115	120	27	27.44	35	34.44	25	25.44
120	125	29	27.78	33	34.56	27	27.00
125	130	27	27.44	36	35.22	29	28.78
130	135	27	27.33	36	35.89	30	30.33
135	140	27	27.44	36	36.89	33	31.44
140	145	28	28.11	38	38.11	32	31.67
145	150	29	29.00	40	39.56	31	32.00
150	155	30	30.00	41	40.89	31	33.11

155	160	31	30.78	42	42.11	36	35.44
160	165	32	30.89	43	43.67	39	36.89
165	170	31	31.11	45	45.56	40	37.56
170	175	28	32.11	49	47.33	32	37.56
175	180	36	33.78	49	47.67	40	39.33
180	185	39	35.56	48	47.67	43	41.56
185	190	31	36.67	43	48.22	44	43.22
190	195	41	39.00	52	50.89	45	43.89
195	200	41	41.56	56	54.11	41	44.00
200	205	45	45.11	56	56.89	47	44.44
205	210	48	48.11	60	58.89	45	44.44
210	215	52	51.11	60	60.33	42	44.67
215	220	54	53.11	62	61.78	46	45.33
220	225	55	54.00	63	62.78	47	46.00
225	230	54	53.67	64	63.56	47	46.33
230	235	53	53.33	64	63.67	45	45.89
235	240	51	52.56	64	63.67	46	45.89
240	245	56	52.22	62	63.33	45	46.22
245	250	48	50.44	65	63.22	48	47.11
250	255	51	49.00	62	62.00	48	47.67
255	260	45	46.89	62	60.89	48	47.78
260	265	46	46.11	56	59.56	48	47.33
265	270	45	45.56	61	59.78	46	46.44
270	275	46	45.78	60	60.22	46	45.56
275	280	46	45.78	61	60.89	44	44.78
280	285	46	45.67	62	60.89	44	44.56
285	290	45	45.22	60	58.22	45	44.56
290	295	45	44.78	60	55.56	45	44.33
295	300	44	44.11	39	52.67	44	43.89
300	305	44	43.67	60	54.44	42	43.56
305	310	42	43.11	57	55.89	44	43.67
310	315	44	42.89	58	57.67	45	43.67
315	320	42	42.56	57	57.00	43	43.22
320	325	42	42.67	57	56.33	42	42.44
325	330	43	43.00	55	55.44	42	41.89
330	335	44	43.44	54	54.89	41	41.44
335	340	44	43.22	55	52.67	42	41.11
340	345	43	42.67	55	48.78	40	41.00
345	350	40	42.22	36	45.00	40	41.11
350	355	43	42.67	38	45.44	44	41.44
355	360	44	43.67	56	49.89	40	41.44
360	365	44	44.33	56	54.33	41	41.78
365	370	47	44.56	57	56.67	43	42.00
370	375	42	44.22	57	56.78	43	42.00
375	380	44	44.44	57	56.67	41	41.44
380	385	46	44.56	56	56.11	40	40.67
385	390	45	44.89	56	55.67	41	40.22
390	395	43	44.33	54	55.44	39	39.89
395	400	47	44.44	56	55.89	40	39.67
400	405	40	44.33	57	56.22	40	39.44
405	410	48	45.89	57	53.89	38	34.89
410	415	46	46.78	55	49.89	40	26.22
415	420	50	47.67	34	43.78		
420	425	47	47.11	45	40.22		
425	430	45	41.44	35	33.00		
430	435	47	30.89	34	24.11		

Table 1: EM raw and tapered horizontal dipole response at Dubalevu

Line Number	Line 1	Site	Turaga ni Koro's farm				
Location	Dubalevu						
RX Station	**Reading position**	**VD**	**VD 10 tapered**	**VD**	**VD 20**	**VD**	**VD 40**

(m)	(m)	10		20	tapered	40	tapered
0	5	34	21.11				
5	10	29	27.22	36	22.67		
10	15	30	30.11	33	28.67		
15	20	30	29.33	30	30.22	24	13.44
20	25	29	28.78	27	28.00	17	15.67
25	30	27	27.78	26	26.56	15	15.44
30	35	28	27.78	26	25.78	12	13.11
35	40	25	27.56	25	24.78	12	11.78
40	45	33	27.56	25	24.22	11	10.67
45	50	24	26.33	20	23.44	9	10.33
50	55	23	25.56	27	23.78	9	10.67
55	60	28	24.33	22	23.56	14	11.78
60	65	24	23.00	24	24.44	12	12.67
65	70	17	21.67	24	25.33	13	13.33
70	75	22	21.33	29	27.11	15	13.67
75	80	24	21.44	28	28.00	13	13.56
80	85	20	21.44	29	28.67	14	13.56
85	90	20	21.00	28	28.22	12	13.11
90	95	23	21.00	30	27.44	15	12.78
95	100	19	21.44	24	25.44	11	12.22
100	105	22	21.33	24	23.78	10	12.22
105	110	26	20.56	21	22.56	15	13.00
110	115	13	20.44	22	23.11	13	13.44
115	120	18	23.89	24	25.11	15	13.67
120	125	35	29.56	28	28.44	12	13.22
125	130	39	33.56	33	31.78	13	14.56
130	135	34	34.33	36	34.56	14	16.44
135	140	29	33.22	35	35.89	25	19.11
140	145	36	32.56	39	36.56	18	19.22
145	150	33	31.11	35	36.11	20	19.33
150	155	27	30.11	36	35.33	15	19.33
155	160	26	30.11	35	34.67	23	20.89
160	165	36	32.56	31	36.33	25	21.44
165	170	34	34.33	38	38.78	19	20.33
170	175	38	33.89	52	42.44	19	19.56
175	180	33	30.44	34	41.56	15	19.56
180	185	21	26.56	51	41.67	26	23.89
185	190	23	26.67	28	39.22	22	28.11
190	195	26	29.89	46	41.33	44	32.33
195	200	44	34.67	41	41.89	32	31.44
200	205	36	36.33	45	41.78	25	27.44
205	210	33	35.56	44	39.89	27	22.22
210	215	39	34.00	25	37.22	10	17.44
215	220	27	33.56	46	38.33	17	16.44
220	225	33	35.56	35	39.56	14	16.44
225	230	44	39.00	43	42.11	22	18.89
230	235	40	40.11	48	41.56	18	20.44
235	240	46	40.22	38	39.11	23	23.00
240	245	28	38.33	33	38.22	26	25.56
245	250	44	40.78	33	41.33	28	27.89
250	255	41	43.78	55	49.11	32	29.00
255	260	51	47.56	59	55.33	28	28.67
260	265	53	47.44	60	56.89	27	29.33
265	270	43	44.22	58	53.33	28	29.33
270	275	39	40.00	43	48.11	39	29.56
275	280	34	37.11	41	45.33	20	26.89
280	285	36	37.44	46	45.33	26	25.11
285	290	39	39.00	49	46.89	24	23.22
290	295	44	41.00	47	46.89	21	22.33
295	300	40	41.89	48	46.44	23	21.56
300	305	43	42.00	41	44.22	18	20.67

305	310	44	41.33	49	42.44	23	21.22
310	315	37	40.67	34	40.00	19	21.78
315	320	40	41.33	37	40.56	25	22.78
320	325	44	42.67	45	42.11	25	23.67
325	330	46	42.78	47	44.56	19	23.78
330	335	43	41.56	42	44.67	31	24.00
335	340	33	39.33	49	45.11	20	21.78
340	345	43	39.11	39	45.89	20	20.00
345	350	37	39.78	50	47.89	15	17.78
350	355	40	41.44	56	46.78	19	18.00
355	360	48	42.33	42	43.78	17	17.78
360	365	40	41.22	30	40.78	21	18.44
365	370	40	39.89	46	40.56	14	18.67
370	375	35	38.33	45	40.22	22	19.44
375	380	41	39.00	35	38.89	23	19.89
380	385	38	39.67	35	37.11	14	20.00
385	390	42	41.00	39	36.11	24	20.56
390	395	42	40.22	36	35.11	22	19.89
395	400	42	38.44	31	33.67	18	18.89
400	405	30	35.00	33	33.33	15	17.67
405	410	34	33.33	33	33.78	18	15.78
410	415	31	33.78	37	35.89	20	12.33
415	420	34	35.89	34	37.11		
420	425	45	37.56	45	38.22		
425	430	35	33.00	35	33.00		
430	435	34	24.11	34	24.11		

Table 2: EM raw and tapered vertical dipole response at Dubalevu

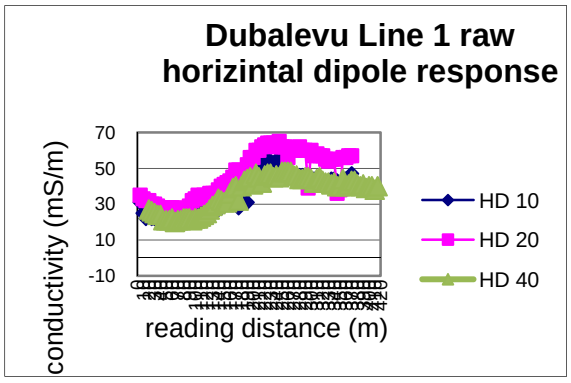

Figure 8: raw horizontal dipole data at Dubalevu

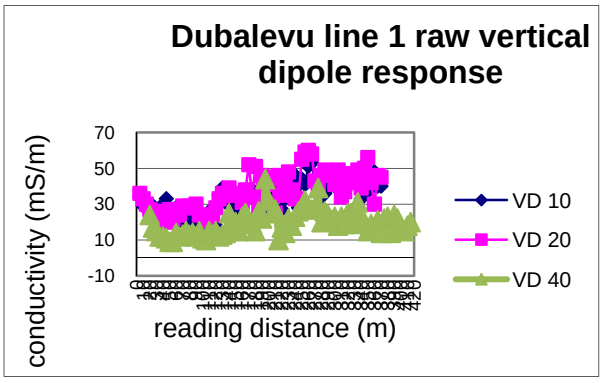

Figure 9: raw vertical dipole response at Dubalevu

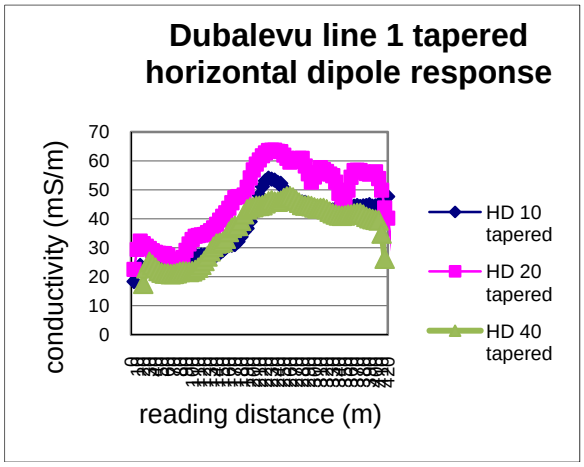

Figure 8: tapered horizontal dipole data at Dubalevu

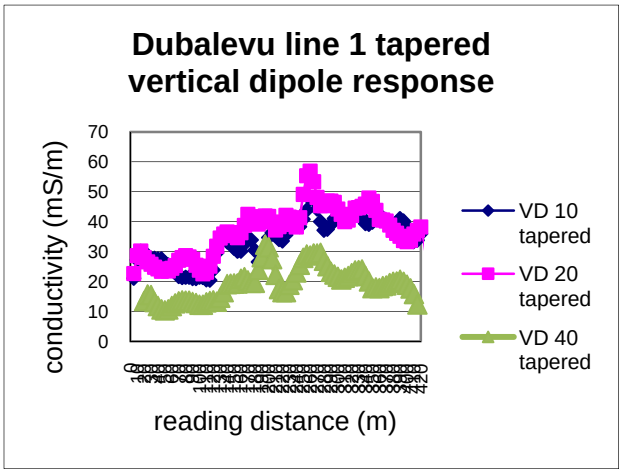

Figure 10: tapered dipole response at Dubalevu

TUBAKELI

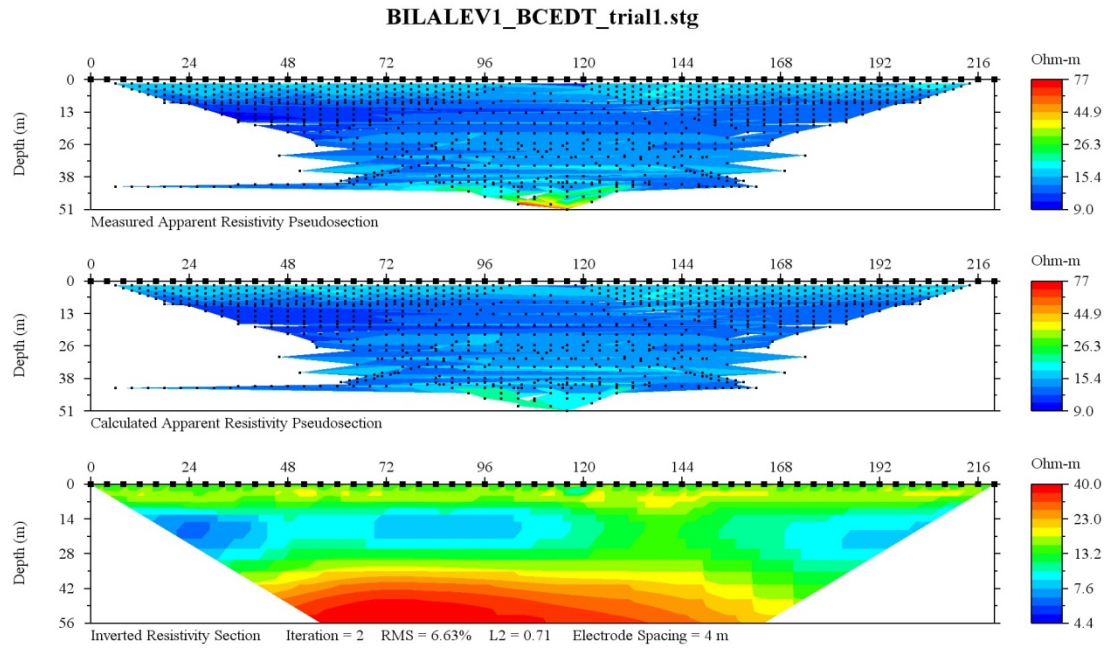

Figure 11: resistivity (DDSG array) profile of line 1 at Tubakeli - improper cable connections

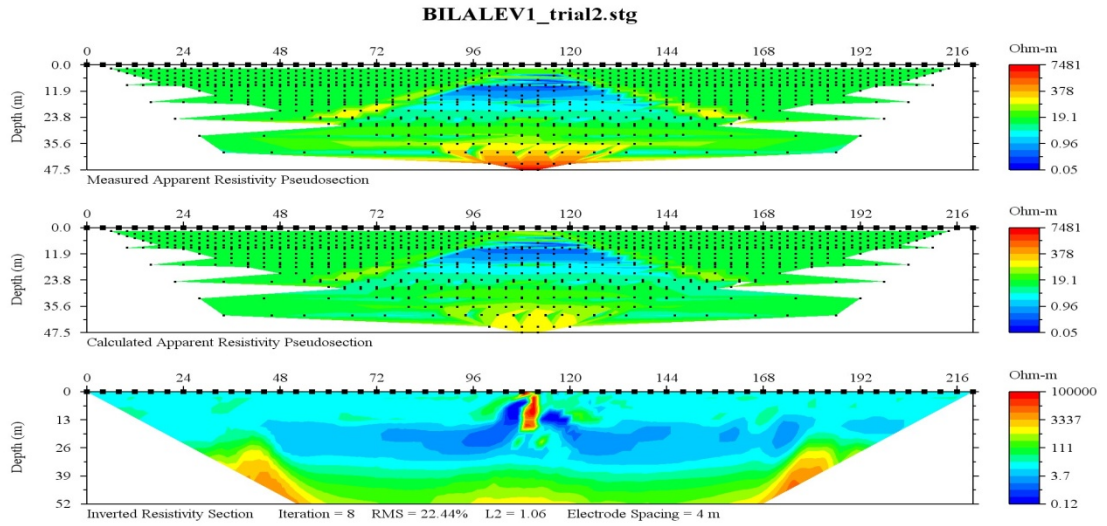

Figure 12: resistivity (Schlumberger array) line 1 profile – improper cable connections

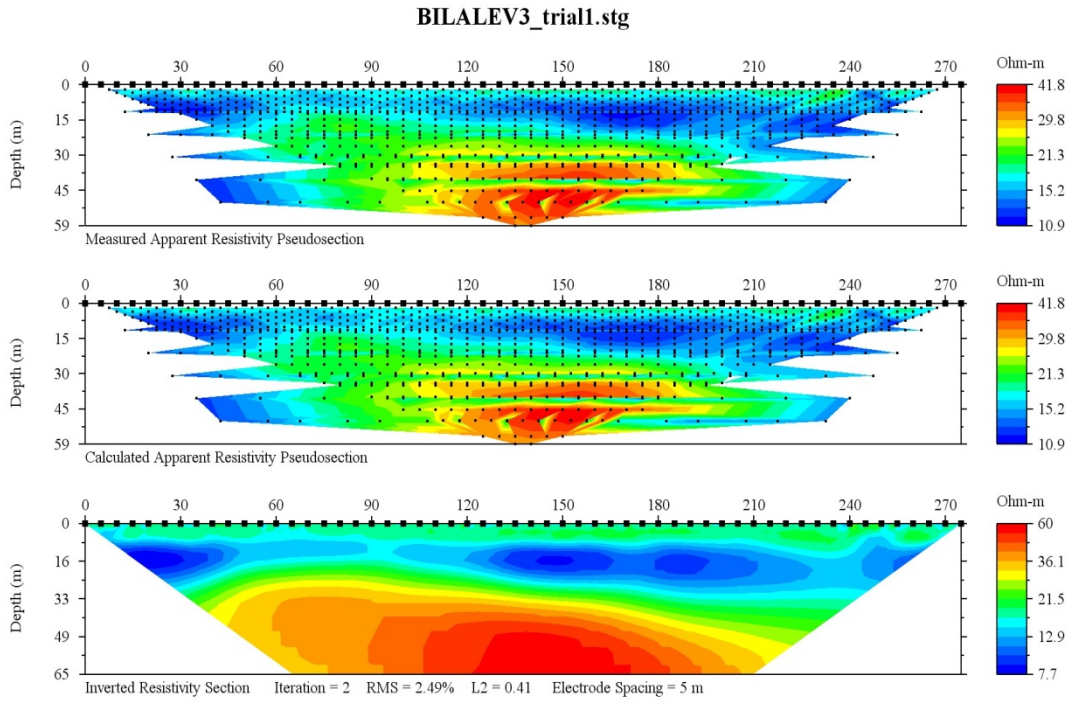

Figure 13: resistivity (DDSG array) line 2 at Tubakeli

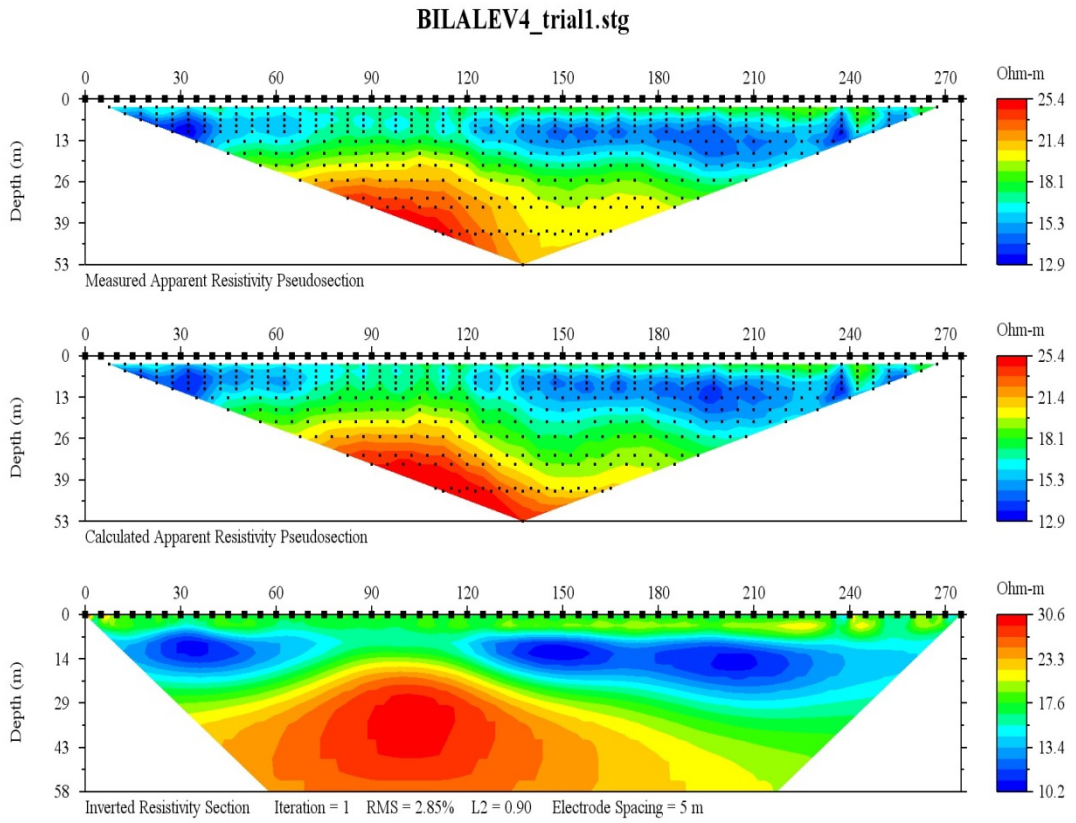

Figure 14: resistivity (Schlumber array) line 2 profile t Tubakeli

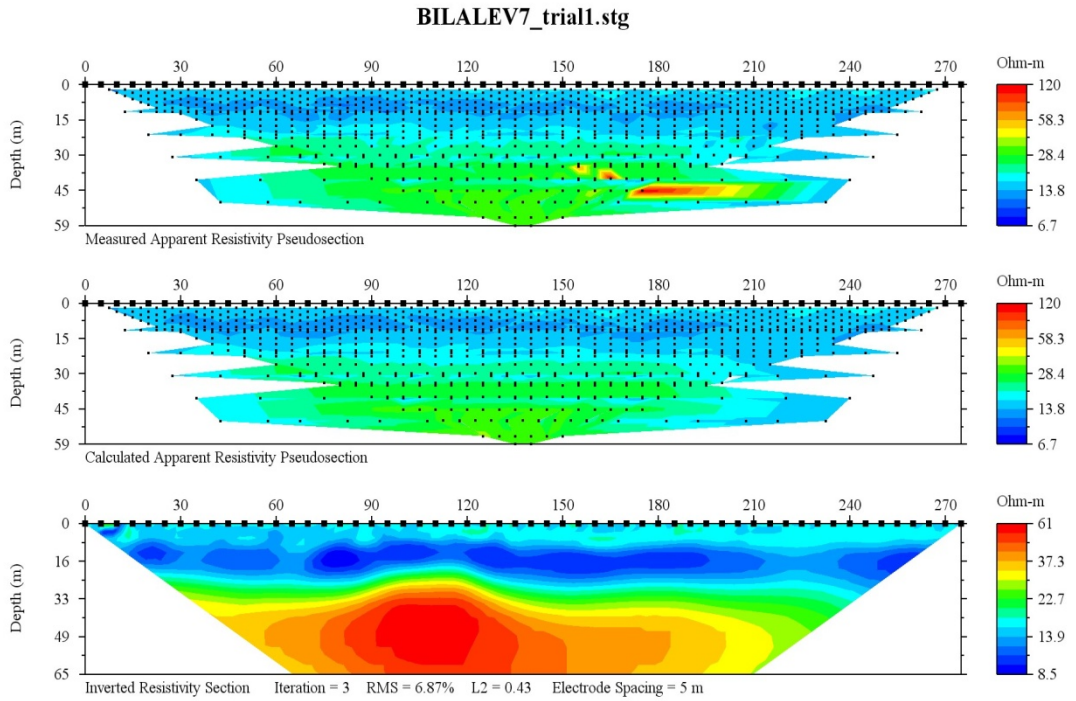

Figure 15 : resistivity (DDSG array) profile line 3 at Tubakeli

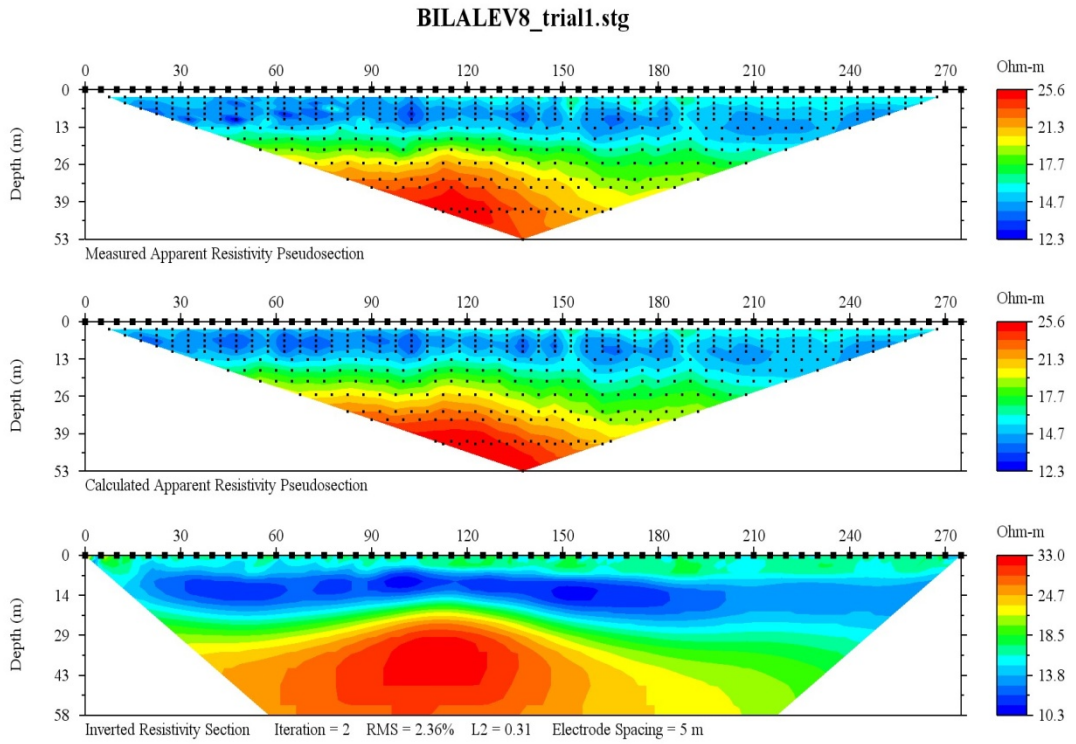

Figure 16: resistivity (Schlumberger array) profile of line 3 at Tubakeli

Line Number	Line 1	Site	Hari Chandra's farm and along Nasovatava Rd		
Location	Tubakeli, Bilalevu				
RX Station (m)	**Reading position (m)**	**HD 20**	**HD 20 tapered**	**HD 40**	**HD 40 tapered**
0	10	55	32.33		
5	15	42	43.56		
10	20	42	53.33	39	24.56
15	25	72	60.67	35	32.00
20	30	71	66.22	34	35.89
25	35	62	71.44	37	36.22
30	40	73	76.22	38	36.89
35	45	97	80.22	36	37.44
40	50	78	77.78	38	38.00
45	55	67	72.44	40	38.78
50	60	65	67.44	38	39.78
55	65	68	65.89	41	41.22
60	70	64	67.44	44	42.89
65	75	64	70.33	44	44.56
70	80	86	74.11	46	46.00
75	85	73	74.22	48	47.78
80	90	71	70.00	48	49.44
85	95	71	65.33	54	51.11
90	100	43	62.56	51	52.11
95	105	74	64.22	52	52.56
100	110	73	68.00	56	52.67
105	115	53	73.67	49	51.89
110	120	96	82.67	53	51.56
115	125	92	86.00	50	50.78
120	130	93	84.44	51	50.89
125	135	67	77.56	50	51.44
130	140	67	74.44	52	52.33
135	145	85	72.67	57	53.22
140	150	72	71.33	50	53.11
145	155	54	65.78	54	53.22
150	160	81	65.11	54	53.11
155	165	39	65.11	52	53.33
160	170	85	70.56	54	53.44
165	175	83	68.78	54	53.67
170	180	55	64.89	53	54.11
175	185	51	57.78	55	54.56
180	190	66	56.22	56	54.11
185	195	42	56.22	54	52.78
190	200	67	55.78	48	51.33
195	205	63	51.56	50	49.78
200	210	25	44.78	54	48.33
205	215	49	40.67	40	45.00
210	220	37	38.44	45	43.33
215	225	32	41.44	37	40.22
220	230	48	45.44	47	38.22
225	235	58	49.89	27	37.11
230	240	48	51.44	30	38.56
235	245	51	51.56	62	42.78
240	250	53	50.89	32	48.89
245	255	51	50.89	48	62.33
250	260	47	51.11	94	87.89
255	265	54	52.00	103	121.44
260	270	56	51.67	175	153.00
265	275	49	50.44	198	166.11
270	280	44	49.22	156	163.67
275	285	53	50.11	136	158.78
280	290	51	50.67	162	157.44
285	295	53	50.11	187	156.78

290	300	47	48.22	129	149.67
295	305	43	46.67	132	145.44
300	310	50	45.78	160	154.00
305	315	44	44.89	148	171.56
310	320	41	44.67	217	197.22
315	325	47	44.89	214	206.89
320	330	47	45.11	240	199.22
325	335	43	45.11	158	170.44
330	340	44	45.00	112	145.78
335	345	48	45.00	142	124.78
340	350	44	43.89	136	105.11
345	355	42	42.56	43	85.44
350	360	39	41.11	56	78.33
355	365	43	40.22	114	85.78
360	370	39	38.67	87	92.89
365	375	35	36.67	101	95.44
370	380	36	34.78	89	92.89
375	385	32	34.22	90	94.33
380	390	32	33.56	100	96.56
385	395	41	33.44	100	100.44
390	400	24	32.11	100	102.89
395	405	34	33.11	114	97.56
400	410	35	34.56	98	80.78
405	415	37	32.78	40	53.33
410	420	40	25.44	25	28.11

Table 3: EM line 1 at Tubakeli showing raw and trapered horizintal response data

Line Number	Line 1	Site	Hari Chandra's farm and along Nasovatava Rd		
Location	Tubakeli, Bilalevu				
RX Station (m)	**Reading position (m)**	**VD 20**	**VD 20 tapered**	**VD 40**	**VD 40 tapered**
0	10	30	29.67		
5	15	57	43.44		
10	20	63	50.56	34.0	22.22
15	25	34	49.56	31.0	29.00
20	30	54	50.67	36.0	32.00
25	35	53	52.00	28.0	30.44
30	40	57	55.78	28.0	29.56
35	45	53	55.56	31.	29.89
40	50	65	57.00	28.0	30.78
45	55	44	54.44	36.0	32.00
50	60	67	52.00	31.0	31.89
55	65	41	44.22	31.0	31.44
60	70	32	41.33	32.0	30.56
65	75	33	42.33	28.0	29.44
70	80	61	48.67	30.0	29.56
75	85	55	52.89	26.0	30.33
80	90	47	53.56	36.0	33.22
85	95	62	51.56	35.0	35.56
90	100	46	47.89	39.0	36.67
95	105	37	44.00	39.0	35.11
100	110	48	42.44	29.0	32.44
105	115	35	45.44	28.0	30.67
110	120	48	50.44	32.0	30.78
115	125	75	56.89	31.0	32.00
120	130	42	62.22	34.0	34.00
125	135	72	69.11	35.0	36.00
130	140	92	72.89	40.0	39.00
135	145	63	71.78	40.0	41.22
140	150	68	68.44	47.0	42.11
145	155	65	63.67	42.0	41.00

150	160	64	61.56	34.0	38.44
155	165	51	57.22	41.0	37.11
160	170	62	53.44	31.0	36.56
165	175	45	45.78	39.0	38.33
170	180	39	41.22	42.0	39.67
175	185	24	39.56	41.0	40.89
180	190	54	45.67	40.0	42.11
185	195	53	51.11	42.0	44.56
190	200	56	54.44	51.0	47.56
195	205	57	53.67	52.0	49.67
200	210	48	50.56	47.0	50.11
205	215	51	46.11	53.0	51.00
210	220	39	39.56	49.0	51.33
215	225	31	34.44	56.0	52.11
220	230	27	32.44	50.0	49.33
225	235	34	34.67	50.0	44.33
230	240	42	37.89	33.0	40.00
235	245	41	40.11	27.0	46.00
240	250	38	39.44	57.0	64.00
245	255	44	38.56	1030	83.11
250	260	29	37.11	112	90.22
255	265	40	38.22	74.0	83.56
260	270	41	39.44	65.0	80.67
265	275	40	40.78	73.0	92.22
270	280	43	40.00	125	117.33
275	285	39	37.67	157	140.89
280	290	32	35.11	156	154.33
285	295	32	34.00	162	159.78
290	300	35	35.11	158	160.44
295	305	37	37.11	167	159.33
300	310	41	39.44	156	155.00
305	315	39	40.67	143	147.00
310	320	45	40.11	149	137.33
315	325	40	38.11	117	123.22
320	330	27	35.78	113	117.78
325	335	40	35.33	91.0	118.22
330	340	36	34.44	156	130.78
335	345	32	33.11	136	134.11
340	350	31	30.44	142	131.78
345	355	28	28.33	112	118.22
350	360	25	26.78	108	110.33
355	365	27	26.11	92.0	105.33
360	370	25	25.67	119	108.89
365	375	26	25.89	106	111.44
370	380	25	25.33	119	113.78
375	385	28	24.44	117	113.22
380	390	20	22.56	102	111.56
385	395	20	21.67	120	110.11
390	400	22	21.78	105	106.33
395	405	23	21.89	100	94.44
400	410	24	21.89	100	74.44
405	415	16	18.78	200	45.56
410	420	25	14.56	25	23.89

Table 4: EM line 1, raw and tapered, vertical dipole response

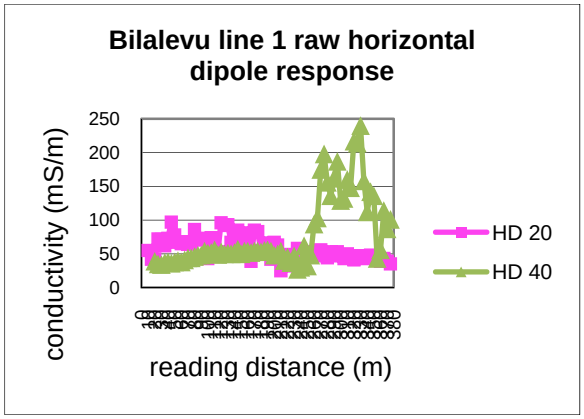

Figure 17: raw EM line 1 horizontal dipole response at Tubakeli

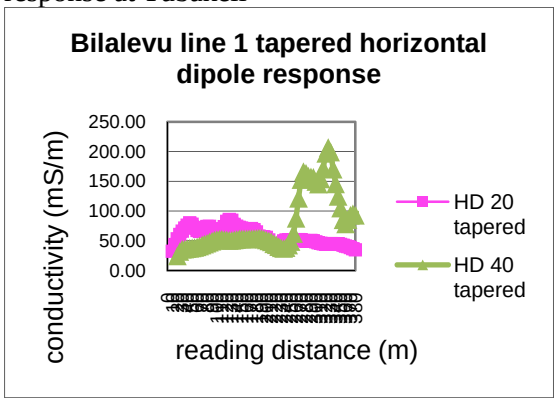

Figure 18: tapered EM line 1 horizontal dipole response at Tubakeli

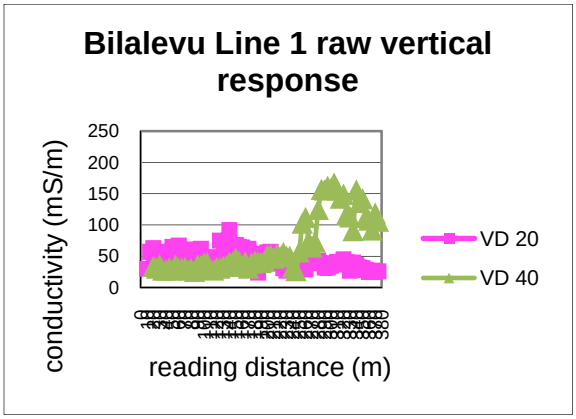

Figure 19: EM line 1raw vertical response at Tubakeli

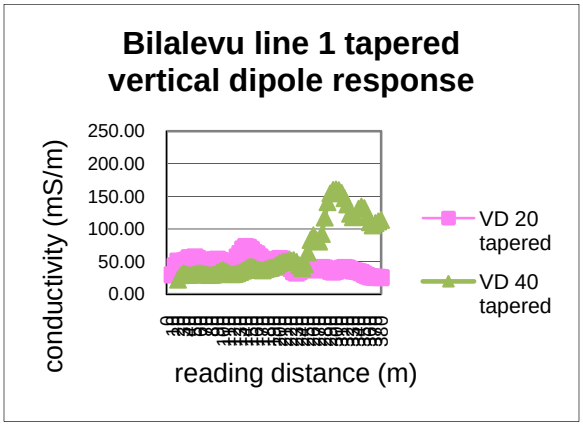

Figure 20: EM line 1 tapered vertical dipole response at Bilalevu.

Line Number	Line 2	Site	Umesh Prasad's farm		
Location	Tubakeli. Bilalevu				
RX Station (m)	**Reading position (m)**	**HD 10**	**HD 10 tapered**	**HD 20**	**HD 20 tapered**
0	5	32	20.67		
5	10	30	27.00	47	31.89
10	15	30	30.56	49	42.78
15	20	29	30.89	48	47.78
20	25	35	32.22	48	47.56
25	30	31	33.00	45	47.22
30	35	35	33.78	49	47.78
35	40	35	34.22	48	47.89
40	45	32	34.78	49	47.78
45	50	38	35.33	46	46.89
50	55	36	35.11	46	46.11
55	60	33	34.78	46	45.56
60	65	34	34.56	44	45.56
65	70	36	34.67	46	46.22
70	75	35	34.89	48	46.56
75	80	33	34.78	48	46.44
80	85	37	34.89	43	45.89
85	90	34	34.67	46	46.00
90	95	34	35.00	48	46.67
95	100	35	35.44	46	47.22
100	105	38	36.33	49	47.33
105	110	36	36.56	47	46.89
110	115	37	36.11	45	46.56
115	120	36	35.11	47	46.44
120	125	32	34.33	47	46.11
125	130	34	34.67	46	45.33
130	135	36	35.78	43	44.22
135	140	38	36.89	43	43.67
140	145	38	37.22	44	43.78
145	150	36	36.78	44	44.11
150	155	37	35.89	45	44.67
155	160	35	34.78	44	45.00
160	165	32	33.67	47	45.33
165	170	34	33.22	45	45.33
170	175	32	33.00	44	45.00
175	180	34	33.22	47	44.78
180	185	33	33.11	42	44.67
185	190	33	33.11	45	45.33
190	195	33	33.22	48	46.22
195	200	33	33.78	46	46.78
200	205	35	34.33	48	47.00
205	210	36	34.56	46	45.44
210	215	33	30.44	47	39.00
215	220	34	22.67	35	27.22

Table 5: EM Line 2, raw and tapered, horizontal dipole response data

Line Number	Line 2	Site	Umesh Chand's farm		
Location	Tubakeli, Bilalevu				
RX Station (m)	**Reading position (m)**	**VD 10**	**VD 10 tapered**	**VD 20**	**VD 20 tapered**
0	5	31	20.67		
5	10	31	28.00	41.00	29.22
10	15	31	32.11	47.00	40.33
15	20	35	32.89	46.00	44.33
20	25	33	32.44	48.00	43.89
25	30	32	31.67	30.00	39.33
30	35	28	31.11	52.00	38.33
35	40	32	31.78	18.00	36.11
40	45	35	32.44	45.00	40.89

45	50	32	33.22	47.00	44.33
50	55	31	32.67	51.00	49.00
55	60	39	32.44	48.00	49.00
60	65	24	31.44	53.00	46.22
65	70	33	32.89	42.00	42.56
70	75	36	34.67	26.00	41.33
75	80	38	35.11	51.00	46.11
80	85	38	32.89	55.00	48.44
85	90	21	30.56	58.00	48.22
90	95	28	29.22	27.00	41.11
95	100	42	29.44	45.00	36.11
100	105	15	28.22	28.00	32.67
105	110	32	28.56	22.00	31.89
110	115	33	27.00	49.00	33.89
115	120	23	28.00	22.00	33.44
120	125	19	29.67	42.00	34.78
125	130	47	34.00	31.00	34.22
130	135	37	34.00	32.00	34.00
135	140	30	31.89	45.00	34.33
140	145	22	28.67	16.00	34.11
145	150	32	29.00	47.00	38.89
150	155	31	30.56	43.00	41.89
155	160	29	33.78	46.00	46.67
160	165	38	36.00	46.00	47.89
165	170	47	38.22	57.00	48.11
170	175	27	38.22	44.00	43.33
175	180	44	38.44	36.00	36.89
180	185	43	38.00	26.00	30.22
185	190	27	37.00	27.00	28.00
190	195	44	36.44	24.00	28.89
195	200	34	34.78	35.00	31.67
200	205	31	33.78	38.00	33.78
205	210	34	32.78	29.00	30.44
210	215	31	29.11	38.00	23.33
215	220	35	22.33		

Table 6: EM Line 2, raw and tapered, vertical dipole response data

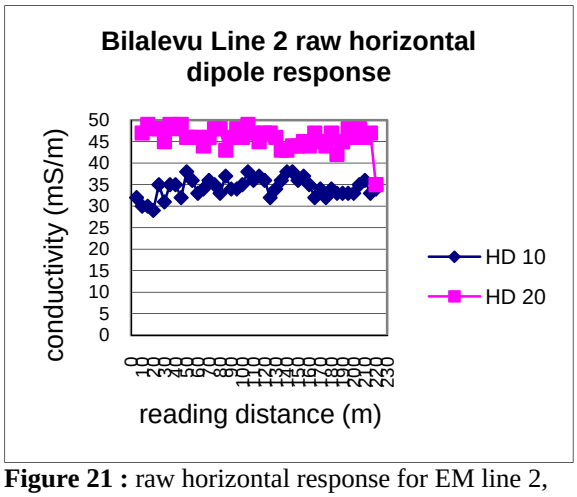

Figure 21 : raw horizontal response for EM line 2, Tubakeli

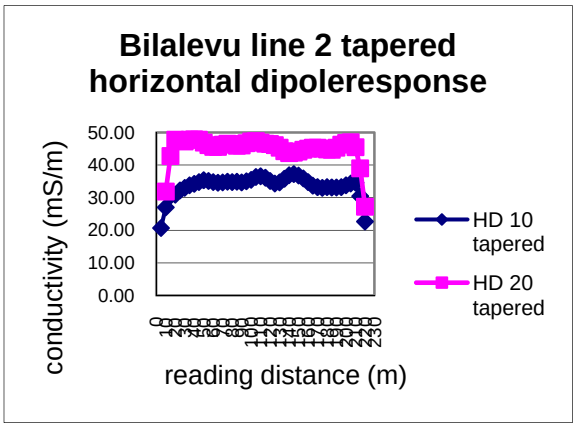

Figure 22: tapered horizontal response for EM line 2, Tubakeli

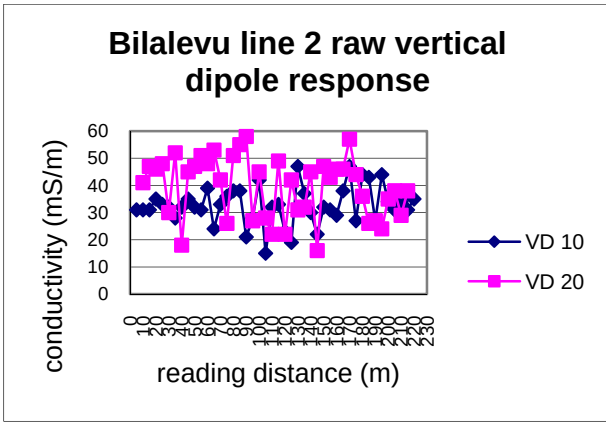

Figure 23: raw vertical response for EM line 2, Tubakeli

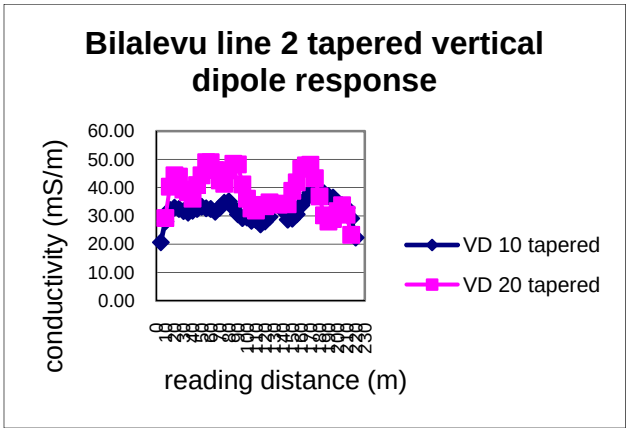

Figure 24: tapered vertical response for EM line 2, Tubakeli

BILA RD

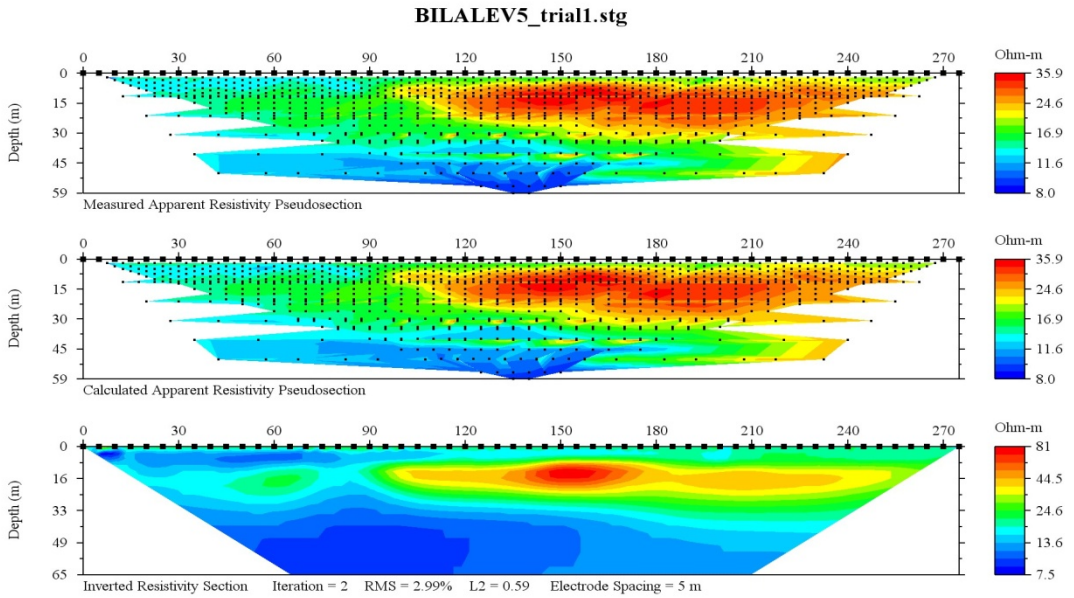

Figure 25: resistivity (DDSG array) profile at Ashok Kumar's farm, Bila Rd

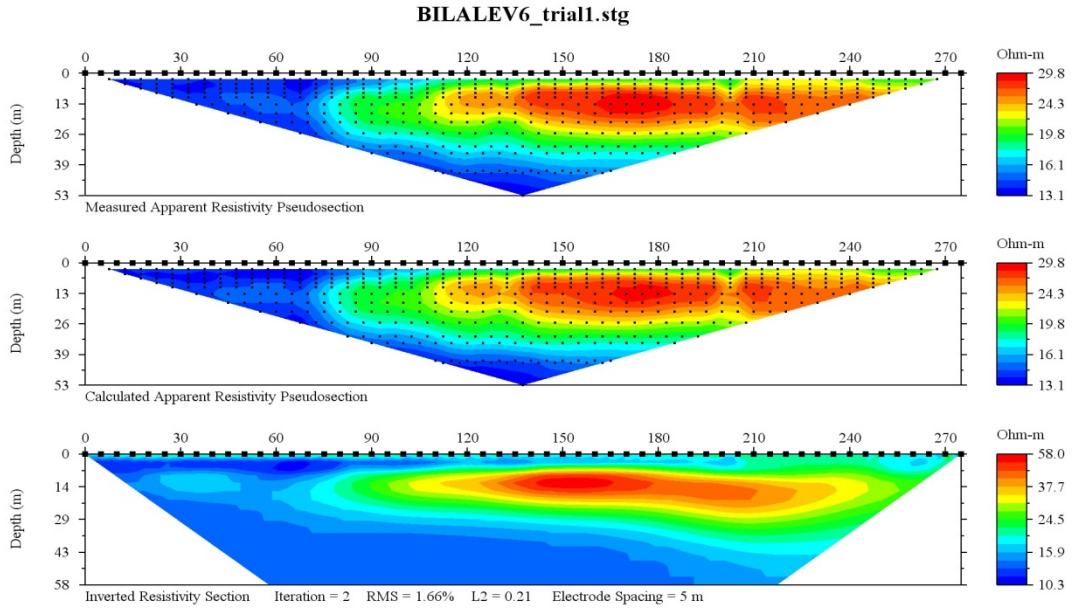

Figure 26: resistivity (Schlumberger array) profile at Ashok Kumar's farm, Bila Rd

Line Number	Line 4	Site	Ashok Kumar's farm				
Location	Bilalevu						
RX Station (m)	**Reading position (m)**	**HD 10**	**HD 10 tapered**	**HD 20**	**HD 20 tapered**	**HD 40**	**HD 40 tapered**
0	5	36	24.00				
5	10	36	31.89	45	30.56		
10	15	36	35.56	46	40.44		
15	20	35	35.11	48	44.44	66	42.67
20	25	34	34.78	40	43.78	65	54.56
25	30	35	34.67	39	45.22	56	57.56
30	35	35	34.44	54	47.33	52	53.33
35	40	34	34.11	54	47.67	50	49.78
40	45	33	33.89	38	45.78	47	47.56
45	50	34	34.11	44	43.67	44	46.00
50	55	35	34.44	48	41.44	47	45.11
55	60	35	34.44	35	38.33	44	44.00
60	65	34	34.11	33	35.67	42	43.11
65	70	33	33.67	34	35.44	42	42.33
70	75	34	33.56	36	37.89	43	41.78
75	80	33	33.44	44	40.78	41	40.89
80	85	34	33.56	44	41.11	39	40.00
85	90	33	33.44	41	39.78	39	39.44
90	95	34	33.44	32	38.22	40	39.33
95	100	33	33.33	39	39.11	39	39.33
100	105	33	33.56	44	40.89	39	39.11
105	110	34	33.78	42	42.22	40	38.44
110	115	35	33.56	42	41.89	37	37.11
115	120	33	32.22	43	40.67	35	35.78
120	125	30	29.44	37	38.89	34	34.89
125	130	27	26.89	37	37.33	35	34.78
130	135	20	25.44	37	36.22	35	34.78
135	140	28	26.56	34	35.44	35	34.78
140	145	29	28.33	36	34.89	34	34.89
145	150	30	30.44	34	34.33	35	35.22
150	155	32	31.89	33	34.33	37	35.56
155	160	34	33.56	35	35.22	35	35.44

160	165	34	35.33	36	36.89	35	35.22
165	170	38	37.44	40	39.11	35	34.89
170	175	40	39.22	41	40.78	35	34.67
175	180	41	40.56	43	42.00	34	34.33
180	185	41	41.00	42	42.44	34	34.22
185	190	42	40.89	43	42.78	34	34.22
190	195	40	40.00	43	42.89	35	34.44
195	200	39	39.00	43	42.78	34	34.11
200	205	37	38.00	43	42.44	35	33.56
205	210	38	37.67	41	41.67	31	32.33
210	215	37	37.33	42	40.89	32	32.22
215	220	38	37.11	39	40.11	30	32.00
220	225	36	36.56	39	39.78	37	32.56
225	230	36	35.89	41	39.67	29	31.56
230	235	36	35.11	39	39.33	32	30.78
235	240	33	34.22	39	38.78	29	29.11
240	245	34	33.78	38	37.89	28	28.00
245	250	33	33.44	37	37.11	26	26.78
250	255	34	33.56	36	36.33	26	25.89
255	260	33	33.33	36	35.67	26	24.89
260	265	34	33.11	35	34.89	23	23.89
265	270	32	32.33	34	34.00	22	23.33
270	275	32	31.56	33	33.00	24	23.33
275	280	30	30.56	32	32.00	24	23.33
280	285	30	29.89	31	31.11	23	23.00
285	290	29	29.22	30	30.44	22	22.44
290	295	29	28.67	30	30.00	22	21.67
295	300	28	28.00	30	29.56	22	20.78
300	305	27	27.22	29	29.00	18	19.67
305	310	27	26.44	28	28.33	19	18.89
310	315	25	25.44	28	27.56	19	18.22
315	320	25	24.33	27	26.56	17	15.78
320	325	23	22.78	25	25.33	17	11.56
325	330	21	20.78	24	24.00		
330	335	19	16.89	23	20.44		
335	340	15	11.56	21	14.78		

Table 7: EM line 3, raw and tapered, horizontal dipole response at Ashok Kumar's farm, Bila Rd, Bilalevu

Line Number	Line 3	**Site**	Ashok Kumar's farm				
Location	Bilalevu						
RX Station (m)	**Reading position (m)**	**VD 10**	**VD 10 tapered**	**VD 20**	**VD 20 tapered**	**VD 40**	**VD 40 tapered**
0	5	28	18.00				
5	10	27	23.67	36	23.11		
10	15	24	26.67	28	32.00		
15	20	28	26.89	44	39.78	29	22.56
20	25	30	27.11	44	41.56	39	33.11
25	30	23	26.67	46	40.11	38	37.44
30	35	28	27.00	34	34.67	47	37.00
35	40	27	28.44	23	30.67	22	33.67
40	45	29	29.67	28	30.00	33	33.44
45	50	38	29.56	37	30.22	39	33.11
50	55	22	26.78	32	30.33	33	32.89
55	60	23	25.22	18	29.56	27	32.33
60	65	24	25.44	39	30.11	32	33.56
65	70	28	26.67	33	29.67	41	36.33
70	75	33	26.78	20	28.78	37	37.67
75	80	19	25.00	32	28.56	39	37.78
80	85	24	24.11	30	30.00	36	35.89
85	90	26	23.78	28	31.67	36	33.89
90	95	22	24.67	40	32.33	28	31.33

95	100	25	26.44	29	32.22	30	29.56
100	105	30	27.44	27	32.44	30	26.78
105	110	33	27.67	41	34.22	24	24.67
110	115	19	26.78	31	35.33	15	24.11
115	120	27	28.11	40	35.33	30	28.78
120	125	34	30.33	36	32.56	34	34.00
125	130	33	34.33	23	30.22	47	38.11
130	135	32	37.56	28	29.78	35	37.00
135	140	51	38.33	35	29.56	34	34.11
140	145	40	33.78	32	28.44	32	30.56
145	150	15	27.56	18	25.44	24	28.22
150	155	20	24.78	26	23.89	28	26.22
155	160	32	25.44	24	22.89	28	23.56
160	165	29	25.89	21	23.00	16	21.00
165	170	20	23.44	22	22.22	16	19.11
170	175	22	23.89	26	21.22	25	17.78
175	180	17	25.22	16	20.00	14	15.33
180	185	46	29.22	16	20.44	9	13.00
185	190	20	28.67	26	22.11	12	12.00
190	195	29	28.00	26	23.44	13	13.33
195	200	31	27.44	21	23.89	14	15.56
200	205	17	27.56	23	24.00	20	17.22
205	210	42	29.11	28	24.44	20	18.00
210	215	22	27.89	23	24.44	14	17.33
215	220	27	27.11	23	24.22	20	16.56
220	225	30	23.78	26	24.33	14	14.44
225	230	17	20.11	23	24.33	13	12.78
230	235	14	17.44	26	24.44	8	10.44
235	240	15	16.78	23	24.44	12	9.67
240	245	21	17.78	24	24.89	6	9.00
245	250	19	17.78	28	25.11	10	9.33
250	255	15	16.89	24	24.11	11	9.11
255	260	16	16.22	23	22.78	8	8.67
260	265	16	16.33	19	21.56	7	8.00
265	270	17	17.56	22	21.56	8	8.78
270	275	18	18.22	23	22.22	8	10.22
275	280	23	18.56	21	23.22	17	12.22
280	285	14	19.11	26	24.11	11	12.56
285	290	17	20.44	26	24.00	13	12.00
290	295	32	22.00	22	23.33	12	10.00
295	300	18	20.78	21	22.78	6	7.78
300	305	18	19.11	24	22.78	5	5.89
305	310	16	17.56	24	21.89	5	5.11
310	315	18	18.78	21	20.11	4	5.11
315	320	20	19.78	14	18.33	7	4.89
320	325	25	19.33	18	16.56	5	3.67
325	330	16	17.00	21	14.33		
330	335	9	13.11	4	9.78		
335	340	17	9.44	8	5.89		

Table 8: EM line 3, raw and tapered, vertical dipole response at Ashok Kumar's farm, Bila Rd, Bilalevu

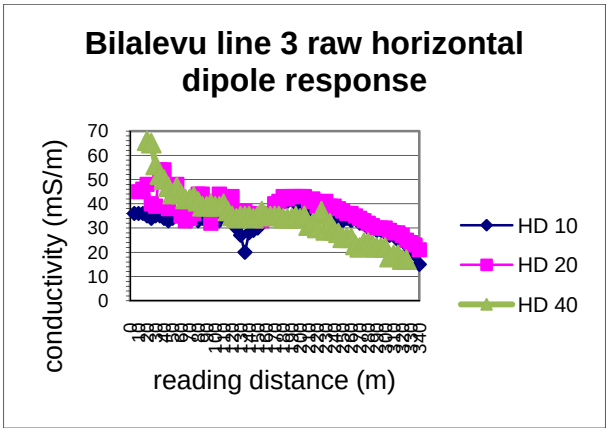

Figure 27: EM line 3 raw horizontal dipole response at Ashok Kumar's farm, Bila Rd, Bilalevu

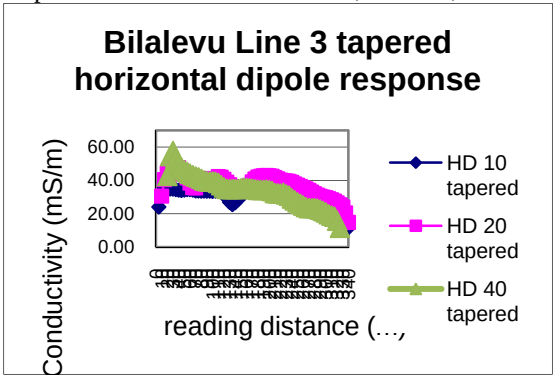

Figure 28: EM line 3 tapered horizontal dipole response at Ashok Kumar's farm, Bila Rd, Bilalevu

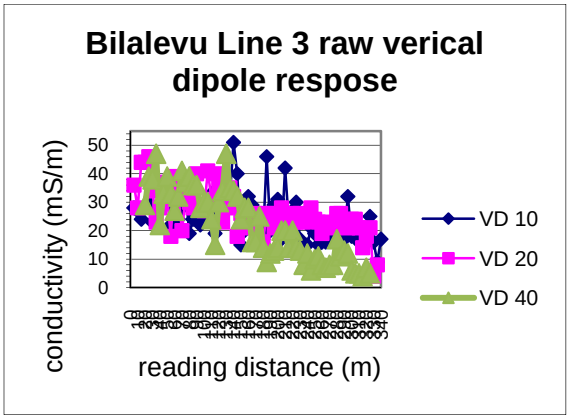

Figure 29: EM line 3 raw vertical dipole response at Ashok Kumar's farm, Bila Rd, Bilalevu

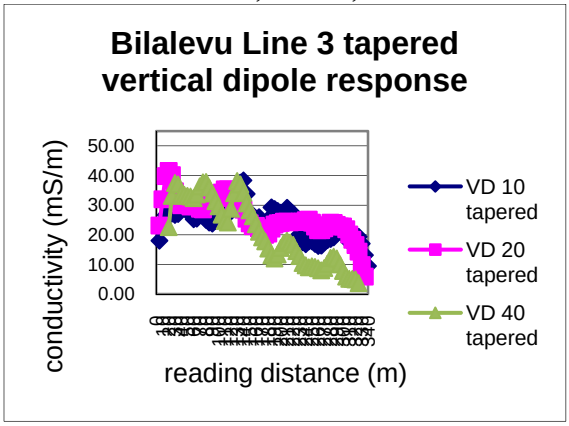

Figure 30: EM line 3 tapered vertical dipole response at Ashok Kumar's farm, Bila Rd, Bilalevu.

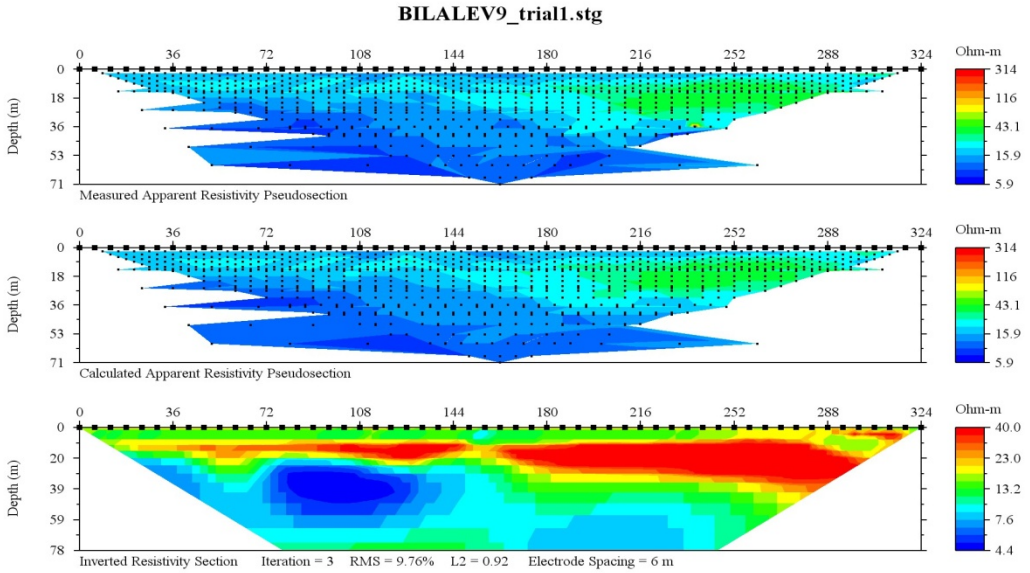

Figure 31: resistivity (DDSG array) profille for line 5 at Sugar Ram's farm, Bila Rd, Bilalevu

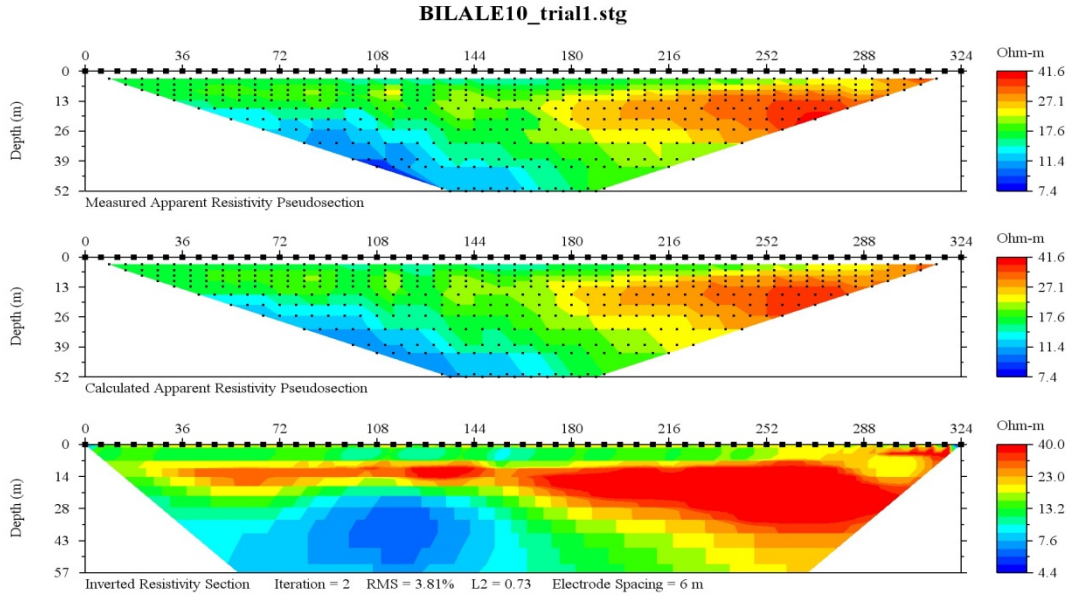

Figure 32: resistivity (Schlumberger array) profille for line 5 at Sugar Ram's farm, Bila Rd, Bilalevu

Line Number	Line 4	Site	Sugar Ram's farm				
Location	Bilalevu						
RX Station (m)	**Reading Positions (m)**	**HD 10**	**HD 10 tapered**	**HD 20**	**HD 20 tapered**	**HD 40**	**HD 40 tapered**
0	5	37	25.22				
5	10	39	34.00	51	34.22		
10	15	38	38.56	51	46.00		
15	20	39	39.22	53	51.89	43	27.89
20	25	40	39.78	53	51.67	40	36.67
25	30	41	40.22	49	50.67	42	41.00
30	35	40	40.22	51	49.78	40	40.44
35	40	40	40.33	48	48.89	40	40.22
40	45	40	40.56	48	48.89	40	40.00
45	50	42	41.11	49	49.11	40	40.00
50	55	41	41.44	51	49.56	40	39.89
55	60	42	40.78	49	49.56	40	39.56
60	65	42	40.00	49	49.67	39	38.89
65	70	33	39.22	50	49.89	38	38.22
70	75	43	40.22	51	50.33	37	37.78
75	80	42	41.00	50	50.44	38	37.56
80	85	41	41.78	51	50.33	38	37.44
85	90	42	41.78	50	49.78	36	37.33
90	95	42	41.78	49	48.89	38	37.33
95	100	42	41.67	48	47.67	38	37.11
100	105	41	41.22	46	46.44	36	36.67
105	110	41	40.78	45	45.56	36	36.11
110	115	40	40.11	45	44.89	36	35.56
115	120	40	39.67	45	44.44	35	35.11
120	125	38	39.22	43	43.89	34	34.56
125	130	40	39.22	44	43.67	35	34.00
130	135	39	39.00	43	43.44	33	33.33
135	140	39	38.78	44	43.22	32	32.78
140	145	38	38.33	43	42.56	33	32.33
145	150	38	37.89	41	41.56	32	31.78
150	155	38	37.22	41	40.56	31	31.11
155	160	36	36.33	39	39.67	30	30.56
160	165	35	35.44	39	39.11	30	30.11

165	170	35	34.78	39	38.67	31	29.67
170	175	34	34.33	38	38.33	28	28.89
175	180	34	34.11	38	38.00	28	28.22
180	185	34	34.11	38	37.33	28	27.67
185	190	34	34.22	37	36.67	27	27.33
190	195	35	34.33	34	36.22	27	27.11
195	200	34	34.11	37	36.44	27	26.89
200	205	34	33.67	38	36.67	27	26.78
205	210	33	32.78	36	36.44	26	26.67
210	215	32	31.89	36	36.00	27	26.67
215	220	30	31.00	35	35.56	27	26.78
220	225	31	30.89	36	35.67	26	26.89
225	230	30	31.33	35	35.89	28	27.00
230	235	33	32.67	37	36.22	27	26.67
235	240	34	34.11	37	36.33	26	26.22
240	245	36	35.33	35	36.33	25	25.89
245	250	37	35.89	37	36.67	26	26.00
250	255	35	35.78	37	36.78	27	26.33
255	260	36	35.67	38	36.89	26	26.33
260	265	35	35.22	35	36.33	27	26.44
265	270	36	34.56	37	36.11	25	26.33
270	275	33	33.11	35	35.78	28	26.22
275	280	31	31.33	36	35.67	26	25.44
280	285	30	29.56	36	35.00	23	24.67
285	290	27	27.89	34	33.89	24	24.00
290	295	27	26.56	32	32.33	25	23.33
295	300	25	25.22	31	30.67	22	22.11
300	305	24	24.11	29	28.89	20	18.56
305	310	23	22.89	27	27.00	19	13.22
310	315	22	21.44	25	23.67		6.44
315	320	20	17.89	23	18.22		
320	325	17	12.56	9	10.89		

Table 9: EM lime 4, raw and tapered, horizontal dipole response at Sugar Ram's farm, Bila Rd, Bilalevu

Line Number	Line 4	Site	Sugar Ram's farm				
Location							
RX Station (m)	**Reading position (m)**	**VD 10**	**VD 10 tapered**	**VD 20**	**VD 20 tapered**	**VD 40**	**VD 40 tapered**
0	5	15	13.78		15.44		
5	10	17	22.44	42	31.56		
10	15	45	31.00	55	43.56		
15	20	31	31.00	48	47.22	53	29.22
20	25	33	30.00	47	45.56	34	36.33
25	30	13	27.00	35	44.00	36	39.00
30	35	38	29.11	48	44.00	47	34.78
35	40	31	28.78	53	43.67	28	27.33
40	45	27	28.22	29	43.11	10	20.22
45	50	23	25.78	45	43.67	12	15.78
50	55	27	24.67	57	42.11	25	16.44
55	60	24	24.56	33	35.33	8	16.22
60	65	20	26.00	23	27.78	23	16.67
65	70	32	30.00	14	22.56	14	14.89
70	75	35	34.22	30	23.78	12	14.11
75	80	40	37.33	22	25.89	14	13.44
80	85	39	37.67	29	28.78	12	14.11
85	90	36	36.78	35	30.33	17	14.56
90	95	35	35.67	28	31.22	17	13.89
95	100	35	34.22	32	31.11	8	13.44
100	105	35	33.11	34	30.67	12	15.11
105	110	27	31.00	25	29.78	22	17.56
110	115	34	30.22	32	29.22	23	19.11

115	120	25	29.00	29	27.89	14	19.00
120	125	31	29.00	25	26.67	19	20.11
125	130	29	27.56	25	25.89	23	21.33
130	135	26	26.33	25	25.44	27	21.89
135	140	22	25.44	29	25.11	17	20.67
140	145	26	26.22	21	24.11	17	21.22
145	150	30	26.67	22	24.44	24	22.78
150	155	28	26.67	27	25.89	31	23.56
155	160	20	24.89	29	28.33	20	21.89
160	165	30	23.78	29	30.00	14	19.67
165	170	18	21.11	34	30.67	23	18.89
170	175	20	20.33	30	29.89	18	17.89
175	180	16	20.22	27	28.67	17	17.00
180	185	25	23.00	28	26.78	13	16.44
185	190	26	24.78	27	25.56	17	17.33
190	195	28	24.89	19	24.33	23	18.22
195	200	23	23.44	28	25.00	16	18.22
200	205	17	22.44	24	24.56	16	17.22
205	210	26	21.78	28	24.78	21	16.44
210	215	25	21.11	18	24.22	10	15.56
215	220	11	19.11	27	26.67	17	15.56
220	225	24	19.00	30	28.11	18	14.89
225	230	15	18.44	35	28.22	12	13.44
230	235	22	19.33	21	25.56	12	11.00
235	240	18	19.00	20	23.89	8	8.89
240	245	18	19.89	27	24.00	5	7.44
245	250	22	21.00	24	24.22	10	7.33
250	255	23	22.00	26	23.44	4	7.56
255	260	23	21.44	20	22.11	10	8.44
260	265	21	19.78	18	22.56	11	8.89
265	270	14	19.00	27	23.89	6	8.89
270	275	18	20.33	29	24.44	11	9.00
275	280	28	23.00	20	23.11	8	8.56
280	285	24	23.89	21	22.44	9	8.56
285	290	25	22.89	21	22.56	7	8.11
290	295	19	20.33	28	24.00	9	7.78
295	300	17	18.33	22	24.44	8	6.89
300	305	18	16.67	25	25.00	4	5.22
305	310	15	15.44	27	24.56	5	3.44
310	315	13	14.00	24	22.22		
315	320	15	11.56	20	17.00		
320	325	9	7.78	9	10.11		

Table 10: EM lime 4, raw and tapered, vertical dipole response at Sugar Ram's farm, Bila Rd, Bilalevu

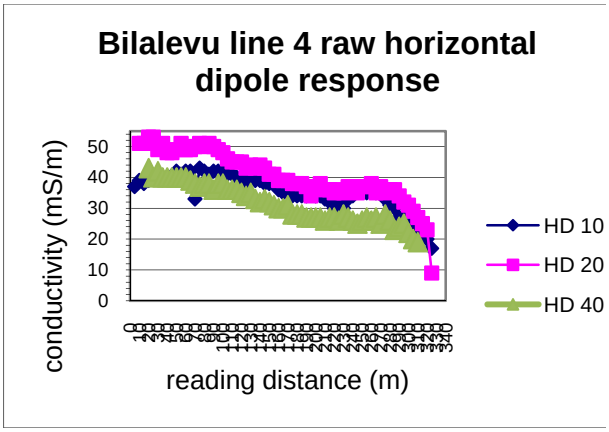

Figure 33: EM line 4 raw horizontal dipole response at Sugar Ram's farm

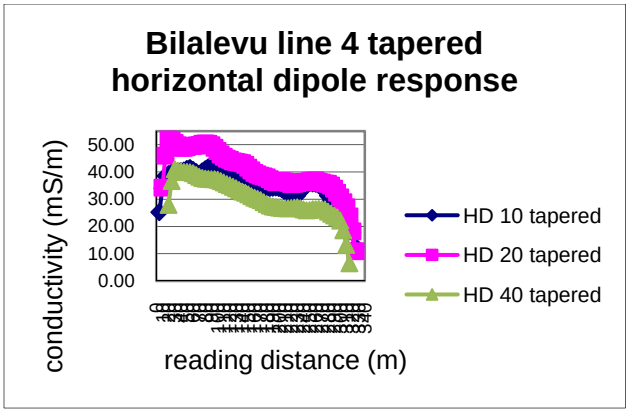

Figure 34: EM line 4 tapered horizontal dipole response at Sugar Ram's farm

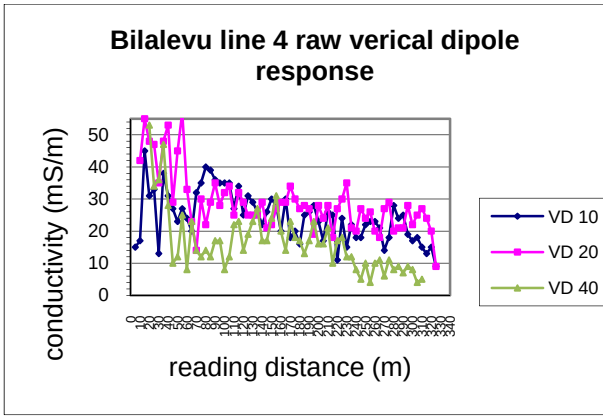

Figure 35: EM line 4 raw verical dipole response at Sugar Ram's farm

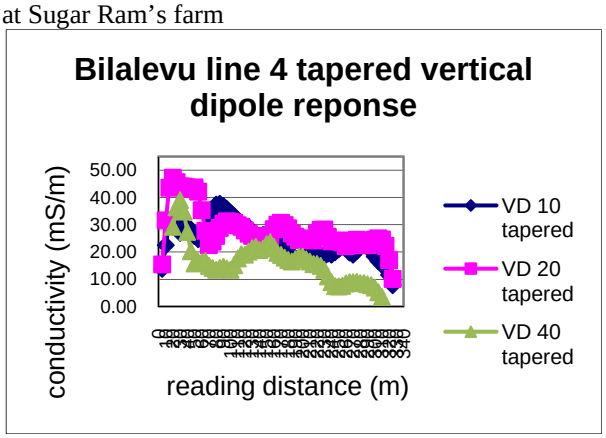

Figure 36: EM line 4 tapered verical dipole response at Sugar Ram's farm

Appendix E: Permeability test results

Soil samples were collected from Dubalevu, Tubakeli and Bila Rd following the digging of mud-pits and prior to the drilling of wells 10/07, 10/11 and 10/15 respectively (Figure 1).

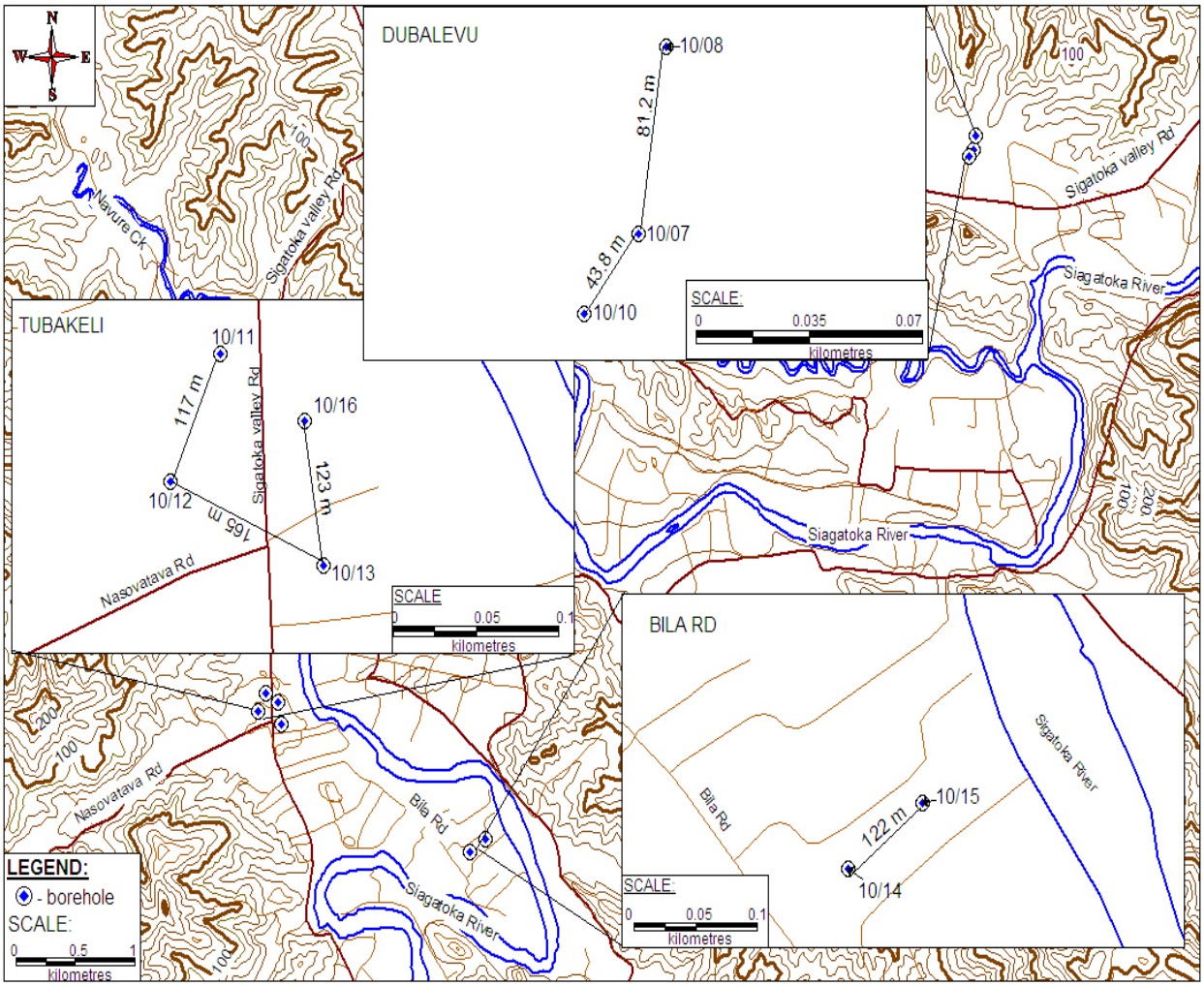

Figure 1: location of wells 10/07, 10/11 and 10/15 where the test soils were collected

$$K = (a/A)\times(L/t)\times\ln\{h_0/h\} \quad K' = 2.3\,(a/A)\times(L/t)\times\log_{10}\{h_0/h\}$$

where K = hydraulic conductivity (m/s)

a = standpipe area (m^2)

A = sample cross sectional area (m^2)

L = sample thickness or height (m)

h_0 = initial head above top of sample (m)

h = measured head during or at the end of test (m)

t = elapsed time from h_0 to h (sec)

Dubalevu

Time (min)	0.16	1	10	40	60	120	470	1100
a (m)	0.000026431	0.000026431	0.000026431	0.000026431	0.000026431	0.000026431	0.000026431	0.000026431
A (m)	0.008107	0.008107	0.008107	0.008107	0.008107	0.008107	0.008107	0.008107
L (m)	0.123	0.123	0.123	0.123	0.123	0.123	0.123	0.123
t (sec)	9.6	60	600	2400	3600	7200	28200	66000
h0	1.620	1.620	1.620	1.620	1.620	1.620	1.620	1.620
H	1.604	1.6	1.54	1.374	1.278	1.07	0.91	0.73
K	4.14157E-07	8.29347E-08	3.38105E-08	2.74891E-08	2.63853E-08	2.30754E-08	8.19231E-09	4.83801E-09
K"	4.14622E-07	8.30279E-08	3.38485E-08	2.752E-08	2.64149E-08	2.31014E-08	8.20152E-09	4.84345E-09

Table 1: permeability test results of soil collected from BH 10/07, Dubalevu, Bilalevu

Average K (m/s) = 7.76103E-08

Tubakeli, Bilalevu

Time (min)	1	5	13	21	40	60	287	360	800
a (m)	0.00002 6431	0.00002 6431	0.00002 6431	0.00002 6431	0.00002 6431	0.00002 6431	0.00002 6431	0.00002 6431	0.00002 6431
A (m)	0.00810 7	0.00810 7	0.00810 7	0.00810 7	0.00810 7	0.00810 7	0.00810 7	0.00810 7	0.00810 7
L (m)	0.123	0.123	0.123	0.123	0.123	0.123	0.123	0.123	0.123
t (sec)	60	300	780	1260	2400	3600	17220	21600	48000
h0	1.862	1.862	1.862	1.862	1.862	1.862	1.862	1.862	1.862
h	1.542	1.502	1.414	1.344	1.23	1.155	0.877	0.837	0.816
K	1.25893 E-06	2.86879 E-07	1.41344 E-07	1.0364E -07	6.92045 E-08	5.31367 E-08	1.75138 E-08	1.48282 E-08	6.88472 E-09
K"	1.26034 E-06	2.87202 E-07	1.41503 E-07	1.03756 E-07	6.92823 E-08	5.31965 E-08	1.75335 E-08	1.48448 E-08	6.89246 E-09

Table 2: permeability test results of soil collected from BH 10/11, Tubakeli, Bilalevu

Average K (m/s) = 2.16929E-07

Bila Rd, Bilalevu

Time (min)	8	20	27	65	381	776	1150
a (m)	0.000026431	0.000026431	0.000026431	0.000026431	0.000026431	0.000026431	0.000026431
A (m)	0.008107	0.008107	0.008107	0.008107	0.008107	0.008107	0.008107
L (m)	0.123	0.123	0.123	0.123	0.123	0.123	0.123
t (sec)	480	1200	1620	3900	22860	46560	69000
h	1.790	1.790	1.790	1.790	1.790	1.790	1.790
h	1.49	1.468	1.464	1.459	1.37	1.24	1.165
K	1.53084E-07	6.6199E-08	4.9711E-08	2.10006E-08	4.68566E-09	3.15831E-09	2.49337E-09
K"	1.53256E-07	6.62734E-08	4.97668E-08	2.10242E-08	4.69093E-09	3.16186E-09	2.49617E-09

Table 3: permeability test results of soil collected from BH 10/15, Bila Rd, Bilalevu

Average K (m/s) = 4.29045E-08

Appendix F – Borehole Logs
Well 10/07 at Dubalevu

Depth (m)	Lithological Description	Geology
0 - 1	dark brown to brown silty loam, friable, with fine sand, very well-well sorted, rooting system visible, moist and slightly sticky	Recent Alluvium
1 - 2	brown to light brown silty loam, fine grained, some coarse sand, moderately sorted,	Recent Alluvium
2 - 3	brown to light brown silty loam, fine grained, some coarse sand, moderately sorted,	Recent Alluvium
3 - 4	brown to light brown silty loam, fine grained, some coarse sand, moderately sorted,	Recent Alluvium
4 - 5	light brown - yellowish brown silty loam with some fine-medium sub-rounded pebbles	Recent Alluvium
5 - 6	light brown - yellowish brown silty loam with some fine-medium sub-rounded pebbles	Recent Alluvium
6 - 7	light brown - yellowish brown silty loam with some fine-medium sub-rounded pebbles	Recent Alluvium
7 - 8	light brown - yellowish brown silty loam with some fine-medium sub-rounded pebbles	Recent Alluvium
8 - 9	light brown - yellowish brown silty loam with some fine-medium sub-rounded pebbles	Recent Alluvium
9 - 10	light brown - yellowish brown silty loam with some fine-medium sub-rounded pebbles	Recent Alluvium
10 - 11	light brown - yellowish brown silty loam with some fine-medium sub-rounded pebbles	Recent Alluvium
11 - 12	light brown - yellowish brown silty loam with some fine-medium sub-rounded pebbles	Recent Alluvium
12 - 13	yellowish brown, fine grained, highly weathered mudstone and siltstone	Cici Sandstone
13 - 14	yellowish brown, fine grained, highly weathered mudstone and siltstone	Cici Sandstone
14 - 15	yellowish brown, fine grained, highly weathered mudstone and siltstone	Cici Sandstone
15 - 16	bluish grey, fresh siltstone	Cici Sandstone
16 - 17	bluish grey, fresh siltstone	Cici Sandstone
17 - 18	bluish grey, fresh siltstone	Cici Sandstone
18 - 19	bluish grey and dark grey siltstone and mudstone	Cici Sandstone
19 - 20	bluish grey and dark grey siltstone and mudstone	Cici Sandstone
20 - 21	bluish grey and dark grey siltstone and mudstone	Cici Sandstone
21 - 22	bluish grey and dark grey siltstone and mudstone	Cici Sandstone
22 - 23	yellowish brown - reddish brown, light grey sandstone with abundant quartz veins and ferrecrete coatings	Cici Sandstone
23 - 24	yellowish brown - reddish brown, light grey sandstone with abundant quartz veins and ferrecrete coatings	Cici Sandstone
24 - 25	yellowish brown - reddish brown, light grey sandstone with abundant quartz veins and ferrecrete coatings	Cici Sandstone
25 - 26	yellowish brown - reddish brown, light grey sandstone with abundant quartz veins and ferrecrete coatings	Cici Sandstone
26 - 27	yellowish brown - reddish brown, light grey sandstone with abundant quartz veins and ferrecrete coatings	Cici Sandstone
27 - 28	yellowish brown - reddish brown, light grey sandstone with abundant quartz veins and ferrecrete coatings	Cici Sandstone
28 - 29	yellowish brown - reddish brown, light grey sandstone with abundant quartz veins and ferrecrete coatings	Cici Sandstone
29 - 30	yellowish brown - reddish brown, light grey sandstone with abundant quartz veins and ferrecrete coatings	Cici Sandstone
30 - 31	yellowish brown - reddish brown, light grey sandstone with abundant quartz veins and ferrecrete coatings	Cici Sandstone
31 - 32	yellowish brown - reddish brown, light grey sandstone with abundant quartz veins and ferrecrete coatings	Cici Sandstone
32 - 33	bluish grey, fine grained, well indurated, extremely strong, unweathered, moderately well-well sorted, fresh Sandstone	Cici Sandstone
33 - 34	bluish grey, fine grained, well indurated, extremely strong, unweathered, moderately well-well sorted, fresh Sandstone	Cici Sandstone

Well 10/08 at Dubalevu

Depth (m)	Lithological Description	Geology
0 - 1	dark brown to greyish brown silty loam with some pebbles	Recent Alluvium
1 - 2	dark brown to greyish brown silty loam with some pebbles	Recent Alluvium
2 - 3	dark brown to greyish brown silty loam with some pebbles	Recent Alluvium
3 - 4	dark brown to greyish brown silty loam with some pebbles	Recent Alluvium
4 - 5	dark brown to greyish brown silty loam with some pebbles	Recent Alluvium
5 - 6	dark brown to greyish brown silty loam with some pebbles	Recent Alluvium
6 - 7	dark brown to greyish brown silty loam with some pebbles	Recent Alluvium
7 - 8	dark brown to greyish brown silty loam with some pebbles	Recent Alluvium
8 - 9	dark brown to greyish brown silty loam with some pebbles	Recent Alluvium
9 - 10	dark brown to greyish brown silty loam with some pebbles	Recent Alluvium
10 - 11	dark brown to greyish brown silty loam with some pebbles	Recent Alluvium
11 - 12	dark grey-bluish sandstone and siltstone	Cici Sandstone
12 - 13	dark grey-bluish sandstone and siltstone	Cici Sandstone
13 - 14	dark grey-bluish sandstone and siltstone	Cici Sandstone
14 - 15	dark grey-bluish sandstone and siltstone	Cici Sandstone
15 - 16	dark grey-bluish sandstone and siltstone	Cici Sandstone
16 - 17	dark grey-bluish sandstone and siltstone	Cici Sandstone
17 - 18	dark grey-bluish sandstone and siltstone	Cici Sandstone
18 - 19	dark grey-bluish sandstone and siltstone	Cici Sandstone
19 - 20	dark grey-bluish sandstone and siltstone	Cici Sandstone
20 - 21	highly discoloured light grey to greenish grey sandstone with some quartz veins and iron oxide coatings	Cici Sandstone
21 - 22	highly discoloured light grey to greenish grey sandstone with some quartz veins and iron oxide coatings	Cici Sandstone
22 - 23	highly discoloured light grey to greenish grey sandstone with some quartz veins and iron oxide coatings	Cici Sandstone
23 - 24	highly discoloured light grey to greenish grey sandstone with some quartz veins and iron oxide coatings	Cici Sandstone
24 - 25	fresh, bluish grey, well indurated, extremely strong, sandstone	Cici Sandstone
25 - 26	fresh, bluish grey, well indurated, extremely strong, sandstone	Cici Sandstone
26-27	fresh, bluish grey, well indurated, extremely strong, sandstone	Cici Sandstone
27-28	fresh, bluish grey, well indurated, extremely strong, sandstone	Cici Sandstone

Well 10/10 - Dubalevu

Depth (m)	Lithological Description	Geology
0 - 1	dark brown silty loam, slightly sticky, low plasticity	Recent Alluvium
1 - 2	dark brown silty loam, slightly sticky, low plasticity	Recent Alluvium
2 - 3	brown silty loam with some very fine sand, non sticky with low plasticity	Recent Alluvium

3 - 4	brown silty loam with some very fine sand, non sticky with low plasticity	Recent Alluvium
4 - 5	brown silt, non plastic, non sticky, well sorted	Recent Alluvium
5 - 6	brown silt, non plastic, non sticky, well sorted	Recent Alluvium
6 - 7	brown silt, non plastic, non sticky, well sorted	Recent Alluvium
7 - 8	brown silt, non plastic, non sticky, well sorted	Recent Alluvium
8 - 9	brown sandy silt with some fine-medium pebble	Recent Alluvium
9 - 10	brown sandy silt with some fine-medium pebble	Recent Alluvium
10 - 11	brown sandy silt with some fine-medium pebble	Recent Alluvium
11 - 12	brown sandy silt with some fine-medium pebble	Recent Alluvium
12 - 13	brown sandy silt with some fine-medium pebble	Recent Alluvium
13 - 14	bluish grey sandy siltstone and sandstone, fine grained, moderate well sorted, unweathered	Cici Sandstone
14 - 15	bluish grey sandy siltstone and sandstone, fine grained, moderate well sorted, unweathered	Cici Sandstone
15 - 16	bluish grey sandy siltstone and sandstone, fine grained, moderate well sorted, unweathered	Cici Sandstone
16 - 17	bluish grey sandy siltstone and sandstone, fine grained, moderate well sorted, unweathered	Cici Sandstone
17 - 18	bluish grey sandy siltstone and sandstone, fine grained, moderate well sorted, unweathered	Cici Sandstone
18 - 19	bluish grey sandy siltstone and sandstone, fine grained, moderate well sorted, unweathered	Cici Sandstone
19 - 20	bluish grey sandy siltstone and sandstone, fine grained, moderate well sorted, unweathered	Cici Sandstone
20 - 21	bluish grey sandy siltstone and sandstone, fine grained, moderate well sorted, unweathered	Cici Sandstone
21 - 22	bluish grey sandy siltstone and sandstone, fine grained, moderate well sorted, unweathered	Cici Sandstone
22 - 23	bluish grey sandy siltstone and sandstone, fine grained, moderate well sorted, unweathered	Cici Sandstone
23 - 24	reddish brown- light grey-greenish brown sandstone with some quartz veins signifying fractured bedrock	Cici Sandstone
24 - 25	reddish brown- light grey-greenish brown sandstone with some quartz veins signifying fractured bedrock	Cici Sandstone
25 - 26	reddish brown- light grey-greenish brown sandstone with some quartz veins signifying fractured bedrock	Cici Sandstone
26 - 27	reddish brown- light grey-greenish brown sandstone with some quartz veins signifying fractured bedrock	Cici Sandstone
27 - 28	reddish brown- light grey-greenish brown sandstone with some quartz veins signifying fractured bedrock	Cici Sandstone
28 - 29	reddish brown- light grey-greenish brown sandstone with some quartz veins signifying fractured bedrock	Cici Sandstone
29 - 30	reddish brown- light grey-greenish brown sandstone with some quartz veins signifying fractured bedrock	Cici Sandstone
30 - 31	reddish brown- light grey-greenish brown sandstone with some quartz veins signifying fractured bedrock	Cici Sandstone
31 - 32	reddish brown- light grey-greenish brown sandstone with some quartz veins signifying fractured bedrock	Cici Sandstone
32 - 33	reddish brown- light grey-greenish brown sandstone with some quartz veins signifying fractured bedrock	Cici Sandstone
33 - 34	reddish brown- light grey-greenish brown sandstone with some quartz veins signifying fractured bedrock	Cici Sandstone
34-35	bluish grey sandy siltstone, fine grained, moderate well sorted, unweathered	Cici Sandstone
35-36	bluish grey sandy siltstone, fine grained, moderate well sorted, unweathered	Cici Sandstone

Well 10/11 –Tubakeli, Bilalevu

Depth (m)	Lithology	Geology
0 - 1	brown to dark brown, non-plastic, fine grained and well sorted silt loam	Recent Alluvium
1 - 2	brown to dark brown, non-plastic, fine grained and well sorted silt loam	Recent Alluvium

2 - 3	brown to dark brown, non-plastic, fine grained and well sorted silt loam	Recent Alluvium
3 - 4	brown to dark brown, non-plastic, fine grained and well sorted silt loam	Recent Alluvium
4 - 5	brown to dark brown, non-plastic, fine grained and well sorted silt loam	Recent Alluvium
5 - 6	yellowish brown to orangy brown sorted silt loam with some fine sand	Recent Alluvium
6 - 7	yellowish brown to orangy brown sorted silt loam with some fine sand	Recent Alluvium
7 - 8	yellowish brown to orangy brown sorted silt loam with some fine sand	Recent Alluvium
8 - 9	yellowish brown to orangy brown sorted silt loam with some fine sand	Recent Alluvium
9 - 10	yellowish brown to orangy brown sorted silt loam with some fine sand	Recent Alluvium
10 - 11	yellowish brown to orangy brown sorted silt loam with some fine sand	Recent Alluvium
11 - 12	yellowish brown to orangy brown sorted silt loam with some fine sand	Recent Alluvium
12 - 13	yellowish brown to orangy brown sorted silt loam with some fine sand	Recent Alluvium
13 - 14	yellowish brown to orangy brown sorted silt loam with some fine sand	Recent Alluvium
14 - 15	yellowish brown to orangy brown sorted silt loam with some fine sand	Recent Alluvium
15 - 16	yellowish brown to orangy brown sorted silt loam with some fine sand	Recent Alluvium
16 - 17	grey, fine grained, well sorted siltstone with some wood or plant chips	Takaro Conglomerate/Rudite
17 - 18	grey, fine grained, well sorted siltstone with some wood or plant chips	Takaro Conglomerate/Rudite
18 - 19	bluish grey-grey, siltstone and sandstone with dacitic, andesite and tonalite clasts, unweathered	Takaro Conglomerate/Rudite
19 - 20	bluish grey-grey, siltstone and sandstone with dacitic, andesite and tonalite clasts, unweathered	Takaro Conglomerate/Rudite
20 - 21	bluish grey-grey, siltstone and sandstone with dacitic, andesite and tonalite clasts, unweathered	Takaro Conglomerate/Rudite
21 - 22	bluish grey-grey, siltstone and sandstone with dacitic, andesite and tonalite clasts, unweathered	Takaro Conglomerate/Rudite
22 - 23	bluish grey-grey, siltstone and sandstone with dacitic, andesite and tonalite clasts, unweathered	Takaro Conglomerate/Rudite
23 - 24	bluish grey-grey, siltstone and sandstone with dacitic, andesite and tonalite clasts, unweathered	Takaro Conglomerate/Rudite
24 - 25	bluish grey-grey, siltstone and sandstone with dacitic, andesite and tonalite clasts, unweathered	Takaro Conglomerate/Rudite
25 - 26	bluish grey-grey, siltstone and sandstone with dacitic, andesite and tonalite clasts, unweathered	Takaro Conglomerate/Rudite
26 - 27	bluish grey-grey, siltstone and sandstone with dacitic, andesite and tonalite clasts, unweathered	Takaro Conglomerate/Rudite
27 - 28	bluish grey-grey, siltstone and sandstone with dacitic, andesite and tonalite clasts, unweathered	Takaro Conglomerate/Rudite
28 - 29	bluish grey-grey, siltstone and sandstone with dacitic, andesite and tonalite clasts, unweathered	Takaro Conglomerate/Rudite
29 - 30	bluish grey-grey, siltstone and sandstone with dacitic, andesite and tonalite clasts, unweathered	Takaro Conglomerate/Rudite
30 - 31	bluish grey-grey, siltstone and sandstone with dacitic, andesite and tonalite clasts, unweathered	Takaro Conglomerate/Rudite
31 - 32	bluish grey-grey, siltstone and sandstone with dacitic, andesite and tonalite clasts, unweathered	Takaro Conglomerate/Rudite
32 - 33	bluish grey-grey, siltstone and sandstone with dacitic, andesite and tonalite clasts, unweathered	Takaro Conglomerate/Rudite
33 - 34	bluish grey-grey, siltstone and sandstone with dacitic, andesite and tonalite clasts, unweathered	Takaro Conglomerate/Rudite
34-35	bluish grey-grey, siltstone and sandstone with dacitic, andesite and tonalite clasts, unweathered	Takaro Conglomerate/Rudite
35-36	bluish grey-grey, siltstone and sandstone with dacitic, andesite and tonalite clasts, unweathered	Takaro Conglomerate/Rudite
36-37	bluish grey-grey, siltstone and sandstone with dacitic, andesite and tonalite clasts, unweathered	Takaro Conglomerate/Rudite
37-38	redish brown to brown sandstone with highly discoloured dacite, andesite, moderately weathered/fractured	Takaro Conglomerate/Rudite
38-39	redish brown to brown sandstone with highly discoloured dacite, andesite, moderately weathered/fractured	Takaro Conglomerate/Rudite
39-40	redish brown to brown sandstone with highly discoloured dacite, andesite, moderately weathered/fractured	Takaro Conglomerate/Rudite
40-41	bluish grey-grey, siltstone and sandstone with dacitic, andesite and tonalite clasts, fresh and unweathered	Takaro Conglomerate/Rudite

Well 10/12 – Tubakeli, Bilalevu

Depth (m)	Lithology	Geology
0 - 1	brown to dark brown, slightly sticky, non-plastic, fine grained and well sorted silt loam	Recent Alluvium
1 - 2	brown to dark brown, slightly sticky, non-plastic, fine grained and well sorted silt loam	Recent Alluvium
2 - 3	brown to dark brown, slightly sticky, non-plastic, fine grained and well sorted silt loam	Recent Alluvium
3 - 4	yellowish brown to orangy brown silt loam with some fine sand	Recent Alluvium
4 - 5	yellowish brown to orangy brown silt loam with some fine sand	Recent Alluvium
5 - 6	yellowish brown to orangy brown silt loam with some fine sand	Recent Alluvium
6 - 7	yellowish brown to orangy brown silt loam with some fine sand	Recent Alluvium
7 - 8	yellowish brown to orangy brown silt loam with some fine sand	Recent Alluvium
8 - 9	yellowish brown to orangy brown silt loam with some fine sand	Recent Alluvium
9 - 10	yellowish brown to orangy brown silt loam with some fine sand	Recent Alluvium
10 - 11	yellowish brown to orangy brown silt loam with some fine sand	Recent Alluvium
11 - 12	yellowish brown to orangy brown silt loam with some fine sand	Recent Alluvium
12 - 13	yellowish brown to orangy brown silt loam with some fine sand	Recent Alluvium
13 - 14	yellowish brown to orangy brown silt loam with some fine sand	Recent Alluvium
14 - 15	yellowish brown to orangy brown silt loam with some fine sand	Recent Alluvium
15 - 16	blish grey, siltstone and sandstone with dacitic, andesite and tonalite clasts, fresh and unweathered	Takaro Conglomerate/Rudite
16 - 17	blish grey, siltstone and sandstone with dacitic, andesite and tonalite clasts, fresh and unweathered	Takaro Conglomerate/Rudite
17 - 18	bluish grey-grey, siltstone and sandstone with dacitic, andesite and tonalite clasts, fresh and unweathered	Takaro Conglomerate/Rudite
18 - 19	bluish grey-grey, siltstone and sandstone with dacitic, andesite and tonalite clasts, fresh and unweathered	Takaro Conglomerate/Rudite
19 - 20	bluish grey-grey, siltstone and sandstone with dacitic, andesite and tonalite clasts, fresh and unweathered	Takaro Conglomerate/Rudite
20 - 21	bluish grey-grey, siltstone and sandstone with dacitic, andesite and tonalite clasts, fresh and unweathered	Takaro Conglomerate/Rudite
21 - 22	bluish grey-grey, siltstone and sandstone with dacitic, andesite and tonalite clasts, fresh and unweathered	Takaro Conglomerate/Rudite
22 - 23	bluish grey-grey, siltstone and sandstone with dacitic, andesite and tonalite clasts, fresh and unweathered	Takaro Conglomerate/Rudite
23 - 24	bluish grey-grey, siltstone and sandstone with dacitic, andesite and tonalite clasts, fresh and unweathered	Takaro Conglomerate/Rudite
24 - 25	bluish grey-grey, siltstone and sandstone with dacitic, andesite and tonalite clasts, fresh and unweathered	Takaro Conglomerate/Rudite
25 - 26	bluish grey-grey, siltstone and sandstone with dacitic, andesite and tonalite clasts, fresh and unweathered	Takaro Conglomerate/Rudite

26 - 27	bluish grey-grey, siltstone and sandstone with dacitic, andesite and tonalite clasts, fresh and unweathered	Takaro Conglomerate/Rudite
27 - 28	bluish grey-grey, siltstone and sandstone with dacitic, andesite and tonalite clasts, fresh and unweathered	Takaro Conglomerate/Rudite
28 - 29	bluish grey-grey, siltstone and sandstone with dacitic, andesite and tonalite clasts, fresh and unweathered	Takaro Conglomerate/Rudite
29 - 30	bluish grey-grey, siltstone and sandstone with dacitic, andesite and tonalite clasts, fresh and unweathered	Takaro Conglomerate/Rudite
30 - 31	bluish grey-grey, siltstone and sandstone with dacitic, andesite and tonalite clasts, fresh and unweathered	Takaro Conglomerate/Rudite
31 - 32	bluish grey-grey, siltstone and sandstone with dacitic, andesite and tonalite clasts, fresh and unweathered	Takaro Conglomerate/Rudite
32 - 33	bluish grey-grey, siltstone and sandstone with dacitic, andesite and tonalite clasts, fresh and unweathered	Takaro Conglomerate/Rudite
33 - 34	bluish grey-grey, siltstone and sandstone with dacitic, andesite and tonalite clasts, fresh and unweathered	Takaro Conglomerate/Rudite
34-35	bluish grey-grey, siltstone and sandstone with dacitic, andesite and tonalite clasts, fresh and unweathered	Takaro Conglomerate/Rudite
35-36	bluish grey-grey, siltstone and sandstone with dacitic, andesite and tonalite clasts, fresh and unweathered	Takaro Conglomerate/Rudite
36-37	redish brown to brown sandstone with highly discoloured dacite, andesite, moderately weathered/fractured	Takaro Conglomerate/Rudite
37-38	redish brown to brown sandstone with highly discoloured dacite, andesite, moderately weathered/fractured	Takaro Conglomerate/Rudite
38-39	redish brown to brown sandstone with highly discoloured dacite, andesite, moderately weathered/fractured	Takaro Conglomerate/Rudite
39-40	redish brown to brown sandstone with highly discoloured dacite, andesite, moderately weathered/fractured	Takaro Conglomerate/Rudite
40-41	redish brown to brown sandstone with highly discoloured dacite, andesite, moderately weathered/fractured	Takaro Conglomerate/Rudite
41-41	bluish grey-grey, siltstone and sandstone with dacitic, andesite and tonalite clasts, unweathered	Takaro Conglomerate/Rudite
42-43	bluish grey-grey, siltstone and sandstone with dacitic, andesite and tonalite clasts, unweathered	Takaro Conglomerate/Rudite

Well 10/13- Tubakeli, Bilalevu

Depth (m)	Lithology	Geology
0 - 1	brown to dark brown, slightly sticky, non-plastic, fine grained and well sorted silt loam	Recent Alluvium
1 - 2	brown to dark brown, slightly sticky, non-plastic, fine grained and well sorted silt loam	Recent Alluvium
2 - 3	brown to dark brown, slightly sticky, non-plastic, fine grained and well sorted silt loam	Recent Alluvium
3 - 4	yellowish brown to orangy brown silt loam with some fine sand	Recent Alluvium
4 - 5	yellowish brown to orangy brown silt loam with some fine sand	Recent Alluvium
5 - 6	yellowish brown to orangy brown silt loam with some fine sand	Recent Alluvium
6 - 7	yellowish brown to orangy brown silt loam with some fine sand	Recent Alluvium
7 - 8	yellowish brown to orangy brown silt loam with some fine sand	Recent Alluvium
8 - 9	yellowish brown to orangy brown silt loam with some fine sand	Recent Alluvium
9 - 10	yellowish brown to orangy brown silt loam with some fine sand	Recent Alluvium
10 - 11	yellowish brown to orangy brown silt loam with some fine sand	Recent Alluvium
11 - 12	yellowish brown to orangy brown silt loam with some fine sand	Recent Alluvium

12 - 13	yellowish brown to orangy brown silt loam with some fine sand	Recent Alluvium
13 - 14	bluish grey, siltstone and sandstone with dacitic, andesite and tonalite clasts, unweathered	Takaro Conglomerate/Rudite
14 - 15	bluish grey, siltstone and sandstone with dacitic, andesite and tonalite clasts, unweathered	Takaro Conglomerate/Rudite
15 - 16	bluish grey, siltstone and sandstone with dacitic, andesite and tonalite clasts, unweathered	Takaro Conglomerate/Rudite
16 - 17	bluish grey, siltstone and sandstone with dacitic, andesite and tonalite clasts, unweathered	Takaro Conglomerate/Rudite
17 - 18	bluish grey, siltstone and sandstone with dacitic, andesite and tonalite clasts, unweathered	Takaro Conglomerate/Rudite
18 - 19	bluish grey, siltstone and sandstone with dacitic, andesite and tonalite clasts, unweathered	Takaro Conglomerate/Rudite
19 - 20	bluish grey, siltstone and sandstone with dacitic, andesite and tonalite clasts, unweathered	Takaro Conglomerate/Rudite
20 - 21	highly discoloured reddish brown to yellowish brown sandstone and mudstone with dacitic and andesitic clasts	Takaro Conglomerate/Rudite
21 - 22	highly discoloured reddish brown to yellowish brown sandstone and mudstone with dacitic and andesitic clasts	Takaro Conglomerate/Rudite
22 - 23	highly discoloured reddish brown to yellowish brown sandstone and mudstone with dacitic and andesitic clasts	Takaro Conglomerate/Rudite
23 - 24	highly discoloured reddish brown to yellowish brown sandstone and mudstone with dacitic and andesitic clasts	Takaro Conglomerate/Rudite
24 - 25	bluish grey-grey, siltstone and sandstone with dacitic, andesite and tonalite clasts, unweathered	Takaro Conglomerate/Rudite
25 - 26	bluish grey-grey, siltstone and sandstone with dacitic, andesite and tonalite clasts, unweathered	Takaro Conglomerate/Rudite
26-27	bluish grey-grey, siltstone and sandstone with dacitic, andesite and tonalite clasts, unweathered	Takaro Conglomerate/Rudite
27-28	bluish grey-grey, siltstone and sandstone with dacitic, andesite and tonalite clasts, unweathered	Takaro Conglomerate/Rudite
28-29	bluish grey-grey, siltstone and sandstone with dacitic, andesite and tonalite clasts, unweathered	Takaro Conglomerate/Rudite
29-30	bluish grey-grey, siltstone and sandstone with dacitic, andesite and tonalite clasts, unweathered	Takaro Conglomerate/Rudite

Well 10/16 – Tubakeli, Bilalevu

Depth (m)	Lithology	Geology
0 - 1	brown to dark brown, slightly sticky, non-plastic, fine grained and well sorted silt loam	Recent Alluvium
1 - 2	brown to dark brown, slightly sticky, non-plastic, fine grained and well sorted silt loam	Recent Alluvium
2 - 3	brown to dark brown, slightly sticky, non-plastic, fine grained and well sorted silt loam	Recent Alluvium
3 - 4	yellowish brown to orangy brown silt loam with some fine sand	Recent Alluvium
4 - 5	yellowish brown to orangy brown silt loam with some fine sand	Recent Alluvium
5 - 6	yellowish brown to orangy brown silt loam with some fine sand	Recent Alluvium
6 - 7	yellowish brown to orangy brown silt loam with some fine sand	Recent Alluvium
7 - 8	yellowish brown to orangy brown silt loam with some fine sand	Recent Alluvium
8 - 9	yellowish brown to orangy brown silt loam with some fine sand	Recent Alluvium
9 - 10	yellowish brown to orangy brown silt loam with some fine sand	Recent Alluvium
10 - 11	yellowish brown to orangy brown silt loam with some fine sand	Recent Alluvium
11 - 12	yellowish brown to orangy brown silt loam with some fine sand	Recent Alluvium
12 - 13	yellowish brown to orangy brown silt loam with some fine sand	Recent Alluvium
13 - 14	bluish grey, siltstone and sandstone with dacitic, andesite and tonalite clasts, unweathered	Takaro Conglomerate/Rudite
14 - 15	bluish grey, siltstone and sandstone with dacitic, andesite and tonalite clasts, unweathered	Takaro Conglomerate/Rudite
15 - 16	bluish grey, siltstone and sandstone with dacitic, andesite and tonalite clasts, unweathered	Takaro Conglomerate/Rudite

16 - 17	bluish grey, siltstone and sandstone with dacitic, andesite and tonalite clasts, unweathered	Takaro Conglomerate/Rudite
17 - 18	bluish grey, siltstone and sandstone with dacitic, andesite and tonalite clasts, unweathered	Takaro Conglomerate/Rudite
18 - 19	bluish grey, siltstone and sandstone with dacitic, andesite and tonalite clasts, unweathered	Takaro Conglomerate/Rudite
19 - 20	bluish grey, siltstone and sandstone with dacitic, andesite and tonalite clasts, unweathered	Takaro Conglomerate/Rudite
20 - 21	bluish grey, siltstone and sandstone with dacitic, andesite and tonalite clasts, unweathered	Takaro Conglomerate/Rudite
21 - 22	bluish grey, siltstone and sandstone with dacitic, andesite and tonalite clasts, unweathered	Takaro Conglomerate/Rudite
22 - 23	bluish grey, siltstone and sandstone with dacitic, andesite and tonalite clasts, unweathered	Takaro Conglomerate/Rudite
23 - 24	highly discoloured reddish brown to yellowish brown sandstone and mudstone with dacitic and andesitic clasts	Takaro Conglomerate/Rudite
24 - 25	bluish grey-grey, siltstone and sandstone with dacitic, andesite and tonalite clasts, unweathered	Takaro Conglomerate/Rudite
25 - 26	bluish grey-grey, siltstone and sandstone with dacitic, andesite and tonalite clasts, unweathered	Takaro Conglomerate/Rudite
26-27	bluish grey-grey, siltstone and sandstone with dacitic, andesite and tonalite clasts, unweathered	Takaro Conglomerate/Rudite
27-28	bluish grey-grey, siltstone and sandstone with dacitic, andesite and tonalite clasts, unweathered	Takaro Conglomerate/Rudite
28-29	bluish grey-grey, siltstone and sandstone with dacitic, andesite and tonalite clasts, unweathered	Takaro Conglomerate/Rudite
29-30	bluish grey-grey, siltstone and sandstone with dacitic, andesite and tonalite clasts, unweathered	Takaro Conglomerate/Rudite

Well 10/14 – Bila Rd, Bilalevu

Depth (m)	Lithology	Geology
0 - 1	dark brown silt with some very fine sand	Recent Alluvium
1 - 2	brown silt with some very fine sand	Recent Alluvium
2 - 3	brown sandy silt with fine-medium sand, moderately sorted	Recent Alluvium
3 - 4	brown sandy silt with fine-medium sand, moderately sorted	Recent Alluvium
4 - 5	brown sandy silt with fine-medium sand, moderately sorted	Recent Alluvium
5 - 6	brown sandy silt with fine-medium sand, moderately sorted	Recent Alluvium
6 - 7	bluish grey-dark grey silty sandstone	Tari Formation
7 - 8	bluish grey-dark grey silty sandstone	Tari Formation
8 - 9	bluish grey-dark grey silty sandstone	Tari Formation
9 - 10	bluish grey-dark grey silty sandstone	Tari Formation
10 - 11	bluish grey-dark grey silty sandstone	Tari Formation
11 - 12	bluish grey-dark grey silty sandstone	Tari Formation
12 - 13	bluish grey-dark grey silty sandstone	Tari Formation
13 - 14	bluish grey-dark grey silty sandstone	Tari Formation
14 - 15	bluish grey-dark grey silty sandstone	Tari Formation
15 - 16	bluish grey-dark grey silty sandstone	Tari Formation
16 - 17	bluish grey-dark grey silty sandstone	Tari Formation
17 - 18	bluish grey-dark grey silty sandstone	Tari Formation
18 - 19	bluish grey-dark grey silty sandstone	Tari Formation
19 - 20	bluish grey-dark grey silty sandstone	Tari Formation

20 - 21	bluish grey-dark grey silty sandstone	Tari Formation
21 - 22	bluish grey-dark grey silty sandstone	Tari Formation
22 - 23	bluish grey-dark grey silty sandstone	Tari Formation
23 - 24	bluish grey-dark grey silty sandstone	Tari Formation
24 - 25	bluish grey-dark grey silty sandstone	Tari Formation
25 - 26	bluish grey-dark grey silty sandstone	Tari Formation
26 - 27	bluish grey-dark grey silty sandstone	Tari Formation
27 - 28	bluish grey-dark grey silty sandstone	Tari Formation
28 - 29	bluish grey-dark grey silty sandstone	Tari Formation
29 - 30	bluish grey-dark grey silty sandstone	Tari Formation
30 - 31	bluish grey-dark grey silty sandstone	Tari Formation
31 - 32	bluish grey-dark grey silty sandstone	Tari Formation
32 - 33	bluish grey-dark grey silty sandstone	Tari Formation
33 - 34	bluish grey-dark grey silty sandstone	Tari Formation
34-35	bluish grey-dark grey silty sandstone	Tari Formation
35-36	bluish grey sandstone with some andesite, tonalite and dacite clasts	Tari Formation
36 - 37	bluish grey sandstone with some andesite, tonalite and dacite clasts	Tari Formation
37 - 38	bluish grey sandstone with some andesite, tonalite and dacite clasts	Tari Formation
38 - 39	bluish grey sandstone with some andesite, tonalite and dacite clasts	Tari Formation
39 - 40	bluish grey sandstone with some andesite, tonalite and dacite clasts	Tari Formation
40 - 41	bluish grey sandstone with some andesite, tonalite and dacite clasts	Tari Formation
41 - 42	bluish grey sandstone with some andesite, tonalite and dacite clasts	Tari Formation
42 - 43	bluish grey sandstone with some andesite, tonalite and dacite clasts	Tari Formation
43 - 44	bluish grey sandstone with some andesite, tonalite and dacite clasts	Tari Formation
44 - 45	bluish grey sandstone with some andesite, tonalite and dacite clasts	Tari Formation
45 - 46	reddish-yellowish brown sandstone and mudstone with tonalitic and dacitic clasts	Tari Formation
46 - 47	reddish-yellowish brown sandstone and mudstone with tonalitic and dacitic clasts	Tari Formation
47 - 48	reddish-yellowish brown sandstone and mudstone with tonalitic and dacitic clasts	Tari Formation
48 - 49	reddish-yellowish brown sandstone and mudstone with tonalitic and dacitic clasts	Tari Formation
49 - 50	reddish-yellowish brown sandstone and mudstone with tonalitic and dacitic clasts	Tari Formation
50 - 51	dark grey, basaltic unit with abundant quartz amygdales	Tari Formation
51 - 52	dark grey, basaltic unit with abundant quartz amygdales	Tari Formation
52 - 53	dark grey, basaltic unit with abundant quartz amygdales	Tari Formation
53 - 54	dark grey, basaltic unit with abundant quartz amygdales	Tari Formation
54 - 55	dark grey, basaltic unit with abundant quartz amygdales	Tari Formation
55 - 56	dark grey, basaltic unit with abundant quartz amygdales	Tari Formation
56 - 57	dark grey, basaltic unit with abundant quartz amygdales	Tari Formation
57 - 58	dark grey, basaltic unit with abundant quartz amygdales	Tari Formation
58 - 59	dark grey, basaltic unit with abundant quartz amygdales	Tari Formation

59 - 60	dark grey, basaltic unit with abundant quartz amygdales	Tari Formation

Well 10/15 – Bila Rd, Bilalevu

Depth (m)	Lithology	Geology
0 - 1	dark brown silt with some very fine sand	Recent Alluvium
1 - 2	brown silt with some very fine sand	Recent Alluvium
2 - 3	brown sandy silt	Recent Alluvium
3 - 4	brown sandy silt	Recent Alluvium
4 - 5	brown sandy silt	Recent Alluvium
5 - 6	brown sandy silt	Recent Alluvium
6 - 7	brown sandy silt	Recent Alluvium
7 - 8	brown sandy silt	Recent Alluvium
8 - 9	brown sandy silt	Recent Alluvium
9 - 10	brown sandy silt	Recent Alluvium
10 - 11	brown silty sand with some medium pebbles	Recent Alluvium
11 - 12	uncondolidated sandy gravels, fine-coarse sub-rounded to sub-angular dacitic, andesitic, tonalitic pebbles	Recent Alluvium
12 - 13	uncondolidated sandy gravels, fine-coarse sub-rounded to sub-angular dacitic, andesitic, tonalitic pebbles	Recent Alluvium
13 - 14	uncondolidated sandy gravels, fine-coarse sub-rounded to sub-angular dacitic, andesitic, tonalitic pebbles	Recent Alluvium
14 - 15	uncondolidated sandy gravels, fine-coarse sub-rounded to sub-angular dacitic, andesitic, tonalitic pebbles	Recent Alluvium
15 - 16	uncondolidated sandy gravels, fine-coarse sub-rounded to sub-angular dacitic, andesitic, tonalitic pebbles	Recent Alluvium
16 - 17	uncondolidated sandy gravels, fine-coarse sub-rounded to sub-angular dacitic, andesitic, tonalitic pebbles	Recent Alluvium
17 - 18	yellowish brown to light brown silty sand, moderately well sorted	Tari Formation
18 - 19	bluish grey-dark grey silty sandstone	Tari Formation
19 - 20	bluish grey-dark grey silty sandstone	Tari Formation
20 - 21	bluish grey-dark grey silty sandstone	Tari Formation
21 - 22	bluish grey-dark grey silty sandstone	Tari Formation
22 - 23	bluish grey-dark grey silty sandstone	Tari Formation
23 - 24	bluish grey-dark grey silty sandstone	Tari Formation
24 - 25	bluish grey-dark grey silty sandstone	Tari Formation
25 - 26	bluish grey-dark grey silty sandstone	Tari Formation
26 - 27	bluish grey-dark grey silty sandstone	Tari Formation
27 - 28	bluish grey-dark grey silty sandstone	Tari Formation
28 - 29	bluish grey-dark grey silty sandstone	Tari Formation
29 - 30	bluish grey-dark grey silty sandstone	Tari Formation
30 - 31	bluish grey-dark grey silty sandstone	Tari Formation
31 - 32	bluish grey-dark grey silty sandstone	Tari Formation
32 - 33	bluish grey-dark grey silty sandstone	Tari Formation
33 - 34	bluish grey-dark grey silty sandstone	Tari Formation
34-35	bluish grey-dark grey silty sandstone	Tari Formation

Appendix G: Pump-test Data

Evaluation of groundwater via pumping test was conducted on 6 of the 9 drilled wells. Well 10/10 and 10/11 were monitored full time for drawdown and recovery analysis due to the difficulty of monitoring pumping wells 10/07 and 10/12, respectively due to the vibration of of the mono-pump column pipes inside the borehole and thus, preventing the free insertion and retrieval of depth probes during the test. Well 10/07 was monitored when 10/08 was pumped; well 10/12 was monitored when well 10/13 was pumped; well 10/15 was monitored when well 10/14 was pumped. Well 10/15, due to no observed drawdown at well 10/14, was conducted as single well test. The estimation of aquifer properties were estimated using Theiss match curve and Cooper-Jacob methods mainly because these wells were penetrating confining aquifers and exhibited non-equilibrium flow conditions. Please note that the average aquifer thickness between the pumping well and observation well is used to calculate K or hydraulic conductivity.

1. Theiss match curve where matchpoint is found at 1/u = 1 and W(u) = 1
    a. $T = Q/(4 \times 22/7 \times d)$
    Where T is transmissivity (m^2/day)
    Q is discharge (L/day)
    d is drawdown in (m) at matchpoint

    b. $S = (4 \times T \times t)/r^2$
    Where S is storativity (dimensionless)
    T is transmissivity (m^2/day)
    t is time at matchpoint (min/1440)
    r is distance from pumping well (m)

    c. $K = T \times b$
    Where K = hydraulic conductivity (m/day)
    T is transmissivity (m^2/day)
    b is thickness of the aquifer

2. Copper-Jacob straight line methods
    a. $T = (2.3 \times Q)/(4 \times 22/7 \times \Delta s)$
    Where T is transmissivity (m^2/day)
    Q is discharge (L/day)
    Δs is change in storage in a log cycle (m)
    b. $K = T \times b$
    Where K = hydraulic conductivity (m/day)
    T is transmissivity (m^2/day)
    b is thickness of the aquifer

Well 10/08 - Dubalevu

Time (min)	DTW (m)	Drawdown	Initial DTW (m):	7.78	
0	7.780	0.000	Distance from Pumping well (m):	0	
1	10.410	2.630	Discharge (L/s)	0.57	
2	11.650	3.870	Discharge (m^3/day)	49.25	
3	12.120	4.340	Thickness of Aquifer	5	
4	12.700	4.920			
5	13.190	5.410	s1	5	
6	13.630	5.850	s2	7.9	
7	13.950	6.170			
8	14.300	6.520			
9	14.650	6.870			
10	15.010	7.230		**Drawdown**	**Recovery**
12	15.560	7.780	**T (m^2/day)**	1.89	1.141
14	16.060	8.280	**K (m/day)**	0.36	0.23
16	16.560	8.780			
18	16.960	9.180			
20	17.330	9.550			
25	18.080	10.300			
30	18.490	10.710			
35	18.590	10.810			
40	18.730	10.950			
50	19.050	11.270			
60	19.250	11.470			
70	19.400	11.620			
80	19.450	11.670			
100	19.710	11.930			
120	19.620	11.840			
145	19.980	12.200			
160	20.380	12.600			
175	19.980	12.200			
189	20.420	12.640			
200	21.550	13.770			
257	22.075	14.295			
300	21.840	14.060			
304	22.060	14.280			
315	22.540	14.760			
337	21.720	13.940			
341	21.670	13.890			
350	21.540	13.760			
354	21.600	13.820			
387	22.540	14.760			
401	22.610	14.830			
442	23.030	15.250			
454	23.280	15.500			
496	23.250	15.470			
512	23.270	15.490			
562	23.600	15.820			
575	23.750	15.970			

Table 1: Drawdown analysis at well 10/08, Dubalevu

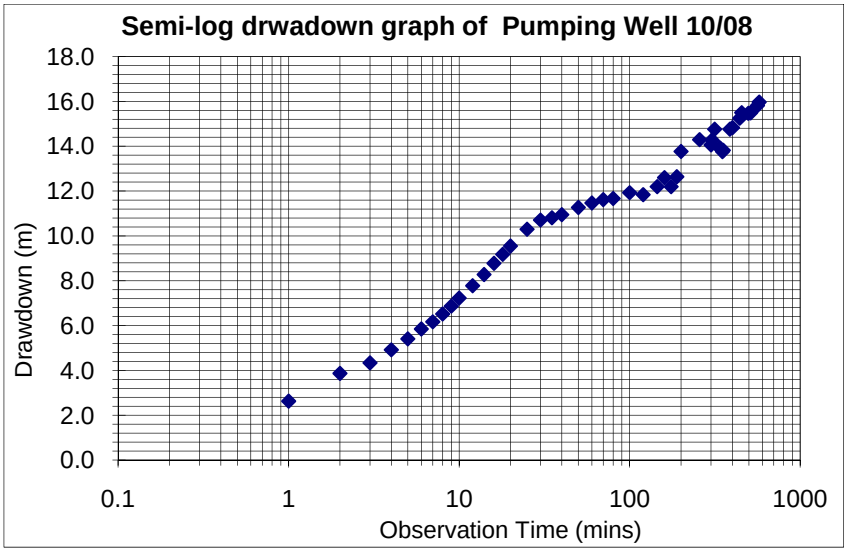

Figure 1: Drawdown graph for well 10/08

Time (minutes)	DTW (m)	Recovery (m)	t/t"	Residual Drawdown
0	23.600	15.820		
3	18.000	10.220	191.67	10.220
3.5	17.270	9.490	164.29	9.49
5.5	16.220	8.440	104.55	8.44
8.6	15.400	7.620	66.86	7.62
9	14.920	7.140	63.89	7.14
10	14.520	6.740	57.50	6.74
11	14.050	6.270	52.27	6.27
12	13.670	5.890	47.92	5.89
13	13.320	5.540	44.23	5.54
14	13.010	5.230	41.07	5.23
15	12.705	4.925	38.33	4.925
17	12.280	4.500	33.82	4.5
19	11.330	3.550	30.26	3.55
21	11.210	3.430	27.38	3.43
23	11.090	3.310	25.00	3.31
25	10.760	2.980	23.00	2.98
35	9.650	1.870	16.43	1.87
40	9.240	1.460	14.38	1.46
45	9.050	1.270	12.78	1.27
65	8.160	0.380	8.85	0.38
85	8.070	0.290	6.76	0.29
115	8.030	0.250	5.00	0.25
155	8.020	0.240	3.71	0.24
188	8.010	0.230	3.06	0.23
725	7.790	0.010	0.79	0.01

Table 2: Recovery analysis data of well 10/08

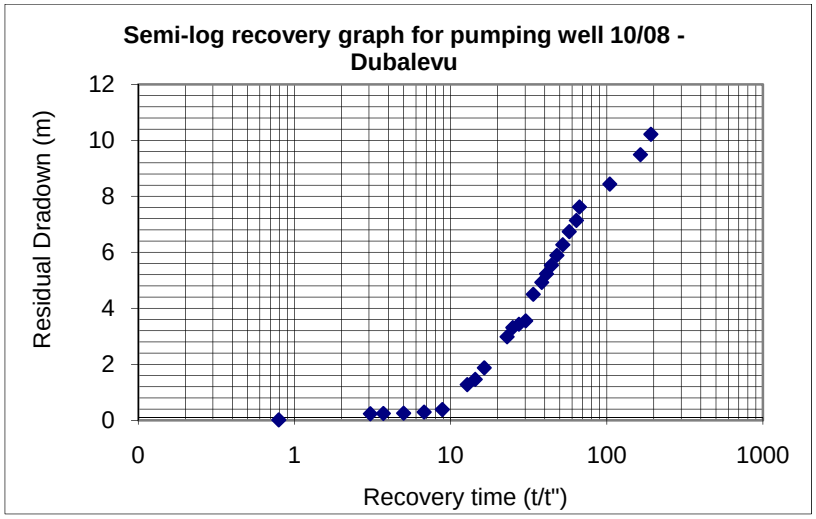

Figure 2: residual drawdown curve for well 10/08

Time (min)	DTW (m)	Drawdown	Distance to pumping well	81.2
0	7.330	0.000	d at match point (m)	0.75
73	7.480	0.150	t_0 at match point (min)	190 minutes
153	7.670	0.340	Q	49.25
195	7.735	0.405	Aquifer thickness	5
266	7.830	0.500		
312	7.880	0.550		
347	7.910	0.580	**T (m^2/day)**	5.22
396	7.960	0.630	**S**	0.0004
451	8.000	0.670	**K (m/day)**	1.04
507	8.050	0.720		
573	8.080	0.750		

Table 3: well 10/07 observation well during pumping of well 10/08

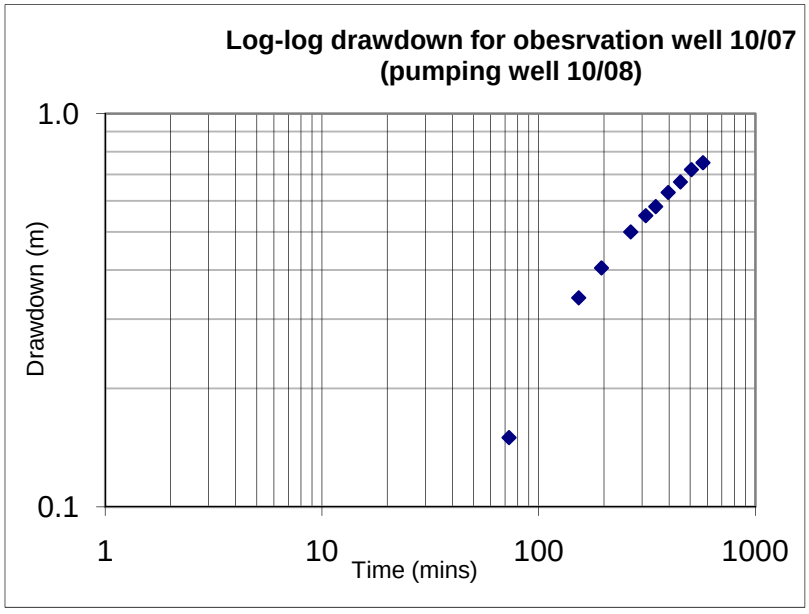

Figure 3: drawdown at observaton well 10/07

Well 10/10 – Dubalevu

Please note that well 10/10 was monitored full time for drawdown and recovery due vibration of column pipes in pumping well 10/07 and hence, preventing the measurement of instantaneous drawdown.

Time (min)	DTW (m)	Drawdown	Initial DTW (m):	0.66
1	0.750	0.0900	Distance from Pumping well (m):	43.8
2	0.840	0.1800	Q (L/s)	10.63
3	1.030	0.3700	Q (m^3/day)	918.432
4	1.260	0.6000	Thickness of Aquifer	10.5
5	1.450	0.7900	Duration of pumping (mins)	1140
6	1.610	0.9500	t_0 at match point (min)	6.85
7	1.790	1.1300	d at match point (m)	2.5
8	1.960	1.3000		
9	2.090	1.4300		
10	2.230	1.5700	t_0 (min/day)	0.013194
12	2.520	1.8600	d	8.9
14	2.740	2.0800	**T (m^2/day)**	8.208662
16	2.950	2.2900	**K (m/day)**	0.781777
18	3.280	2.6200	**S**	0.000226
20	3.330	2.6700		
25	3.840	3.1800		
30	4.100	3.4400		
35	4.350	3.6900		
40	4.590	3.9300		
50	5.350	4.6900		
60	5.560	4.9000		
70	5.970	5.3100		
80	6.360	5.7000		
101	7.060	6.4000		
121	7.650	6.9900		
140	8.230	7.5700		
160	8.650	7.9900		
180	9.070	8.4100		
200	9.270	8.6100		
230	9.700	9.0400		
260	10.220	9.5600		
290	10.460	9.8000		
320	10.830	10.1700		
350	11.040	10.3800		
380	11.330	10.6700		
420	11.620	10.9600		
460	11.790	11.1300		
500	11.890	11.2300		
540	12.380	11.7200		
600	12.490	11.8300		
660	12.780	12.1200		
720	12.920	12.260		
780	13.020	12.360		
840	13.060	12.400		
900	13.160	12.5000		
960	13.350	12.6900		
1020	13.440	12.7800		
1080	13.520	12.8600		
1140	13.630	12.9700		

Table 4: drawdown response on observation well 10/10 during the pumping of well 10/07

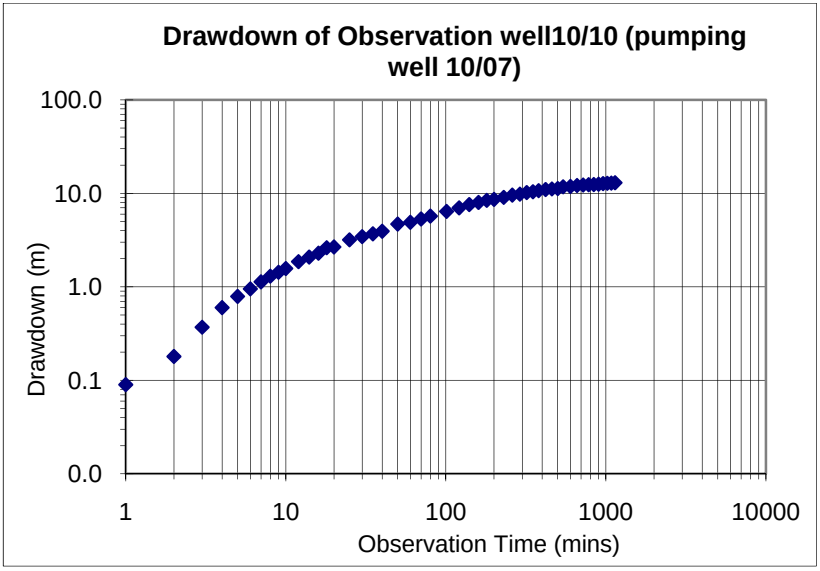

Figure 4: drawdown curve at observation well 10/10 during the pumping of well 10/07

T (min)	DTW (m)	Recovery (m)	t/t"	Residual Drawdown	Initial DTW (m):	0.66
1	13.520	12.860	1140.00	12.860	Distance from Pumping well (m):	43.8
2	13.240	12.580	570.00	12.580	Discharge	918.432
3	13.010	12.350	380.00	12.350	Thickness of Aquifer	10.5
4	12.740	12.080	285.00	12.080	Duration of pumping (min)	1140
5	12.350	11.690	228.00	11.690	d at match point (m)	7
6	11.890	11.230	190.00	11.230	t_0 at match point (min)	9.5
7	11.600	10.940	162.86	10.940		
8	11.350	10.690	142.50	10.690	d (m)	7
9	11.200	10.540	126.67	10.540	t_0 (min/day)	0.007
10	11.010	10.350	114.00	10.350	**T (m^2/day)**	29.2
12	10.680	10.020	95.00	10.020	**K (m/day)**	2.8
14	10.370	9.710	81.43	9.710	**S**	0.0004
16	10.100	9.440	71.25	9.440		
18	9.770	9.110	63.33	9.110		
20	9.580	8.920	57.00	8.920		
25	9.090	8.430	45.60	8.430		
30	8.580	7.920	38.00	7.920		
35	8.240	7.580	32.57	7.580		
40	7.890	7.230	28.50	7.230		
50	7.210	6.550	22.80	6.550		
60	6.720	6.060	19.00	6.060		
70	6.250	5.590	16.29	5.590		
80	5.940	5.280	14.25	5.280		
100	5.320	4.660	11.40	4.660		
120	4.800	4.140	9.50	4.140		
140	4.400	3.740	8.14	3.740		
160	4.130	3.470	7.13	3.470		
190	3.640	2.980	6.00	2.980		
220	3.390	2.730	5.18	2.730		
250	3.150	2.490	4.56	2.490		
280	2.950	2.290	4.07	2.290		
320	2.630	1.970	3.56	1.970		
360	2.480	1.820	3.17	1.820		

Table 5: residual drawdown response on observation well 10/10 during the cessation of pumping at well 10/07

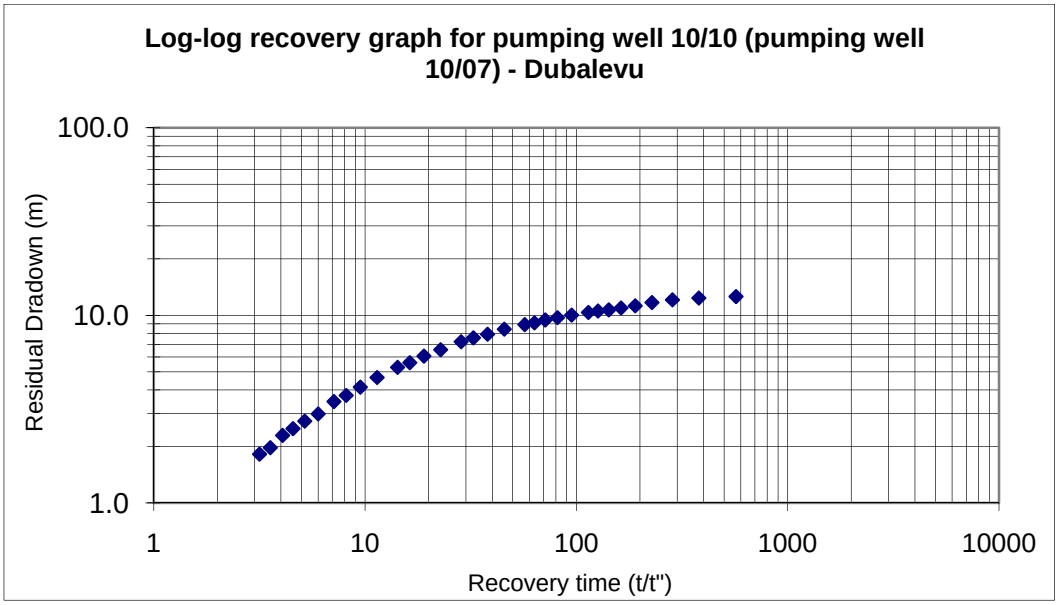

Figure 5: residual drawdown plot of well 10/10

Well 10/13, Tubakeli, Bilalevu

Time (min)	DTW (m)	Drawdown	Initial DTW (m):	8.465
0	8.465	0.000	Distance from Pumping well (m):	0
1	9.960	1.495	Discharge (L/s)	0.92
2	11.010	2.545	Thickness of Aquifer	3
3	11.560	3.095	Q (m3/day)	79.488
4	11.950	3.485	S	1.4
5	12.100	3.635	T (m2/day)	10.38764
6	12.200	3.735	K	3.462545
7	12.300	3.835		
8	12.370	3.905		
9	12.480	4.015		
10	12.550	4.085		
12	12.700	4.235		
14	12.780	4.315		
16	12.880	4.415		
18	12.950	4.485		
20	13.010	4.545		
27	13.210	4.745		
30	13.280	4.815		
35	13.350	4.885		
40	13.420	4.955		
50	13.560	5.095		
60	13.680	5.215		
70	13.760	5.295		
80	13.850	5.385		
90	13.890	5.425		
100	13.970	5.505		
120	14.030	5.565		
140	14.100	5.635		
160	14.210	5.745		
180	14.280	5.815		
200	14.370	5.905		
220	14.410	5.945		
240	14.470	6.005		
260	14.500	6.035		
280	14.530	6.065		
300	14.600	6.135		

330	14.620	6.155		
360	14.730	6.265		
390	14.745	6.280		
420	14.770	6.305		
450	14.840	6.375		
480	14.870	6.405		
510	14.900	6.435		
540	14.930	6.465		
570	14.950	6.485		
600	14.980	6.515		
630	15.000	6.535		
660	15.010	6.545		
690	15.010	6.545		
720	15.010	6.545		
750	15.010	6.545		
780	15.010	6.545		
810	15.010	6.545		
840	15.010	6.545		
870	15.010	6.545		
600	15.010	6.545		
960	15.010	6.545		

Table 6: drawdown data of well 10/13 constant rate test

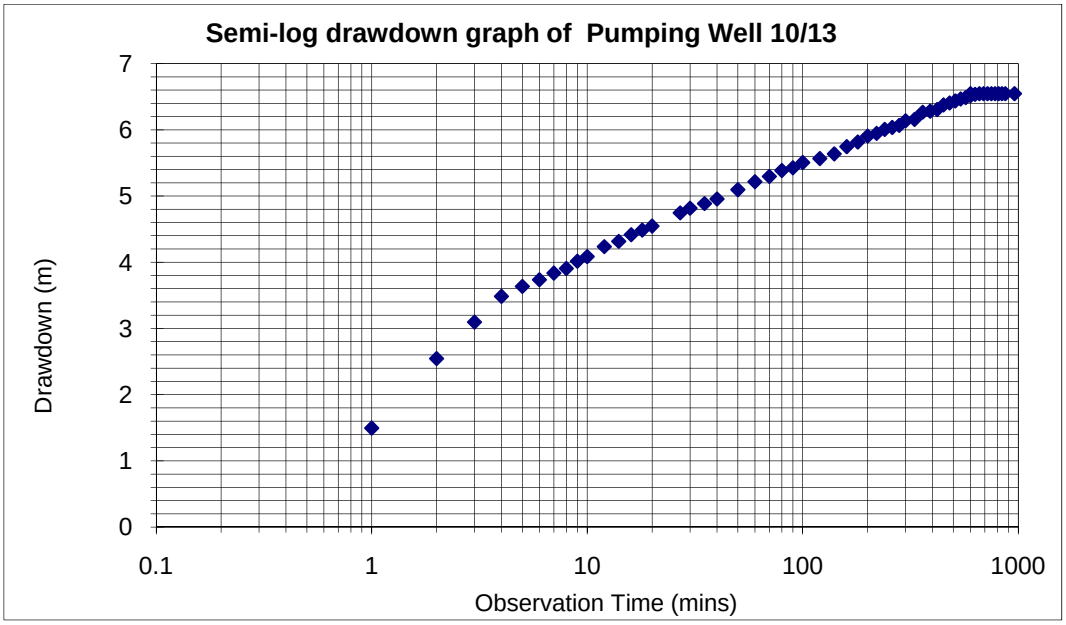

Figure 6: drawdown graph of well 10/13

T(minutes)	DTW (m)	Recovery (m)	t/t''	Residual Darwdown	Initial DTW (m):	8.465
0	15.010	6.545			Aquifer thickness (m):	3
0.5	14.500	6.035	1920.00	6.035	Q (l/s)	0.9
1	13.100	4.635	960.00	4.635	Q (m3/day)	77.76
2	11.940	3.475	480.00	3.475	Test Duration (mins)	960
3	11.500	3.035	320.00	3.035	s'	1.2
4	11.260	2.795	240.00	2.795		
5	11.100	2.635	192.00	2.635		
6	11.010	2.545	160.00	2.545	**T (m^2/day))**	11.85545
7	10.920	2.455	137.14	2.455	**K (m/day)**	3.951818
8	10.850	2.385	120.00	2.385		

9	10.780	2.315	106.67	2.315		
10	10.750	2.285	96.00	2.285		
12	10.680	2.215	80.00	2.215		
14	10.600	2.135	68.57	2.135		
16	10.550	2.085	60.00	2.085		
18	10.510	2.045	53.33	2.045		
20	10.460	1.995	48.00	1.995		
25	10.360	1.895	38.40	1.895		
30	10.270	1.805	32.00	1.805		
40	10.180	1.715	24.00	1.715		
50	10.145	1.680	19.20	1.68		
60	10.060	1.595	16.00	1.595		
70	9.880	1.415	13.71	1.415		
80	9.840	1.375	12.00	1.375		
100	9.760	1.295	9.60	1.295		
120	9.630	1.165	8.00	1.165		
150	9.510	1.045	6.40	1.045		

Table 7: residual drawdown data of well 10/13 constant rate test

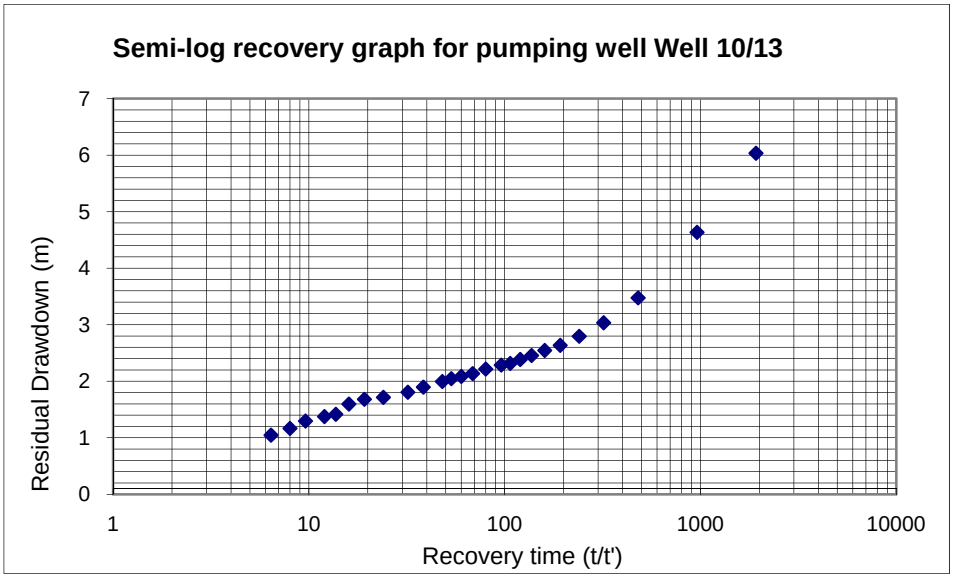

Figure 7: recovery graph of well 10/13

Time (min)	DTW (m)	Drawdown	Initial DTW (m):	6
2	6.000	0.000	Q (L/s)	0.92
200	6.025	0.025	Q (m3/day)	79.488
235	6.060	0.060	Distance from Pumping well (m):	165
290	6.095	0.095	d at match point (m)	0.29
320	6.121	0.121	t_0 at match point (min)	400
365	6.141	0.141		
425	6.150	0.150	d	0.29
500	6.157	0.157	t	0.277778
550	6.162	0.162	**T (theiss method) m^2 /day**	21.80313
600	6.169	0.169	**K m/day**	5.450784
650	6.178	0.178	**S**	0.00089

700	6.185	0.185		
750	6.193	0.193		
801	6.200	0.200		
855	6.200	0.200		
924	6.200	0.200		

Table 8: drawdown at observation well 10/12 during constant-rate pumping of well 10/13

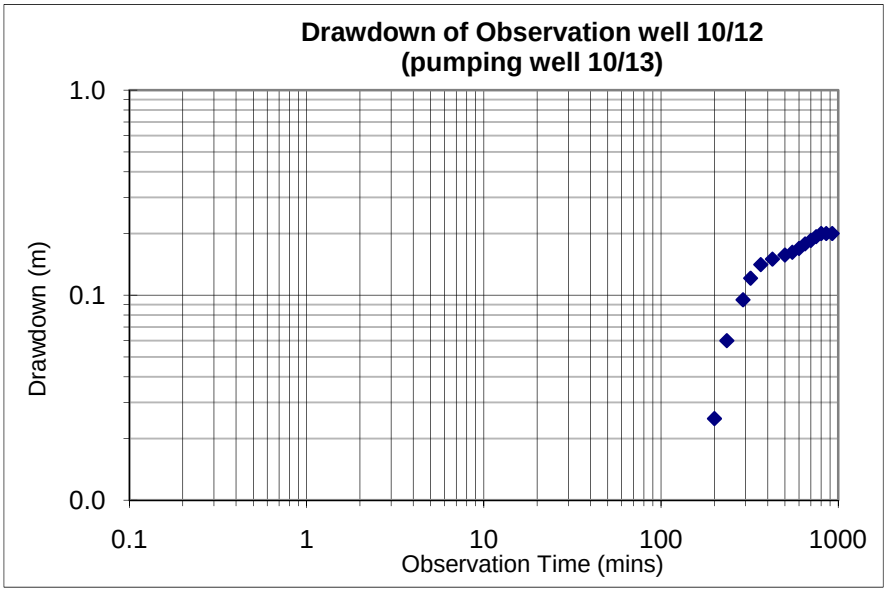

Figure 8: drawdown at observation well 10/12 during the constant-rate pumping of well 10/13

WELL 10/11, Tubakeli, Bilalevu

This well was monitored full time for drawdown and recovery due vibration of column pipes in pumping well 10/12 and hence, preventing the measurement of instantaneous drawdown.

Time (min)	DTW (m)	Drawdown	Initial DTW (m):	7.83
1	7.830	0.0000	Distance from Pumping well (m):	117
2	7.830	0.0000	Discharge	437.184
3	7.830	0.0000	Thickness of Aquifer	4.5
4	7.830	0.0000	Duration of pumping (mins)	1320
8	7.830	0.0000	d at match point (m)	0.65
9	7.830	0.0000	t at match point (min)	61
10	7.830	0.0000		
12	7.830	0.0000	d (m)	0.65
14	7.843	0.0130	t (min/day)	0.04
16	7.830	0.0000		
18	7.840	0.0100	**T (m^2/day)**	**53.50154**
20	7.850	0.0200	**S**	**0.000673**
25	7.853	0.0230	**K m/day**	**11.88923**
30	7.862	0.0320		
35	7.881	0.0510		
40	7.894	0.0640		
50	7.921	0.0910		

65	7.975	0.1450		
70	7.994	0.1640		
80	8.031	0.2010		
90	8.072	0.2420		
100	8.107	0.2770		
120	8.182	0.3520		
140	8.265	0.4350		
160	8.341	0.5110		
180	8.415	0.5850		
200	8.482	0.6520		
230	8.575	0.7450		
260	8.673	0.8430		
290	8.752	0.9220		
320	8.833	1.0030		
350	8.910	1.0800		
380	8.985	1.1550		
437	9.118	1.2880		
460	9.175	1.3450		
500	9.250	1.4200		
540	9.300	1.4700		
580	9.360	1.5300		
620	9.434	1.6040		
660	9.510	1.6800		
720	9.560	1.730		
780	9.630	1.800		
840	9.692	1.862		
900	9.740	1.910		
960	9.800	1.970		
1020	9.850	2.020		
1080	9.890	2.060		
1140	9.960	2.130		
1200	9.990	2.160		
1260	10.020	2.190		
1320	10.100	2.270		

Table 9: drawdwon at observation wel 10/11 during constant-rate pumping of well 10/12

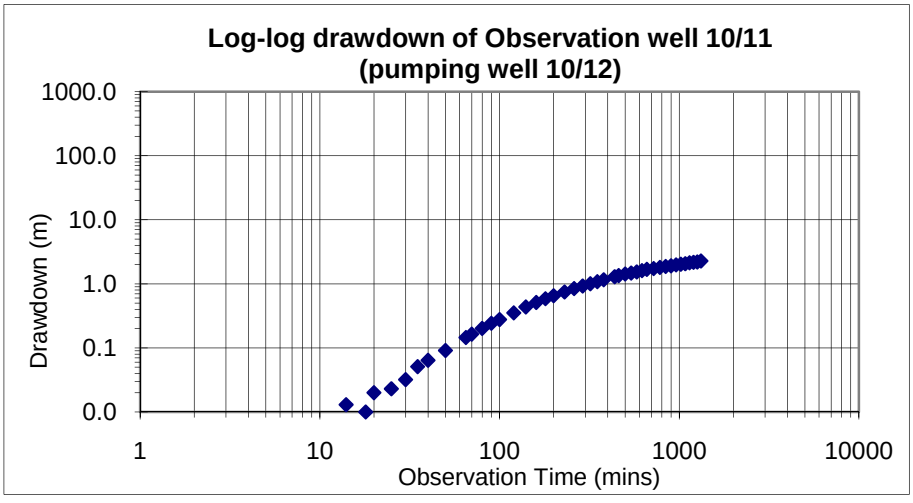

Figure 9: drawdown of observation well 10/11 during constant-rate pumping of well 10/12

T (mins)	DTW (m)	Recovery (m)	t/t''	Residual Drawdown	Initial DTW (m):	7.83
1	10.102	2.272	1320.0	2.272	Distance from Pumping well (m):	117
2	10.103	2.273	660.0	2.273	Q (L/s)	5.06
3	10.103	2.273	440.0	2.273		
4	10.103	2.273	330.0	2.273	Q (m/day)	437.2
5	10.103	2.273	264.0	2.273	Thickness of Aquifer	27.9
6	10.103	2.273	220.0	2.273	Duration of pumping (mins)	1320
7	10.103	2.273	188.6	2.273	d at match point (m)	1.8
8	10.102	2.272	165.0	2.272	t at matchpoint (mins)	2.2
9	10.101	2.271	146.7	2.271		
10	10.101	2.271	132.0	2.271	**T (m^2/day)**	19.32
12	10.099	2.269	110.0	2.269	**S**	8.6×10^{-6}
14	10.097	2.267	94.29	2.267	**K m/day**	4.33
16	10.095	2.265	82.50	2.265		
18	10.093	2.263	73.33	2.263		
20	10.091	2.261	66.00	2.261		
25	10.086	2.256	52.80	2.256		
30	10.075	2.245	44.00	2.245		
35	10.068	2.238	37.71	2.238		
40	10.059	2.229	33.00	2.229		
47	10.045	2.215	28.09	2.215		
50	10.036	2.206	26.40	2.206		
60	10.003	2.173	22.00	2.173		
70	9.977	2.147	18.86	2.147		
80	9.934	2.104	16.50	2.104		
90	9.902	2.072	14.67	2.072		
100	9.871	2.041	13.20	2.041		
120	9.810	1.980	11.00	1.980		
140	9.740	1.910	9.43	1.910		
160	9.670	1.840	8.25	1.840		
180	9.538	1.708	7.33	1.708		
200	9.474	1.644	6.60	1.644		
230	9.445	1.615	5.74	1.615		
260	9.355	1.525	5.08	1.525		
290	9.273	1.443	4.55	1.443		
300	9.247	1.417	4.40	1.417		
420	8.943	1.113	3.14	1.113		
540	8.690	0.860	2.44	0.86		
620	8.500	0.670	2.13	0.67		
790	8.260	0.430	1.67	0.43		
1042	8.000	0.170	1.27	0.17		
1102	7.940	0.110	1.20	0.11		
1162	7.850	0.020	1.14	0.02		

Table 10: residual drawdwon at observation wel 10/11 after constant-rate pumping of well 10/12

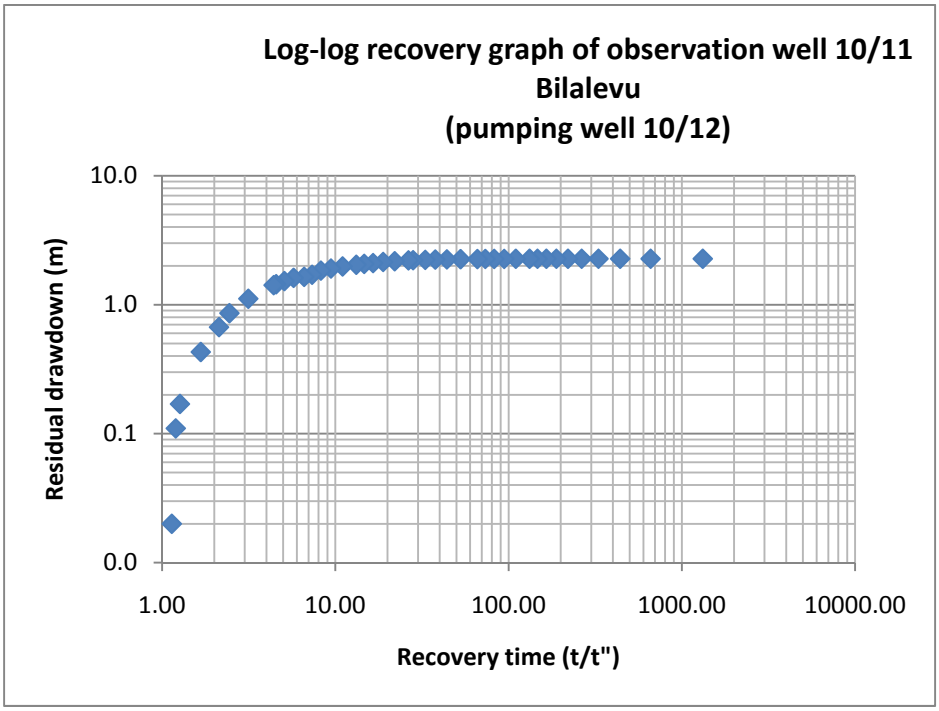

Figure 10: plot of residual drawdwon at observation wel 10/11 after constant-rate pumping of well 10/12

WELL 10/14, Bila Rd, Bilalevu

Time (min)	DTW (m)	Drawdown	Initial DTW (m):	9.89
1	10.530	0.640	Discharge (L/s)	1.4
2	10.760	0.870	Thickness of Aquifer	5
3	11.230	1.340	Duration of pumping (mins)	1230
4	11.570	1.680	Discharge (m3/day)	120.96
5	11.880	1.990	s	0.95
6	11.890	2.000	T (m²/day)	23.29493
7	11.910	2.020	K (m/day)	4.658986
8	11.910	2.020		
9	11.920	2.030		
10	11.925	2.035		
12	11.930	2.040		
14	11.935	2.045		
16	11.940	2.050		
18	11.940	2.050		
20	11.950	2.060		
25	11.980	2.090		
30	12.210	2.320		
35	12.360	2.470		
40	12.390	2.500		
50	12.450	2.560		
65	12.495	2.605		
70	12.530	2.640		
80	12.610	2.720		
90	12.635	2.745		
100	12.680	2.790		
120	12.730	2.840		
140	12.860	2.970		
148	12.905	3.015		
180	12.930	3.040		

202	12.970	3.080		
230	13.000	3.110		
280	13.010	3.120		
310	13.030	3.140		
340	13.112	3.222		
360	13.170	3.280		
390	13.210	3.320		
420	13.240	3.350		
450	13.310	3.420		
480	13.320	3.430		
540	13.370	3.480		
600	13.460	3.570		
660	13.500	3.610		
720	13.510	3.620		
780	13.550	3.660		
840	13.590	3.700		
900	13.615	3.725		
960	13.660	3.770		
1020	13.680	3.790		
1088	13.700	3.810		
1140	13.745	3.855		
1200	13.763	3.873		
1230	13.768	3.878		

Table 11: drawdown data of well 10/14 constant rate test

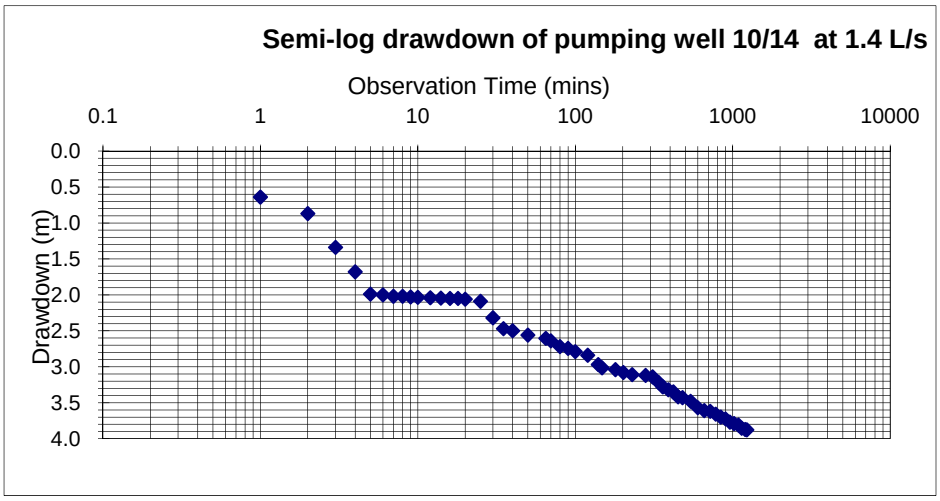

Figure 11: drawdown plot of well 10/14 constant-rate pumping

T (min)	DTW (m)	Recovery (m)	t/t"	Residual Drawdown	Initial DTW (m):	9.89
1	13.150	3.260	1230	3.260	Distance from Pumping well (m):	0
2	12.520	2.630	615	2.630	Discharge	1.4
3	11.725	1.835	410	1.835	Thickness of Aquifer	5
4	11.795	1.905	307.5	1.905	Duration of pumping (mins)	1230
5	11.690	1.800	246.00	1.800	Discharge (m3/day)	120.96
6	11.665	1.775	205.00	1.775	s'	0.4
7	11.643	1.753	175.71	1.753	T (m^2/day)	55.3
8	11.630	1.740	153.75	1.740	K (m/day)	11.1
9	11.608	1.718	136.67	1.718		
10	11.595	1.705	123.00	1.705		
12	11.565	1.675	102.50	1.675		
14	11.545	1.655	87.86	1.655		
16	11.523	1.633	76.88	1.633		
18	11.512	1.622	68.33	1.622		

20	11.497	1.607	61.50	1.607		
25	11.450	1.560	49.20	1.560		
30	11.417	1.527	41.00	1.527		
37	11.375	1.485	33.24	1.485		
42	11.355	1.465	29.29	1.465		
46	11.335	1.445	26.74	1.445		
52	11.310	1.420	23.65	1.420		
60	11.275	1.385	20.50	1.385		
70	11.242	1.352	17.57	1.352		
81	11.205	1.315	15.19	1.315		
90	11.180	1.290	13.67	1.290		
105	11.138	1.248	11.71	1.248		
120	11.100	1.210	10.25	1.210		
144	11.048	1.158	8.54	1.158		
160	11.018	1.128	7.69	1.128		
200	10.960	1.070	6.15	1.070		
360	10.670	0.780	3.42	0.780		
690	10.490	0.600	1.78	0.600		
900	10.270	0.380	1.37	0.380		
1200	10.120	0.230	1.03	0.230		

Table 12: recovery data at well 10/14

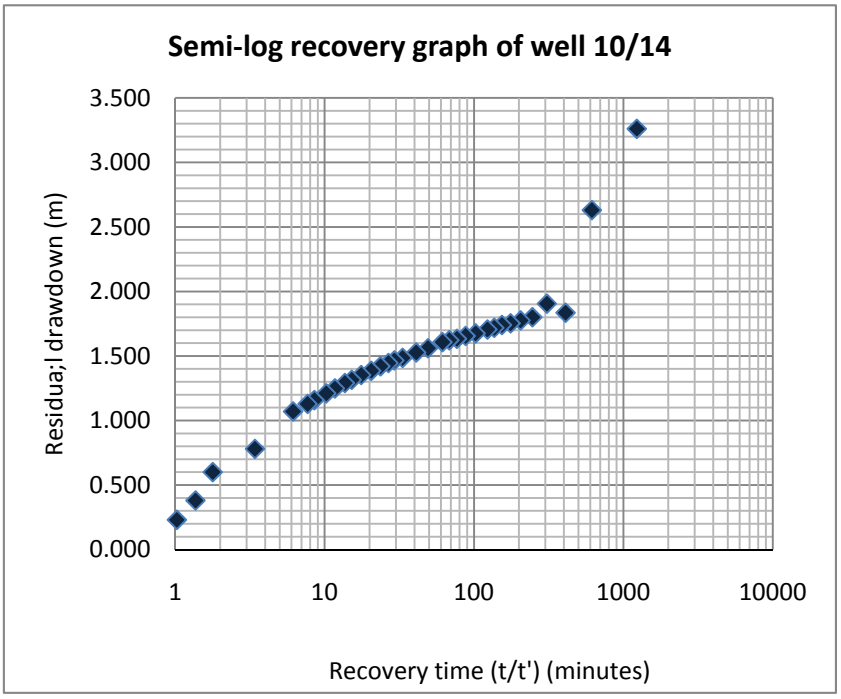

Figure 12: residual drawdown plot of well 10/14 constant-rate pumping

Time (min)	DTW (m)	Drawdown	Initial DTW (m):	9.87
1	9.870	0.0000	Distance from Pumping well (m):	122
2	9.870	0.0000	Discharge (L/s)	1.4
3	9.870	0.0000	Discharge (m^3/day)	
4	9.870	0.0000		
5	9.870	0.0000	Thickness of Aquifer	5.5
6	9.870	0.0000	Duration of pumping (mins)	1230
7	9.870	0.0000	d at match point (m)	0.13
8	9.870	0.0000	t_0 at match point	0.083333
9	9.870	0.0000	**T Theiss method (m2/day)**	74.01399
10	9.870	0.0000	**K (m/day)**	13.45709
12	9.880	0.0100	**S**	0.001658
14	9.880	0.0100		

16	9.880	0.0100		
18	9.880	0.0100		
20	9.880	0.0100		
25	9.900	0.0300		
30	9.920	0.0500		
35	9.930	0.0600		
40	9.930	0.0600		
50	9.930	0.0600		
65	9.930	0.0600		
70	9.930	0.0600		
80	9.930	0.0600		
90	9.930	0.0600		
100	9.935	0.0650		
120	9.940	0.0700		
140	9.940	0.0700		
148	9.940	0.0700		
180	9.940	0.0700		
202	9.940	0.0700		
230	9.950	0.0800		
280	9.950	0.0800		
310	9.960	0.0900		
340	9.960	0.0900		
360	9.970	0.1000		
390	9.970	0.1000		
420	9.970	0.1000		
450	9.970	0.1000		
480	9.970	0.1000		
540	9.970	0.1000		
600	9.980	0.1100		
660	9.990	0.1200		
720	9.990	0.1200		
780	9.990	0.1200		
840	9.990	0.1200		
900	10.000	0.1300		
960	10.000	0.1300		
1020	10.000	0.1300		
1088	10.000	0.1300		
1140	10.000	0.1300		
1209	10.005	0.1350		
1230	10.010	0.140		

Table 13: drawdown at observation well 10/15 during constant-rate pumping of well 10/14

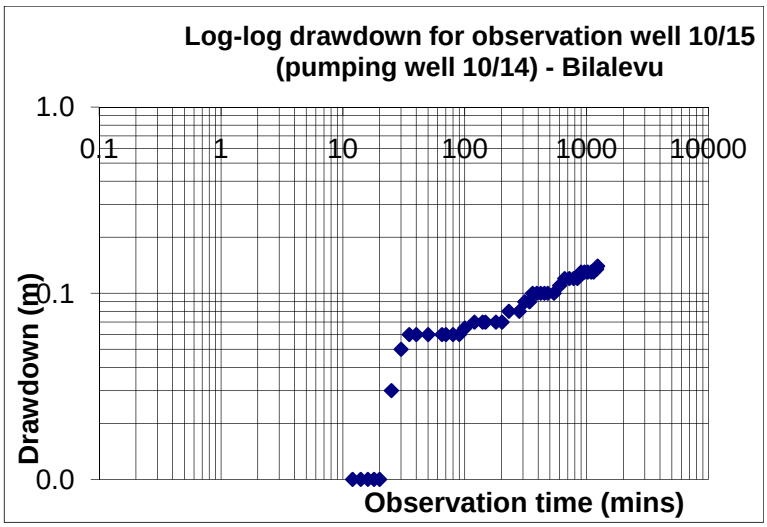

Figure 13: drawdown at observation well 10/15 during constant-rate pumping of well 10/14

WELL 10/15, Bila Rd, Bilalevu

Time (min)	DTW (m)	Drawdown	Initial DTW (m):	10.02
2	10.460	0.440	Discharge	1.85
4	10.470	0.450	Thickness of Aquifer	6
12	10.470	0.450	Depth of suction (m bgl)	30
14	10.490	0.470	Duration of pumping (mins)	920
16	10.520	0.500	Discharge (m3/day)	159.84
18	10.520	0.500	s (m)	0.015
20	10.520	0.500	**T (m^2/day)**	1949.564
30	10.535	0.515	**K (m/day)**	324.9273
35	10.540	0.520		
480	10.550	0.530		
840	10.560	0.540		
920	10.565	0.545		

Table 14: drawdown at pumping well 10/15

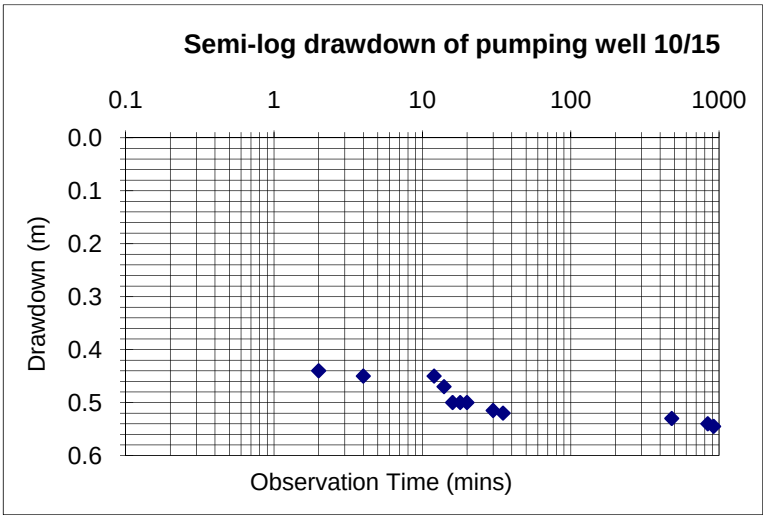

Figure 14: drawdown at well 10/15 during constant-rate pumping test

Time (minutes)	DTW (m)	t/t"	Residual Drawdown	Initial DTW (m):	10.02
1	10.210	920.00	0.190	Distance from Pumping well (m):	0
2	10.100	460.00	0.080	Discharge (L/s)	1.85
3	10.090	306.67	0.070	Thickness of Aquifer	6
4	10.085	230.00	0.065	Duration of pumping (mins)	920
5	10.085	184.00	0.065	Discharge (m^3/ day)	159.84
6	10.084	153.33	0.064	s" (m)	0.019
7	10.083	131.43	0.063	**T (m^2/day)**	**1338.373**
8	10.082	115.00	0.062	**K (m/day)**	**223.0622**
9	10.081	102.22	0.061		
10	10.080	92.00	0.060		
12	10.080	76.67	0.060		
14	10.079	65.71	0.059		
16	10.078	57.50	0.058		
18	10.077	51.11	0.057		
20	10.075	46.00	0.055		
25	10.073	36.80	0.053		
30	10.070	30.67	0.050		
35	10.069	26.29	0.049		
40	10.068	23.00	0.048		
50	10.066	18.40	0.046		
60	10.065	15.33	0.045		
80	10.062	11.50	0.042		

100	10.060	9.20	0.040		
120	10.059	7.67	0.039		
150	10.058	6.13	0.038		
180	10.057	5.11	0.037		
240	10.056	3.83	0.036		
300	10.054	3.07	0.034		
360	10.053	2.56	0.033		
420	10.052	2.19	0.032		
480	10.052	1.92	0.032		
540	10.052	1.70	0.032		

Table 15: recovery analysis data at well 10/15

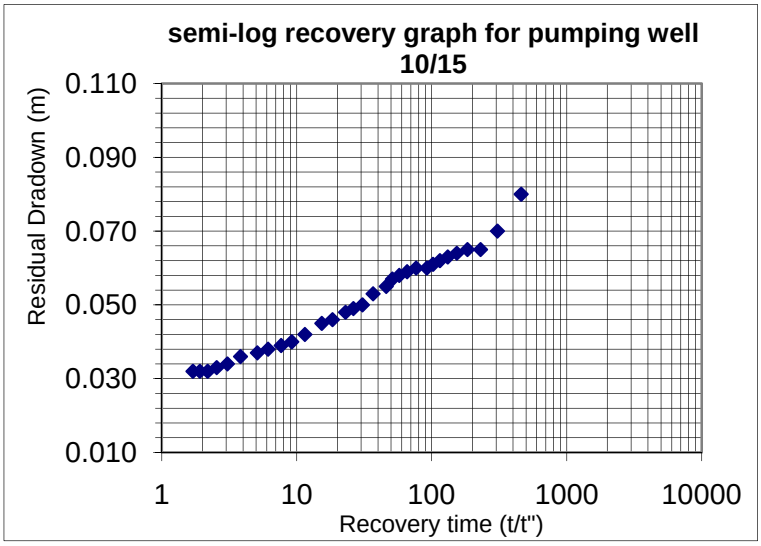

FIgute 15: recovery graph from well 10/15 after constant-rate long-tem pumping

Appendix H: Physical Water Balance calculation

Parameters	Calculations	Wet season	Dry season
Land area (m^2)	A	40000000	40000000
Precipitation (m/month)	P	0.223	0.089
Evapotranspiration (m/month)	ET	0.138	0.098
Total Precipitation (m^3/month)	TP = A×P	8920000	3560000
Total Evapotranspiration (m^3/month)	TET = A×ET	5520000	3920000
Total runoff (m^3/m^{-1}) (4.1 % of P)	Ru = (A×P)×0.041	365720	145960
Total number of Groundwater sources	Num_GW_sources	26	29
Average pumping rate (L/s)	Q	1.06	1.19
Average daily abstraction duration (hrs)	Hr1	5.15	4.93
Daily groundwater abstraction (m^3/day)	(Q×3600×Hr1×Num_GW_sources)/1000	510.96	612.48
Total groundwater abstraction (m^3/month)	GA = ((Q×3600×Hr1×Num_GW_sources)/1000)×30	15328.87	18374.50
Total number of low lift pump	Num_LL_Pumps	-	14
average pumping rate (L/s)	Q	-	9
average pumping duration (hrs)	Hr2	-	6
Daily low-lift pump abstraction (m^3/day)	(Q×3600×Hr2×Num_LL_Pumps)/1000		2721.6
Low-lift pump abstraction (m^3/month)	Low-lift abstraction = ((Q×3600×Hr2×Num_LL_Pumps)/1000)×30	-	81648
Total number of groundwater irrigation source	Num_GW_Pumps	-	3
average pumping rate (L/s)	Q	-	2.3
average abstraction duration (hrs)	Hr3	-	3
Daily groundwater abstraction	(Q×3600×Hr3×Num_GW_Pumps)/1000		74.52
Groundwater irrigation (m^3/month)	GW irrigation =((Q×3600×Hr3×Num_GW_Pumps)/1000)×30	-	2235.6
Total irrigation (m^3/month)	TI = Low-lift abstraction + GW irrigation	-	83883.6
Total Recharge (m^3/m)	Recharge (m^3/month) = (TP+TI) - (TET+GA+Ru)	3018951.13	-440450.90
Total Recharge (m/month)	Recharge (m/month) = (((TP+TI) - (TET+GA+Ru))/A))	0.08	-0.01

Table 1: physical water balance calculation

Appendix I: Individual Chemical Results

Chemical sampling, as mentioned in section 3.5, was conducted on monthly basis. Due to the spatial extent of the study area, cost of analysis and logistical costs, coverage of the entire field area was difficult. Consequently, sites were sampled, at least, twice in the course of the project. The samples were then grouped in to location areas, namely Bilalevu (B), Dubalevu (D), Nabaka (Na), Nabitu (Nb)Siminilaya (S) and Vunarewa (V) and were given unique ID for ease of referencing. A total of 93 samples were collected during the coarse of the project (September, 2009 – January, 2011) and the individual results are provided below with the Site ID added for reference. The table below presents the sites, location, physical parameters and site ID before the individual results area provided. As discussed earlier in sections 3.5 and 4.3, the samples were averaged, to provide a snapshot of hydrochemistry of the sampled water source.

Site, Location	Depth	Location	Source	ID	pH	EC	Salinity	Temp
Tubakeli Project	35	Bilalevu	GW	B1	7.1-7.3	367-410	0.01	27-27.2
Tore Project	37	Bilalevu	GW	B2	6.9-7.4	369-419	0.01	27-27.2
Manoj Kumar	39	Bilalevu	GW	B3	7.5	465	0.01	27.1
Waiwai Project	23	Bilalevu	GW	B4	6.9-7.1	440-473	0.01	27-27.2
Tavuto Project	47	Bilalevu	GW	B5	6.9-7.3	510-514	0.02	26-26.8
Bulatale Store	40	Bilalevu	GW	B6	6.8-7.4	282-393	0.01	27.5-29.1
Shiu Shankar	40	Bilalevu	GW	B7	6.8-7.3	350-383	0.01	26.8-28.3
Ashok Kumar	20	Bilalevu	GW	B8	5.9-6.6	201-254	0	27.5-27.6
Mahen's Export	40	Bilalevu	GW	B9	7-7.2	578-638	0.02	28.5-30
Shiu Prasad	43	Bilalevu	GW	B10	7.1-7.2	343-421	0.01	26.2
Sunil Prasad	45	Bilalevu	GW	B11	7.5-8	381	0.01	27.2
Arjun Lal	20	Bilalevu	GW	B12	6.7	279	0.01	29.5
Oxbow Lake	0	Bilalevu	OL	B14	7.3-7.7	31-136	0	26.8-30
Bilalevu Meander	0	Bilalevu	Rr	B15	6.9-7.9	113-184	0	26.7-31.4
BH 10/12	43	Bilalevu	GW	B16	7.5-8.5	240-280	0.01	25.5-27.1
BH 10/13	30	Bilalevu	GW	B17	7.6-7.9	380-403	0.01	26-27
BH 10/14	60	Bilalevu	GW	B18	7-6-8.1	370-385	0.01	26.6-28
BH 10/15	35	Bilalevu	GW	B19	6.4-8	288-300	0.01	27.5-28
Ami Chand	60	Dubalevu	GW	D1	6.3-7.8	350-389	0.01	27-28
BH 90/15	40	Dubalevu	GW	D2	6.1-6.9	243-294	0-0.01	26.2-26.6
BH 90/16	45	Dubalevu	GW	D3	6.1-7.2	260-279	0.01	26.2-30.7
BH 89/15	43	Dubalevu	GW	D4	6.6-6.9	315-341	0.01	26.6-27.5
BH 10/07	34	Dubalevu	GW	D5	7.1-7.7	243-248	0	25-26.3
BH 10/08	26	Dubalevu	GW	D6	6.1-6.8	224-299	0.01	25-26
Jubairata village	38	Dubalevu	GW	D7	7.3	404	0.01	28.7
MPI Station	40	Dubalevu	GW	D8	6.8-7.5	363-396	0.01	27-28.2
Raunitogo meander	0	Dubalevu	Rr	D9	7.34	189	0	28.1
Jubairata meander	0	Dubalevu	Rr	D10	7.2-7.4	150-212	0	27-27.8
Nakavika settlement	26	Nabaka	GW	Na1	6.8-7.5	394-407	0.01	26.5-27.2
Qalitala Creek	0	Nabaka	Ck	Na2	7.1-7.4	147-171	0	27.1
Oxbow Lake	0	Nabaka	OL	Na3	7.2-7.5	63-82	0	27.8-32
Janmin Jay	40	Nabaka	GW	Na4	6.5-7.8	257-327	0.01	27-30.7
Paras Ram	18	Similaya	GW	S1	7.3-7.6	304-310	0.01	27.8-28
Hari Chand	40	Similaya	GW	S2	6.4-7.1	580-592	0.02-0.03	27-27.5
Nabitu Community	27	Nabitu	GW	Nb1	6.9-7.6	397-477	0.01	27.1-28.6
Kamal Kishor	40	Nabitu	GW	Nb2	6.9-8.3	400-653	0.01-0.02	27.5-27.9
Pramend Singh	25	Nabitu	GW	Nb3	6.7-7.1	293-388	0.01	27.2-28.2
Nabitu Primary Sch	30	Nabitu	GW	Nb4	7.1-7.4	406-421	0.01	27.2
Anil Prasad	40	Nabitu	GW	Nb5	6.5-7.2	182-187	0	27.5-28
Ram Deo	37	Nabitu	GW	Nb6	7.12	301	0.01	27.6

Koroira Spring	0	Qalimare	SP	Q1	7.7-8.5	250-256	0	23.4-24.1
Nacule Spring	0	Qalimare	SP	Q2	7.1-7.4	310-315	0.01	25.3-25.6
Matanitavuni Spring	0	Qalimare	SP	Q3	7.15	390	0.01	24.9
Mataukaba Spring	0	Vunarewa	SP	V1	7.7	229	0	25
Navala Spring	0	Mavua	SP	M1	7.5-7.6	355-392	0.01	24.1-25.5

Table 1: summary table of all chemical sampling sites, showing depth (m), location, type (i.e. groundwater (GW), spring (SP), river (Rr) and creek (Ck), pH, EC (µS/cm), temperature (°C), and salinity (%).

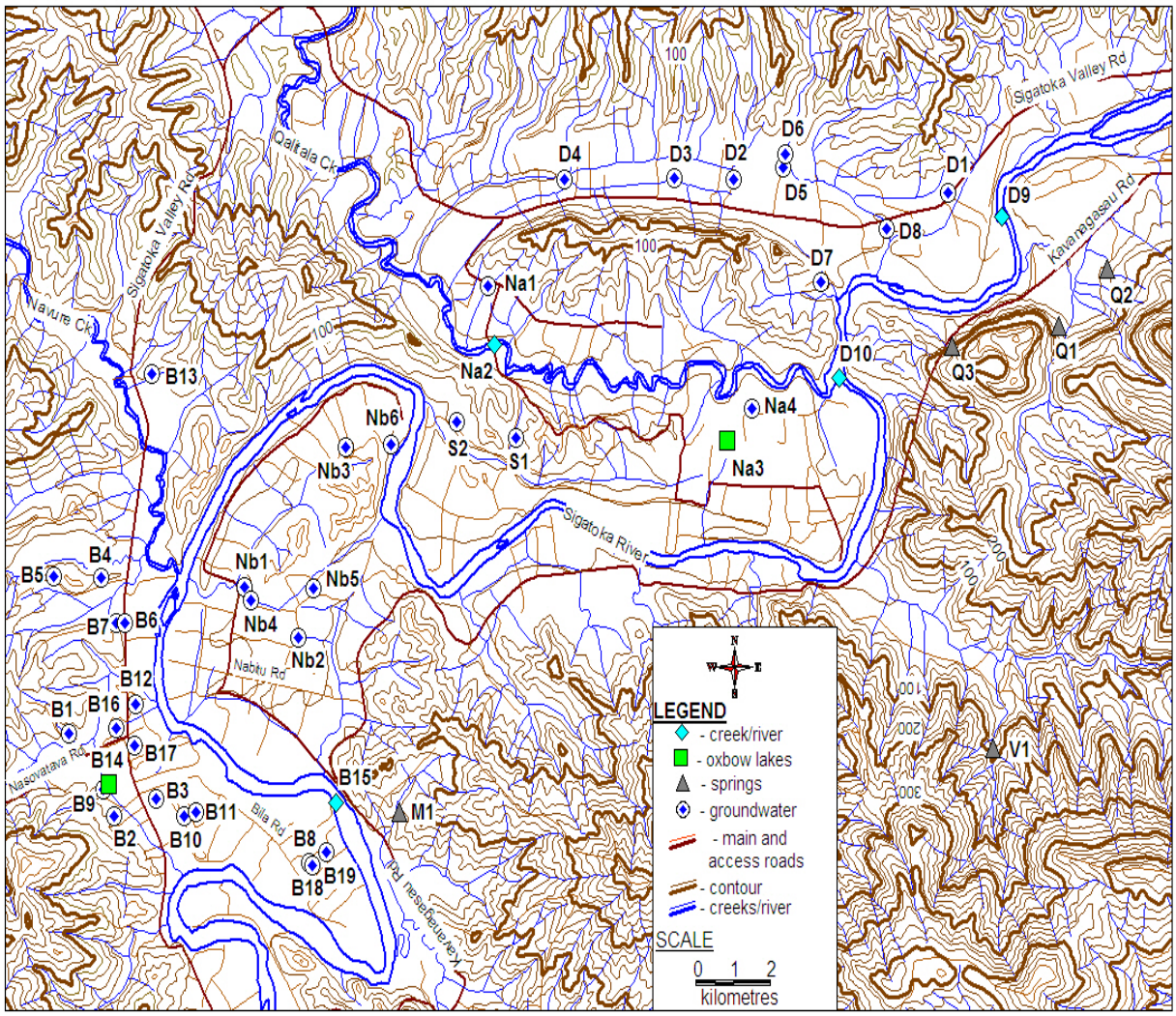

Figure 1: Location of map of chemical sampling sites with Site ID.

Individual results are shown the following pages: